

Engineering and characterizing nonclassical states of light in quantum optical networks

Présentée le 19 août 2022

Faculté des sciences de base
Laboratoire de physique théorique des nanosystèmes
Programme doctoral en physique

pour l'obtention du grade de Docteur ès Sciences

par

Kilian Robert SEIBOLD

Acceptée sur proposition du jury

Prof. F. Mila, président du jury
Prof. V. Savona, directeur de thèse
Prof. M. Wouters, rapporteur
Prof. D. Gerace, rapporteur
Prof. C. Galland, rapporteur

Abstract

The exploration of open quantum many-body systems —systems of microscopic size exhibiting quantum coherence and interacting with their surrounding— has emerged as a key research area over the last years. The recent advances in controlling and preserving quantum coherence at the level of a single particle, developed in a wide variety of physical platforms, have been a major driving force in this field. The driven dissipative nature is a common characteristic of a wide class of modern experimental platforms in quantum science and technology, such as photonic systems, ultracold atoms, optomechanical systems, or superconducting circuits. The interplay between the coherent quantum dynamics and dissipation in open quantum systems leads to a wide range of novel out-of-equilibrium behaviours. Among them, the emergence in these systems of dynamical phases with novel broken symmetries, topological phases and the occurrence of dissipative phase transitions are of particular interest.

This thesis aims at establishing a theoretical framework to engineer, characterize and control nonclassical states of light in photonic quantum optical networks in different regimes. The emphasis is put on its implementation, in particular with respect to integration and scalability in photonic platforms.

In this thesis, we tackle some interesting aspects arising in the study of the dynamics of driven dissipative coupled nonlinear optical resonators. In that context, we consider the dynamics of two coupled nonlinear photonic cavities in the presence of inhomogeneous coherent driving and local dissipations using the Lindblad master equation formalism. We show that this simple open quantum many-body system can be subject to dynamical instabilities. In particular, our analysis shows that this system presents highly nonclassical properties and its dynamics exhibits dissipative Kerr solitons (DKSs), characterized by the robustness of its specific temporal or spatial waveform during propagation.

In a second step, our intuition gained from this system composed of only few degrees of freedom is expanded to the study of systems of bigger size. In particular, we study DKSs originating from the parametric gain in Kerr microresonators. While DKSs are usually described using a classical mean-field approach, our work proposes a quantum-mechanical model formulated in terms of the truncated Wigner formalism. This analysis is motivated by the fact that technological implementations push towards

the realization of DKSs in miniaturized integrated systems. These are operating at low power, a regime where quantum effects are expected to be relevant.

Using the tools provided by the theory of open quantum systems, we propose a detailed investigation of the impact of quantum fluctuations on the spectral and dynamical properties of DKSs. We show that the quantum fluctuations arising from losses engender a finite lifetime to the soliton, and demonstrate that DKSs correspond to a specific class of dissipative time crystals.

Keywords: Open quantum many-body systems, Lindblad quantum master equation, Truncated Wigner method, Non-equilibrium dynamics, Collective dynamics, Optical parametric oscillators, Dissipative phase transitions, Dissipative Kerr solitons, Dissipative time crystals.

Zusammenfassung

Die Erforschung offener Quanten-Vielteilchensysteme—Systeme mikroskopischer Grösse, die Quantenkohärenz aufweisen und mit ihrer Umgebung interagieren— hat sich in den letzten Jahren zu einem wichtigen Forschungsgebiet entwickelt. Die jüngsten Fortschritte bei der Kontrolle und Erhaltung der Quantenkohärenz auf der Ebene eines einzelnen Teilchens, die in einer Vielzahl von physikalischen Plattformen entwickelt wurden, waren eine wichtige Triebkraft in diesem Bereich. Der Getrieben-Dissipativ-Charakter ist ein gemeinsames Merkmal einer breiten Klasse von modernen Experimentierplattformen in der Quantenwissenschaft und -technologie, wie zum Beispiel photonische Systeme, ultrakalte Atome, optomechanische Systeme oder supraleitende Schaltkreise. Das Zusammenspiel zwischen der kohärenten Quantendynamik und der Dissipation in offenen Quantensystemen führt zu einem breiten Spektrum neuartiger Verhaltensweisen ausserhalb des Gleichgewichts. Von besonderem Interesse sind dabei die Entstehung dynamischer Phasen mit neuartigen gebrochenen Symmetrien, topologische Phasen und das Auftreten dissipativer Phasenübergänge in diesen Systemen.

Diese These zielt darauf ab, einen theoretischen Rahmen für die Entwicklung, Charakterisierung und Kontrolle von nichtklassischen Zuständen des Lichts in photonischen quantenoptischen Netzwerken in verschiedenen Regimen zu schaffen. Der Schwerpunkt liegt auf seiner Umsetzung, insbesondere im Hinblick auf die Integration und Skalierbarkeit in photonischen Plattformen.

In dieser These befassen wir uns mit einigen interessanten Aspekten, die sich bei der Untersuchung der Dynamik von getriebenen dissipativen gekoppelten nichtlinearen optischen Resonatoren ergeben. In diesem Zusammenhang betrachten wir die Dynamik von zwei gekoppelten, nichtlinearen photonischen Kavitäten in Gegenwart von inhomogenen kohärenten Antrieben und lokalen Dissipationen unter Verwendung der Lindblad Mastergleichung.

Wir zeigen, dass dieses einfache offene Quanten-Vielteilchensystem dynamischen Instabilitäten unterliegen kann. Insbesondere, dass dieses System höchst unklassische Eigenschaften aufweist und seine Dynamik dissipative Kerr-Solitonen (DKSs) hervorbringt, die durch die Robustheit ihrer spezifischen zeitlichen oder räumlichen Wellenform während der Ausbreitung gekennzeichnet sind.

In einem zweiten Schritt wird unsere Intuition, die wir aus diesem System mit nur wenigen Freiheitsgraden gewonnen haben, auf die Untersuchung von Systemen mit einer Grosszahl von Freiheitsgraden erweitert. Insbesondere untersuchen wir DKSs, die durch die parametrische Verstärkung in Kerr-Mikroresonatoren entstehen. Während DKSs normalerweise mit einem klassischen Molekularfeldtheorie-Ansatz beschrieben werden, schlagen wir in unserer Arbeit ein quantenmechanisches Modell vor, das in Form des trunkierten Wigner-Formalismus ausgedrückt wird. Diese Analyse ist durch die Tatsache motiviert, dass technologische Implementierungen in Richtung der Realisierung von DKSs in miniaturisierten integrierten Systemen vorstossen. Diese werden mit geringer Leistung betrieben, einem Bereich, in dem Quanteneffekte relevant sein dürften. Unter Verwendung der Werkzeuge der Theorie offener Quantensysteme schlagen wir eine detaillierte Untersuchung der Auswirkungen von Quantenfluktuationen auf die spektralen und dynamischen Eigenschaften von DKSs vor. Wir zeigen, dass die Quantenfluktuationen, die durch Verluste entstehen, dem Soliton eine endliche Lebensdauer verleihen, und demonstrieren, dass DKSs einer bestimmten Klasse von dissipativen Zeitkristallen entsprechen.

Schlüsselwörter: Offene Quantensysteme, Lindblad Quanten-Mastergleichung, Trunkierte Wigner-Methode, Nicht-Gleichgewichtsdynamik, Kollektive Dynamik, Optische parametrische Oszillatoren, Dissipative Phasenübergänge, Dissipative Kerr-Solitonen, Dissipative Zeitkristalle.

Résumé

L'exploration des systèmes quantiques ouverts à plusieurs corps —des systèmes de taille microscopique présentant une cohérence quantique et interagissant avec leur environnement — est devenue un domaine de recherche essentiel au cours des dernières années. Les récentes avancées dans le contrôle et la préservation de la cohérence quantique au niveau d'une seule particule, développées dans une grande variété de plateformes physiques, ont été une force motrice majeure dans ce domaine. La nature dissipative entraînée est une caractéristique commune d'une large classe de plateformes expérimentales modernes en science et technologie quantiques, telles que les systèmes photoniques, les atomes ultrafroids, les systèmes optomécaniques ou les circuits supraconducteurs. L'interaction entre la dynamique quantique cohérente et la dissipation dans les systèmes quantiques ouverts conduit à un large éventail de nouveaux comportements hors équilibre. Parmi ceux-ci, l'émergence dans ces systèmes de phases dynamiques avec de nouvelles symétries brisées, de phases topologiques et l'apparition de transitions de phase dissipatives sont particulièrement intéressantes.

Cette thèse vise à établir un cadre théorique pour concevoir, caractériser et contrôler les états non classiques de la lumière dans les réseaux optiques quantiques photoniques dans différents régimes. L'accent est mis sur sa mise en œuvre, en particulier en ce qui concerne l'intégration et la scalabilité dans les plateformes photoniques.

Dans cette thèse, nous abordons certains aspects intéressants de l'étude de la dynamique des résonateurs optiques non linéaires couplés et dissipatifs. Dans ce contexte, nous considérons la dynamique de deux cavités photoniques non linéaires couplées en présence d'un pompage cohérent inhomogène et de dissipations locales en utilisant le formalisme des équations maîtresses de Lindblad.

Nous montrons que ce simple système quantique ouvert à plusieurs corps peut être sujet à des instabilités dynamiques. En particulier, notre analyse montre que ce système présente des propriétés hautement non-classiques et que sa dynamique présente des solitons de Kerr dissipatifs (SKDs), caractérisés par la robustesse de sa forme d'onde temporelle ou spatiale spécifique pendant la propagation.

Dans un deuxième temps, notre intuition acquise à partir de ce système composé de seulement quelques degrés de liberté est étendue à l'étude de systèmes de plus grande taille. En particulier, nous étudions les SKDs provenant du gain paramétrique dans

les microrésonateurs de Kerr. Alors que les SKDs sont généralement décrits par une approche classique de champs moléculaires, notre travail propose un modèle quantique formulé en termes du formalisme de Wigner tronqué. Cette analyse est motivée par le fait que les implémentations technologiques poussent à la réalisation de SKDs dans des systèmes intégrés miniaturisés. Ceux-ci fonctionnent à faible puissance, un régime où les effets quantiques sont censés être non négligeables.

En utilisant les outils fournis par la théorie des systèmes quantiques ouverts, nous proposons une investigation détaillée de l'impact des fluctuations quantiques sur les propriétés spectrales et dynamiques des SKDs. Nous montrons que les fluctuations quantiques résultant des pertes engendrent une durée de vie finie au soliton, et démontrons que les SKDs correspondent à une classe spécifique de cristaux de temps dissipatifs.

Mots clés : Systèmes quantiques ouverts, équation maîtresse quantique de Lindblad, méthode de Wigner tronquée, dynamique de non-équilibre, dynamique collective, oscillateurs paramétriques optiques, transitions de phase dissipatives, solitons de Kerr dissipatifs, cristaux de temps dissipatifs.

Sinossi

L'esplorazione dei sistemi quantistici aperti a molti corpi —sistemi di dimensioni microscopiche che mostrano coerenza quantistica e interagiscono con il loro ambiente — è diventata un'area di ricerca chiave negli ultimi anni. I recenti progressi nel controllo e nella conservazione della coerenza quantistica a livello di una singola particella, sviluppati in un'ampia varietà di realizzazioni sperimentali, hanno rappresentato una forza trainante in questo campo. La natura dissipativa forzata (*driven dissipation*) è una caratteristica comune a un'ampia classe di moderne realizzazioni sperimentali nella scienza e nella tecnologia quantistica, come i sistemi fotonici, gli atomi ultrafreddi, i sistemi optomeccanici o i circuiti superconduttori. L'interazione tra dinamica quantistica coerente e dissipazione nei sistemi quantistici aperti porta a un'ampia gamma di nuovi comportamenti fuori dall'equilibrio. Tra questi, l'emergenza in questi sistemi di fasi dinamiche con nuove rotture di simmetrie, fasi topologiche e transizioni di fase dissipative è particolarmente interessante.

Questa tesi mira a stabilire un quadro teorico per ingegnerizzare, caratterizzare e controllare gli stati non classici della luce in reti ottiche fotoniche quantistiche in diversi regimi. L'accento è posto sulla sua implementazione, in particolare per quanto riguarda l'integrazione e la scalabilità delle piattaforme fotoniche.

In questa tesi affrontiamo alcuni aspetti interessanti che emergono nello studio della dinamica di risonatori ottici non lineari accoppiati e dissipativi. In questo contesto, consideriamo la dinamica di due cavità fotoniche non lineari accoppiate in presenza di un pompaggio coerente disomogeneo e di dissipazioni locali, utilizzando il formalismo della master equation di Lindblad. Mostriamo che questo semplice sistema quantistico aperto a molti corpi può essere soggetto a instabilità dinamiche. In particolare, la nostra analisi mostra che questo sistema presenta proprietà altamente non classiche e che la sua dinamica presenta solitoni dissipativi di Kerr (SDK), caratterizzati dalla robustezza della loro specifica forma d'onda temporale o spaziale durante la propagazione.

In una seconda fase, l'intuizione acquisita da questo sistema composto da pochi gradi di libertà viene estesa allo studio di sistemi più grandi. In particolare, studiamo i SDK originati dal guadagno parametrico nei microresonatori di Kerr. Mentre i SDK sono generalmente descritti da un approccio classico di campo medio, il nostro lavoro propone un modello quantomeccanico formulato in termini di formalismo di Wigner troncato.


Questa analisi è motivata dal fatto che le implementazioni tecnologiche si spingono verso la realizzazione di SDK in sistemi integrati miniaturizzati. Questi funzionano a bassa potenza, un regime in cui si prevede che gli effetti quantistici non siano trascurabili. Utilizzando gli strumenti forniti dalla teoria dei sistemi quantistici aperti, proponiamo un'indagine dettagliata dell'impatto delle fluttuazioni quantistiche sulle proprietà spettrali e dinamiche dei SDK. Dimostriamo che le fluttuazioni quantistiche derivanti dalle perdite generano tempi di vita finiti per i solitoni e dimostriamo che i SDK corrispondono a una classe specifica di cristalli temporali dissipativi.

Parole chiave: Sistemi quantistici aperti e a molti corpi, equazione quantistica di Lindblad, metodo di Wigner troncato, dinamica di non-equilibrio, dinamica collettiva, oscillatori ottici parametrici, transizioni di fase dissipative, solitoni di Kerr dissipativi, cristalli temporali dissipativi.

Publication List

- K. Seibold, R. Rota, and V. Savona, *Dissipative time crystal in an asymmetric nonlinear photonic dimer*, [Physical Review A **101**, 033839 \(2020\)](#)
- J. Vasco, D. Gerace, K. Seibold, and V. Savona, *Monolithic silicon-based nanobeam cavities for integrated nonlinear and quantum photonics*, [Physical Review Applied **13**, 034070 \(2020\)](#)
- K. Seibold, R. Rota, F. Minganti, and V. Savona, *Quantum dynamics of dissipative kerr solitons*, [Phys. Rev. A **105**, 053530 \(2022\)](#)
- M. D. Anderson, S. T. Velez, K. Seibold, H. Flayac, V. Savona, N. Sangouard, and C. Galland, *Two-color pump-probe measurement of photonic quantum correlations mediated by a single phonon*, [Physical Review Letters **120**, 233601 \(2018\)](#)
- S. T. Velez, K. Seibold, N. Kipfer, M. D. Anderson, V. Sudhir, and C. Galland, *Preparation and decay of a single quantum of vibration at ambient conditions*, [Physical Review X **9**, 041007 \(2019\)](#)

Contents

Abstract (English/Deutsch/Français/Italiano)	i
Publication List	ix
Contents 	xi
General Introduction	1
0.1 A brief history of Quantum Mechanics	1
0.2 Open quantum systems	4
0.2.1 On the importance of dissipation	5
0.3 Critical phenomena and phase transitions	7
1 Light-matter interaction and quantum states of light	11
1.1 Preliminary background	12
1.1.1 Hilbert space and quantum states	12
1.1.2 Time-evolution	14
1.1.3 Physical observables and measurements	15
1.1.3.1 Observable	15
1.1.3.2 Standard measurement	15
1.1.3.3 Generalized Measurements (POVMs)	16
1.1.4 Composite systems and entanglement	17
1.2 The quantum harmonic oscillator	18
1.2.1 Quantizing the electromagnetic field	22
1.2.2 Correlation functions	23
1.3 Coherent states	24
1.3.1 Definition	24
1.3.2 Properties	25
1.4 Physical platforms of quantum many-body physics	28
1.4.1 Optical resonators and photonic structures	28
1.4.2 Superconducting architectures	29
1.4.3 Ultracold atoms	30
1.4.4 Quantum optomechanical systems	31
1.4.5 ... and a lot of other platforms	32

2	Theory of open quantum systems	35
2.1	Opening	37
2.1.1	What	37
2.1.2	Why	38
2.1.3	How	39
2.2	Time evolution of open quantum systems	40
2.2.1	Time evolution of closed quantum systems	40
2.2.2	Let there be interaction!	42
2.2.3	Time evolution of open quantum system	43
2.2.3.1	Universal Dynamical Maps of Open Quantum Systems	43
2.3	The Lindblad quantum master equation	46
2.3.1	Some approximations	46
2.3.2	The Lindblad master equation	47
2.3.3	Environment types and modeling approaches	49
2.3.3.1	Bosons	49
2.3.3.2	Fermions	51
2.3.3.3	Drive	51
2.3.4	Intermezzo: example of a single bosonic (cavity) mode	51
2.4	The Liouvillian superoperator	52
2.4.1	The Liouvillian superoperator	52
2.4.2	Vectorization: the Choi-Jamiolkowski isomorphism	54
2.4.3	Spectral properties of the Liouvillian superoperator	56
2.5	Various open quantum system methods	58
2.5.1	Stochastic approaches	59
2.5.1.1	The quantum trajectory technique	59
2.5.2	Other approaches	61
3	Truncated Wigner method for simulating dissipative many-body dynamics	65
3.1	The Truncated Wigner formalism	66
3.2	Phase-space representations of quantum optics	69
3.3	The Weyl-Wigner phase-space representation	70
3.3.1	The Weyl and Wigner transformations	71
3.3.1.1	The Wigner function	72
3.3.2	Expectation values	73
3.3.3	Operator correspondences	74
3.3.4	The multi-mode generalization	75
3.4	Time evolution of the Wigner function	75
3.4.1	Partial differential equation for the Wigner distribution	76
3.5	From PDE to FPE : the Truncated-Wigner approximation	76
3.6	The Truncated Wigner-function Fokker-Planck equation	77

3.7	Expectation values within the TWA formalism	78
3.8	Remarks	79
3.8.1	Accuracy	79
3.8.2	Limitations of this numerical technique	79
3.8.3	Single trajectory interpretation	79
3.8.4	Extensions	79
3.8.5	Exact limit	80
3.8.6	Connection with path-integral approach	80
3.9	Application to the driven dissipative harmonic oscillator	80
4	Dissipative phase transition and dissipative time crystals	81
4.1	Equilibrium phase transition	82
4.1.1	Classical phase transitions	82
4.1.2	Quantum phase transition	84
4.1.2.1	First order quantum phase transitions	86
4.1.2.2	Continuous quantum phase transitions	87
4.1.2.3	Extension to Finite Temperatures	88
4.1.2.4	Symmetry Breaking and phase transitions	88
4.2	Dissipative phase transitions	89
4.2.1	Theoretical framework	90
4.2.2	Universal critical behavior and scaling invariance	92
4.2.3	Optical bistability	92
4.2.4	Numerical methods	93
4.3	Dissipative time crystals	93
4.3.1	Time crystals	93
4.3.2	Dissipative time crystals	96
4.3.3	Theoretical description of dissipative time-crystals	97
4.3.3.1	Spectral Requirements for Dissipative Time Crystals	99
4.3.3.2	From Finite to Infinite Dissipative Time Crystals	99
4.4	One mode critical phenomena: dynamical optical hysteresis in the Kerr model	100
4.4.1	Semiclassical analysis	100
4.4.2	Quantum analysis	101
4.5	Two mode critical phenomena: dissipative time crystal in an asymmetric nonlinear photonic dimer	101
5	Dissipative Kerr solitons as dissipative time crystals	113
5.1	Optical frequency combs	114
5.1.1	Introduction.	114
5.1.2	Generation of frequency combs	115
5.2	Kerr frequency combs	115

5.2.1	Kerr comb generation	116
5.3	Temporal cavity solitons	118
5.3.1	Dissipative solitons	118
5.3.2	Temporal cavity solitons	118
5.4	Dissipative Kerr soliton	119
5.4.1	A rich dynamic	119
5.4.2	Solitons and frequency combs	120
5.4.3	Theoretical description of solitons in a microresonator	120
5.4.4	Anatomy of KFCs	120
5.4.5	Lugiato–Lefever equation	121
5.5	Multi mode critical phenomena: quantum dynamics of dissipative Kerr solitons	122
6	General discussion and outlook	137
	Bibliography	141

General Introduction

Quantum mechanics is a very successful mathematical theory explaining a wide range of phenomena that occur at very small scales (including atoms, electrons, and photons), where classical theories formulated by Galileo, Newton, Lagrange, Hamilton, Maxwell and others, fail. Quantum physics has broadened our understanding of nature and sparked a slew of technological breakthroughs.

0.1 A brief history of Quantum Mechanics

The first years of quantum mechanics. The quantum journey began with Max Planck’s pioneering work in 1900, when he postulated that energy exchanges between light and matter occurs in discrete irreducible quanta, with energy E proportional to the frequency of radiation ν ,

$$E = h\nu, \tag{1}$$

with h the Planck constant [6]. This new perspective allowed him to accurately describe the spectrum of black body radiation — which can be used to approximately describe the energy emitted by the sun for instance. Albert Einstein then generalized Planck’s concept by theorizing that energy itself (not just the process of energy absorption and emission) is quantized according to Eq. (1), with the energy E actually corresponding to the energy of a particle. The concept that light must consist of tiny bullet-like particles —the photons— allowed him to explain the photo-electric effect in 1905 [7], work for which he received the Nobel Prize in Physics.

First quantum revolution (1920’s - 1980’s). These early accomplishments led to the development of a full-fledged theory of quantum mechanics in the 1920s, which describes how nature works at the quantum level —at least for isolated systems. Standard quantum mechanics considers closed or isolated systems, i.e. systems that are perfectly isolated from their surroundings. Such systems evolve deterministically, their dynamics is unitary and is fully governed by the Schrödinger equation

$$i\hbar\frac{\partial}{\partial t}|\psi(t)\rangle = \hat{H}(t)|\psi(t)\rangle. \tag{2}$$

In the above, $\hbar = h/(2\pi)$ denotes the reduced Planck constant, $|\psi(t)\rangle$ is the ket (vector in the Hilbert space) describing the state of the system at a given time t , and $\hat{H}(t)$ is the Hamiltonian of the system. Important aspects of quantum mechanics in closed systems are reviewed in [Chap I Sec. 1](#), and [Chap II Sec. 2](#).

A striking outcome of the quantum theory is the existence of two kinds of elementary particles in nature: fermions and bosons, distinguished by their quantum statistics. Fermions¹ have half-integer spin, obey Fermi–Dirac statistics, and are the building blocks of matter. Bosons² on the other hand have integer spin, obey Bose–Einstein statistics, and are the mediators of interactions. An important interaction that will play a central role in this thesis is the interaction between light (photons) and matter (e.g. electrons). A fully quantum description of interactions between photons and electrons is provided by a quantum field theory, namely quantum electrodynamics. Dirac quantized in particular the electromagnetic field and more generally bosonic fields, introducing the concept of quantum harmonic oscillators (QHO). The elemental notions of the QHO and its importance in the treatment of the electromagnetic field is presented in [Chap. I Sec. 2](#).

Quantum mechanics can be formulated within the formalism of Schrödinger (wave mechanics, as described above) or Heisenberg (matrix mechanics).³ Besides the Schrödinger and Heisenberg formulation, in 1932, Eugene Wigner introduced a phase space formulation of quantum mechanics. This formulation shares interesting common points with the classical phase space formalism. An important ingredient to phase space methods is the concept of coherent states. Some basic concepts of these specific set of states are presented in [Sec. 3 of Chap. I](#), while some intriguing aspects of phase space approaches are examined in [Sec. 2 to 4 of Chap. III](#).

The success of these various formalisms of quantum mechanics was enormous and allowed to understand the periodic table of elements, quantized energy levels of atoms [8], chemical interactions, amazing properties of matter such as superconductivity or superfluidity, or describe particle physics. This also led to discovery and debate about the weirdness of quantum mechanics. The wave-particle duality was established: light and matter can behave as either a particle or a wave. Entanglement — a spooky action at a distance — was brought to light.

This sparked a technological revolution, with the invention of technologies based on emergent quantum physics phenomena. The so-called first quantum revolution enabled inventions such as the transistor (1948), atomic clock (1949) and laser (1960). These

¹Described by E. Fermi, P. Dirac and W. Pauli. Leptons and quarks are fermions, as well as entities made up of them like e.g protons, neutrons, atoms, molecules and humans.

²Described by S. Bose A. Einstein. Photons, gluons, the W, Z and Higgs bosons are bosons.

³The two formalisms were demonstrated equivalent by P. Dirac.

³At the time of its invention, the laser was called “a solution looking for a problem” [9]. Today its ubiquity of applicability is striking in our society, ranging from medical and industrial applications to fundamental biological or nuclear fusion research.

inventions are at the heart of computers, the Global Positioning System, and optical fiber telecommunications, all of which are vital to today's world economy. However, these technologies do not harness the full power of quantum mechanics.

Second quantum revolution (starts ~ 1980's). Today, researchers and scientists are working towards a second technological leap. This second quantum revolution builds upon fundamental research at the crossroads between quantum mechanics (i.e. atoms, photons, Josephson junctions, physics of computation) and information science (i.e. computer science, communications, cryptography), giving birth to a new discipline called Quantum Information Science.

The trademark of this second quantum revolution lies in overcoming the passive observer status of the quantum world as it exists in nature, and to start using quantum effects to tailor novel quantum states of our own design. For instance, in addition to providing an explanation of the periodic table, new artificial atoms can be created —like e.g. quantum dots, excitons or superconducting qubit— that can be engineered to have the desired electronic and optical properties.

Puzzling properties of quantum mechanics —superposition principle, entanglement and teleportation — are used to this aim.

This audacious program was pioneered by the experiments conducted in the 1970s and 1980s, including the works by Serge Haroche and David J. Wineland, allowing to measure and manipulate individual quantum systems (as said in their Nobel Prize). Since then, more progress has been made in that direction, and it has become possible to generate quantum states of coherent or entangled matter and energy that exist (probably) nowhere else in the Universe. These new manufactured quantum states offer novel properties—like e.g. sensitivity, entanglement or correlations— that are extremely desirable in quantum devices.

Some interesting experimental platforms used extensively within this framework are exposed in [Chap I Sec. 4](#).

Still (a lot of) work to do! Recently, large companies like Google and Microsoft started pouring a lot of energy into this field with the aim of building a quantum computer. With all these technology-driven perspectives, one might believe that the theory of quantum physics is completely and perfectly established. But even more than a hundred years after Planck and Einstein's ground breaking works, quantum physics still presents conceptual challenges for the scientific community.

On one side, this is due to the fact that the quantum world is host to a plethora of strange phenomena that are not yet fully under control. We can mention for instance the superposition of states, the EPR paradox ⁴, the collapse of the wave function,

⁴Named after Einstein, Podolsky and Rosen the EPR paradox is a thought experiment questioning the "completeness" of quantum mechanics.

the paradox of measurement as well as the existence of non-locality, which all raise interesting physical and philosophical questions.

Also, some general question are not well understood. Among them, the transition between the microscopic world—governed by the laws of quantum physics— and the macroscopic world described by classical physics, remain unanswered. A particularly rapidly expanding field of quantum science and technology is the research related to nonclassical states of light. By “nonclassical” it is meant that the outcome of measurements cannot be explained in terms of a classical probability distribution, but only in terms of quantum mechanics. Prominent examples are sub-Poissonian photon number statistics, and quantum entanglement. This thesis aims at establishing a theoretical framework to

engineer, characterize and control nonclassical states of light in photonic quantum optical networks in different regimes.

These nonclassical states of light emerge from the interaction between driving — a laser source is generally applied to the optical network — and dissipation. To describe such driven-dissipative system it is necessary to go beyond the framework of isolated quantum system and use the tools of open quantum systems instead.

0.2 Open quantum systems

The theory of quantum mechanics initially was solely limited to the description of isolated systems — systems that are perfectly isolated, with none of its degrees of freedom coupling to the rest of the Universe. This constitutes of course an idealization; in nature every system is open and interacts with its environment, exchanging energy, matter and information. While some physical platforms are characterized by a particularly weak interaction between the system and its environment, legitimating to treat them as being isolated, in this thesis we shall be (mostly) interested in those setups where interactions with the environment is of critical importance.

A significant part of modern experimental platforms in quantum science and technology—like e.g. photonic, ultracold atoms, optomechanical, and superconducting circuits systems— are open quantum systems by nature. In view of their omnipresence in experimental setups, it is of paramount importance to understand the dynamics of open quantum systems.

An introduction to open quantum systems can be found in [Chap. II Sec. 1](#). Some physical platforms realizing open quantum optical many body systems are presented in [Chap. I Sec. 4](#).

Dynamics of open quantum systems. Open quantum systems can be divided into two components: the system of interest and its environment, with non-trivial coupling between them.

In practice we often can only track the physics of the system while the behavior of the surrounding environment is far too complex to be grasped. A consequence of this lack of knowledge is that one can no longer work in terms of pure quantum states — kets $|\psi(t)\rangle$ — but rather one needs to introduce a new quantity — the density matrix $\hat{\rho}(t)$ describing a statistical mixture of quantum states. In 1976 the Lindblad master equation (or Gorini-Kossakowski-Sudarshan-Lindblad (GKSL) equation) was derived. This is the most general equation describing the dynamics of an open quantum system under Markovian dynamics, and reads

$$\frac{d\hat{\rho}(t)}{dt} = \mathcal{L}(t)\hat{\rho}(t) , \quad (3)$$

where $\mathcal{L}(t)$ is the Liouvillian superoperator, encoding the coherent and incoherent evolution. The Lindblad master equation and Liouvillian superoperator are discussed in [Chap. II Sec. 3](#) and [Chap. II Sec. 4](#) respectively.

A computational challenge. From a theoretical standpoint, the description of closed interacting many-body quantum systems is already challenging. The dimension of the Hilbert space expands namely exponentially with the number of particles since a quantum mechanical state is defined as the superposition of all possible configurations. The task becomes even more challenging when treating quantum many-body systems within the master equation formalism. Indeed, in this scenario, the density matrix—with corresponding Hilbert space dimension being the square of the dimension of the original space — must be time-evolved. The computational challenges associated with the numerical simulation of the Lindblad dynamics are discussed in [Chap. II](#) and [Chap. III](#). Different approaches have been established to overcome this challenge. Some of these various theories are exposed in [Chap. II Sec. 5](#)

Truncated Wigner. In this thesis we will focus on one specific method, the truncated Wigner approximation approach, which is a phase space method. It is an efficient numerical method describing quantum fluctuations to leading order in \hbar .

In [Chap. III Sec. 1](#) I propose a general discussion to the truncated Wigner formalism, in [Chap. III Sec. 5](#) to [Sec. 8](#) the truncated Wigner formalism is addressed.

While in [Chap. III Sec. 9](#) the TW is applied to a simple system of a driven dissipative quantum harmonic oscillator.

0.2.1 On the importance of dissipation

The interest generated in the field of open quantum systems in the last decades is motivated at least by two reasons. Within this paradigm the fundamental, experimental and technological actors are entangled.

Dissipation as an obstacle. Tackling the dissipative nature of the dynamics of quantum many-body systems is particularly relevant in the experimental area and for the development of quantum technologies. Indeed, in these domains, a major aim consists in creating complex quantum states and controlling them.

It comes as no surprise that the quantum properties of a quantum system can be altered by the dissipation and decoherence induced by the interaction of quantum devices with its surrounding.

It is therefore of paramount importance to achieve better understanding of these destructive processes and develop techniques to protect quantum systems from them ⁵. Note that understanding dissipation is fundamental to reaching the goal of a large-scale quantum computer. Notably, progress has been so significant in this area that Google very recently announced that their quantum computer has achieved “quantum supremacy” [10].

Dissipation as a resource. While the inclusion of a dissipative coupling to an environment often appears to be harmful to the generation and preservation of quantum states, it turns out that non-equilibrium effects can also be used constructively. ⁶

Any cooling procedure, for example, relies on artificially introducing dissipation and transferring the heat of a system into a cold bath, thereby lowering the system’s temperature and entropy. This is common practice in laser cooling of atoms and is of paramount importance in various experimental setups.

Moreover, fundamental theoretical work was performed around the 2000s to utilize dissipation for the preparation and protection of quantum states [11–15]. Building upon this idea, various dissipative processes have been harnessed over the year to create non-classical states [16–24]. Non-classical states of light, such as squeezed and entangled states of light, are valuable resources for both, fundamental and applied research of quantum mechanics. For example they constitute a key ingredient in quantum information sciences, paving the way for more precise quantum metrology, more secure quantum communication, and faster quantum computation[25–27].

The ability to control and protect quantum states also plays a central role for the implementation of quantum computation protocols [28–32].

The so obtained states of matter are stable against perturbations and are therefore candidates for emerging quantum technologies.

⁵This is especially true in the realm of quantum information processing. Indeed, in this field, the study is often initially inferred from the perspective of a closed system for the sake of simplicity, and only after re-examined in an open system situation.

⁶Thermal cycles—where the functioning of a given cycle is enabled by the dissipation induced by the heat baths—are prime examples of such protocols.

0.3 Critical phenomena and phase transitions

The presence of dissipation causes open quantum systems' dynamics to become non-unitary. This leads to an additional layer of complexity and offers novel potentials in comparison to the unitary dynamics of closed systems. In particular, the competition between the different coherent and dissipative processes can lead to quantum phase transitions and the emergence of new phases of matter. This leads to applications spanning from novel paradigms of quantum simulators [33, 34] to the accurate modeling of noise in modern quantum computing platforms [35]. In particular, reservoir engineering [12–14, 23, 36–46] made it possible to realize previously inaccessible quantum phases of matter.

Quantum phase transitions. Phase transitions occur when the physical properties of a system change radically as one varies a parameter. A common example are phase transitions associated with a change in temperature, such as the phase transition between the solid, liquid and gaseous phases of water. In classical thermodynamics, critical phenomena⁷ can be driven by the competition between the energy of the system and the entropy produced by thermal fluctuations [47]. Quantum phase transitions (QPTs) on the other hand are phase transitions that occur at absolute zero temperature. They are a central theme of many-body physics [48]. Quantum critical phenomena⁸ originate from collective behavior of strongly correlated particles. At zero temperature the system is always in its ground state — which by definition is the state with lowest energy — and a QPT results in an brusque change of the ground-state wave function, with different qualitative features. A common example is the Bose-Hubbard model, which describes bosons residing on a lattice with on-site interactions and nearest-neighbour hopping. A quantum phase transition from a strongly localized (Mott insulator) to a delocalized one (superfluid) occurs as the ratio between hopping and interaction is varied. [Chap. IV Sec. 1.1](#) discusses quantum phase transition. While equilibrium quantum phase transitions have historically received a lot of attention, the nonequilibrium scenario generates a whole new set of open questions.

Dissipative phase transitions. In open quantum systems, the competition between Hamiltonian evolution and driving and dissipation processes can engender a non-analytical change in the system's steady state [49]. These critical phenomena emerging in the nonequilibrium steady state of an open quantum system are dubbed as dissipative phase transitions [33, 49–88]. These are discussed in [Chap. IV Sec. 2](#)

⁷The so-called contact process—a toy model for the propagation of an infection—is an (not so random) example. This classical non-equilibrium system exhibit a phase transition in the long-time limit, between a state where the population is healthy and a state where the infection becomes endemic.

⁸The notion of critical phenomena describes the particular behavior of a system which is exactly at, or close to, the phase transition point.

Critical phenomena in driven-dissipative many-body quantum systems have attracted recently a lot of interest [89], propelled by the quest for new classes of phase transitions. Examples of criticality and critical phenomena are e.g. hysteresis [63, 78, 90, 91] and slowing-down [64, 67, 92].

Dissipative time crystals. Dissipative time crystals (DTCs) [93, 94] are a peculiar phase of a driven-dissipative quantum system where the time-translational symmetry of the equation of motion is broken and non-stationary long-lived states spontaneously occur [95]. DTCs will be discussed in more detail in [Chap. IV Sec. 3](#). From a theoretical perspective, they are characterized by the presence of multiple eigenvalues in the Liouvillian spectrum with vanishing real but finite imaginary parts. In [Chap. IV Sec. 5](#) we explore the dynamics of two coupled nonlinear photonic cavities, in the presence of inhomogeneous coherent driving and local dissipations. This section features the results of an article published in *Physical Review A* [1]:

K. Seibold, R. Rota, and V. Savona, *Dissipative time crystal in an asymmetric nonlinear photonic dimer*, [Physical Review A 101, 033839 \(2020\)](#).

We numerically solve the quantum master equation in two different ways —by diagonalizing the Liouvillian superoperator and using the approximated truncated Wigner approach — and show that this system exhibits a dissipative phase transition with the emergence of a time crystalline phase. Moreover, our work investigates the onset of these dynamical instabilities in the framework of dissipative phase transitions, whereby the soliton emerges as a critical phenomenon in the “thermodynamic” limit of large field amplitude.

Dissipative Kerr solitons. When a powerful source of light such as a laser is applied on a material, this can alter its refractive index — a number characterizing how fast light can travel within the material. This non-linear effect is called “Kerr non-linearity”. Kerr frequency combs are systems in which the Kerr non-linearity results in an optical frequency comb, with the initial single-frequency spectrum of the laser converted into a series of discrete, equally spaced frequency lines. If the material is also dispersive, meaning that the speed of light in the medium will depend on the frequency, then the dispersion and non-linearity effects can conspire to give birth to solitons. These dissipative Kerr solitons (DKSs) are wave packets that propagate at constant velocity and which maintain their form.

Optical frequency combs and Kerr frequency combs will be discussed in [Chap. V Sec. 1](#) and [Chap V sec 2](#) respectively, while [Chap. V Sec. 1](#) focuses on the intriguing concept of solitons. Combining our knowledge of open quantum systems, and in particular the study of the Liouvillian gap, together with the truncated Wigner method, we explore in [Chap. IV Sec. 4](#) a simple and solvable system: namely a single Kerr cavity oscillator

subject to single-photon driving and one-photon dissipation. In this minimal model, there exists a first-order driven-dissipative quantum phase transition and hysteresis. We then extend this analysis in [Chap. IV Sec. 4](#) to analyse DKSs in Kerr microring resonator. Up to now, DKS have been investigated according to classical mean-field approach. Here we provide an analysis using an open quantum system approach, in particular using the truncated wigner approximation to include first order quantum fluctuations. This last section reproduces the article submitted to *Physical Review A* [3]:

K. Seibold, R. Rota, F. Minganti, and V. Savona, *Quantum dynamics of dissipative kerr solitons*, [Phys. Rev. A](#) **105**, 053530 (2022).

Description of other quantum states of light. During the journey of my thesis, I got the great chance and pleasure to bring my theoretical knowledge to a project of an experimental group.

Perfectly in phase with the goals of my thesis, this project explores the quantum correlations between photons and phonons modes, theoretically modelled as QHOs. In particular, this work presents techniques for creating, controlling, and measuring vibrational modes in the quantum regime.

This bridge between the theoretical and the experimental world was crowned with 2 published papers; the first one in *Physical Review Letters* [4]:

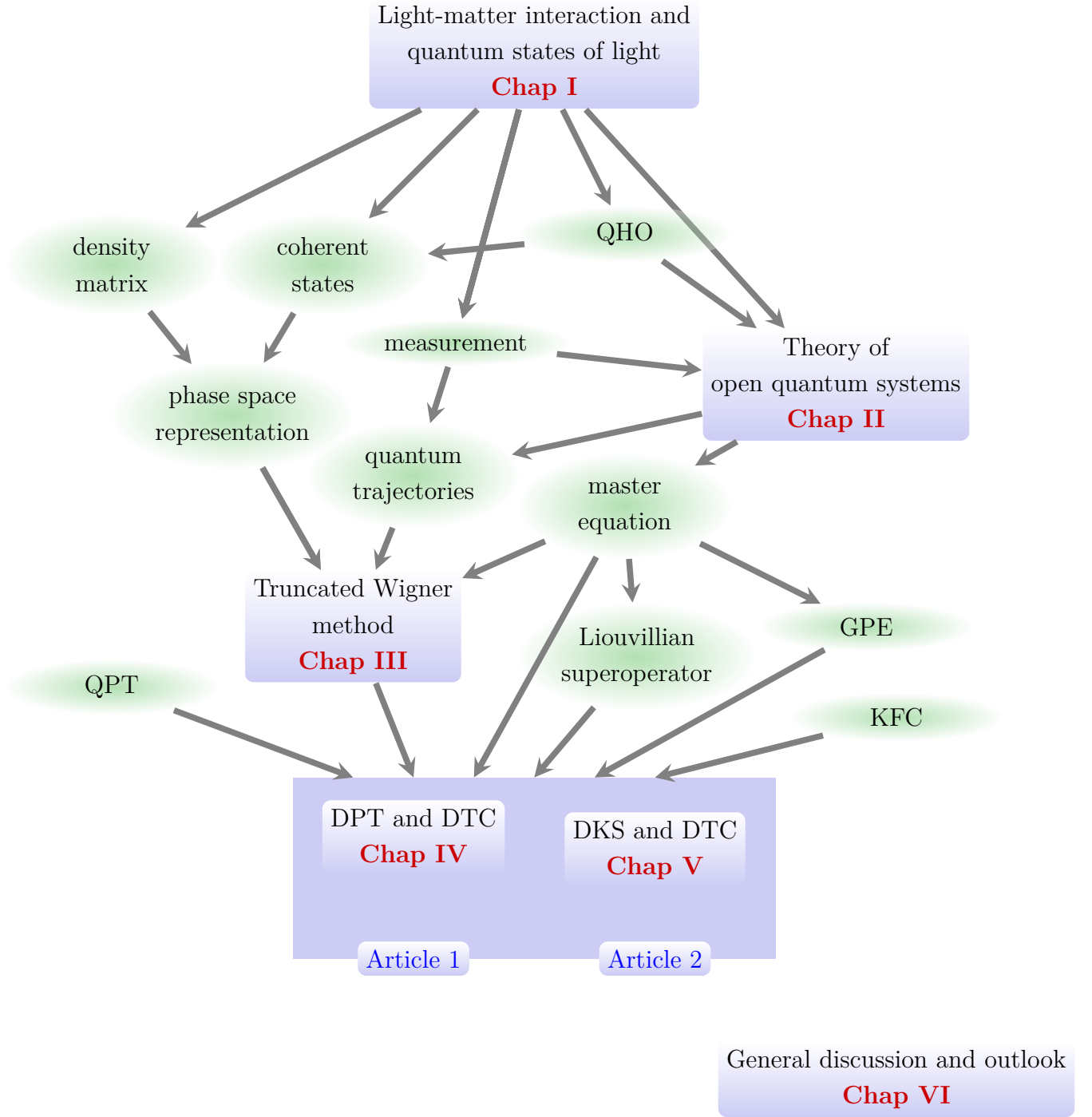
M. D. Anderson et al., *Two-color pump-probe measurement of photonic quantum correlations mediated by a single phonon*, [Physical Review Letters](#) **120**, 233601 (2018)

and the second one in *Physical Review X* [5] :

S. T. Velez et al., *Preparation and decay of a single quantum of vibration at ambient conditions*, [Physical Review X](#) **9**, 041007 (2019).

This very enriching experience allowed me to have an insight into the world of experimental physics. In particular, it is very instructive to handle the vocabulary, jargon, or tools of this other word, and also to realize the constraints of experimental physics, which can be completely different from theory. I am convinced that physics benefits tremendously of such collaborations. I thank Vincenzo Savona and Christophe Galland for having granted me their trust for this collaboration.

Finally, this document closes with a general discussion and outlook in [Chap. VII](#).



Abbreviations:

- QHO: Quantum Harmonic Oscillator
- GPE: Gross–Pitaevskii Equation
- QPT: Quantum Phase Transition
- DPT: Dissipative Phase Transition
- DTC: Dissipative Time Crystal
- DKS: Dissipative Kerr Soliton
- KFC: Kerr Frequency Comb⁹

⁹Nothing to do with chicken.

Chapter 1

Light-matter interaction and quantum states of light

The interaction between light and matter plays a fundamental role in science and technology. The emission and absorption of light by electrons in matter is at the heart of an impressive number of emerging and well-established technologies.

This chapter begins with an overview of some general (and relevant) concepts of quantum physics. We continue with a brief summary of the quantum harmonic oscillator, a headstone at the heart of the quantum description of bosonic fields (the electromagnetic field, mechanical vibrations or environmental degrees of freedom can all be modeled by Harmonic oscillators). This will lead us to the concept of coherent states, an important building block of the Gross–Pitaevskii and Truncated Wigner methods.

We round off this first chapter by giving various paramount examples of experimental platforms.

Contents

1.1 Preliminary background	12
1.1.1 Hilbert space and quantum states	12
1.1.2 Time-evolution	14
1.1.3 Physical observables and measurements	15
1.1.4 Composite systems and entanglement	17
1.2 The quantum harmonic oscillator	18
1.2.1 Quantizing the electromagnetic field	22
1.2.2 Correlation functions	23
1.3 Coherent states	24
1.3.1 Definition	24
1.3.2 Properties	25
1.4 Physical platforms of quantum many-body physics	28
1.4.1 Optical resonators and photonic structures	28
1.4.2 Superconducting architectures	29
1.4.3 Ultracold atoms	30

1.4.4	Quantum optomechanical systems	31
1.4.5	... and a lot of other platforms	32

1.1 Preliminary background

This introductory chapter aims at giving the reader all the tools necessary to grasp and enjoy the discussions presented in this thesis and pinpoint the important aspects connected to our work. We do not go into too much detail as this would be beyond the scope of this document, but all the nitty-gritty details can be found e.g in these resources [96–101] and we also provide abundant bibliographic references in this chapter. We begin this chapter with a lightening review of quantum mechanics, the mathematical model of the physical (quantum) world. In the specific case of closed systems—systems which are perfectly isolated from their environment—this model can be characterized by five axioms [102] that specify the representation of states, observable, measurements, the system dynamics, and the recipe to obtain a composite system.

1.1.1 Hilbert space and quantum states

The *state* of a physical quantum system encodes all the accessible information about the system.

Pure states. The description of a quantum system in terms of pure states is possible provided (a) we have complete knowledge about the system, and (b) there is no entanglement with other systems. A pure state is represented with a normalized state vector in a complex vector space, denoted, for example, as a ket $|\psi\rangle$ in the Dirac formalism [103]¹, and may be seen as a normalized column vector².

For a given physical system, the set of all possible state vectors forms a complex vector space \mathcal{H} , known as the *Hilbert space* (or state space) of the system. Any quantum system is thus characterized by its Hilbert space \mathcal{H} . The latter is equipped with a scalar product that is complete with respect to the norm induced by the scalar product. For what follows, we can assume that this space is of finite size.

To each ket $|\psi\rangle$ belonging to \mathcal{H} , there is a unique associated bra (its adjoint) $\langle\psi|$, belonging to the dual space \mathcal{H}^* .

If a quantum system can be in multiple (pure) states $|\psi_j\rangle$, the *superposition principle*³ stipulates that the superposition of states

$$|\psi\rangle = \sum_j c_j |\psi_j\rangle \quad (1.1)$$

¹The wavefunction is a representation of the state vector in a particular basis, usually the position basis.

²A state vector is defined up to a (physically insignificant) phase: $|\psi\rangle$ and $e^{i\theta}|\psi\rangle$ describe the same state.

³The superposition principle is a cornerstone of the quantum theory and represents a major departure from the classical one [104].

1. Light-matter interaction and quantum states of light

is also a (pure) quantum state, with the coefficients c_j denoting arbitrary complex coefficients.

Beyond the bra-ket notation, states of a system can be expressed in the density matrix (also called density operator⁴) representation [103, 105, 106]⁵. The density matrix⁶ corresponding to the pure state $|\psi\rangle$ is

$$\hat{\rho}_{\text{pure}} := |\psi\rangle\langle\psi|. \quad (1.2)$$

For pure states, the density matrix and the ket description are equivalent⁷. However, this representation becomes essential for describing the most general states, the so-called mixed states. We will now explore the concept behind this terminology.

Mixed states. Sometimes, the knowledge of the state of a quantum system is not maximal. This incomplete information about the physical state of the system requires to introduce the concept of *mixed states* or *mixture*.

The lack of knowledge can either arise from the preparation (subjective lack of knowledge) or from the embedding in a larger Hilbert space (objective lack of knowledge). In the first case the system has been prepared in a completely known (pure) state, but the observer has insufficient information about this state, while in the second case, the system is entangled with one or several other systems.

This is in particular the case for open quantum systems, which will be discussed in more detail in the dedicated [chapter 2](#).

A mixed state implements two probabilistic layers, one coming from the intrinsic probabilistic nature of quantum mechanics (resulting from the probabilistic “collapse” of the state onto an eigenstate of the observable), and the second arising from the classical averaging (resulting from the observer’s lack of knowledge about the (pure) state of the system).

State vectors by themselves are not able to capture the statistical (incoherent) mixtures characterizing the mixed states. For this one needs to introduce the density matrix formalism, which encapsulates both probabilistic layers and thus completely encodes all statistical properties of the system.

For an arbitrary basis $\{|\psi_j\rangle\}_{j=1}^N$ of the Hilbert space, the density matrix in this basis is written as

$$\hat{\rho} = \sum_{i,j=1}^N \rho_{ij} |\psi_i\rangle\langle\psi_j|. \quad (1.3)$$

⁴This (ab)use of notation between the abstract density operator and the corresponding density matrix expressed in some basis is generalized in most of the literature, and will also be used here.

⁵The density-matrix formalism was introduced in 1927 by John von Neumann [107]. The theory of density matrix can be looked up at e.g. [108].

⁶The density matrices describing a system belong to (form) the Hilbert space of that system.

⁷However the density matrix representation gets rid of the global phases : $\hat{\rho}_{\text{pure}} = |\psi\rangle\langle\psi| = (e^{i\theta}|\psi\rangle)(e^{-i\theta}\langle\psi|)$.

⁷To be precise, every quantum mechanical state, even those requiring a density matrix description, can be associated to a (a priori purely algebraic) state description (described with a vector) through the so-called Gelfand–Naimark–Segal (GNS) construction. Nevertheless, this vector representation is often complicated and does not provide any advantage, in contrary of the density-matrix formalism.

The (real, non-negative) diagonal elements $\rho_{ii} \in \mathbb{R}_0^+$ are called populations. They quantify the probability of the quantum system to be in state $|\psi_j\rangle$, and verify $\sum_i \rho_{ii} = 1$ (the density matrix has a unit trace, all probabilities add up to one).

The (complex valued) off-diagonal elements $\rho_{ij} \in \mathbb{C}$ are called coherences, they characterize the superposition between state $|\psi_i\rangle$ and $|\psi_j\rangle$, and verify $\rho_{ij} = \rho_{ji}^*$ (the density matrix is Hermitian). Note that the density matrix is dependent on the choice of basis vectors.

Properties of the density matrix. The density matrix is a positive semi-defined hermitian operator on a Hilbert space⁸ with a unit-trace [105]. The Hermiticity and non negativity conditions ensure respectively real and not negative eigenvalues, and the unit-trace imposes eigenvalues summing to one.

Since the density matrix is Hermitian, it can always be diagonalised in an orthogonal eigenstate basis $(|\varphi_j\rangle)_{j=1}^N$ of \mathcal{H} ,

$$\hat{\rho} = \sum_{i=1}^N p_i |\varphi_i\rangle \langle \varphi_i|, \quad (1.4)$$

where $0 \leq p_i \leq 1$ and $\sum_i p_i = 1$.

From this point of view, the density matrix can be interpreted as an incoherent statistical mixture (superposition) of pure states $\{p_i, |\varphi_i\rangle\}$; “incoherent” means that the relative phases of the $|\varphi_j\rangle$ ’s are experimentally inaccessible [109].

This representation is not unique as it was for pure states.

Purity. The quantity $\text{Tr}(\hat{\rho}^2)$ is called the purity and it is a good measure of the mixedness of a density matrix.

For a Hilbert space of dimension N , the purity takes values between $1/N$ and 1, corresponding respectively to the values of a maximally mixed state and pure state⁹. Mixed states verify $1/N \leq \text{Tr}(\hat{\rho}_{mix}^2) < 1$.

Entropy. Another useful measure for the heterogeneity of a quantum system is the von Neumann entropy, a quantum extension of the Shannon entropy, which measures how much is missing from the maximal information. It is defined as

$$S(\hat{\rho}) \equiv -\text{Tr}(\hat{\rho} \log \hat{\rho}) = -\sum_i p_i \log p_i,$$

where the p_i are the eigenvalues of $\hat{\rho}$. The von Neumann entropy takes values between 0 and $\log N$, corresponding respectively to the values of a pure state and a maximally mixed state.

1.1.2 Time-evolution

On the one hand, the time-evolution of a state vector $|\psi(t)\rangle$ is given by the Schrödinger equation

$$i\hbar \frac{d}{dt} |\psi(t)\rangle = \hat{H}(t) |\psi(t)\rangle,$$

⁸An operator is said to be positive-semidefinite (or non-negative) if it is an Hermitian operator with nonnegative eigenvalues (due to hermicity, the eigenvalues are necessarily real).

⁹Since $\hat{\rho}_{pure}$ is an idempotent operator, $\text{Tr}(\hat{\rho}_{pure}^2) = \text{Tr}(\hat{\rho}_{pure}) = 1$.

1. Light-matter interaction and quantum states of light

where $\hat{H}(t)$ denotes the Hamiltonian of the system.

On the other hand, the time evolution of the density matrix is governed by the Von Neumann-equation^{10,11}

$$i\hbar \frac{\partial}{\partial t} \hat{\rho}(t) = [\hat{H}(t), \hat{\rho}(t)], \quad (1.5)$$

where $[A, B] = \hat{A}\hat{B} - \hat{B}\hat{A}$ denotes the commutator of the operators \hat{A} and \hat{B} .

1.1.3 Physical observables and measurements

1.1.3.1 Observable

Consider an experimentally measurable quantity \mathcal{A} (for instance, this could be position, momentum, spin or energy) of a quantum system described by a Hilbert space \mathcal{H} . The *observable* \hat{A} associated to the quantity \mathcal{A} is a Hermitian operator on \mathcal{H} , i.e. an operator satisfying $\hat{A}^\dagger = \hat{A}$, where the “dagger” \dagger operation denotes the complex conjugate transpose. The expectation value of the observable \hat{A} for a given state $\hat{\rho}$ is

$$\langle \hat{A} \rangle = \text{Tr}(\hat{\rho}\hat{A}). \quad (1.6)$$

Spectral representation Since an observable \hat{A} is a Hermitian operator, it can be diagonalized. The (real) eigenvalues^{12,13} a_j are the only possible outcomes of a (idealized projective) measurement of \hat{A} . The (normalized) eigenstates $|a_j\rangle$ associated to the a_j ’s¹⁴ form a complete orthonormal basis¹⁵ in \mathcal{H} , and thus \hat{A} has the spectral decomposition

$$\hat{A} = \sum a_j \hat{\Pi}_j \quad (1.7)$$

with $\hat{\Pi}_j = |a_j\rangle\langle a_j|$, the projector operator relative to the eigenvector $|a_j\rangle$. This spectral representation generates a projection-valued measure (PVM).

1.1.3.2 Standard measurement

A measurement is a process in which an observer acquires information about the state of a physical system. The information encapsulated in the density matrix does not imply a deterministic, but rather a statistical prediction of the outcome of the measurement, leading to an intrinsic randomness of the measurement process. In the case of projective measurements (also called von Neumann measurements, projection-valued measures or PVMs), the probability to find the eigenvalue a_j of \hat{A} in outcome is given by

¹⁰This equation can be derived from the Schrödinger equation.

¹¹The Von Neumann equations are analogous to the Liouville equation in classical statistical mechanics (See Dirac rule [110, 111]).

¹²Or rigorously the spectral values, if we also include Hilbert spaces of infinite dimension.

¹³The eigenvalues of an Hermitian operator are real. This is a desirable feature if one wants to interpret the eigenvalues of observables as measurement outcomes.

¹⁴ $\hat{A}|a_j\rangle = a_j|a_j\rangle$

¹⁵The eigenstates verify the orthogonality relation $\langle a_i|a_j\rangle = \delta_{ij}$ and the completeness relation $\sum_j |a_j\rangle\langle a_j| = \mathbb{1}$.

$$p_j = \langle \hat{\Pi}_j \rangle = \text{Tr}(\hat{\rho} \hat{\Pi}_j) \quad ^{16} \quad (1.8)$$

and the measurement of the observable \hat{A} projects the system into the eigenstate $|a_j\rangle$ associated to the eigenvalue a_j .

The expected value of the measurement is given by the observable

$$\langle \hat{A} \rangle = \text{Tr}(\hat{A} \hat{\rho}) = \sum_j a_j p_j \quad ^{17}. \quad (1.9)$$

The concept of projective measurement is insufficient. In reality, the experimenter never directly measures the system, but rather the effect of the system on its environment¹⁸.

In the same spirit of the density operators which generalize the ket states description, projective measurements can be generalized to the so-called generalized measurements or positive operator-valued measurements (POVMs).

1.1.3.3 Generalized Measurements (POVMs)

The generalized measurement, or positive operator-valued measurement (POVM), of a system, is described by a set of *measurement operators* $\{M_j\}$ that act in the Hilbert space of the system. The index j refers to the possible outcomes of the measurement. The M_j are positive operators (not necessarily projectors). Thus, they constitute a non-orthogonal decomposition of the identity operator¹⁹.

If a quantum system is in a state ρ just before the measurement, then the outcome of the measurement is j with an a priori probability

$$p_j = \langle E_j \rangle = \text{Tr}\{\rho E_j\} \quad (1.10)$$

where the $E_j = M_j^\dagger M_j$ ²⁰ do not need to be projectors, but must be positive (to guarantee that p_j is always positive) and must satisfy the completeness equation²¹ $\sum_j E_j = \mathbb{1}$. Right after the measurement with outcome j , the (normalized) state of the system is [97]

$$\rho_j = \frac{M_j \rho M_j^\dagger}{p_j} \quad (1.11)$$

¹⁶Since the $|a_j\rangle$'s come from a complete set of orthonormal states, then the completeness relation $\sum_j \Pi_j = \mathbb{1}$ ensures that $\sum_j p_j = 1$, phew!

¹⁷ $\langle \hat{A} \rangle$ is a prediction of the average value of repeated measurements, whereas $A|a_j\rangle = a_j|a_j\rangle$ is the value of 1 (just 1) single measurement.

¹⁸For example, if an experimenter observes the spontaneous emission from an atom, they measure the radiation emitted (effect of the system on the environment) by the atom (the system) as a result of its interaction with the ambient electromagnetic field (the environment). However, the experimenter does not directly observe the emitted radiation.

¹⁹Note that if the M_j 's are taken to be a complete set of orthonormal projection operators i.e. $M_j = |j\rangle\langle j|$, leading to $E_j = |j\rangle\langle j|$, we recover the usual projective measurement.

²⁰Note that while the M_i determine the E_i , the other way around is not true ($(M_i^\dagger U^\dagger)(U M_i) = M_i^\dagger M_i$).

²¹Which translates to probabilities summing to 1.

1. Light-matter interaction and quantum states of light

It is important to note that, unless $\hat{\rho}$ is an eigenvector of the observable \hat{A} , a finite uncertainty —the variance $\Delta\hat{A} = \sqrt{\langle\hat{A}^2\rangle - \langle\hat{A}\rangle^2}$ — remains. This directly relates to the Heisenberg uncertainty relation.

Heisenberg uncertainty relation. Given two symmetric operators \hat{A} and \hat{B} satisfying $[\hat{A}, \hat{B}] = \hat{C}$, the (Robertson–Schrödinger) uncertainty relation states that²²

$$\Delta A \Delta B \geq \frac{1}{2} |\langle\hat{C}\rangle| \quad (1.12)$$

The Heisenberg uncertainty principle follows and reads²³

$$\Delta x \Delta p \geq \frac{\hbar}{2}. \quad (1.13)$$

States that satisfy the Heisenberg uncertainty principle with equality are called minimum uncertainty states. As we will see hereafter, the ground state of the harmonic oscillator and coherent states satisfy the minimum uncertainty relation. Quantum fluctuations stem from the uncertainty principle²⁴.

1.1.4 Composite systems and entanglement

Consider now two distinct quantum systems A and B with associated Hilbert space \mathcal{H}_A and \mathcal{H}_B respectively²⁵. We also denote by $\{|a_i\rangle\}$ and $\{|b_i\rangle\}$ the orthonormal basis in each subspace.

Compose. The Hilbert space of the composite system $\{A, B\}$ is given by the tensor product $\mathcal{H}_{AB} = \mathcal{H}_A \otimes \mathcal{H}_B$. We have $\dim(\mathcal{H}_{AB}) = \dim(\mathcal{H}_A) \times \dim(\mathcal{H}_B)$, expressing the exponential complexity when interconnecting several quantum systems.

The tensor product construction applies for Hilbert spaces, vectors, and operators. For instance, if system A is prepared in the state ρ_A and system B is prepared in the state ρ_B , then the composite system's state is the product $\rho_{AB} = \rho_A \otimes \rho_B$.

Reduce. The partial trace operation allows to obtain the state of system A when considered alone, given by its reduced density operator

$$\hat{\rho}_A = \text{Tr}_B(\hat{\rho}_{AB}) = \sum_j \langle b_j | \hat{\rho}_{AB} | b_j \rangle. \quad (1.14)$$

²²The uncertainty in operators is defined as the standard deviation $\Delta A = \sqrt{\langle A^2 \rangle - \langle A \rangle^2}$.

²³While the version of the Heisenberg uncertainty principle for the position-momentum variables is the one always present in the textbooks, this principle also applies to all canonical pairs, such as phase and action, or time and energy.

²⁴Quantum fluctuations play a critical role in various physical phenomena. E.g. the inhomogeneity in the structure of the Universe in the temperature fluctuations of the cosmic microwave background [112].

²⁵A bipartite system is used in this discussion for the sake of simplicity. It is straightforward to generalize to a multipartite system.

Starting from a bipartite system in a pure state (complete knowledge), we end up with a mixed state (limited knowledge) by tracing out one subsystem²⁶.

Separability. The density operator ρ_{AB} of the composite system $\{A, B\}$ is separable if it can be expressed as a convex combination of product states

$$\hat{\rho}_{AB} = \sum_j p_j \hat{\rho}_{jA} \otimes \hat{\rho}_{jB}$$

for some set of density operators $\{\hat{\rho}_{jA}\}$ on \mathcal{H}_A and similarly for B , with $p_j \geq 0$ and $\sum_j p_j = 1$.

Quantum Entanglement. A state that is not separable is called *entangled state*. [113]²⁷.

Entangled states are characterized by the existence of quantum correlations between the subsystems and are considered to be the most non-classical manifestations of quantum physics. It is crucial to point out the fundamental difference between quantum correlations (i.e. entanglements) and classical correlations. They lead to new and puzzling phenomena, allowing e.g. quantum teleportation [114]. For this reason, entangled states have attracted a lot of attention both from experimental and theoretical point of view.

For more details on entanglement, see e.g. [113] for a complete review, or [115] discussing more general types of quantum correlations.

1.2 The quantum harmonic oscillator

In this part, we address the main aspects of the one-dimensional quantum harmonic oscillator. The model of the quantum harmonic oscillator is built in complete analogy with the model of a classical harmonic oscillator. It models the behavior of a plethora of physical systems, including the electromagnetic field or the vibrational modes in a molecule. The reason for this ubiquity is that any smooth potential can usually be approximated by a harmonic potential close to a stable equilibrium point²⁸.

In particular, the quantum harmonic oscillator also plays a central role in open quantum systems, since for instance the environment of a quantum system subject to relaxation processes can be modeled with an infinite set of quantum oscillators weakly coupled with the system of interest.

We will now review some simple aspects of the harmonic oscillator and we refer to [102, 116] for more detailed discussions.

The classical harmonic oscillator. Let us recall the good ol' times of classical mechanics lectures and write the Hamiltonian describing a classical one-dimensional harmonic oscillator with angular oscillation frequency ω and mass m [117, 118]

²⁶And the other way around, the so-called purification procedure turns a mixed state into a pure one, but living in a higher dimensional Hilbert space

²⁷Verschränkung in German.

²⁸“The career of a young theoretical physicist consists of treating the harmonic oscillator in ever-increasing levels of abstraction” —Sidney Coleman.

1. Light-matter interaction and quantum states of light

$$H = \frac{p^2}{2m} + \frac{1}{2}m\omega^2 x^2, \quad (1.15)$$

where we use the dynamical variables $\{x, p\}$ for position and conjugate momentum.

Phase space. Using the conjugate variables x and p , we can define

$$\alpha = \sqrt{\frac{m\omega}{2}} \left(x + \frac{i}{m\omega} p \right). \quad (1.16)$$

In the complex phase space plane (α, α^*) , the oscillator traces out a circle (with $\alpha_0 = \alpha(t = 0)$)

$$\alpha(t) = \alpha_0 e^{-i\omega t}. \quad (1.17)$$

The time evolution of the variables x and p can be recovered from (1.17) and we have

$$\begin{cases} x(t) = \frac{1}{\sqrt{2m\omega}} (\alpha(t) + \alpha^*(t)) = \sqrt{\frac{2}{m\omega}} \operatorname{Re}[\alpha(t)] \\ p(t) = -i\sqrt{\frac{m\omega}{2}} (\alpha(t) - \alpha^*(t)) = \sqrt{2m\omega} \operatorname{Im}[\alpha(t)]. \end{cases} \quad (1.18a)$$

$$(1.18b)$$

The energy of the system is given by

$$H(t) = \omega |\alpha_0|^2. \quad (1.19)$$

An established classic among the classics. We shall now consider the quantum harmonic oscillator.

One-dimensional quantum harmonic oscillator. Moving to the quantum mechanical description, the canonical variables x and p for the classical system are upgraded to their operator equivalents \hat{x} and \hat{p} .

In complete analogy to the classical case, the Hamiltonian of the quantum harmonic oscillator reads

$$\hat{H} = \frac{\hat{p}^2}{2m} + \frac{1}{2}m\omega^2 \hat{x}^2. \quad (1.20)$$

The conjugate variables of position and momentum satisfy the canonical commutation relation

$$[\hat{x}, \hat{p}] = i\hbar \mathbb{1}, \quad (1.21)$$

with the reduced Planck constant \hbar .

To solve this model, and in analogy with (1.16), we introduce the so-called creation and annihilation operators²⁹, respectively \hat{a}^\dagger and \hat{a}

$$\hat{a} = \sqrt{\frac{m\omega}{2\hbar}} \left(\hat{x} + \frac{i}{m\omega} \hat{p} \right), \quad (1.22a)$$

$$\hat{a}^\dagger = \sqrt{\frac{m\omega}{2\hbar}} \left(\hat{x} - \frac{i}{m\omega} \hat{p} \right). \quad (1.22b)$$

²⁹These operators are also called ladder operators. They were introduced by Paul Dirac.

These operators verify the commutation relation

$$[\hat{a}, \hat{a}^\dagger] = \mathbb{1}, \quad (1.23)$$

and provide the useful expression for the conjugate position and momentum operators³⁰

$$\begin{aligned} \hat{x} &= \sqrt{\frac{\hbar}{2m\omega}} (\hat{a}^\dagger + \hat{a}), \\ \hat{p} &= i\sqrt{\frac{\hbar m\omega}{2}} (\hat{a}^\dagger - \hat{a}). \end{aligned} \quad (1.24)$$

The Hamiltonian of the harmonic oscillator in terms of the ladder operators reads

$$\hat{H} = \hbar\omega \left(\hat{a}^\dagger \hat{a} + \frac{1}{2} \right). \quad (1.25)$$

The constant term $\hbar\omega/2$ in the Hamiltonian represents the vacuum fluctuation energy³¹. We can define the *number operator* $\hat{N} = \hat{a}^\dagger \hat{a}$, whose eigenstates are also the eigenstates of \hat{H} . Thus, solving the Harmonic oscillator problem is equivalent to finding the eigenvalues of \hat{N} . For this later, we have the eigenvalue equation $\hat{N}|n\rangle = n|n\rangle$, where n is the eigenvalue associated to the eigenvector $|n\rangle$ of \hat{N} . The ket $|n\rangle$ is called *number states* or *Fock states*.

The operator \hat{N} is Hermitian, thus its eigenvalues n are real and its eigenvectors $|n\rangle$ form a complete set of orthogonal states. Hence, we have the closure relation $\sum_{n=0}^{\infty} |n\rangle\langle n| = \mathbb{1}$, where $\mathbb{1}$ is the identity operator in the Hilbert space of the single-mode system.

The spectrum of the HO Hamiltonian is

$$E_n = \hbar\omega \left(n + \frac{1}{2} \right), \quad (1.26)$$

and is illustrated in Fig. 1.1.

It is the energy of n quanta $\hbar\omega$ and can correspond to phonons or photons.

The allowed energy-levels of the quantum harmonic oscillator are discrete and equidistant, of value $\hbar\omega$. In particular, the ground state of the QHO $|0\rangle$ has energy $E_0 = \hbar\omega/2$. This means that, unlike a classical oscillator, a quantum oscillator is never at rest and undergoes quantum fluctuations. The wave-function of the ground state of the Ho is given by $\varphi_0(x) = \sqrt{\text{centered normal distribution with standard deviation } \Delta x}$.

The action of the ladder operators on the energy eigenstates $|n\rangle$ gives

$$\begin{aligned} \hat{a}^\dagger |n\rangle &= \sqrt{n+1} |n+1\rangle \\ \hat{a} |n\rangle &= \sqrt{n} |n-1\rangle \quad \text{with} \quad \hat{a}|0\rangle = 0. \end{aligned} \quad (1.27)$$

All Fock states can be expressed in terms of the ground state $|0\rangle$ by repeated action of the creation operator:

³⁰Bear in mind that the operator \hat{x} and \hat{p} are Hermitian while the operator \hat{a} is not.

³¹While this term can be canceled by redefining the energy origin, it can have drastic influence on the system.

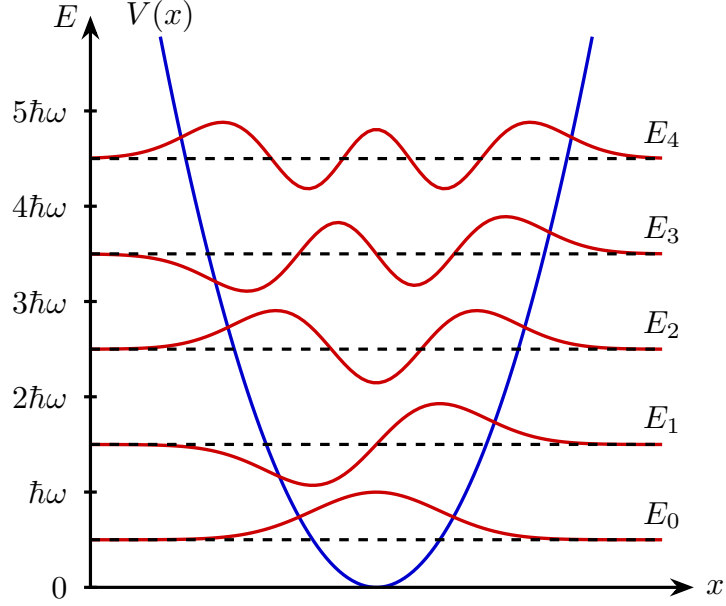


Figure 1.1: Energy level diagram of the canonical quantum harmonic oscillator. The ground state energy is $E_0 = \hbar\omega/2$, and the energy levels form an equidistant ladder with spacing $\hbar\omega$.

$$|n\rangle = \frac{(a^\dagger)^n}{\sqrt{n!}}|0\rangle. \quad (1.28)$$

We can point out that the Hilbert space dimension of a HO is unbounded.

Time evolution. In analogy to the Hamilton equation, the dynamics of the quantum operators is given by the Heisenberg equation

$$\frac{d\hat{O}}{dt} = \frac{1}{i\hbar}[\hat{H}, \hat{O}] \quad (1.29)$$

From the Heisenberg point of view, all oscillator states become stationary and the operators evolve in time. The dynamical equation for the annihilation operator is ³²

$$\frac{d\hat{a}}{dt} = \frac{1}{i\hbar}[\hat{a}, H] = -i\omega\hat{a}. \quad (1.30)$$

which has the solution

$$\hat{a}(t) = \hat{a}(0)e^{-i\omega t}. \quad (1.31)$$

³²In what follows, we use systematically a tilde to denote the operators or state vectors in an interaction representation with respect to a part or to the totality of the system's Hamiltonian. This convention applies to the Heisenberg point of view, which corresponds to the interaction representation with respect to the total Hamiltonian.

1.2.1 Quantizing the electromagnetic field

Maxwell's equations³³ describe electricity and magnetism in terms of the electric and magnetic fields.

We show here that a quantum approach to the electromagnetic field leads to its description in terms of the quantum harmonic oscillator.

This enables the description of a single photon, and the emission and absorption of photons is described via the creation and annihilation operators.

This quantization drove to the description of stimulated and spontaneous emissions (and absorptions) of photons, leading to the study of Lasers, LEDs and photodiodes.

Wave equations resulting from Maxwell equations. Combining the Maxwell equations in vacuum leads to the wave equations for the electric field \mathbf{E} and magnetic field \mathbf{B} ,

$$\nabla^2 E - \frac{1}{c^2} \frac{\partial^2 E}{\partial t^2} = 0, \quad \nabla^2 B - \frac{1}{c^2} \frac{\partial^2 B}{\partial t^2} = 0, \quad (1.32)$$

with c the speed of light.

By considering an electromagnetic field in a finite empty (no charges or currents) cavity of dimension $L \times L \times L$, and fixing periodic boundary conditions, the general solution of these two wave equations consists in a sum of normal modes, each normal being equivalent to a (classical) harmonic oscillator [109]. Hence, the electric (or magnetic) field is equivalent to an infinite collection of independent harmonic oscillators.

The modes are labeled by the wave-vector $\mathbf{k}_n = 2\pi/L(n_x, n_y, n_z)$, with $n_\alpha \in \mathbb{N}$. The dispersion relation is (in free space) $\omega_n = c\sqrt{k_{n,x}^2 + k_{n,y}^2 + k_{n,z}^2}$, and the associated polarization vector of the light mode contained in the unit vector $\boldsymbol{\epsilon}_n$ verifying $\boldsymbol{\epsilon}_n \cdot \mathbf{k}_n = 0$. The quantization leads to the following expressions for the electric field \mathbf{E} and magnetic field \mathbf{B}

$$\begin{aligned} \mathbf{E}(\mathbf{r}, t) &= -i \sum_n \sqrt{\frac{\hbar \omega_n}{2\epsilon_0 V}} (\hat{a}_n e^{-i\omega_n t + i\mathbf{k}_n \cdot \mathbf{r}} - c.c.) \boldsymbol{\epsilon}_n \\ \mathbf{B}(\mathbf{r}, t) &= \frac{1}{c} \sum_n \sqrt{\frac{\hbar \omega_n}{2\epsilon_0 V}} (\hat{a}_n e^{-i\omega_n t + i\mathbf{k}_n \cdot \mathbf{r}} + c.c.) \mathbf{k}_n \times \boldsymbol{\epsilon}_n \end{aligned} \quad (1.33)$$

where $V = L_x L_y L_z$ is the volume of the cavity³⁴.

The electric and magnetic fields represent the two quadratures of the electromagnetic field in analogy of the position x_n and momentum p_n of an ensemble of quantum harmonic oscillators.

The creation (annihilation) operator produces (destroys) an excitation of a given plane wave mode and verify $[\hat{a}_n, \hat{a}_{n'}^\dagger] = \delta_{nn'}$.

³³In classical electrodynamics, a free electromagnetic field (in vacuum) satisfies the source-free Maxwell's equations

$$\begin{aligned} \nabla \cdot \mathbf{E} &= 0 & \nabla \times \mathbf{E} &= -\partial_t \mathbf{B} \\ \nabla \cdot \mathbf{B} &= 0 & \nabla \times \mathbf{B} &= \frac{1}{c} \partial_t \mathbf{E} \end{aligned}$$

with the speed of light $c = 1/\sqrt{\epsilon_0 \mu_0}$.

³⁴The quantity $\sqrt{\frac{\hbar \omega_n}{2\epsilon_0 V}}$ corresponds to the electric field per photon

1. Light-matter interaction and quantum states of light

Thus, the Hamiltonian of the quantized free electromagnetic field is

$$H_{EM} = \frac{1}{2} \int_V d\mathbf{r} \left(\varepsilon_0 \hat{\mathbf{E}}^2(\mathbf{r}) + \frac{1}{\mu} \hat{\mathbf{B}}^2(\mathbf{r}) \right) = \sum_{\mathbf{k}} \hbar \omega_k \left(a_{\mathbf{k}}^\dagger a_{\mathbf{k}} + \frac{1}{2} \right). \quad (1.34)$$

Zero-Point Energy and the Casimir Force Let's point out that the lowest energy of a HO is $\hbar\omega/2$, and corresponds to the zero-point energy. Since Eq. (1.34) accounts for an infinite number of modes in a finite volume V , it follows that there is an infinite amount of energy present in any finite volume of space. This can lead to some interesting effects such as the vacuum-induced Casimir force [119, 120].

1.2.2 Correlation functions

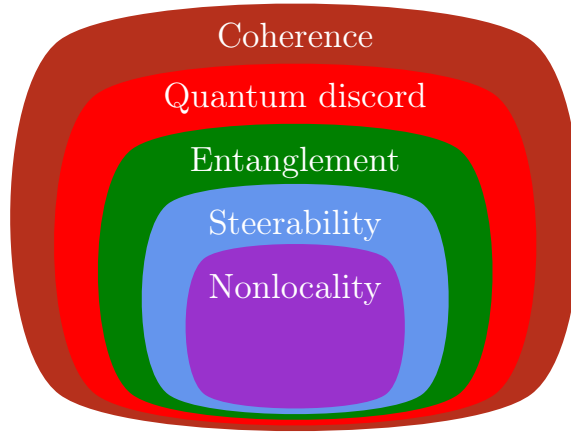


Figure 1.2: Hierarchical structure among the various quantum correlations: quantum coherence \supseteq (is the superset of) quantum discord \supseteq quantum entanglement \supseteq quantum steering \supseteq Bell non-locality.

The superposition principle of quantum states (Eq.(1.1)) which is at the heart of quantum mechanics leads to the concept of quantum coherence [104, 121–123]. Not only can quantum coherence even arise in monopartite systems, but it can also encompass all different flavor of quantum correlations, see Fig. 1.2. Therefore, it goes without saying that this feature is an important resource in diverse quantum technologies including design of strongly correlated photons [124, 125] and new light sources [126], quantum metrology [127, 128], quantum computing [129], quantum simulation [130] and quantum cryptography [131].

In this context, the coherence properties of a quantum state and in particular the non-classical nature of light can be characterized via *correlation functions* [132–138]. A highly valuable correlation function is the normalized second order coherence function that describes intensity correlations and reads

$$g^{(2)}(\tau) = \frac{\langle : \hat{I}(t) \hat{I}(t + \tau) : \rangle}{\langle : \hat{I}(t) : \rangle^2} = \frac{\langle \hat{a}^\dagger(t) \hat{a}^\dagger(t + \tau) \hat{a}(t + \tau) \hat{a}(t) \rangle}{\langle \hat{a}^\dagger(t) \hat{a}(t) \rangle^2} \quad (1.35)$$

where \hat{I} is the measured instantaneous intensity, and the colon “:” denotes normal ordering³⁶.

The zero-delay second-order correlation function gives the field statistic, while the derivative of the time-delayed correlation function characterises the arrival time distribution [139]³⁷.

The condition $g^{(2)}(0) > 1$ corresponds to a super-Poissonian statistics and $g^{(2)}(\tau) < g^{(2)}(0)$ indicates photon bunching. In these two cases, the field is of classical nature. The condition $g^{(2)}(0) = 1$ corresponds to a Poissonian statistics and $g^{(2)}(\tau) = g^{(2)}(0) \forall \tau$ indicates a coherent field.

Finally, the condition $g^{(2)}(0) < 1$ corresponds to a sub-Poisson statistics and $g^{(2)}(\tau) > g^{(2)}(0)$ indicates photon antibunching. In the two later cases, the field is purely quantum and has no classical counterpart.

Two particular cases are squeezed light, that verifies $g^{(2)}(0) < 1$, and $g^{(2)}(0) = 2$, which corresponds to a thermal field.

The first order and cross correlation function are other useful correlation functions. A particularly adequate method for studying the photon statistics is the quantum jump approach (see next chapter).

1.3 Coherent states

In quantum optics, a coherent state [98, 136, 141–145]³⁸ refers to the specific state of the quantum harmonic oscillator whose dynamics is closest to that of a classical harmonic oscillator, and shows maximal coherence³⁹.

Coherent states are important since they describe the quantum state of a laser, superfluids and super-conductors. In this section, we present the concept of coherent states, which is the basis of the truncated Wigner method, used in the simulation of the works presented in this thesis, and presented in chapter 3.

1.3.1 Definition

The state of a classical harmonic oscillator can be described by using the continuous variables x and p and is represented in phase space by the complex variable $x + ip$. The quantum counterpart is given by the concept of *coherent state* α with $\alpha = \text{Re}(\alpha) + i\text{Im}(\alpha) \in \mathbb{C}$.

A coherent state $|\alpha\rangle$ is defined as the (unique) eigenstate of the annihilation operator \hat{a} with corresponding (complex) eigenvalue α :

$$\hat{a}|\alpha\rangle = \alpha|\alpha\rangle. \quad (1.36)$$

³⁵The second-order correlation function can be experimentally measured with using a Hanbury-Brown-Twiss (HBT) setup.

³⁶Normal ordering consists in putting the hermitian conjugate operators on the left

³⁷The precise correspondence between (anti)bunching and the $g^{(2)}(\tau)$ (see hereafter) needs special care in the definitions [137, 139, 140]

³⁸Or sometimes called Glauber Coherent States, or displaced ground states. They were introduced by Schrödinger and reintroduced by Glauber.

³⁹These states are not more “coherent” than other pure states, but they efficiently maintain their coherence in the presence of dissipation.

1. Light-matter interaction and quantum states of light

Since \hat{a} is not hermitian, α is, in general, a complex number⁴⁰.

1.3.2 Properties

Decomposition in the Fock basis. Because the Fock states are a complete orthonormal system of vectors (see [section 1.2](#)), a coherent state can be expanded in terms of Fock states as

$$|\alpha\rangle = e^{-\frac{|\alpha|^2}{2}} \sum_{n=0}^{\infty} \frac{\alpha^n}{\sqrt{n!}} |n\rangle = e^{-\frac{|\alpha|^2}{2}} \sum_{n=0}^{\infty} \frac{\alpha^n (\hat{a}^\dagger)^n}{\sqrt{n!}} |0\rangle = e^{-\frac{|\alpha|^2}{2}} \exp(\alpha \hat{a}^\dagger) |0\rangle. \quad (1.37)$$

We can see from this expression that the distribution along the Fock states follows a Poissonian distribution. The Fock state occupation probability amplitudes $p_\alpha(n) = |c_n|^2$ follow a Poisson distribution of mean α , leading to an average phonon number $\bar{n} = |\alpha|^2$ and variance $\sqrt{\bar{n}}$ (see [Fig. 1.3](#)).

Displacement operator. Coherent states can be viewed as displaced vacuum states in phase space,

$$|\alpha\rangle = \hat{D}(\alpha)|0\rangle \quad (1.38)$$

with the displacement operator⁴¹

$$\hat{D}(\alpha) = e^{\alpha \hat{a}^\dagger - \alpha^* \hat{a}} \quad (1.39)$$

which satisfies

$$\hat{D}^{-1}(\alpha) = \hat{D}^\dagger(\alpha) = \hat{D}(-\alpha). \quad (1.40)$$

Time evolution The time evolution of the coherent state $|\alpha\rangle$ can be inferred from [Eq. \(1.31\)](#) and reads

$$\alpha(t) = \alpha_0 e^{-i\omega t}. \quad (1.41)$$

Thus coherent states remain coherent states during their time evolution and evolve as a classical particle (this equation is identical to the one found for the classical HO in [Eq. \(1.17\)](#)).

Expectation values The expectation values of \hat{x} and \hat{p} correspond to the classical variables [\(1.18\)](#) with $\hbar = 1$

$$\begin{cases} \langle \alpha | \hat{x} | \alpha \rangle = \sqrt{\frac{\hbar}{2m\omega}} (\alpha + \alpha^*) = \sqrt{\frac{2\hbar}{m\omega}} \text{Re}(\alpha) \\ \langle \alpha | \hat{p} | \alpha \rangle = -i\sqrt{\frac{\hbar m\omega}{2}} (\alpha - \alpha^*) = \sqrt{2\hbar m\omega} \text{Im}(\alpha) \end{cases} \quad (1.42a)$$

$$\begin{cases} \langle \alpha | \hat{x} | \alpha \rangle = \sqrt{\frac{\hbar}{2m\omega}} (\alpha + \alpha^*) = \sqrt{\frac{2\hbar}{m\omega}} \text{Re}(\alpha) \\ \langle \alpha | \hat{p} | \alpha \rangle = -i\sqrt{\frac{\hbar m\omega}{2}} (\alpha - \alpha^*) = \sqrt{2\hbar m\omega} \text{Im}(\alpha) \end{cases} \quad (1.42b)$$

⁴⁰Applying the creation operator on the coherent state leads to a more complicated result: $\hat{a}^\dagger |\alpha\rangle = (\partial_\alpha + \alpha^*) |\alpha\rangle$

⁴¹As its name suggests, the displacement operator displaces the state to which it is applied.

The probability density of a general coherent state $|\alpha\rangle$ is a Gaussian distribution with constant width, whose centroid oscillates in a harmonic oscillator potential⁴², with frequency ω of the HO, and amplitude $\sqrt{2}x_0|\alpha|$ in position and $\sqrt{2}\hbar|\alpha|/x_0$ in momentum ($x_0 = \sqrt{\frac{\hbar}{m\omega}}$).

The coherent state wave-function is the ground state wave-function shifted in momentum and position. It corresponds to a minimal-uncertainty wave-packet. Thus, coherent states correspond to the closest analogue to the free classical single mode field.

The transition from quantum to classical HO can be seen in the limit of large n as the index of dispersion $\sqrt{\bar{n}}/\bar{n}$ tends to 0, leading to a localized distribution.

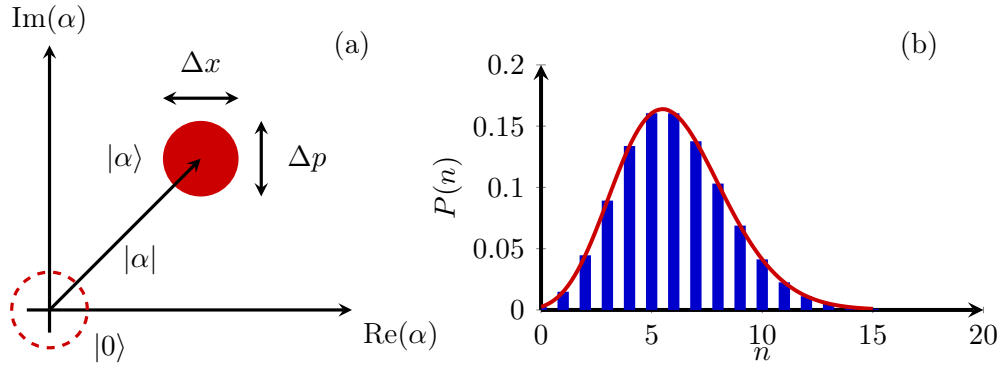


Figure 1.3: Representation of coherent states in phase space (a) and Fock space (b). In (a), the coherent state $|\alpha\rangle$ (red disc) can be obtained by displacing the ground state $|0\rangle$ (red dashed) with the displacement operator $\hat{D}(\alpha)$. A coherent state is represented in phase space by a disc, which corresponds to a Gaussian wave packet with minimum uncertainty. In (b) representation of a coherent state—of amplitude $\alpha = \sqrt{6}$ (population $n = |\alpha|^2 = 6$)—using the Fock space representation.

Phase space In classical mechanics, a configuration at point \mathbf{x} with momentum \mathbf{p} is represented by a point (\mathbf{x}, \mathbf{p}) in phase space.

Eqs. (1.42) show that similarly, in quantum optics, it is possible to build a 2D-phase space associated with a single-mode field by mapping the complex α -space to the phase space of a coherent state.

Minimum Uncertainty States For a coherent state $|\alpha\rangle$, the Heisenberg uncertainty relation (1.13) saturates i.e.

$$\Delta x|_{\alpha} \Delta p|_{\alpha} = \frac{\hbar}{2}. \quad (1.43)$$

Thus, coherent states are states of minimal uncertainty. This is one of the reasons why we say they are “most classical”.

Coherent state basis: orthogonality and completeness relations.

⁴²Since all terms in the expansion are in phase, the wave packet of the coherent state is not spreading.

1. Light-matter interaction and quantum states of light

Orthogonality. Let us consider $|\alpha\rangle$ and $|\beta\rangle$ two coherent states, so $\hat{a}|\alpha\rangle = \alpha|\alpha\rangle$ and $\hat{a}|\beta\rangle = \beta|\beta\rangle$.

The coherent states corresponds to the eigenstates of the not Hermitian annihilation operator \hat{a} .

Therefore, we cannot automatically assume the coherent states to be orthogonal.

Since $\langle\alpha|\beta\rangle \neq 0$ if $\alpha \neq \beta$ ⁴³, the coherent states are not orthogonal⁴⁴.

Completeness of coherent states. However, coherent states satisfy the completeness (closure) relation

$$\int_{\mathbb{C}} \frac{d^2\alpha}{\pi} |\alpha\rangle\langle\alpha| = \hat{1} \quad (1.44)$$

where the integral is over the whole complex plane, ie, where we used the notation

$$d^2\alpha/\pi \equiv d\text{Re}[\alpha]d\text{Im}[\alpha]/\pi = d\alpha d\alpha^* . \quad (1.45)$$

Thus, $\{|\alpha\rangle\}$ produces a *non-orthogonal over-complete basis* to span the Hilbert space [96]⁴⁵.

Coherent representation of states and operators In the coherent state representation, states can be decomposed as

$$|\psi\rangle = \int_{\mathbb{C}} \frac{d^2\alpha}{\pi} \langle\alpha|\psi\rangle |\alpha\rangle \quad (1.46)$$

and operators as

$$\hat{F} = \frac{1}{\pi^2} \iint d^2\alpha d^2\beta \left\{ \exp\left(-\frac{1}{2}(|\alpha|^2 + |\beta|^2)\right) \mathcal{F}(\bar{\alpha}, \beta) \right\} |\alpha\rangle\langle\beta| \quad (1.47)$$

where we have defined the function $\mathcal{F} = \exp(|\alpha|^2 + |\beta|^2) \langle\alpha|\hat{F}|\beta\rangle$.

Diagonal coherent-state representation of quantum operators. Let $\hat{\mathcal{B}}$ be a bounded operator, or a polynomial in \hat{a} and \hat{a}^\dagger . The trace of the operator $\hat{\mathcal{B}}$ may be calculated by [146]

$$\text{Tr}(\hat{\mathcal{B}}) = \frac{1}{\pi} \int d^2\alpha \langle\alpha|\hat{\mathcal{B}}|\alpha\rangle \quad (1.48)$$

These properties of the coherent states will be important when we will be considering the phase space representations and in particular it is at the basis of the Truncated Wigner method. This will be discussed in [chapter 3](#).

⁴³We have the scalar product/overlap $\langle\alpha|\beta\rangle = e^{-\frac{|\alpha|^2 + |\beta|^2}{2} + \alpha^*\beta}$, and thus $|\langle\alpha|\beta\rangle|^2 = e^{-|\alpha - \beta|^2} \neq 0$ if $\alpha \neq \beta$.

⁴⁴Two coherent states are never exactly orthogonal. We may note that they become approximately orthogonal for $|\alpha - \beta| \gg 1$

⁴⁵The coherent states form an “overcomplete” basis. Thus—as a consequence of the nonorthogonality—any coherent state can be expanded in terms of all the other coherent states.

1.4 Physical platforms of quantum many-body physics

The light-matter interaction is an ubiquitous process occurring in nature. Its simplest realisation is through the interaction of a single atom with a single photon.

Reaching this regime attracts lot of interest in the fast evolving and interdisciplinary⁴⁶ field of many-body physics. This led to the development of a variety of experimental platforms. Different systems provide different opportunities for control and measurement.

1.4.1 Optical resonators and photonic structures

Optical resonators provide spatially confined, spectrally filtered and temporally re-circulated light fields⁴⁷.

Typically, in a Fabry-Perot cavity, light bounces back and forth between two highly reflecting mirrors facing each other, leading to a standing-wave pattern.

Cavity QED Within the framework of cavity-QED, the linear system of a single bosonic mode in a cavity is turned into a nonlinear (interesting) system by coupling to a two level system. The typical model of a cavity-QED system is pictured in Fig. 1.4. The quantum treatment of this paradigm gives rise to the Rabi model [147, 148] and its approximate Jaynes Cummings model [149] (which is fully analytically solvable). The Rabi Hamiltonian reads

$$H = \hbar\omega_c\left(\hat{a}^\dagger\hat{a} + \frac{1}{2}\right) + \frac{1}{2}\hbar\omega_a\sigma^z + \hbar g_a(\sigma^+\hat{a} + \sigma^-\hat{a}^\dagger) \quad (1.49)$$

where \hat{a} (\hat{a}^\dagger) are the destruction (creation) operators for a single bosonic mode of frequency ω_c , σ^ν are the Pauli matrices for a two-level system with level splitting ω_a , and g_a denotes the coupling strength between the two systems.

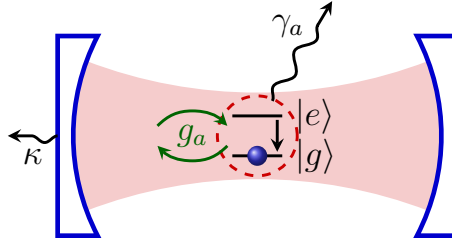


Figure 1.4: Typical model of a cavity QED platform. A single mode of the electromagnetic field in a cavity (frequency ω_c , decay rate κ) interacts with a two-level system (transition frequency ω_a , spontaneous decay rate γ_a). The interaction between the two-level system and the cavity is characterized by the coupling strength g_a .

The optical ring resonator Apart from the linear resonators, in ring resonators the confined light propagates in a low-loss bulk material in a circular path [150]. These resonators are auspicious for exhibiting high-quality factors (small mode volumes and large intracavity photon lifetime) leading to strong light-matter interactions. This platform can generate dissipative Kerr solitons. This will be studied in [chapter 5](#).

⁴⁶At the convergence of quantum optics, photonics, condensed matter physics and quantum technologies.

⁴⁷Optical resonators are at the base of the invention of the laser.

Photonic crystals A Photonic crystal is a periodic arrangement of materials with different refractive indices, affecting the propagation of light. In ordinary (spatial) crystals, the periodic arrangement of atoms and molecules affects the propagation of electrons by introducing gaps in the band structure, with allowed and forbidden energy regions. Similarly, the periodic arrangement in photonic crystals creates gaps in the light spectrum: only certain states (modes) can propagate throughout the crystal (see Fig. 1.5). Similar to solid states crystals, we can also have defects in photonic crystals which give rise to light localization or guiding. In the case of 0-dimensional defects, they are commonly named cavities. A lot of effort is put into optimizing the quality factor of these cavities. The current theoretical world record of quality factors (February 2022) in these systems has been established by a work of Juan Vasco and Vincenzo Savona [151].

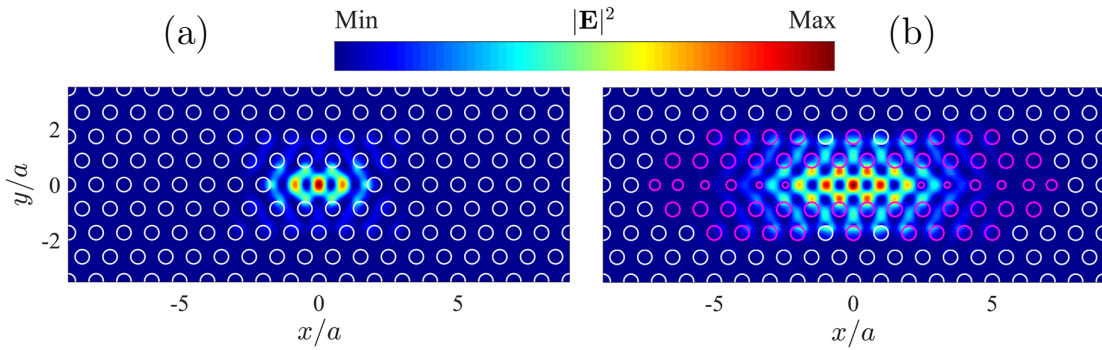


Figure 1.5: Field intensity in a specific photonic crystal, an L3 cavity. Lot of interest is devoted to the optimization of these structure to reach higher Q-factors. This picture is taken from [151], and represents the non-optimized (a) and optimized cavity (b). More details can be found in [151].

1.4.2 Superconducting architectures

In this section, we explore the world/circuitry of superconducting circuits. This is a particularly prominent platform since it provides numerous useful building blocks to explore the quantum, like e.g. quantum simulation, quantum information processing and scalable quantum technology.

In this paradigm, a microwave cavity (modeled as a harmonic oscillator) couples to nonlinear elements —the *superconducting qubits* (or higher-dimensional qudits)⁴⁸, as pictured in Figs. 1.6 and 1.7.

Superconducting qubits are implemented under the form of Josephson junctions [152, 153], existing in three basic types: charge qubits [154–157], flux qubits [158–160] and phase qubits [161]⁴⁹.

This offers exceptionally large nonlinearity with negligible dissipation and a very rich parameter space of possible qubit properties and operation regimes.

The Hamiltonian for a phase-qubit is

$$H = \frac{1}{2C} \hat{Q}^2 - \frac{I_0 \Phi_0}{2\pi} \cos \hat{\delta} - \frac{I \Phi_0}{2\pi} \hat{\delta}, \quad (1.50)$$

⁴⁸Superconducting qubits are also commonly referred to as artificial atoms.

⁴⁹These varieties of qubits depends on the specific circuit and coupling, but have similar attributes.

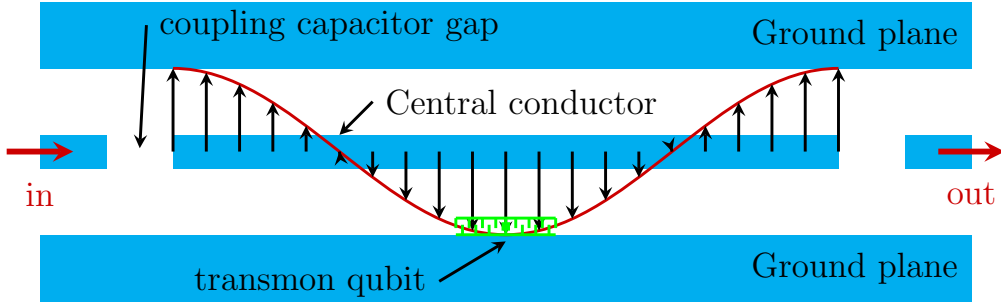


Figure 1.6: Typical model of a circuit-QED platform. A single mode of the electromagnetic field in a coplanar waveguide resonator interacts with a transmon qubit. This model is analogue to the cavity-QED setup showed in Fig. 1.4

where C is the capacitance of the tunnel junction, I_0 is the critical-current, and $\phi_0 = h/2e$ the superconducting flux quantum. The operators charge \hat{Q} and phase difference $\hat{\delta}$ obey the commutation relationship $[\hat{\delta}, \hat{Q}] = 2ei$.

The Hamiltonians for charge and flux qubits can e.g. be found in [162].

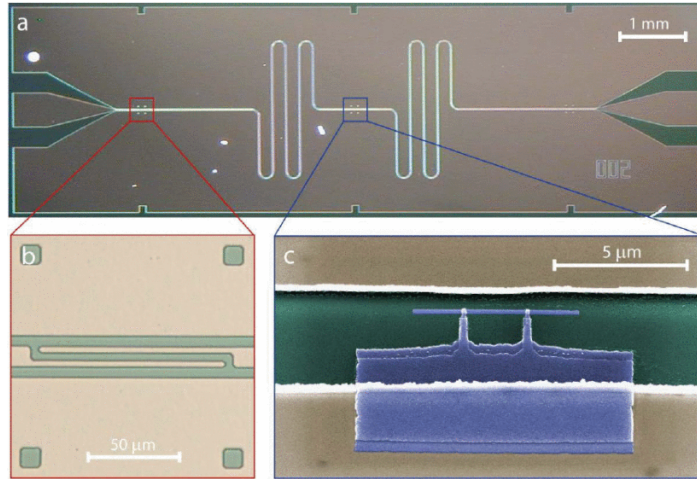


Figure 1.7: Picture of an integrated circuit QED device. Picture taken from [163].

More details can be found in the reviews [164, 165].

The theory of the canonical system is known as Circuit QED [60, 92, 166, 167]

Applications Superconducting architectures have applications such as high-fidelity readout [152], quantum memory [168, 169], or quantum computation with cat states [170–172]

1.4.3 Ultracold atoms

The field of ultra-cold atoms [174–178] attracts lots of interest in both fundamental and applied science. In this realm, the dynamics of trapped atoms is controlled and manipulated through the interaction with laser beams⁵⁰ [174, 176, 177, 179,

⁵⁰For this application it is necessary to reach spectral purity, with a high degree of coherence and gain control on the direction and polarization of laser beams.

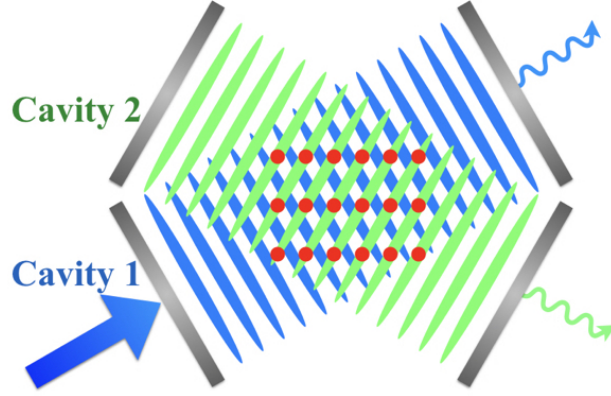


Figure 1.8: Schematic view of trapped cold atoms (red dots) in a cavity assisted ultracold atoms platform. atom interferometer. Figure taken from [173].

[180]. In an ultracold atom experiment, atoms are cooled down in optical lattices⁵¹. Optical lattices are optical potentials in periodic form, analogue to the structures of real crystal lattices in solid-state physics. The interaction among the atoms can be controlled with light fields⁵² (see Fig. 1.8). When atoms are moving slowly (in the order of mm/s), the wave nature becomes important, enabling the regime of non-linear optics with atom-atom interaction. The beginnings of cold atom physics led to the observation and study of Bose-Einstein condensate (BEC), where a phase-space density of the order of one is reached.

Applications Cold atoms are valuable resources in spectroscopy [181], precision measurements ranging from enhanced atomic clocks [182, 183] to sensing and navigation, quantum simulation [184], and quantum information processing [185, 186]. On the fundamental side, the strong analogy between the physics of ultra-cold atoms and solid-state physics crystals provides an ideal platform for analog quantum simulations [178, 187]. In particular, many-body systems models such as the Bose-Hubbard or Fermi-Hubbard models [188] can be implemented. It also enables the study of many-body localization [189, 190], quantum phase transitions and engineering of desired atomic states [191]. Moreover, ultra-cold atom physics is also a candidate for quantum computation.

1.4.4 Quantum optomechanical systems

Light and mechanical degrees of freedom can interact through the radiation pressure force [192]. The field of quantum optomechanics [193–197] harness this interplay and explores the interaction of optical or microwave radiation with micro- or nanomechanical resonators.

⁵¹The interference arising from the intersection of two or more laser beams creates a periodic spatial pattern for the light intensity, inducing a force on the atom (via the radiation pressure force), called optical dipole force. This tightly traps the atoms in minima of the light potential.

⁵²Via radiation pressure force.

Hamiltonian and definition The canonical systems with one optical mode (\hat{a} , frequency ω_c , cavity with a mirror separation L) interacting with one mechanical mode (\hat{b} , mass m , frequency ω_{om}) is described with the optomechanical coupling term

$$\hat{H}_{\text{om}} = \hbar g_m \hat{a}^\dagger \hat{a} (\hat{b} + \hat{b}^\dagger) \quad (1.51)$$

Here, $g_m = \omega_c x_{\text{ZPF}}/L$ with the mechanical zero-point fluctuations⁵³ $x_{\text{ZPF}} = (\hbar/2m\omega_{\text{om}})^{1/2}$ quantifies the interaction strength between a single photon and the mechanical mode. The typical model of an optomechanical system is pictured in Fig. 1.9 and a gallery featuring some of the various experimental implementations is pictured in 1.10.

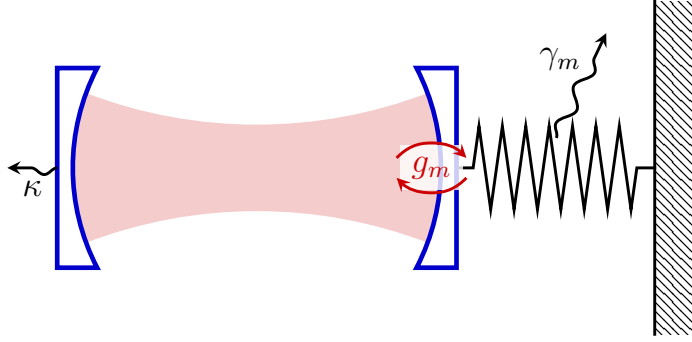


Figure 1.9: Typical model of a cavity optomechanical platform. A single mode of the electromagnetic field in a cavity (frequency ω_c , decay rate κ) interacts with a mechanical oscillator (frequency ω_m , dissipation rate γ_m). The interaction between the mechanical and optical mode is characterized by the coupling strength g_m .

Applications Optomechanics have lots of technological applications [198], among them ground state cooling of macroscopic mechanical resonators [199–202], quantum squeezing of mechanical motions [203–206], production of squeezed light [207–209], nonclassical correlations between an optical field and a mechanical resonator [210], quantum entanglement between mechanical resonators [211, 212], coherent conversion between optical and microwave signals [213] and non-reciprocal photonic devices [214–219]. Optomechanical setups also find application in gravitational-wave detectors [220]. It is also a prime system for the study of the quantum to classical “transition” [221].

1.4.5 ... and a lot of other platforms

Of course, the creativity of scientists makes this list quite incomplete. Some other experimental platforms are electron spins in silicon [222–227], quantum dots [228–231], polaritons [232–234], trapped ions [235–239] and nitrogen-vacancies in diamonds [240, 241].

⁵³Width of the mechanical ground state wave function.

1. Light-matter interaction and quantum states of light

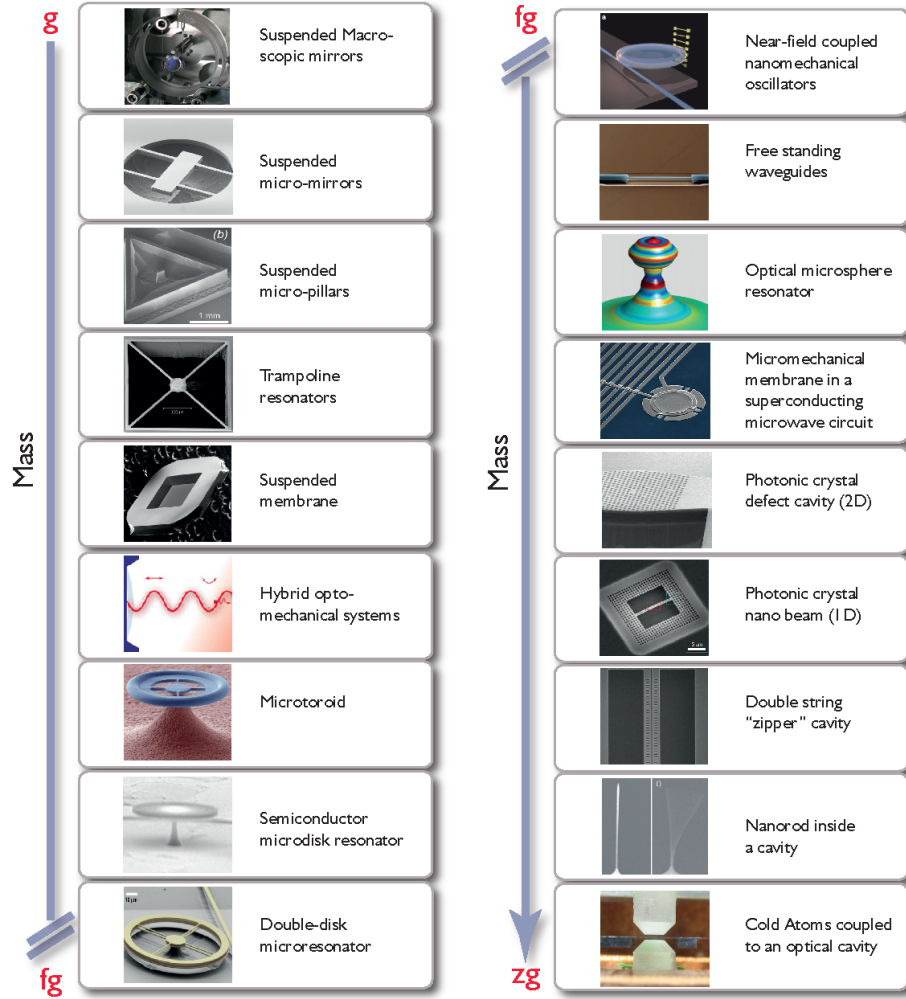


Figure 1.10: The more the merrier: a gallery featuring the variety of optomechanical platforms. Picture taken from [193].

Chapter 2

Theory of open quantum systems

An open quantum system is a (small, or not so small¹) quantum system —“what we are interested in”— interacting with its (macroscopic) environment (see Fig. 2.1).

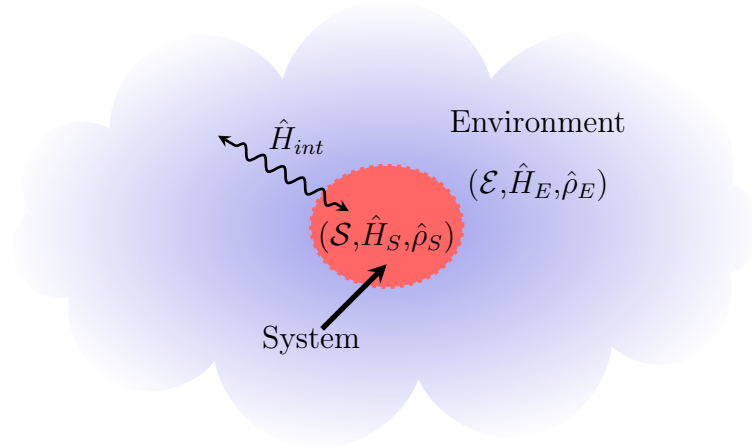


Figure 2.1: Schematic representation of an open quantum system, with the notation used in this chapter. The system \mathcal{S} (Hamiltonian \hat{H}_S , density matrix $\hat{\rho}_S$) interacts with its environment \mathcal{E} (Hamiltonian \hat{H}_E , density matrix $\hat{\rho}_E$) through the interaction Hamiltonian \hat{H}_{int} .

In many real-world situations, the coupling with the external environment cannot be neglected², making the application of the standard toolkit of coherent (close/pure) quantum dynamics (e.g. Schrödinger or von Neumann equations) insufficient³. Not only is the treatment as an open quantum system closer to

¹E.g. a superconducting qubit is of macroscopic size.

²It's worth noting that the concept of “openness” isn't limited to quantum mechanics; understanding the dynamics of systems in relation to their surroundings is relevant to a large number of natural sciences. In fact, all systems are open.

³In general the large number of degrees of freedom of these systems (and precisely of the environment) prevent an exact treatment with the current resources. Imagine solving the Schrödinger equation for $\sim 10^{23}$ quantum particles...

reality⁴, but also it often unveils a much richer physics compared to closed systems. The theory of open quantum systems thus turns out to be a fundamental paradigm in quantum mechanics and its applications.

The special interest in the study of an open quantum system is on the one hand the steady-state properties, and on the other hand the relaxation dynamics towards the steady state. The guiding idea of the theory of open quantum systems is to focus only on the dynamics of a small number of degrees of freedom (d.o.f) of interest (Hilbert space \mathcal{H} , dimension of the Hilbert space $\dim \mathcal{H} = N$), and trace out all the other d.o.f. The precise dynamics of the environment is lost and only its influence on the subsystem of interest is accounted for. Assuming simple (and often reasonable) assumptions such as weak coupling of a small system to a much larger memoryless environment, the reduced dynamics of the subsystem can be found. The state of an open quantum system can be described by the $N \times N$ (reduced) density operator $\hat{\rho}_S$ which is an element of the Liouville space (also called operator or coherence space, is of $\dim \mathcal{L} = N^2$) [242].

The Lindblad master equation formalism for $\hat{\rho}_S$ is a successful theoretical framework for describing the dynamics of open quantum systems.

However, analytic solutions to the master equation are only available for very few cases [243–249], and it can become challenging to solve numerically (memory problems), since $\mathcal{O}(N^2)$ memory is needed at each timestep to store $\hat{\rho}_S$.

This problem can be mitigated in the framework of stochastic unraveling methods of the Lindblad equations (also called quantum trajectories or Monte Carlo methods). The basic concept behind this framework is to average over a large set of stochastically time-evolved quantum state trajectories until convergence criterion is met⁵. It reduces the cost from evolving a $N \times N$ density matrix, to a wave-functions $|\psi\rangle$ of only N elements⁶. The stochastic simulation technique lies at the basis of the Truncated Wigner method, which is a central topic of this thesis.

In this chapter, we will first introduce the theory of open quantum systems with the goal of setting the state for the original work presented in this thesis. Afterward, we will have a brief overview of different methods used for solving the dynamics of open quantum systems. Moreover, we will focus on the general formalism leading to the Lindblad master equation. Among other aspects, we address the dynamical map approach and bosonic bath. Then, we will analyze the different spectral properties of the Liouvillian superoperator. We will end up taking a look at the stochastic approach.

Contents

2.1	Opening	37
2.1.1	What	37
2.1.2	Why	38
2.1.3	How	39
2.2	Time evolution of open quantum systems	40
2.2.1	Time evolution of closed quantum systems	40

⁴The theory of open quantum systems has benefit of renewed interest through the advent of quantum technologies. It's due to the fact that a major obstacle to the elaboration of quantum devices is decoherence caused by interaction with the environment.

⁵A lot of trajectories can be needed to reach convergence, but the process can be highly parallelized.

⁶Depending on the nature of the problem, additional approximations to the state can be made that overcome the still exponential scaling (both when working with the master equation directly or with trajectories) such as Gutzwiller, tensor network, neural network or Gaussian Ansatzes.

2.2.2	Let there be interaction!	42
2.2.3	Time evolution of open quantum system	43
2.3	The Lindblad quantum master equation	46
2.3.1	Some approximations	46
2.3.2	The Lindblad master equation	47
2.3.3	Environment types and modeling approaches	49
2.3.4	Intermezzo: example of a single bosonic (cavity) mode	51
2.4	The Liouvillian superoperator	52
2.4.1	The Liouvillian superoperator	52
2.4.2	Vectorization: the Choi-Jamiolkowski isomorphism	54
2.4.3	Spectral properties of the Liouvillian superoperator	56
2.5	Various open quantum system methods	58
2.5.1	Stochastic approaches	59
2.5.2	Other approaches	61

2.1 Opening

We introduce here the general framework of the theory of open quantum systems, by laying out the motivations, purposes and context.

2.1.1 What

Over the last years, the theory of open quantum systems (OQS) has received renewed attention due to its utmost importance from both fundamental physics and applied quantum science viewpoints.

The reason is simple: all systems found in nature, quantum or classical, are never perfectly isolated from their surroundings. They continuously interact with their environment in the form of heat transfer, decoherence etc⁷, leading to a time-irreversible dynamics.

In general, classical systems tend to be much less sensitive to external influences (e.g. trajectories of celestial bodies) than quantum systems. In classical systems, tracing out the environment makes the Hamiltonian descriptions incomplete and gives the system a stochastic nature (e.g. the case of Brownian motion). Similarly, in open quantum systems, the openness of a quantum system leads to additional “classical” fluctuations. Different types of environments can affect the quantum system of interest.

The environment can be of quantum or classical nature. In the quantum environment scenario, one can deal with bosonic or fermionic environments, stationary or non-stationary environments. Within stationary environments there can be thermal environments (often called reservoirs) and non-thermal environments (e.g. squeezed reservoirs [250, 251]⁸).

⁷Within this regard, the environment can be viewed as a quantum version of Orwell’s Big Brother, as it continuously monitors the system and collects information about it.

⁸Squeezed environment are important physical resource especially for quantum information processing [252], and precision measurements like gravitational wave detection [253].

When considering a single atom, the natural environment is the electromagnetic field surrounding the atom⁹.

For an atom in a solid crystal instead, a possible environment is an assembly of phonons (vibrational excitations) describing the vibrational motion of the crystalline structure. In both examples above, the quantum environment is bosonic and is described in terms of an infinite set of quantum harmonic oscillators representing the normal modes of the electromagnetic or vibrational field.

Photons (or phonons) are quantum excitations of quantum harmonic oscillators having different frequencies. The frequency spectrum of the environment and its density of modes play a significant part in the description of open quantum system dynamics. One should mention at this point that, due to the system-environment coupling, the system could also influence the environment. However, under some general assumptions (e.g. size and energy of the reservoir much greater than the ones of the system¹⁰), the changes induced by the system onto the environment are negligible, and the latter can be considered as stationary.

2.1.2 Why

The theory of open quantum systems was born out of the aim to describe lasers [255, 256] and nuclear magnetic resonance (NMR) [257–259].

Then, from a fundamental perspective, the theory of open quantum systems attracts interests as their dynamics, especially in a driven-dissipative context, exhibit a large number of features not encountered in closed or equilibrium systems [14, 260] in particular the emergence of novel out of equilibrium behaviors.

Of particular interest are dissipative phase transitions and critical behavior and the appearance of dynamical phases with new broken symmetries [261–264]. These emergent phenomena will be addressed in [chapter 4](#) and [chapter 5](#).

On the practical side, technological advances in the last few decades made possible to manipulate quantum systems at the level of individual atoms or photons. The theory of open quantum systems has an essential importance for these developments, enabling the realization of quantum devices [265–270], including in particular the very trendy quantum computers [10, 271–276], the description of chemical reactions [277–280], or understanding biological complexes [281–286].

It turns out that the coherent dynamics of quantum systems—a key feature for quantum technologies—is altered by their inevitable coupling to the external environment. The latter, by continuously “reading” the state of the system, prevents quantum interference. Thus, it appears to be crucial to consider the effects of dissipation when modeling realistic quantum systems by numerical methods or quantum simulation.

The impressive variety of environments and system-environment interactions are responsible for a vast spectrum of interesting physical phenomena. Among them, and just to name a few, there are fluctuations and dissipation of course, but also loss of

⁹The coupling between the atom and the electromagnetic field is the source of the phenomenon of spontaneous emission.

¹⁰Note however that in some cases the open quantum systems approach can be used to study finite-size environments [254].

quantum coherence, irreversibility and relaxation to equilibrium, processes enhancement or the emergence of classical stochastic dynamics [105, 287–290].

An additional reason is that it allows to assess some important questions as for example the quantum measurement problem, or the quantum to classical transition¹¹. It has even cross field application as it is for example used for the theory of gravity [291].

From the applied perspective, open quantum many-body systems are at the centre of the era known as the second quantum revolution¹².

These quantum technologies rely on the most definitively quantum features of microscopic systems, such as quantum superpositions and entanglement. In open quantum systems the parameter offered by the dissipation channels can be used to engineer specific desired quantum manybody steady-states. The quantum technologies become commercially distributed and available on the market. These technologies include quantum computers, quantum sensors, quantum cryptographic devices and so on and so forth.

2.1.3 How

When a quantum system’s state is clearly defined (in a pure state), it can be described in terms of vectors in Hilbert space, so called kets. However, for statistical mixtures, e.g. the most general state a physical system can be in, this description is no longer possible. The mathematical object used for the representation of statistical mixtures, and also valid for pure states, is called density operator, which is defined in [chapter 1](#). Such mixed states inevitably arise in OQS. In general, the dynamics between an OQS and its environment results in correlations (e.g., entanglement) between both parts, so the state of the system can only be defined in terms of a density operator.

In OQs, the properties of special interest are the steady-state properties and the relaxation dynamics toward this steady-state.

With the intention to determine the time evolution of the system, we could, in principle, resort to basic quantum mechanics [293, 294] and solve the Schrödinger or von Neumann equation, for the state describing the entire system constituted of the system and its environment.

This total system can indeed be considered as “closed” and therefore remains in a pure state at all times¹³. The system’s state could then be determined anytime by tracing out the environment.

The problem, however, is that this approach is usually inconvenient and almost always unfeasible, due to the far too large number of environmental degrees of freedom. Instead,

¹¹The question about the border between the quantum description of reality, which generally applies to microscopic objects such as atoms or electrons, and the classical description of the objects of our every day experience. See e.g. [288]

¹²Why the second? Because there was already a first (see also discussion in the general introduction of this thesis). The first quantum revolution is the one that led to a whole new range of technologies based on the understanding of the quantum structure of microscopic systems as, for instance, the invention of the laser, which is now widely used in a number of technologies. In the early 2000’s, 30% of the gross national product of the United States came from inventions enabled by quantum physics [292].

¹³If one wants to be completely rigorous, the only system that is really closed is the whole Universe (multiverse?)!

by analyzing the structure of the Hamiltonian, an effective, and/or approximate equation of motion for the density operator describing the system can be derived.

This equation of motion —the so called quantum master equation 2.2.2— plays a major role throughout this chapter. A general unified approach to open quantum many-body systems doesn't exist yet, but a large number of different simulation methods exists for different scenarios (see e.g. [295] for a nice overview).

In the framework of closed system, solving the Schrödinger equation leads to a family of unitary operators parameterized by time that, when applied to the initial state, yield the state at later (all) times. The situation is rather different for open quantum systems, because the time evolution is not unitary anymore. In this case, solving a master equation results in a family of channels, physically consistent superoperators mapping density operators into density operators, that go by the name of dynamical maps and account for the temporal evolution of the system.

What about the treatment of the environment? A widely used approach is the so-called harmonic bath assumption. It consists in modeling the environment with an infinite ensemble of quantum harmonic oscillators which do not interact between each other [296]¹⁴.

2.2 Time evolution of open quantum systems

In open quantum systems, the interaction of the system of interest with the external environment is essential for an appropriate description of the dynamics of the system. In most (almost all) cases, a model including all of the external degrees of freedom that interact with the system is unsuitable. Indeed, their numbers is excessive, and their dynamics aren't sufficiently known to enable an explicit treatment.

A more refined approach consists in implementing the effect of the macroscopic environment on the dynamics by partial trace operation, thereby averaging at any time over the unknown state of the environment. This is the idea behind the open quantum system approach that we will look at now.

2.2.1 Time evolution of closed quantum systems

We begin with an overview of the formalism treating the time evolution of closed systems, i.e. systems which are fully isolated from their environment. These systems are characterized by a unitary dynamics. Physical systems cannot be completely isolated from their environment, hence this is an idealized vision.

Given an isolated quantum system described by a pure state $|\psi(t)\rangle$, and governed by the Hamiltonian $\hat{H}(t)$, its dynamics is described via the *Schrödinger equation*¹⁵

$$i\hbar \frac{d}{dt} |\psi(t)\rangle = \hat{H}(t) |\psi(t)\rangle. \quad (2.1)$$

The generalization to an equation of motion for a mixed state described via a density

¹⁴While this approach is intuitive, it is however still unjustified [297].

¹⁵Postulate V) of quantum mechanics, see chapter 1.

matrix $\hat{\rho}(t)$ ¹⁶ is given by the Liouville-von Neumann equation¹⁷

$$i\hbar \frac{d}{dt} \hat{\rho}(t) = [\hat{H}(t), \hat{\rho}(t)] . \quad (2.2)$$

Eqs. (2.1) and (2.2) are first order differential equations.

The linearity of these equations and the Hermiticity of the Hamiltonian allows to express their respective solution in terms of a handy unitary operator¹⁸, the so-called time evolution/propagator operator $\hat{U}(t, t_0)$. The operator $\hat{U}(t, t_0)$ represents a finite time translation.

In the general case of a time dependent Hamiltonian, the expression of the time evolution operator is given as a time-ordered exponential¹⁹

$$\hat{U}(t, t_0) = \mathcal{T} \exp \left(-\frac{i}{\hbar} \int_{t_0}^t ds \hat{H}(s) \right) , \quad (2.3)$$

and in the case of a time independent Hamiltonian, its expression boils down to

$$\hat{U}(t, t_0) = \exp \left(-\frac{i}{\hbar} \hat{H}(t - t_0) \right) . \quad (2.4)$$

The evolution operator obeys the combination law for all t and τ

$$\hat{U}(t + \tau, t_0) = \hat{U}(t, \tau) \hat{U}(\tau, t_0) , \quad (2.5)$$

and deterministically relates the states at the initial and final times²⁰.

Given the initial condition at an initial time t_0 , $|\psi(t_0)\rangle$, respectively $\hat{\rho}(t_0)$, the state at a later time $t > t_0$ is given by

$$|\psi(t)\rangle = \hat{U}(t, t_0) |\psi(t_0)\rangle , \quad (2.6)$$

and respectively

$$\hat{\rho}(t) = \hat{U}(t, t_0) \hat{\rho}(t_0) \hat{U}^\dagger(t, t_0) . \quad (2.7)$$

Having at hand the state at time t , we can compute the time dependence of the expectation value of an observable \hat{A} using (postulate number)

$$\langle \hat{A} \rangle(t) = \langle \psi(t) | \hat{A} | \psi(t) \rangle , \quad (2.8)$$

in wave mechanics, or for matrix mechanics we have

$$\langle \hat{A} \rangle(t) = \text{Tr}(\hat{A} \hat{\rho}(t)) . \quad (2.9)$$

¹⁶Note that a mixed state, as defined in (1.2), cannot in general be expressed in terms of a wave function and there is no Schrödinger equation that describes the dynamics of the corresponding system.

¹⁷The Liouville-von Neumann is isomorphic to the Heisenberg equation of motion, since $\hat{\rho}$ is also an operator.

¹⁸An operator U is unitary if $U^\dagger = U^{-1}$ or $UU^\dagger = \mathbb{1}$.

¹⁹The time ordering operator \mathcal{T} ensures that in a product of operators, the operators have increasing time arguments from right to left.

²⁰In other words, the knowledge of the state of the system —described either by a wave function or a density matrix— at a particular time t_0 determines the entire trajectory at all times, in complete analogy to the Hamilton or Euler–Lagrange equations of motion of classical mechanics.

Note that due to the cyclic invariance of the trace, the time-dependent expectation value of an operator can be calculated either by propagating the density matrix (Schrödinger or interaction picture), or the operator \hat{A} (Heisenberg picture). In the latter case we have $\langle \hat{A} \rangle(t) = \text{Tr}(\hat{A}(t)\hat{\rho}(t_0))$.

Thereby, the Schrödinger and Liouville-von Neumann equations establish a continuous group of unitary transformations via the map $U(t, t_0)$, parameterized by the parameter t and t_0 . This unitarity implies the reversible character of the system dynamics.

The reversible character of the dynamics of a closed system can be challenged when a measurement of the system is performed. The measurement projects the system into a new state—determined according to the probability distribution of the possible outcomes of the POVM — breaking the smoothness and determinism of the time evolution. Under this scenario, it becomes impossible to retrieve the state the system was in just prior to the measurement, and this, even knowing the state of the system after the measurement and the evolution operator.

Oppositely, we will observe that the evolution of an open system is generally irreversible, even if no measurements are made: it is a probabilistic time evolution.

2.2.2 Let there be interaction!

We consider a generic open quantum system \mathcal{S} (e.g. a two-level atom or a single-mode optical cavity), coupled to an environment \mathcal{E} ²¹. For the nomenclature, the subsystem of interest \mathcal{S} (environment \mathcal{E}) lives in Hilbert space \mathcal{H}_S (\mathcal{H}_E) and is described by the reduced density matrix $\hat{\rho}_S$ ($\hat{\rho}_E$). This ensemble forms a large quantum system described by the density matrix $\hat{\rho}_{tot}$ in Hilbert space $\mathcal{H}_S \otimes \mathcal{H}_E$.

The total Hamiltonian describing the system coupled to its environment can be written under the form

$$\hat{H}_{tot} = \hat{H}_S + \hat{H}_E + \hat{H}_{SE} . \quad (2.10)$$

where \hat{H}_S and \hat{H}_E are respectively the bare/free system and environment Hamiltonians (embedded in the total Hilbert space using the tensor product²²), and \hat{H}_{SE} denotes a suitable interaction Hamiltonian.

The combined ensemble {system+environment} is considered as closed. Its state described equivalently by $|\psi_{tot}\rangle$ or $\hat{\rho}_{tot} = |\psi_{tot}\rangle\langle\psi_{tot}|$ evolves according to Eq. (2.7), with the global unitary evolution operator defined as in Eq. (2.3).

We are interested in describing the system \mathcal{S} solely, leaving aside what happens to \mathcal{E} . The system of interest treated alone is an open one and its state is expressed in terms of the density operator $\hat{\rho}_S$.

The reduced dynamics of the system $\hat{\rho}_S(t)$ is obtained by tracing over the environmental degrees of freedom:

²¹Special type of environments are reservoirs and heat baths (see Fig. 2.1). A reservoir describes an environment with an infinite number of degrees of freedom, and continuous energy spectrum of the reservoir modes. On the other hand, a heat bath is a reservoir in thermal equilibrium state.

²²The Hamiltonian describing the composite system is obtained by embedding the free Hamiltonians in the higher dimensional Hilbert space using the tensor product i.e. $H_S = h_s \otimes \mathbb{1}_E$, where h_s is the system operator in \mathcal{H}_S and $\mathbb{1}_E$ is the identity operator in \mathcal{H}_E .

$$\hat{\rho}_S(t) := \text{Tr}_E(\hat{\rho}_{tot}(t)), \quad (2.11)$$

where Tr_E denotes the partial trace²³.

The expectation value of the observable \hat{O}_S at time t is given by²⁴

$$\langle \hat{O}_S(t) \rangle = \text{Tr}_S(\hat{O}_S \rho_S(t)). \quad (2.13)$$

The dynamics of $\hat{\rho}_S$ takes the following form

$$\hat{\rho}_S(t) = \text{Tr}_E(\hat{U}(t, t_0) \hat{\rho}(t_0) \hat{U}^\dagger(t, t_0)). \quad (2.14)$$

In general, the time evolution for $\hat{\rho}_S$ described in Eq. (2.14) is not unitary like Eq. (2.7). The presence of the interaction term \hat{H}_{SE} in the total Hamiltonian has the effect of entangling the system with its environment during the time evolution: due to these correlations, the reduced density matrix $\rho_S(t)$ is subject to a non-unitary evolution. The type of non-unitary dynamics of a system depends on the characteristics of the environment and coupling type and strength between the system and the environment. It can involve several and different kind of dissipation and/or decoherence “channels” and can lead to exotic features such as critical phenomena, and the occurrence of phase transitions (See chapter 4) or superselection sectors.

In the framework of open quantum systems, it is common to resort to the assumptions that \mathcal{S} and \mathcal{E} are weakly coupled (i.e. \mathcal{S} does not affect the state of \mathcal{E}), and initially uncorrelated i.e. we can write $\rho_{tot}(0) = \rho_S(0) \otimes \rho_E(0)$.

2.2.3 Time evolution of open quantum system

2.2.3.1 Universal Dynamical Maps of Open Quantum Systems

Equation (2.14) gives the time evolution of the reduced density matrix $\hat{\rho}_s$ for closed quantum systems, using a unitary operator.

Similarly, we are now interested in defining the most general map that gives the time evolution of the reduced density matrix $\hat{\rho}_s$ from a time t_0 to t_1 in the case of open quantum systems.

This is given by the concept of universal dynamical map²⁵ [98, 298–300]. In this context, the adjective “universal” means that the definition of these maps is independent from the density matrix they are acting on²⁶.

²³The partial trace of an operator living in the product space of the system and environment is defined as

$$\hat{\rho}_S = \text{Tr}_E(O_S \otimes O_E) := \text{Tr}(O_E) O_S = \sum_k \langle \psi_k^E | \hat{\rho} | \psi_k^E \rangle, \quad (2.12)$$

with $\{|\psi_k^E\rangle\}$ a basis of the Hilbert space \mathcal{H}_E .

$$\rho_A = \sum_b (I_A \otimes \langle b |) \rho_{AB} (I_A \otimes |b\rangle) = (\text{id} \otimes \text{tr}_B) \rho_{AB}$$

²⁴We have $\langle \hat{O}_S(t) \rangle = \text{Tr}((\hat{O}_S \otimes \mathbb{1}_E) \rho(t)) = \text{Tr}_S(\hat{O}_S \text{Tr}_E(\rho(t))) = \text{Tr}_S(\hat{O}_S \rho_S(t))$, and voilà!

²⁵Other names are used, such as quantum dynamical map or quantum operation. Quantum operation is particularly used in the context of quantum computation.

²⁶Indeed, the initial state of the system has to be independent from the environment.

Formally, a dynamical map transforms quantum states into quantum states (e.g. through time evolution, measurement, coupling to another system, etc...) and preserves the superposition principle. Thus, a quantum dynamical map between two systems with Hilbert spaces \mathcal{H}_1 and \mathcal{H}_2 can be identified with a linear homomorphism \mathcal{M} mapping $D(\mathcal{H}_1)$ into $D(\mathcal{H}_2)$ such that²⁷

$$\mathcal{M}_{t,t_0}: D(\mathcal{H}_1) \rightarrow D(\mathcal{H}_2) \quad (2.15)$$

$$\hat{\rho}(t_0) \mapsto \hat{\rho}(t) = \mathcal{M}[\hat{\rho}(t_0)] . \quad (2.16)$$

In this instance, we have

$$\hat{\rho}_s(t) = \mathcal{M}_{t,t_0}[\hat{\rho}_s(t_0)] . \quad (2.17)$$

The quantum map \mathcal{M} is a superoperator, since it transforms an operator into another and can be interpreted as the evolution superoperator for the the reduced density matrix of the system.

Now, in addition to meeting the generic structure defined in Eq. (2.17), the map \mathcal{M} must also preserve the properties of the density operator during the time evolution. This request of the physicality of the time evolution is guaranteed if the map satisfies the following properties [105, 301]:

1. Linearity: $\mathcal{M}[\lambda_1 \rho_1 + \lambda_2 \rho_2] = \lambda_1 \mathcal{M}[\rho_1] + \lambda_2 \mathcal{M}[\rho_2]$.
2. Trace preserving: $\text{Tr}(\mathcal{M}[\rho]) = \text{Tr}(\rho)$.
3. Completely positive²⁸: if $\rho \geq 0$ then $\mathcal{M}[\rho] \geq 0$.

A map satisfying these properties is called a Completely Positive Trace Preserving (CPTP) map [105].

Kraus-operator representation. Kraus-operator [302], also called operator-sum [97, 303] representation is common representation of CPTP-maps.

The Kraus sum representation is given by a (not unique) set of Kraus operators $\{M_k\}$ such that the evolution of a density matrix ρ_S is given by [98, 298, 304–307]

$$\mathcal{M}[\hat{\rho}(t)] = \sum_k M_k \hat{\rho}(t) M_k^\dagger \quad (2.18)$$

with the property that the Kraus operators resolve the identity

$$\sum_k M_k^\dagger M_k = \mathbb{1} . \quad (2.19)$$

The representation set out in Eq. (2.18) generalizes the unitary evolution expressed in Eq. (2.7). A Kraus description of the map \mathcal{M} need a maximal number of N^2 Kraus operators, where N is the dimension of the Hilbert space \mathcal{H}_S (an thus N^2 is the size of the Liouville space). At the opposite, the minimum number of Kraus operators corresponds to a unitary evolution parameterized by just one Kraus operator.

²⁷The notation $D(\mathcal{H})$ stands for the representation of the Hilbert space \mathcal{H} .

²⁸Complete positivity means that the extended map is positive for any dimension of the extended space. Partial trace and transposition are examples of positive but not completely positive maps.

Unicity. The Kraus representation of the map \mathcal{M} is not unique. There is unitary freedom in choosing the Kraus operators and any linear unitary transformation mixing them leaves the quantum map unchanged. Thus, the equivalent expressions of the Kraus operators can be expressed as $\tilde{M}_\mu(t) = \sum_\nu M_\nu(t) V_{\mu\nu}$, where $V_{\mu\nu}$ are the elements of an arbitrary unitary matrix.

A special representation—the Canonical Kraus Representation [308] — corresponds to the unique set of Kraus operators satisfying the orthogonality relation

$$\text{Tr}(M_\alpha^\dagger M_\beta) = \lambda_\alpha \delta_{\alpha\beta} . \quad (2.20)$$

Besides being elegant, the representation in terms of Kraus operators is also very powerful since the entire description of the influence of the environment onto the system is cast into a set of operators M_μ .

Choi-Kraus decomposition theorem. Given a system originally in a state ρ_S , coupled to an environment originally in a state ρ_E . In the forgoing, the dynamics of open quantum systems have been addressed following two different ways.

On the one hand the dynamics is expressed by Eq. (2.14). The system evolves jointly with the environment according to a unitary evolution operator, and then the environmental degrees of freedom are disregarded (i.e. traced out).

On the other hand, the evolution is expressed in terms of a linear, completely positive, and trace preserving map —a universal dynamical map— that time evolve the density matrix describing the system.

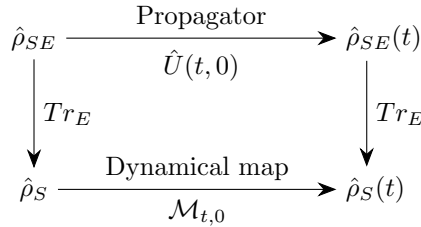


Figure 2.2: Equivalence of the two formulations

$$\hat{\rho}_S(t) = \text{Tr}_E(\rho_{tot}(t)) = \mathcal{M}_{t,t_0}[\hat{\rho}_S(t_0)] \quad (2.21)$$

The Choi-Kraus decomposition theorem states that these two formulations are equivalent (see fig. 2.2)

Markovianity. The dynamical map is divisible if it can be written as the composition of two CPTP maps

$$\mathcal{M}_{t,0} = \mathcal{M}_{t,t'} \mathcal{M}_{t',0} \quad \forall t' \leq t . \quad (2.22)$$

If the dynamical map is divisible, the time evolution of the open quantum system is memoryless, and the dynamic is called *Markovian*.

A typical scenario leading to Markovian dynamics is the weak coupling between system and environment in addition to the condition that the environmental correlations decay

much faster than the timescales of the system dynamics.

Conversely, open quantum systems can exhibit pronounced memory effects: the dynamics is then called non-Markovian.

Common origin of memory effects are e.g. structured spectral densities, nonlocal correlations between environmental degrees of freedom and correlations in the initial system-environment state [309, 310].

As we will see in the next section, the Markovian dynamics can be described via a so called master equation in Lindblad form.

In the case of a non-Markovian dynamics, a similar unified framework does not exist. Instead, various methods have been developed, each being characterized by its proper assumptions, and range of validity [311].

When it happens that maps are not very useful, it is preferable to have a differential equation for $\rho_S(t)$. In the next section, we are seeking for an equation of motion describing the dynamics of the system alone, and accounting for its coupling to the environment.

2.3 The Lindblad quantum master equation

We focus here in particular on the case where the system bath interaction is Markovian, i.e. we assume that the environment has no memory of its previous states.

The most general generator of Markovian dynamics is given by the Lindblad (or Gorini-Kossakowski-Sudarshan-Lindblad) master equation.

This equation turns out to be an essential tool in a variety of fields as e.g. quantum optics [287], condensed matter [312], atomic physics [313], quantum information [15, 314], decoherence [315, 316] and quantum biology [317].

2.3.1 Some approximations

It is necessary to resort to some approximations to derive²⁹ a master equation in a specific operatorial form, known as the Gorini-Kossakowski-Sudarshan-Lindblad (GKSL) form, often referred to as the Lindblad form.

To begin with, note that the dynamics of the open quantum system is characterized by three (independent) time scales

- the environment correlation time τ_c
- the environment relaxation time τ_r , inversely proportional to the strength of the system-environment interaction
- the characteristic time scale of the intrinsic evolution of the system $\tau_S = 1/\omega_S$

An important step in the system-reservoir interaction description is to establish a clear separation of timescales and to control the accuracy of the approximations we undertake. We can usually make the three following approximations:

²⁹Note that these approximations can fail to capture the effects of the interaction of the system with its environment e.g. in the configuration where the timescales of the system-environment interaction is comparable to those characteristic of the open system.

2. Theory of open quantum systems

1. *Weak-coupling (or Born) approximation* [105]: the system-environment interaction is weak, so that the dynamics of the open quantum system does not affect the dynamics of the environment. In other words, the characteristic time scale of the time evolution of $\rho_S(t)$ is such that it can always be assumed that $\rho_E(t) = \rho_E(t_0)$ and treats the two systems as uncorrelated. This assumption allows to write the initial state

$$\hat{\rho}_{tot}(t_0) \approx \hat{\rho}_S(t_0) \otimes \hat{\rho}_E(t_0) \quad (2.23)$$

2. *Markov approximation*: the relevant time scale of the system is much larger than the time scale over which the environmental correlation functions decay³⁰.

Thus, the time evolution of $\rho_S(t)$ only depends on its actual state and not on its past states.

3. *Rotating-wave (secular) approximation*: this approximation consists in neglecting fast oscillating terms (with regard to a characteristic time scales of the system)³¹. There exist two different manners to implement this type of approximation.

In the rotating-wave approximation (RWA), the fast oscillating terms appearing in the Hamiltonian expressed in the interaction picture [250, 318] are dropped. In the secular approximation (SA) on the other hand, terms appearing in the master equation for the reduced density operator, written in the interaction picture are removed [105, 319].

2.3.2 The Lindblad master equation

Within these approximations (the Born-Markov approximation), the time evolution of the density matrix $\hat{\rho}$ is governed by the so-called Lindblad master equation (or Gorini-Kossakowski-Sudarshan-Lindblad [320]), which reads in its most general form [105, 287, 321–325]

$$\frac{d\hat{\rho}_S(t)}{dt} = \frac{1}{i\hbar} [\hat{H}_S, \hat{\rho}_S(t)] + \sum_{k=1}^{N_S^2-1} \left[L_k \hat{\rho}_S(t) L_k^\dagger - \frac{1}{2} (L_k^\dagger L_k \hat{\rho}_S(t) + \hat{\rho}_S(t) L_k^\dagger L_k) \right]. \quad (2.24)$$

Here $\hat{\rho}_S$ is the density matrix of the system, \hat{H}_S is the system Hamiltonian on the Hilbert space \mathcal{H}_S , of dimension $N_S = \dim \mathcal{H}_S$.

The superoperators L_j are the so-called Lindblad (or quantum jump, or collapse) operators. They are not necessarily Hermitian and they can be time-dependant. They have to be bounded and fulfill the property $\sum_j L_j^\dagger L_j = 1$. Their maximum number is $N_S^2 - 1$, one less than the square of the dimension of the system. The operators L_j model the different dissipation channels.

In what follows, we will drop the subscript S to lighten the notations, i.e. $\hat{\rho}_S \rightarrow \hat{\rho}$, $\hat{H}_S \rightarrow \hat{H}$, and $\mathcal{H}_S \rightarrow \mathcal{H}$.

³⁰In a nutshell, time scales related to the environment are fast, whereas time scales related to the system are slow. See e.g. ref. [105] for more details.

³¹Intuitively, the terms with fast frequencies will average to zero when integrating over a period.

It can be convenient to introduce $\hat{L}_k = \sqrt{\gamma_k} \hat{\Gamma}_k$, with the γ_k 's being non-negative quantities, and the dissipator superoperator

$$\mathcal{D}[\hat{\Gamma}_j]\hat{\rho} = \hat{\Gamma}_j\hat{\rho}\hat{\Gamma}_j^\dagger - 1/2(\hat{\Gamma}_j^\dagger\hat{\Gamma}_j\hat{\rho} + \hat{\rho}\hat{\Gamma}_j^\dagger\hat{\Gamma}_j). \quad (2.25)$$

so that the master equation Eq. (2.24) can be written as

$$i\hbar \frac{d\hat{\rho}(t)}{dt} = [\hat{H}, \hat{\rho}(t)] + \sum_j \gamma_j \mathcal{D}[\hat{\Gamma}_j]\hat{\rho}(t). \quad (2.26)$$

Each quantum jump operator $\hat{\Gamma}_j$ is associated with a dissipation channel (decoherence and loss processes) occurring at the characteristic rate γ_j .

We should also point out that the jump operators $\hat{\Gamma}_k$ do not need to be Hermitian, despite the fact that by inverting the situation, it is always possible to interpret them as resulting from a continuous measurement of Hermitian operators having an effect just on the environment. In the specific situation where all the $\hat{\Gamma}_k$'s are Hermitian, the master equation can be seen as a continuous measurement of the system operators $\hat{\Gamma}_k$. The Lindblad equation contains more physics than the Schrödinger equation (which is obtained in a limit).

Also note that the Lindblad equation (2.26) implies the trace-preserving property of the master equation³² i.e. $\text{Tr}\left(\frac{d\hat{\rho}}{dt}\right) = 0$, which guarantees probability conservation.

Derivation of the Lindblad master equation. There are many ways to derive the Markovian master equation (see, e.g. [105, 287, 317, 323, 326]). The master equation in the Lindblad form can be derived in (at least) two distinct ways:

- A microscopic and specific derivation which has to be carried out for each type of system under consideration.
- A general and abstract derivation which does not relate directly to a particular system [321, 322].

Computational aspect. In general, the resolution of the master equation for the determination of the density matrix $\hat{\rho}(t)$ admits no analytic solution and must therefore be solved numerically. While in theory this can be done with an arbitrary high precision [327], it can lead to computational challenges due to the exponential scaling of the size of Hilbert space. The exact simulation of the time evolution given by the master equation is therefore often prohibited and computational improvement without resorting to other methods (see subsection 2.5.2) seems to be limited [328, 329].

Adjoint master equation. The Liouvillian super-operator \mathcal{L} allows also to express the dynamics of the Heisenberg operator $O_H(t)$, corresponding to the time-independent operator \mathcal{O} in the Schrödinger picture. The dynamics of $O_H(t)$ is governed by the so-called adjoint master equation and reads

³²Due to the cyclic property of the trace.

$$\frac{d}{dt}O_H = \mathcal{L}^\dagger(O_H) = \frac{i}{\hbar}[H, O_H] + \sum_{k=1}^{N_S^2-1} \gamma_k \left(A_k^\dagger O_H A_k - \frac{1}{2} \{A_k^\dagger A_k, O_H\} \right). \quad (2.27)$$

Non-Markovian dissipation. Let me note the existence of non-Markovian dynamics. Numerous quantum systems exhibit pronounced memory effects [309–311, 330–337]. Memory effects of the environment originates from correlations in the initial system-environment state, nonlocal correlations between environmental degrees of freedom, and structured spectral densities [309, 310].

2.3.3 Environment types and modeling approaches

The environment of an open quantum system can be of various type and can be constituted of several different microscopic degrees of freedom as elementary constituent. A correct accounting of the effect of the environment on the dynamics of the system of interest does not necessarily require an *explicit* definition of the microscopic structure of the environment. The degree of accuracy with which the environment must be accounted for a given model to be relevant varies considerably. Some scenarios allow for approximations that significantly simplify the description of the system dynamics, without compromising the accuracy of the model. In others, the system dynamics shows extreme sensitivity to details of the environment, and requires a precise and detailed model.

In the following, we will introduce some common types of environments. We will also discuss how the environment can be effectively modeled, the coupling to a system of interest, the different regimes that can arise.

Bosonic and fermionic environment. This thesis tackles open quantum systems subject to irreversible dynamics: in absence of external driving, the system relaxes toward equilibrium due to its coupling to its environment.

This behavior requires an environment of infinite size (infinite number of degrees of freedom) in order to prevent quasi-periodic recurrences. In fact, irreversibility requires a continuous energy spectrum [338, 339]. However, every physical environment is of finite size, and thus has discrete energy levels. A good way to model an environment for irreversible dynamics is to take a continuous infinite set of finite systems, whose characteristics depend on the type of environment we want to model.

An ubiquitous type of quantum environment is an infinite set of quantum harmonic oscillators. This can model a gas of bosons or an environment composed of a large number of degrees of freedom oscillating around their equilibrium point.

2.3.3.1 Bosons

An environment consisting of a set of infinitely many bosonic modes (one dimensional harmonic oscillators) labeled by the continuous frequency parameter ω can be described by the standard Hamiltonian of the form

$$\hat{H}_{\text{bos}} := \int_0^\infty d\omega \hbar \omega \hat{b}^\dagger(\omega) \hat{b}(\omega), \quad (2.28)$$

where $\hat{b}^\dagger(\omega)$ ($\hat{b}(\omega)$) is a bosonic creation (annihilation) operator of the mode at frequency ω obeying the canonical commutation relations

$$[\hat{b}(\omega), \hat{b}(\omega')] = 0, \quad \text{and} \quad [\hat{b}(\omega), \hat{b}^\dagger(\omega')] = \delta(\omega - \omega'). \quad (2.29)$$

where $\delta(\omega)$ denotes the Dirac delta function.

It is worth noticing that the density of modes $g(\omega)$ of the reservoir is in general frequency-dependent.

This Hamiltonian models the interaction of a system with degrees of freedom obeying the Bose-Einstein statistics such as photons and phonons.

Note that the Hamiltonian defined in Eq. (2.28) is quadratic in the creation and annihilation operators. This leads to a Gaussian dynamics of the bosonic environment.

The interaction Hamiltonian. By assuming that the system-bath interaction is linear in the bath harmonic oscillator operators, the interaction Hamiltonian can be written as

$$\hat{H}_{\text{int}} = \hbar \int_0^\infty d\omega g(\omega) (\hat{c} + \hat{c}^\dagger) [\hat{b}(\omega) + \hat{b}^\dagger(\omega)]. \quad (2.30)$$

where the $g(\omega)$ is the bath-system coupling strength and \hat{c} denotes exemplarily one of the system's operator. In the specific case of an harmonic oscillator, we have $\hat{c} = \hat{a}$, if the system is a two-level system, we would have $\hat{c} = \hat{\sigma}^-$.

Passing via the interaction picture, we can perform a rotating wave approximation leading to the Hamiltonian³³

$$\hat{H}_{\text{int}} = \hbar \int_{-\infty}^\infty d\omega g(\omega) [\hat{b}^\dagger(\omega) \hat{c} + \hat{c}^\dagger \hat{b}(\omega)] \quad (2.31)$$

Moreover, we assume that the bath-system coupling constant is independent from the frequency and can be written as

$$g(\omega) \simeq g(\omega_c) = \sqrt{\frac{\kappa}{2\pi}} \quad (2.32)$$

³³Moving into the interaction picture using the operator $\hat{U}_I(t) = \exp(i(\hat{H}_S + H_E)t)$, the interaction Hamiltonian (2.30) rewrites

$$\begin{aligned} \hat{H}_{\text{int}} &= \hat{U}_I(t) \hat{H}_{\text{int}} \hat{U}_I^\dagger(t) \\ &= \hbar \int_{-\infty}^\infty d\omega g(\omega) (\hat{c} e^{-i\omega_c t} + \hat{c}^\dagger e^{i\omega_c t}) [\hat{b}(\omega) e^{-i\omega t} + \hat{b}^\dagger(\omega) e^{i\omega t}]. \end{aligned}$$

By developing the Hamiltonian defined in Eq. (2.30), two sorts of terms appear:

the terms $\hat{c}^\dagger \hat{b}$ and $\hat{b}^\dagger \hat{c}$ whose time dependence is given by $e^{-i(\omega - \omega_c)t}$ and $e^{i(\omega - \omega_c)t}$ respectively, and the counter-rotating terms $\hat{b}^\dagger \hat{c}^\dagger$ and $\hat{b} \hat{c}$ evolving according to $e^{i(\omega_c + \omega)t}$ and $e^{-i(\omega_c + \omega)t}$ respectively.

The counter-rotating terms are rapidly varying in comparison to the time dependence of the co-rotating terms, especially when $\omega_c \approx \omega$. As a result, the counter-rotating terms can be left aside.

Assuming $g(\omega)$ to be small, the only interaction terms which will contribute significantly in Eq. (2.31) are those close to resonance $\omega_c \approx \omega$. Thus, the lower integration limit can be sent towards $-\infty$.

where κ will be referred to as decay rate (i.e. the inverse of the lifetime). This approximation is known as the Markov approximation.

2.3.3.2 Fermions

An environment consisting in a set of infinitely many one dimensional fermionic fields can be described by the standard Hamiltonian of the form

$$H_{\text{fer}} := \int_0^\infty d\eta \hbar \eta \hat{a}_\eta^\dagger \hat{a}_\eta, \quad (2.33)$$

with the fermionic creation and annihilation operators \hat{a}_η and \hat{a}_η^\dagger obeying the canonical anticommutation relations

$$\{\hat{a}_\eta, \hat{a}_{\eta'}^\dagger\} = 0, \quad \{\hat{a}_\eta, \hat{a}_{\eta'}^\dagger\} = \delta(\eta - \eta') \quad (2.34)$$

with the definition of the commutator $\{\hat{A}, \hat{B}\} := \hat{A}\hat{B} + \hat{B}\hat{A}$.

This Hamiltonian models the interaction of a system with degrees of freedom obeying the Fermi-Dirac statistics such as electrons, half-integer spin particles or fermionic atoms or nuclei.

Since H_{fer} is also quadratic in the fermionic creation and annihilation operators, the dynamics of the fermionic reservoir is Gaussian, as in the bosonic case.

2.3.3.3 Drive

The previous discussion considered a system weakly coupled to its environment, composed of an infinite number of degrees of freedom.

We will end this part by considering the case where the system coherently exchanges excitations with its environment. Instead of appearing in the dissipative part of the master equation, this will result in an additional effective term in the Hamiltonian. As a typical example, we can consider the coherent driving of a cavity mode by an external laser of frequency ω_0 .

The Hamiltonian describing this coupling has the form

$$\hat{H}_{\text{drive}} = g(\omega_0)(\hat{a}^\dagger \hat{b} + \hat{a} \hat{b}^\dagger), \quad (2.35)$$

where \hat{a} is the annihilation operator for the cavity mode, and \hat{b} of the laser field. Now, we assume the laser to be in a coherent state $|\beta\rangle$ of the operator \hat{b} (i.e. $\hat{a}|\beta\rangle = \beta|\beta\rangle$). Tracing out the environmental degree of freedom, we obtain the Hamiltonian describing a coherent drive

$$\hat{H}_{\text{drive}} = F\hat{a}^\dagger + F^*\hat{a}. \quad (2.36)$$

2.3.4 Intermezzo: example of a single bosonic (cavity) mode

In order to illustrate how this works, we will loose full generality, and write explicitly the master equation for the simple and ubiquitous case of a single bosonic (cavity) mode.

Let us consider a single quantum harmonic oscillator with frequency ω_c , coupled to a set of quantum harmonic oscillators of frequencies ω_j modeling the environmental degree of

freedom. Typically, this could model e.g. the coupling of a single mode of the electromagnetic field in a cavity with its environment in a cavity-QED setup (see [section 1.4](#)). The system, environment and interaction Hamiltonian reads

$$\hat{H}_S = \hbar\omega_c \hat{a}^\dagger \hat{a} , \quad (2.37)$$

$$\hat{H}_E = \hbar \sum_j \omega_j \hat{b}_j^\dagger \hat{b}_j \quad \text{and} \quad (2.38)$$

$$\hat{H}_{SE} = \hbar \sum_j \left(\lambda_j \hat{a}^\dagger \hat{b}_j + \lambda_j^* \hat{a} \hat{b}_j^\dagger \right) , \quad (2.39)$$

where \hat{a} (\hat{b}_j) is the annihilation operator in the system (of the j th mode in the environment) Hilbert space, and λ_j is the coupling strength between the system and the j th mode of the environment.

Assuming that there are no correlations between the system and reservoir at $t = 0$, the initial density matrix is of the separable form

$$\hat{\rho}(t = 0) = \hat{\rho}_S(0) \otimes \hat{\rho}_E . \quad (2.40)$$

By assuming a broadband environment —so that in the time domain, it returns to its steady state value on a time scale far quicker than system dynamics— the density operator describing the environment has no time dependence. We can also assume that the total density matrix will stay separable at all times.

The environment is assumed to be in thermal equilibrium at temperature T , which is described by

$$\hat{\rho}_E = \frac{\exp(-\frac{\hat{H}_E}{k_B T})}{\text{Tr}_E(-\frac{\hat{H}_E}{k_B T})} . \quad (2.41)$$

by following one of the standard procedure to derive the master equation, that can be found for instance in [\[105, 340\]](#), we eventually obtain the Lindblad master equation for the damped harmonic oscillator

$$\frac{d\hat{\rho}}{dt} = \kappa(\bar{n} + 1)\mathcal{D}[\hat{a}]\hat{\rho} + \kappa\bar{n}\mathcal{D}[\hat{a}^\dagger]\hat{\rho} , \quad (2.42)$$

with the dissipator $\mathcal{D}[\hat{a}]\hat{\rho} = \hat{a}\hat{\rho}\hat{a}^\dagger - \frac{1}{2}(\hat{a}^\dagger\hat{a}\hat{\rho} + \hat{\rho}\hat{a}^\dagger\hat{a})$, the decay rate $\kappa = 2\pi\mathcal{D}(\omega_c)|\lambda(\omega_c)|^2$, where $\mathcal{D}(\omega)$ is the density of states of the environment, and $\bar{n} = \text{Tr}_E(\hat{b}^\dagger\hat{b}\hat{\rho}_E)$, the average number of excitations in the reservoir.

2.4 The Liouvillian superoperator

2.4.1 The Liouvillian superoperator

The linearity of the Lindblad master³⁴ equation (2.24) in the density matrix $\hat{\rho}$, makes it possible to recast it into the following synthetic form

³⁴Master equation is a historical name supposing to mean an equation from which all other properties can be derived from.

$$\frac{d\hat{\rho}}{dt} = \mathcal{L}\hat{\rho}, \quad (2.43)$$

where \mathcal{L} is the so-called Liouvillian superoperator [341]. Superoperators are linear operators acting on the vector space of operators. As operators act on vectors to produce new vectors, superoperators act on operators to produce new operators. Let me fix the nomenclature here; in the remaining of this document, operators will be indicated with a hat (e.g., \hat{O}) and superoperators with calligraphic symbols (e.g., \mathcal{O}). Moreover, we will assume a time-independent Liouvillian.

The superoperator \mathcal{L} is trace-preserving and generates a completely positive map $\mathcal{M}_t = \exp(\mathcal{L}t)$.

Eq. (2.43) is a first order homogeneous linear differential equation. Thus, given a system initially in a state described by $\hat{\rho}(0)$, the solution of Eq. (2.43) at a time t is formally given by the theory of ordinary differential equations

$$\hat{\rho}(t) = \mathcal{M}_t[\hat{\rho}(0)] = \exp(\mathcal{L}t)\hat{\rho}(0). \quad (2.44)$$

The structure of Eq. (2.43) also implies that \mathcal{M}_t must satisfy the semigroup property³⁵

$$\mathcal{M}_{t_2}\mathcal{M}_{t_1} = \mathcal{M}_{t_2+t_1}. \quad (2.45)$$

The structure of Eq. (2.44) justifies that the superoperator \mathcal{L} is also called the time evolution generator (note the parallel with (2.6)). \mathcal{L} contains all the information on the dynamics of the system.

Properties. The Lindblad's theorem [321] postulates that the generator of any quantum operation satisfying the semigroup property must have the form:

$$\mathcal{L}\hat{\rho} = \frac{1}{i\hbar}[\hat{H}, \hat{\rho}(t)] + \sum_j \gamma_j/\hbar \left[\hat{\Gamma}_j \hat{\rho} \hat{\Gamma}_j^\dagger - \frac{1}{2} \left\{ \hat{\Gamma}_j^\dagger \hat{\Gamma}_j, \hat{\rho} \right\} \right] \quad (2.46)$$

For a time-independent Liouvillian, and assuming a Hilbert space of finite dimension, there is always at least one steady state [342], i.e., a matrix such that

$$\frac{d\hat{\rho}_{ss}}{dt} = \mathcal{L}\hat{\rho}_{ss} = 0. \quad (2.47)$$

Mathematically speaking, Eq. (2.47) means that the steady-state density matrix is an eigenmatrix of the superoperator \mathcal{L} associated to the zero eigenvalue.

The steady-state density matrix ρ_{ss} does not evolve anymore under the action of the Lindblad master equation, meaning that ρ_{ss} represents the long-time dynamics of the system

$$\hat{\rho}_{ss} = \lim_{t \rightarrow \infty} e^{\mathcal{L}t} \hat{\rho}(0). \quad (2.48)$$

³⁵It is a semigroup because the inverse is not necessarily a member of the group.

Moreover, under quite general conditions (see Refs. [343, 344]), it can be highlighted that the steady state is unique and any initial state converges to it. In particular, Spohn's theorem shows that the Liouvillian for a finite system has a unique steady state, provided the quantum dynamical semigroup is irreducible [345, 346].

Lately, systems that do not satisfy the criteria for Spohn's theorem —and do not reach a unique steady state— have raised considerable interest.

For example, and as we will see in the next chapter (chapter 4), dissipative phase transitions are strictly related to the violation of this unicity condition.

Competition. A master equation such as (2.46) can be seen as a competition between different terms. The effective steady-state will correspond to a compromise.

The first term in the dissipative part removes excitations and the second term adds excitations into the system. Consequently, the system eventually settles down in the steady state (2.47).

The terms coming from the unitary evolution also contribute to the competition and this interaction of unitary and dissipative elements can lead to remarkable effects.

Spaces and dimensions. A note about spaces and dimensions. Let us call \mathcal{H} the Hilbert space of the system. Operators and density matrices belong to the operator space $\mathcal{H} \otimes \mathcal{H}$. The Liouvillian superoperator space, instead, is $(\mathcal{H} \otimes \mathcal{H})^* \otimes (\mathcal{H} \otimes \mathcal{H})$.

2.4.2 Vectorization: the Choi-Jamiolkowski isomorphism

We notice that in the master equation, it is recurrent to multiply the density matrix on both sides, e.g. $\hat{\Gamma}\rho\hat{\Gamma}^\dagger$. From linear algebra courses, we recall that matrices also form a vector space. Hence, we can picture superoperators (such as the Liouvillian) as big matrices multiplying a big vector (the density operator). This idea is formalized using the Choi-Jamiolkowski isomorphism [298, 347–349] or vectorization.

The representation of matrices as vectors on a higher dimensional Hilbert space is referred to as vectorization. It transforms a $p \cdot q$ matrix \hat{A} into a $pq \cdot 1$ column vector denoted by $\text{vec}(\hat{A}) \equiv \hat{A}_\#$ [350].

For example for a 2×2 matrix, we have

$$\hat{A} = \begin{pmatrix} a & b \\ c & d \end{pmatrix} \longrightarrow \hat{A}_\# = \begin{pmatrix} a \\ b \\ c \\ d \end{pmatrix}. \quad (2.49)$$

The following relation illustrates the concept of vectorization

$$|a\rangle\langle b| \longrightarrow |a\rangle \otimes |b\rangle \quad (2.50)$$

Thus, the density matrix can be rewritten as a one dimensional vector, and the superoperators that act on the density matrices can be rewritten as a matrix.

Properties. This vectorization trick is very useful, especially due to two main properties.

The first is related to the Hilbert-Schmidt inner product, defined as

$$\langle \hat{A}, \hat{B} \rangle = \text{Tr}(\hat{A}^\dagger \hat{B}) \quad (2.51)$$

in the vectorized representation, takes the intuitive

$$\text{Tr}(\hat{A}^\dagger \hat{B}) = \text{vec}(A)^\dagger \text{vec}(B) \equiv A_\#^\dagger B_\#. \quad (2.52)$$

The vectorized version of the identity operator is another important relation

$$\mathbb{1} = \sum_i |i\rangle \langle i| \longrightarrow \mathbb{1}_\# = \sum_i |i\rangle \otimes |i\rangle \quad {}^{36}. \quad (2.53)$$

Thus, connecting this result to the normalization of a density matrix leads to

$$\text{Tr}(\hat{\rho}) = \mathbb{1}_\#^\dagger \rho_\# = 1 \quad (2.54)$$

The second useful/not intuitive property is the vectorization of the product of three matrices ABC :

$$\text{vec}(ABC) = (C^T \otimes A) \text{vec}(B) \quad {}^{37}. \quad (2.55)$$

The vectorized master equation. The linearity of the Liouvillian³⁸ allows to represent it as a matrix. These considerations and properties encountered above, allows to write for the general Liouvillian structure such as (2.43):

$$\partial_t \hat{\rho} = \mathcal{L} \hat{\rho} \quad \implies \quad \partial_t |\hat{\rho}\rangle_\# = \mathcal{L}_\# |\hat{\rho}\rangle_\# \quad (2.56)$$

In line with Eq. (2.44), the time evolution of the density operator can then be rewritten as

$$|\hat{\rho}(t)\rangle_\# = \exp(\mathcal{L}_\# t) |\hat{\rho}(0)\rangle_\#. \quad (2.57)$$

The dynamics is now encapsulated by the matrix $\mathcal{L}_\#$. It is then possible to use an eigendecomposition to extract all information from the time evolution. Bipartite positive semidefinite operators

$$\begin{aligned} \mathcal{L}_\# \equiv & \frac{1}{i\hbar} (\mathbb{1} \otimes H - H^T \otimes \mathbb{1}) \\ & + \sum_k \left(L_k^* \otimes L_k - \frac{1}{2} \mathbb{1} \otimes L_k^\dagger L_k - \frac{1}{2} L_k^T L_k^* \otimes \mathbb{1} \right) \end{aligned} \quad (2.58)$$

Note that the crossed product $\mathcal{L}_\#^\dagger \mathcal{L}_\#$ is non-local. Since \mathcal{L} is not Hermitian, its eigenvectors are, in general, not orthogonal.

³⁶Note that the vectorization of the identity is the (unnormalized) maximally entangled Bell state.

³⁷Note that what appears here is not the dagger, but the transpose.

³⁸We have $\mathcal{L}[\alpha_1 \hat{\sigma}_1 + \alpha_2 \hat{\sigma}_2] = \alpha_1 \mathcal{L}[\hat{\sigma}_1] + \alpha_2 \mathcal{L}[\hat{\sigma}_2]$ for any operator σ_j , and for any complex number α_j .

Dimensions. Within the procedure of vectorization, if we are initially working in a Hilbert space of dimension $\dim(\mathcal{H}) = N$, the density operator —a matrix of dimension $N \times N$ — becomes a vector of size N^2 . The Liouvillian becomes a matrix $N^2 \times N^2$. Except for some very rare cases where the quantum master equation can be solved analytically, in general, the quantum master equation needs to be solved numerically to determine the time evolution of $\hat{\rho}$. This can be done with arbitrarily high precision [327]. Nevertheless, because of the exponential scaling of the size of Hilbert and Liouville space, the computational effort can rapidly become challenging.

On the one hand, the exact diagonalization of the Liouvillian can be extremely memory consuming due to the quartic scaling of the Liouvillian superoperator with respect to Hilbert space of the system that is already of exponentially large dimension. On the other hand, a direct time evolution implies to time evolve a $N \times N$ density matrix, which can also turn out to be computationally challenging.

It may be worthwhile to use other methods, such as the stochastic method presented in subsection 2.5.1 or the phase space methods presented in chapter 3.

2.4.3 Spectral properties of the Liouvillian superoperator

When considering closed systems, the eigendecomposition³⁹ of the Hamiltonian provides all the informations on the system [75, 351]. Indeed, the diagonalisation of \hat{H} makes possible to express the system dynamics in terms of the energies and eigenvectors of \hat{H} . In open quantum systems obeying the quantum Lindblad master equation, this role is awarded to the eigendecomposition of the Liouvillian superoperator.

Assuming a Liouvillian $\mathcal{L}_\#$ of dimension $N^2 \times N^2$, the diagonalisation provides us with a set of (complex⁴⁰) eigenvalues λ_j and eigenmatrices (eigenstates) $|\hat{\rho}_j\rangle_\#$ such that

$$\mathcal{L}_\# |\hat{\rho}_j\rangle_\# = \lambda_j |\hat{\rho}_j\rangle_\# \quad (2.59)$$

with $j = 0, 1, 2, \dots, N^2$. Moreover, the left and right eigenvectors will in general be different, and we have

$$_\# \langle \hat{\sigma}_j | \mathcal{L}_\# = _\# \langle \hat{\sigma}_j | \lambda_j, \quad (2.60)$$

where $_\# \langle \hat{\sigma}_j |$ is the left eigenvectors of the Liouvillian $\mathcal{L}_\#$.

Physically, the eigenvalues λ_j represent the timescales of the system, while the eigenvectors $\hat{\rho}_j$ correspond to the states explored along the system dynamics.

Since all the eigenvalues have negative real part ($\text{Re}(\lambda_j) \leq 0$), it is convenient to order the eigenvalues by their real part, so that

$$|\text{Re}(\lambda_0)| \leq |\text{Re}(\lambda_1)| \leq |\text{Re}(\lambda_2)| \leq \dots \quad (2.61)$$

A typical Liouvillian spectrum is depicted in Fig. 2.3. A noticeable feature is the reflexion symmetry of the eigenvalues with respect to the real axis. This is due to the fact that the Lindblad master equation Eq. (2.43) preserves Hermiticity such that

$$\mathcal{L} \hat{\rho}^\dagger = (\mathcal{L} \hat{\rho})^\dagger. \quad (2.62)$$

³⁹In linear algebra, the eigendecomposition corresponds to represent a matrix in terms of its eigenvalues and eigenvectors.

⁴⁰Note that the eigenvalues are complex since the Liouvillian is non-hermitian.

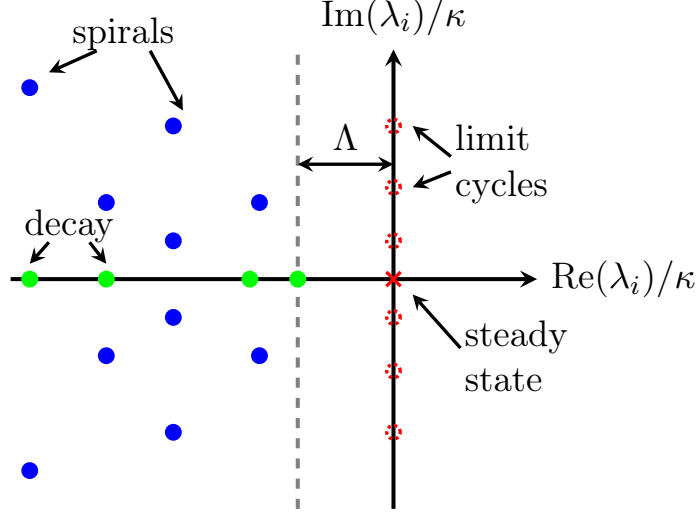


Figure 2.3: Schematic view of the spectrum of the Liouvillian \mathcal{L} . The eigenvalues lie on the negative complex plane, and the complex-valued eigenvalues exist in complex conjugate pairs. The losses in the system are caused by the eigenvalues depicted by solid circles. The real part contribution of the eigenvalues induces decay, the imaginary part oscillations. The red cross represents the steady state, the eigenvalue that survives in the infinite time limit. Λ is the Liouvillian gap: it determines the slowest non-zero rate of convergence towards the steady state. The eigenvalues laying on the imaginary axis (red dashed circles) induce limit cycles.

This implies that for each eigenvalue of \mathcal{L} , we can write $\lambda_j = \text{Re}(\lambda_j) + i\text{Im}(\lambda_j)$ with $\text{Im}(\lambda_j) \neq 0$, its complex conjugate $\lambda_j^* = \text{Re}(\lambda_j) - i\text{Im}(\lambda_j)$ is also an eigenvalue of \mathcal{L} .

Note that in the special case where the Liouvillian superoperator corresponds to the description of a closed system the eigenvalues are purely imaginary.

The Liouvillian spectrum provides the steady state and all the dynamical features of an open quantum system. Indeed, according to Eq. (2.57), all properties can be determined by exponentiating and therefore by the spectral properties of $\mathcal{L}_\#$.

The low-lying part of the Liouvillian spectrum turns out to be particularly useful in several problems, where the nontrivial role of the Liouvillian long-lived metastable states allows to correctly determine the scaling towards the thermodynamic limit.

This is particularly the case in the study of dissipative critical phenomena such as dissipative phase transitions [49, 75], (boundary) time crystals [1, 352, 353], synchronization [354] and dissipative freezing [355]. Dissipative phase transitions and time crystals will be the subject of the next chapter.

Starting at the origin of the complex plane, we retrieve the steady state density matrix

$$\hat{\rho}_{ss} = \frac{\hat{\rho}_0}{\text{Tr}(\hat{\rho}_0)}, \quad (2.63)$$

associated to the eigenvalue $\lambda_0 = 0$.

Another set of eigenvalue and eigenstate of particular interest are λ_1 and $\hat{\rho}_1$ that correspond to the slowest time dependent process present in the dynamics of the

system. The timescale of the associated process is determined by $\Lambda = \text{Re}(\lambda_1)$, called the *Liouvillian gap* or *asymptotic decay rate*. As we will see in the next chapter, the Liouvillian gap plays an important role in the study of dissipative phase transition and dissipative time crystals.

Spectral decomposition of density matrices. Consider a system that admits a single steady state. The condition of its physicality imposes to a density matrix to be Hermitian, positive-definite with trace equal to one. Knowing the Liouvillian spectrum it is possible to determine the time evolution of an open quantum system. Indeed, any initial state can be recast as

$$\hat{\rho}(t=0) = \hat{\rho}_{ss} + \sum_{j \geq 1} c_j \hat{\rho}_j \quad (2.64)$$

Then, knowing $\hat{\rho}_j$ and λ_j , we can determine the time evolution of any density matrix by applying

$$\hat{\rho}(t) = \hat{\rho}_{ss} + \sum_{j \geq 1} c_j e^{\lambda_j t} \hat{\rho}_j. \quad (2.65)$$

Tricky numerical simulations. Let's examine a moment from a computational perspective, and assume that we are interested in the steady state ρ_{ss} , or Liouvillian gap Λ of an open quantum system.

As we mentioned previously, $\{\lambda_1, \hat{\rho}_1\}$ corresponds to the slowest process present in the dynamics of the system, and therefore, λ_1 is small or approximately zero. This is not an issue if an exact eigendecomposition of the Liouvillian is possible. On the contrary, methods based on a time evolution e.g. master equation, quantum trajectory or truncated Wigner approach are needed (due to e.g. memory issues, due to the $N^2 \times N^2$ size of the vectorized Liouvillian), this becomes a problem since the system has to be time-evolve for a very long time.

2.5 Various open quantum system methods

In both closed and open quantum systems, the computational complexity scales exponentially with the system size. Moreover, in addition to the exponential scaling due to the system size, the computational cost is even quadratically larger in OQS than in closed systems, because of the need to work with density matrices.

The explicit matrix representation of operators [356] allows, in principle, an exact diagonalisation by brute force using standard numerical software packages. While this may work when dealing with small systems, it becomes numerically infeasible when multiple modes come into play, or if these modes are fairly populated.

The use of sophisticated computational modeling and simulation methods are required to obtain the desired results⁴¹.

⁴¹It is interesting to notice that while it is experimentally easier to obtain the stationary state of an open quantum system, compared of preparing a closed system in its ground state, it is (quadratically) more difficult to numerically simulate open quantum systems than closed system on a classical computer.

In recent years, great steps forward have been made. In this part, we review some methods that are commonly used to solve the quantum master equation. The first class of techniques we will be focusing on are the stochastic approaches. These methods are based on an exact numerical treatment of the full Hilbert space of the problem. We will then address other methods.

2.5.1 Stochastic approaches

Within this formalism, the deterministic dynamics described by the Markovian master equation in the Lindblad form defined in Eq. (2.24) for the density matrix is *unraveled* into a stochastic differential equation for a pure quantum state.

In trajectory-based methods, quantum effects are included via the concept of *quantum trajectories*, which can be traced back to the early work by de Broglie and Bohm [357, 358]. A quantum trajectory corresponds to a single solution for one realization of the noise, and the unraveling is not unique.

The master equation is then reproduced by averaging the solutions over all realizations of the noise.

In the early 1990s, different implementations of stochastic approaches have emerged, among them the *jump methods*—divided in Monte Carlo wavefunction simulations (MCWF) (Dalibard, Castin, Molmer), and the quantum trajectories techniques (Zoller, Carmichael)—and the quantum state diffusion (QSD) methods (Diosi, Gisin, Percival...) [359, 360].

These algorithms were developed in order to study various open-quantum system phenomenons like laser cooling [361–365], continuous measurements [366, 367], the generation of non-classical states of light [368], and the modeling of a single radiating atom [369, 370].

While all of these approaches are mathematically essentially equivalent, the numerical implementations differ. Hereafter, we will focus on the quantum trajectories techniques.

2.5.1.1 The quantum trajectory technique

Quantum trajectory techniques [361, 362, 368, 371] can be applied for any open quantum system whose dynamics can be described by the quantum master equation in the Lindblad form Eq. (2.24).

The method. To begin with, recall the Lindblad operators, also called jump operators L_k ($L_k = \gamma_k^{-1/2}\Gamma_k$) and note that the Lindblad master equation Eq. (2.24) can be expressed in the alternative form

$$i\hbar \frac{d\rho}{dt} = \frac{1}{i\hbar} (H_{\text{eff}}\hat{\rho} - \hat{\rho}H_{\text{eff}}^\dagger) + \sum_m \hat{L}_m \hat{\rho} \hat{L}_m^\dagger.$$

H_{eff} , a non-Hermitian “effective” Hamiltonian including a decay part, and is defined by

$$H_{\text{eff}} \equiv H - \frac{i\hbar}{2} \sum_m \hat{L}_m^\dagger \hat{L}_m.$$

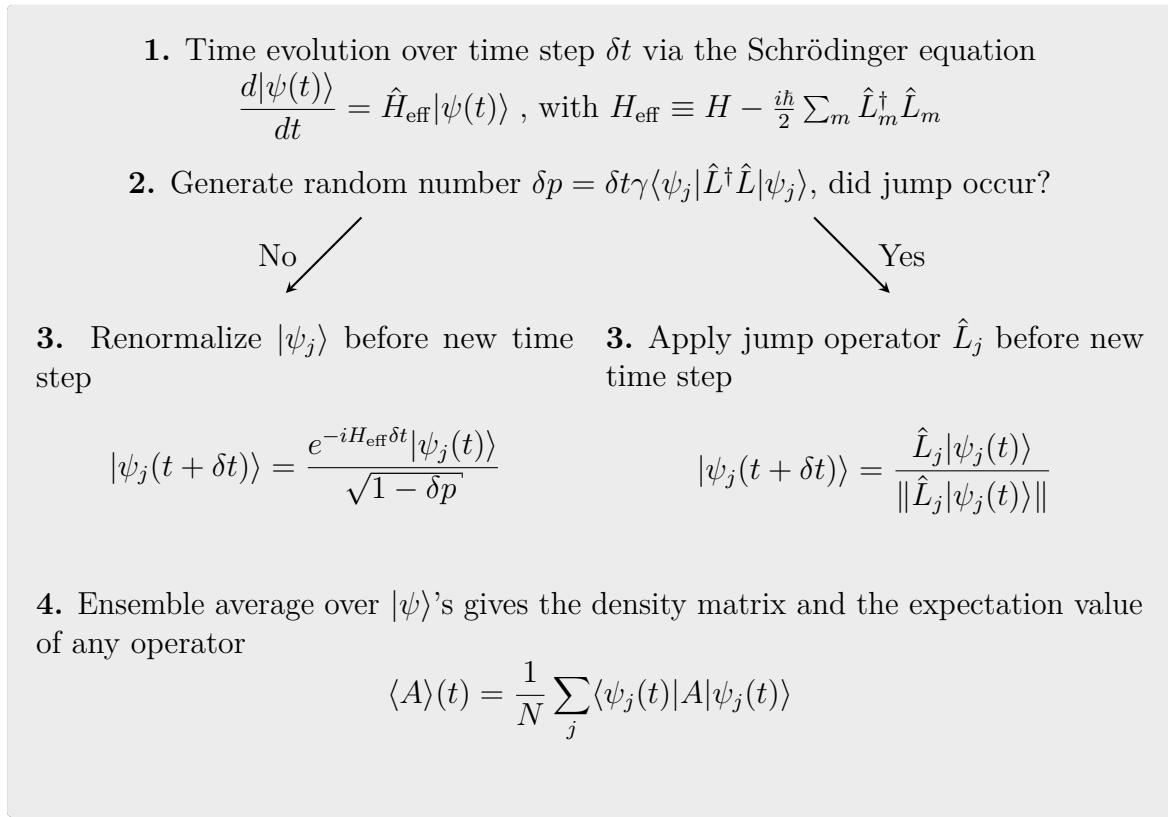
With this in mind, let us jump into the formalism.

This method provides numerical solution of a master equation without propagating a density matrix directly.

Instead, pure states are propagated in time under the non-Hermitian effective Hamiltonian H_{eff} , and experience quantum jumps —sudden changes in the state— at certain points in time, defined with a certain probability.

The solution of the quantum master equation is then retrieved by taking an appropriate stochastic average over all the obtained trajectories. The stochastic average is weighting the different times at which the jumps occur and all of the different types of jumps that can occur. Expectation values can be reconstructed within well-controlled statistical errors.

This formalism is particularly interesting with respect to continuous measurement theory, as it can provide physical insight into the effects of the dissipative process on the physical system.



Motivations. The quantum jump method can be motivated twofold:

- On the one hand, the quantum jump method is a computational tool that allows the unraveling of the quantum master equation into a set of quantum trajectories.

Within this formalism, the master equation is rewritten as a stochastic average over individual realizations (trajectories), evolving in time as pure states.

Assume a system with Hilbert space dimension N .

The resolution of the quantum master equation which requires to time evolve a full density matrix —an object of size N^2 — in time, is replaced by the propagation of a state vector of size N only. The significant reduction of the dimension of the numerical problem makes larger systems tractable.

However, there is no such thing as a free lunch, and this benefit in terms of computational resources should be balanced with the stochastic sampling. Indeed, if one is interested in ensemble statistics, many trajectories can be needed in order to minimize statistical errors⁴². On a computational aspect, this method can be highly parallelized, but trajectories are not orthogonal (redundancy).

- On the other hand, the quantum jump method is a physical model reflecting the dynamics of *single realizations* of small quantum systems. The method provides physical interpretation for the physics induced by the environment on single realizations of the system. In fact each individual trajectory can be considered as physical. Its evolution in time will depend on how the system is observed, in accordance with the quantum measurement theory. Within the framework of this method, we obtain insight into the dynamics of the system by measuring the environment.

Equivalence to the master equation. It is possible to prove that the stochastic propagation is equivalent to the master equation (see e.g. [371])

Different unraveling. There are different unraveling methods like e.g. the photon (jump) counting unraveling method and the Homodyne and heterodyne unraveling methods (see e.g. [373] for details).

Further details on this method would go beyond the scope of this section. Additional details, references, examples of applications, as well as details of its physical interpretation can be found e.g. in refs [371].

2.5.2 Other approaches

A lot of other techniques constitute the vast constellation of methods for the simulation of open quantum systems. Hereafter, we propose a small overview of some of them. More details can be found e.g. in this review and references therein [315, 374].

Analytical model. First, there are some (rare) analytically solvable models [52, 243–249, 375–377] and integrable models [312, 378–381].

Also, the Keldysh formalism [382–385], based on the mathematical object of the non-equilibrium Green’s function (NEGF), or the diagrammatic expansions like the linked-cluster expansion [386, 387], provide a systematic way to study non-equilibrium systems [388].

Mean-Field. A simple approach to the master equation is the (coherent) mean-field approximation, which also exists in closed systems. Fluctuations are disregarded by replacing field operators with their expectation values⁴³.

⁴²For these methods to be efficient, it is important that the required sample remains smaller than N , the size of the Hilbert space. Even if there is no clear cut in the advantage compared to direct master equation simulation [372], some many body open quantum systems occur to have so many degrees of freedom that even a single copy of the full density matrix would exceed all memory limits.

⁴³This comes down to a coherent state Ansatz.

This approach leads, for example, to the Gross-Pitaevskii equation [126]⁴⁴ or Lugiato–Lefever equation [389]. The validity of such approaches is strongly limited to semiclassical behaviour, typically arising in the limit of large occupation, but they may be the only workable ones.

Tensor network. Simulation techniques based on tensor network aim to describe the “physical corner” of the Hilbert space, i.e., it only considers the quantum states that are most relevant to describe the dynamical and steady states properties of the quantum systems.

A particularly suited method for low-entropy systems is the so-called Corner-Space Renormalization (CSR) method [390, 391], where the goal is to target a small corner of the Hilbert space hosting the relevant states for the density matrix.

Variational methods. The variational methods approximate the true state “as close as possible” by a variational state with a few adjustable parameters.

In the vast family of variational methods, the gaussian trajectory method combines quantum trajectories with a Gaussian Ansatz [87, 126, 371, 392].

Density-Matrix Renormalization Group. These variational methods based on a faithful representation of the density matrix formalized in tensor networks [374], in terms of either Matrix-Product States (MPS) or Matrix-Product operators (MPO) for systems in 1 dimension, and Projected Entangled-Pair States (PEPS) in 2D. The guiding idea in tensor networks is to write the state of the full system as a contraction over local tensors. This method can be generalized to a master equation for open quantum systems [393, 394].

Recently, several groups converged in parallel to a method, combining the quantum monte-carlo approach with a variational neural network ansatz [395–398].

Factorized solution. The assumption of a factorized density matrix, leads, for example, to the Gutzwiller monte carlo approach [399–401]. This “refined mean field methods” method can be generalized into the cluster Gutzwiller method [69, 402]. The factorized solution shows limitations for capturing non-local correlations.

Phase-space methods. Finally, the phase space methods are based on the fact that quantum mechanical states can be described as quasi-probability distributions in phase-space. Of particular importance is the Truncated Wigner Approximation [126], effective in the semiclassical limit characterized by high occupation and positive Wigner functions. The approximation in this case consists of neglecting derivatives of order higher than two, typically proportional to interaction constants. Noise enters both the initial conditions and the dissipative evolution. This method will be detailed in the next chapter.

⁴⁴The (time-dependent) GPE is commonly known as the (cubic) nonlinear Schrödinger equation (NLSE) in other areas of physics and in mathematics.

Numerically exact approaches. There is also a variety of numerically exact approaches that were worked out over the last two decades [311].

These approaches can be used to describe features that aren't accurately expressed by other methods. The hierarchical equations of motion [403–405], path integral methods [406–408], and Dissipation-Assisted Matrix Product Factorization [409] are examples of exact approaches.

Chapter 3

Truncated Wigner method for simulating dissipative many-body dynamics

The Truncated Wigner Approximation (TWA) approach provides a paradigm for the numerical simulation of open quantum many-body systems. A crucial point in the theoretical study of non-equilibrium systems is to go beyond the classical analysis provided by standard mean field approximations by incorporating quantum fluctuations into the model.

Precisely, the TWA is a phase space method that provides a practical framework for solving the dynamics of a quantum system near the classical limit [410].

This chapter articulates around four points. First, we provide a general introduction, meant as a road-map for this chapter. Then, we lay the groundwork for the TWA, introducing the general framework of phase space methods. Next, we propose a digest unwinding of the derivation of the TWA. Finally, we address some important remarks and explicit a simple example of application. This method has been the race horse in the two results presented in the next two chapters. Ah-lon-zee!

Contents

3.1	The Truncated Wigner formalism	66
3.2	Phase-space representations of quantum optics	69
3.3	The Weyl-Wigner phase-space representation	70
3.3.1	The Weyl and Wigner transformations	71
3.3.2	Expectation values	73
3.3.3	Operator correspondences	74
3.3.4	The multi-mode generalization	75
3.4	Time evolution of the Wigner function	75
3.4.1	Partial differential equation for the Wigner distribution	76
3.5	From PDE to FPE : the Truncated-Wigner approximation	76
3.6	The Truncated Wigner-function Fokker-Planck equation	77
3.7	Expectation values within the TWA formalism	78

3.8	Remarks	79
3.8.1	Accuracy	79
3.8.2	Limitations of this numerical technique	79
3.8.3	Single trajectory interpretation	79
3.8.4	Extensions	79
3.8.5	Exact limit	80
3.8.6	Connection with path-integral approach	80
3.9	Application to the driven dissipative harmonic oscillator	80

3.1 The Truncated Wigner formalism

Introduction The truncated Wigner approximation (TWA) [126, 318, 410–421] is a common and convenient approach to simulate weakly interacting bosons in the limit of a large mode occupation, where direct diagonalization approaches [422] become computationally impossible and standard mean-field approximations are too coarse to capture some important physical properties.

Motivation As discussed in [chapter 2](#), the exponential growth of the Hilbert space dimension with the number of particles¹ makes the numerical approaches challenging. Concretely, imagine we want to simulate $M = 100$ interacting bosons on classical computers. Further, we assume that the state of the system is encoded in double². A double needs 64 bits or 8 bytes of memory and thus, a complex number needs 16 bytes. Imagine we cut the Hilbert-space of each mode j at $N_j = 99 + 1$ excitations. The size of the total Hilbert-space is³ $\dim(\mathcal{H}) = 10^{100}$. To fit the state vector describing this system into a computer, we would need $\sim 10^{91}$ Gigabytes. This number can e.g. be compared to 10^{82} , the estimated total number of atoms in the (observable) universe [424]. This definitely does not fit into the memory of my personal computer and illustrates the fact that the simulation of the master equation for systems with no particularly low numbers of modes and excitation numbers nor approximation, is computationally challenging [137].

From another side, standard mean-field approximations ([chapter 2](#)), such as the Gross-Pitaevskii (GP) equation [425–429], treat the dynamics of the macroscopically occupied wave function, but neglect atomic correlations and fluctuations [430]. This turns out to be a coarse approximation/bad description for numerous cases, especially when modes with low occupation become relevant.

For example, experiments involving Bose-Einstein condensates (BEC) of ultracold atoms are not always well modelled by the GP equation in general [431, 432].

The general idea The TWA method describes efficiently the dynamics beyond the mean-field level, by taking into account both thermal and leading-order quantum fluctuations.

¹This led to the trademark “Hilbert space is a big place!” [423].

²Double-precision floating-point data type.

³Here, we do not consider some refined applicable truncations like e.g. imposing $\sum_{j=1}^N N_j \leq N_{max}$.

This approach is non-perturbative, and while quantum fluctuations are not incorporated exactly, they can be well approximated. Their effect on the dynamics of the system enters by (see also Fig. 3.1)

- a) the initial value of the complex field is sampled over the Wigner quasi-distribution of the initial quantum state. As a result, each unoccupied mode is populated by fluctuations equivalent to one half of a particle.
- b) the coupling to a reservoir is modeled by additional noise sources leading to stochastic equations of motion i.e. classical random process are used to mimic quantum mechanics.

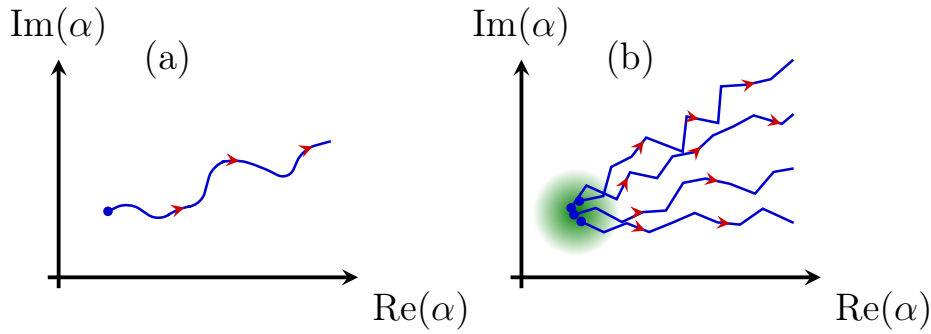


Figure 3.1: Schematic representation of the time evolution in phase space, obtained with the Gross–Pitaevskii equation (GPE) method in (a), and with the truncated Wigner method in (b). The red arrows indicate the flow of time. In (a), the GPE evolution brings deterministically an initial state (blue point) to a further time. In (b), the TWA method stochastically time evolve an initial states (blue points), taken within a specific distribution (green area).

Applications of the TWA method. The Truncated Wigner method found numerous applications in quantum optics [287] and cold atom systems [414, 431, 433–435] (chapter 1), where it predicted and/or explained various phenomena [436]. This includes dynamical instabilities [437], quantum optical parametric oscillators [438], dark solitons [439, 440], decoherence [441], and squeezing [442, 443].

While the TWA was traditionally used in various interacting spinless bosonic systems, the method was recently extended to broader situations. It was e.g. successfully applied to study the dynamics of the Dicke model [444], spinor condensates [445], or the delicate computation of multi-time correlation functions [419].

In general, excellent agreement between the theoretical prediction of the TWA and experiments are reported [432, 446].

The TWA method. In this chapter, we provide an overview (in a condensed way) of the main key ingredients, tools and concepts involved in the derivation of the truncated Wigner method. More details can be found e.g. in ref. [287, 413, 447]. The plan of this chapter goes with the flow of the derivation of the TWA method and is as follows.

Phase space representation. First of all, the truncated Wigner formalism is part of the broad class of *phase space methods*, and thus is based on the formulation of quantum mechanics in phase space. We will present an overview of the phase space representation in [section 3.2](#). An important ingredient in the Truncated Wigner formalism is the coherent state phase space [\[142, 144\]](#), which was introduced in [chapter 1](#). Indeed, the starting point consists in expressing/expanding the density matrix $\hat{\rho}$ in the over-complete set of coherent states $|\alpha\rangle$, with $\alpha \in \mathbb{C}$ [\[415\]](#).

Wigner phase-space representation. The TWA is a method based on the Wigner quasi-probability distribution function [\[287, 318\]](#) of a bosonic mode⁴. We will discuss the aspects of the Wigner phase space representation in [section 3.3](#). In particular, we will see the Weyl and Wigner transform, the Wigner function (or Wigner quasi-probability distribution) and the computation of expectation values of symmetrized product of operators. The considerations will be made on a single bosonic field—in order to dodge the notational cumbersomeness inherent to the full many-mode problem—but the results can be easily expanded to the multi-modes case.

From master equation for $\hat{\rho}$ to PDE for W . We will see in [section 3.4](#) that in general, the Lindblad master equation—describing the evolution of the density operator—(see [chapter 2](#)) can be mapped exactly into an equivalent third-order differential equation for the quasi-probability Wigner function [\[318, 448\]](#). The resulting partial differential equation (also called Wigner-Moyal time-evolution equation or in this context Fokker Planck-like equation) is exact and is equivalent to the master equation.

From PDE to FPE: the truncated Wigner approximation. The motivation behind this step-by-step reasoning resides in the observation that any Fokker-Planck equation (FPE) with a positive-definite diffusion matrix can be recast as a stochastic differential equations (also called Langevin equations) [\[449, 450\]](#).

In a first step, the PDE for the Wigner quasi-probability distribution function is “truncated” by mean of the truncated Wigner approximation. Under certain conditions [\[318, 450\]](#)—broadly speaking with a high number of excitations in each mode or small nonlinearity—the third order derivative terms can be neglected. The resulting equation is a FPE. This step will be addressed in [section 3.5](#).

From FPE for W to SDE for bosonic fields The obtained FPE—a differential equation for the truncated Wigner function (following this truncation, the Wigner function is positively defined)—can be mapped to a stochastic differential equation (SDE) for the bosonic fields (phase-space variables). This mapping is exposed in [section 3.6](#). More specifically, the determination of a coherent (in a not quantum optical sense) initial condition will also be discussed.

Expectation values. To finish our trajectory in the truncated Wigner formalism, in [section 3.7](#), we show that the expectation values of symmetrized products of operators [\[126, 412\]](#) can be retrieved by averaging over a set of interdependent stochastic trajectories.

⁴A bosonic mode can be described with the ladder operator \hat{a} and \hat{a}^\dagger (see [chapter 1](#)).

Épilogue and application to a single bosonic mode. We then close the chapter by making some remarks on the TWA in [section 3.8](#). In particular, we discuss the limitations of this numerical technique and the physical interpretation of single truncated Wigner trajectories.

Finally, in [section 3.9](#), we provide a concrete illustration of the truncated Wigner method by applying it to a driven dissipative harmonic oscillator.

3.2 Phase-space representations of quantum optics

Phase-space representations. There are several mathematical formulations of quantum mechanics [\[451\]](#). Among them, the Schrödinger wave function and Heisenberg matrix formulations were the first to be established in 1925⁵.

Another approach is the Feynman path integral introduced in 1948⁶.

A further approach tackling quantum mechanics is the *phase-space formulation* (See refs. [\[142, 144, 411, 453–458\]](#) for the pioneering works and [\[287, 459–462\]](#) for textbook treatments). It is based on quasi-distribution functions and Weyl’s correspondence [\[463, 464\]](#) establishing a correspondence between quantum-mechanical operators defined on a Hilbert space and ordinary functions in phase space.

This formulation has recently attracted increasing interest propelled by its numerous applications in quantum optics [\[415\]](#), e.g. in the field of cold atoms (see e.g. Ref. [\[410\]](#) for a review), or in quantum technologies, especially for state tomography [\[465, 466\]](#). From the dawning of quantum mechanics, drawing on the classical phase space formulation, many theoretical works have explored the possibility of formulating quantum mechanics using exclusively the language of phase space variables.

Within this context, several phase space functions playing a similar role of the probability distribution for the phase space variables in classical physics have been developed, including the Wigner quasi-probability distribution function⁷ [\[411\]](#), the Glauber-Sudarshan P-representation [\[142–144, 287, 318, 414, 456, 467–469\]](#) and the Husimi Q-representation [\[470, 471\]](#).

Beside these phase space functions, the capture of the additional layer of quantum fluctuations characteristic of quantum mechanics is treated by mean of statistical theories. Within this framework, it is necessary to have a full parametrization Ω of the phase space. This parametrization can e.g. be in terms of position and momentum coordinates or eigenvalues of the annihilation operators.

Phase-space formulation of a bosonic system A system of M bosonic modes can be represented using the annihilation and creation operators, respectively \hat{a}_j and \hat{a}_j^\dagger , with $j = 1, \dots, M$ (see [chapter 1](#)). These satisfy the commutation relations

$$[\hat{a}_i, \hat{a}_j^\dagger] = \delta_{ij} \quad \text{and} \quad [\hat{a}_i, \hat{a}_j] = [\hat{a}_i^\dagger, \hat{a}_j^\dagger] = 0. \quad (3.1)$$

⁵This formulation builds around kets and operators in Hilbert space and was developed by Heisenberg, Schrodinger, Dirac among others.

⁶This approach was already suggested by Dirac [\[452\]](#), but one had to wait the important work of Feynman [\[406\]](#) to have a complete construction.

⁷It is called a quasi-probability rather than a probability distribution because it is not necessarily everywhere positive.

Coordinate-Momentum representation. The phase space can be constructed in complete analogy with classical physics by placing on an equal footing the c-number corresponding to canonical pairs of position and momentum (or any two quadratures associated with orthogonal angles)⁸.

In quantum physics, this is realized in order to satisfy Heisenberg's principle preventing the simultaneous exact determination of the momentum and the position [472].

Coherent state representation. A coherent account of the concepts of coherent states, needed in this part, was tackled in chapter 1. In particular, we have seen that for a coherent state $|\alpha\rangle$ with $\alpha \in \mathbb{C}$

$$\langle\alpha|\hat{x}|\alpha\rangle \sim \text{Re}(\alpha) \quad (3.2)$$

$$\langle\alpha|\hat{p}|\alpha\rangle \sim \text{Im}(\alpha) , \quad (3.3)$$

so that the conjugate pair (α, α^*) of the coherent state can be regarded as phase-space parametrization for the bosonic field⁹.

Hereafter, all considerations will be developed using a coherent-states phase space parameterization, but it would be equivalent to present this in position and momentum representation.

3.3 The Weyl-Wigner phase-space representation

Introduction. The successive works of Wigner [411], Weyl [463], Moyal [457], von Neumann [454], Groenewold [455], Berezin [458] and others led to the Wigner phase space representation.

Foremost, the Wigner quasi-distribution function —obtained via the expansion of the density operator $\hat{\rho}$ in the overcomplete set of coherent states $|\alpha\rangle$ — provides a complete representation in phase space of the density matrix.

The Wigner quasi-distribution function corresponds to a quantum moment-generating functional, by enabling the computation of the expectation values of quantum operators, analogously to classical probability distribution of phase space variables.

On another side, Weyl's correspondence introduces a map between functions in phase space and operators living in a Hilbert space.

Finally, the expectation values of symmetrically ordered product of operators is obtained by averaging over the Wigner distribution.

The Wigner functions have found a significant number of applications in various fields, both experimental and theoretical [473–482]. The strong analogy to classical mechanics makes it a powerful tool in the study of the quantum-classical transition [483–485].

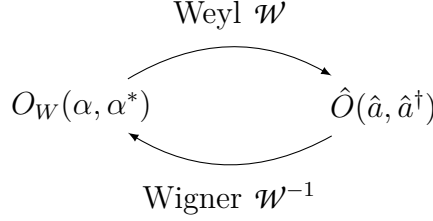
In the subsequent section, we will address the major ingredients of this approach in the simple case of a single mode of a bosonic field.

⁸The dimension of the phase-space is twice the configuration-space's dimension.

⁹Note that α, α^* are treated as independent variables.

3.3.1 The Weyl and Wigner transformations

The Wigner-Weyl transform¹⁰ for bosons [462, 486] is a one-to-one (invertible) mapping between an arbitrary quantum operator $\hat{O}(\hat{a}, \hat{a}^\dagger)$ defined on a Hilbert space (e.g. a quantum observable) and a classical function $O_W(\alpha, \alpha^*)$ defined in the phase space (e.g. classical observable):



Wigner transform The Wigner transform¹¹ \mathcal{W} is a mapping from an arbitrary operator $\hat{O}(\hat{a}, \hat{a}^\dagger)$ (written in the second quantization) on a Hilbert space¹² to its *Weyl symbol* $O_W(\alpha, \alpha^*)$, a function defined on the phase space and defined through [453, 487]

$$O_W(\alpha, \alpha^*) = \mathcal{W}[\hat{O}(\hat{a}, \hat{a}^\dagger)] = \frac{1}{2} \iint d\eta d\eta^* \left\langle \alpha - \frac{\eta}{2} \left| \hat{O}(\hat{a}, \hat{a}^\dagger) \right| \alpha + \frac{\eta}{2} \right\rangle e^{\frac{1}{2}(\eta^* \alpha - \eta \alpha^*)}, \quad (3.4)$$

where $|\alpha\rangle$ denote coherent states, and η is a complex variable¹³. An important observation is that \hat{O} is Hermitian if and only if O_W is real valued.

There are two other convenient and equivalent definitions of this transform.

- a) By defining the *Wigner operator*^{14,15} as the displaced parity operator $\Delta(\alpha) = \hat{D}(\alpha)\Pi\hat{D}^\dagger(\alpha)$ with the displacement operator $\hat{D}(\alpha) = \exp(\alpha\hat{a}^\dagger - \alpha^*\hat{a})$ and the parity operator $\Pi = e^{i\pi\hat{a}^\dagger\hat{a}}$ ¹⁶, the Wigner transform can also be written as [488–490]

$$O_W(\alpha, \alpha^*) = 2 \operatorname{Tr}(\hat{O}\Delta(\alpha)). \quad (3.5)$$

- b) By defining the *quantum characteristic function* (also called moment-generating function)

$$\chi_O(\alpha) \equiv \operatorname{Tr}(\hat{O}\hat{D}(\alpha)), \quad (3.6)$$

we have

$$O_W(\alpha, \alpha^*) = \frac{1}{\pi} \int d^2\eta \chi_O(\eta) e^{\eta^* \alpha - \eta \alpha^*} \quad (3.7)$$

¹⁰Also called Wigner-Weyl representation, correspondence or quantization.

¹¹Or sometimes called inverse Weyl transform.

¹²It is possible to unwind this reasoning either with the phase space variables \hat{x} and \hat{p} , or equivalently with the bosonic operators.

¹³Here, the integral is over the configuration space and the integration measure is defined as $d^2\eta/\pi^2 = d\eta d\eta^*/2 = d\operatorname{Re}\eta d\operatorname{Im}\eta/\pi$ where $|\eta\rangle, \eta \in \mathbb{C}$ is a coherent state. $d^2\lambda/\pi = d\operatorname{Re}[\lambda] d\operatorname{Im}[\lambda]$.

¹⁴The Wigner operator is also sometimes called kernel, seed operator or Stratonovich-Weyl kernel.

¹⁵The Wigner operator is Hermitian.

¹⁶Note that the parity operator can also be expressed as $\Pi = (-1)^{\hat{a}^\dagger\hat{a}} = \int dx |-x\rangle\langle x|$.

The Wigner transformation admits an inverse [410, 453]: the *Weyl transformation*.

Weyl transform. The Weyl transform is a mapping from functions on phase space to operators in Hilbert space [463, 491] and is given by

$$\hat{O} = \mathcal{W}^{-1}[O_W] = \frac{1}{\pi} \int d^2\eta \chi_O(\eta) \hat{D}^\dagger(\eta) \quad (3.8a)$$

$$= \frac{1}{\pi} \int d^2\eta O_W(\eta) \Delta(\eta) \quad {}^{18}, \quad (3.8b)$$

Operator ordering. Provided that the Weyl symbol $O_W(\alpha, \alpha^*)$ only contains terms linear in α and α^* the corresponding operator $\hat{O}(a, a^\dagger)$ is uniquely defined. An ambiguity however arises if $O_W(\alpha, \alpha^*)$ contains products like $\alpha\alpha^*$: while the two functions $\alpha\alpha^*$ and $\alpha^*\alpha$ are identical, since the classical phase space variables α and α^* commute, they lead to two different operators upon applying the Weyl transform. In order to define uniquely the quantum mechanical operator, one need to specify an ordering rule.

Within the Weyl-Wigner formalism, the operators are symmetrically (or Weyl) ordered¹⁹.

A symmetrically ordered product of operators is denoted by $\{\cdots\}_{sym}$ and corresponds to the average of all ways of ordering the operators. We have e.g.

$$\{\hat{a}\hat{a}^\dagger\}_{sym} = \frac{1}{2} \{\hat{a}\hat{a}^\dagger + \hat{a}^\dagger\hat{a}\}. \quad (3.9)$$

The Moyal product [455, 491]²⁰ and Bopp operators [492–494]²¹ are practical tools in Wigner-Weyl quantization facilitating the computation of symmetrized products.

3.3.1.1 The Wigner function

The Weyl symbol of a density matrix $\hat{\rho}$ is of particular interest, and corresponds to the *Wigner phase-space quasi-distribution* or *Wigner function* [410, 411, 486]²²

$$W(\alpha, \alpha^*) = \rho_W(\alpha, \alpha^*) = \frac{1}{2} \iint d\eta d\eta^* \left\langle \alpha - \frac{\eta}{2} | \hat{\rho} | \alpha + \frac{\eta}{2} \right\rangle e^{\frac{1}{2}(\eta^* \alpha - \eta \alpha^*)}. \quad (3.10)$$

Thus the Wigner function is the phase-space distribution associated to the density matrix. It allows the computation of expectation values of symmetrically ordered operators.

¹⁷The Weyl symbol corresponds to the Fourier transform of the symmetrically-ordered quantum characteristic function of the operator.

¹⁸An advantage in the Wigner function (with respect to other quasiprobability distribution functions) lies in the fact that the same kernel is used for transforming the Wigner function to the operator and for the reverse transformation.

¹⁹There are three types of ordering of operators : the normal ordering, the symmetric ordering and the anti-normal ordering.

²⁰Moyal product, which is the phase space product related to the Weyl transform, is denoted by \star_M .

²¹The Bopp operators provide a natural interpretation of commutation relations through jumps in the classical phase space.

²²Presented in 1932 by Eugene Wigner.

Properties of the Wigner function

- Any density matrix can be mapped to a Wigner function (see [287] for a proof). The Wigner distribution and density matrix contain the exact same informations.
- Since any (physical) density matrix is Hermitian, it can be showed that the Wigner function is a real-valued function.
- The Wigner function is not positively defined on the whole phase space for a general density matrix. For this reason, it is often referred to as the Wigner quasi-probability distribution. In the case where the Wigner function is positive, it behaves like a probability distribution for the phase space variables α and α^* .
Conditions for non-negativity of the Wigner quasi-probability distributions have been worked out. While for pure states this corresponds to Gaussian states [495, 496], it is still ongoing work in the case of mixed states [497, 498].
- For any physically valid density matrix, the Wigner function is normalized such that

$$\frac{1}{\pi} \int d^2\alpha W = 1. \quad (3.11)$$

3.3.2 Expectation values

Weyl symbols of quantum operators and the Wigner function provide a complete phase-space description of a given system.

A key property of the Weyl transform is that for two operators \hat{A} and \hat{B} we have (see e.g. [487])²³

$$\text{Tr}(\hat{A}\hat{B}) = \frac{1}{\pi} \int d^2\alpha A_W(\alpha, \alpha^*) B_W(\alpha, \alpha^*). \quad (3.12)$$

It follows from (3.12) that the expectation value of a symmetrically ordered operator \hat{O} in the state defined with the density matrix $\hat{\rho}$ is given by²⁴ (see e.g. [499])

$$\langle \hat{O}(\hat{a}, \hat{a}^\dagger) \rangle = \text{Tr}(\hat{\rho}\hat{O}) = \frac{1}{\pi} \int d^2\alpha O_W(\alpha, \alpha^*) W(\alpha, \alpha^*) \quad (3.13)$$

Thus—and in complete analogy to an ordinary phase-space probability density—the Wigner function can be used for calculating averages²⁶.

²³Remark that we have $\text{Tr}(\hat{O}) = \frac{1}{\pi} \int d^2\alpha O_W(\alpha, \alpha^*)$ as a direct consequence of $\hat{1} = \frac{1}{\pi} \int_{-\infty}^{\infty} d^2\alpha |\alpha\rangle\langle\alpha|$.

²⁴Note that this is always true, even for negative Wigner functions.

²⁵This equation is correct whether in the Schrödinger $\text{Tr}(\hat{\rho}(t)\hat{O})$ or Heisenberg $\text{Tr}(\hat{\rho}\hat{O}(t))$ picture.

²⁶The Wigner function plays the role of a (quasi) probability distribution. In fact, the Wigner function was historically exactly introduced for this reason.

Expectation value of symmetric ordered operators. In statistics, a probability distribution can be completely characterized by mean of its *moments* $\langle x^n \rangle$ [500]²⁷. The moments of the Wigner distribution correspond to symmetrically ordered operator averages²⁸.

In particular for the case of a product of bosonic operators $\hat{a}^s(\hat{a}^\dagger)^r$ for integers $r, s \geq 0$, we have

$$\left\langle \left\{ \hat{a}^r (\hat{a}^\dagger)^s \right\}_{\text{sym}} \right\rangle = \int d^2\alpha \alpha^r (\alpha^*)^s W(\alpha, \alpha^*). \quad (3.14)$$

Quantum fluctuations As a result of the symmetric averaging, the vacuum $|0\rangle\langle 0|$ receives a virtual occupation of half a particle. In order to yield the correct result of zero occupation in the vacuum mode it is necessary to subtract the virtual half occupation after the averaging is performed.

This population of virtual particles can lead to an ultraviolet divergence if no truncation of the modes (momentum cutoff) is carried out [431].

3.3.3 Operator correspondences

In order to put in context, the operator correspondence will be a crucial result for transforming the master equation into an equation for the Wigner function. The operator correspondences translate the action of the ladder operators \hat{a} and \hat{a}^\dagger on an operator \hat{O} with an equivalent expression defined as the action of differential operators on the associated Weyl symbol. For any Hilbert-Schmidt operator \hat{O} we have

$$\mathcal{W}[\hat{a}\hat{O}] = \left(\alpha + \frac{1}{2} \frac{\partial}{\partial \alpha^*} \right) \mathcal{W}[\hat{O}] \quad (3.15a)$$

$$\mathcal{W}[\hat{a}^\dagger \hat{O}] = \left(\alpha^* - \frac{1}{2} \frac{\partial}{\partial \alpha} \right) \mathcal{W}[\hat{O}] \quad (3.15b)$$

$$\mathcal{W}[\hat{O}\hat{a}] = \left(\alpha - \frac{1}{2} \frac{\partial}{\partial \alpha^*} \right) \mathcal{W}[\hat{O}] \quad (3.15c)$$

$$\mathcal{W}[\hat{O}\hat{a}^\dagger] = \left(\alpha^* + \frac{1}{2} \frac{\partial}{\partial \alpha} \right) \mathcal{W}[\hat{O}]. \quad (3.15d)$$

The correspondence of eq. (3.15) translates immediately to the specific case where the operator is a density matrix i.e. we take $\hat{O} = \hat{\rho}(t)$, and we have $\mathcal{W}[\hat{\rho}] = W(\alpha, \alpha^*, t)$. The correspondences for the density matrix can be used to recast a master equation—expressed in terms of ladder operators—as a partial differential equation for the Wigner function.

²⁷The four first moments are called: mean, variance, skewness, and kurtosis.

²⁸This is found by integrating by parts the expression of the Wigner function in terms of characteristic function and observing that symmetrically ordered moments are identified as derivatives of χ_W at $\lambda = 0$.

3.3.4 The multi-mode generalization

The previous results can be generalized to the multi-mode case of M bosonic modes. For example for an operator \hat{O} and a complex vector of coherent states α , we have

$$O_W(\alpha, \alpha^*) = \frac{1}{2^M} \int d\eta^* d\eta \left\langle \alpha - \frac{\eta}{2} | \hat{O} | \alpha + \frac{\eta}{2} \right\rangle \exp \left\{ \frac{1}{2} \sum_j (\eta_j^* \alpha_j - \eta_j \alpha_j^*) \right\} \quad (3.16a)$$

$$= 2^M \text{Tr}(\hat{O} \Delta(\alpha)) \quad (3.16b)$$

$$= \frac{1}{\pi^M} \int d\eta^* d\eta \chi_O(\eta) e^{\sum_j (\eta_j^* \alpha_j - \eta_j \alpha_j^*)} \quad (3.16c)$$

where $\hat{D}(\alpha) = e^{\sum_j \alpha_j a_j^\dagger - \alpha_j^* a_j}$ is the displacement operator.

On the other hand, taking advantage of the Bopp operators, we can find e.g. the correspondence between the multimode operator products

$$\hat{a}_j^\dagger \hat{a}_k \rightarrow \alpha_j^* \alpha_k \quad \text{for } j \neq k \quad (3.17a)$$

$$\hat{a}_j^\dagger \hat{a}_j \rightarrow \left(\alpha_j^* - \frac{1}{2} \frac{\partial}{\partial \alpha_j} \right) \left(\alpha_j + \frac{1}{2} \frac{\partial}{\partial \alpha_j^*} \right) 1 = |\alpha_j|^2 - \frac{1}{2} \quad (3.17b)$$

$$\hat{a}_j^\dagger \hat{a}_j^\dagger \hat{a}_j \hat{a}_j \rightarrow \left(\alpha_j^* - \frac{1}{2} \frac{\partial}{\partial \alpha_j} \right) \left(\alpha_j^* - \frac{1}{2} \frac{\partial}{\partial \alpha_j} \right) \alpha_j^2 = |\alpha_j|^4 - 2|\alpha_j|^2 + \frac{1}{2} \quad (3.17c)$$

3.4 Time evolution of the Wigner function

In this part we seek to write an equation governing the time evolution of any observable of a system of bosonic modes. The general idea is made of two steps.

A first step consists in mapping the Markovian master equation in the Lindblad form for a density matrix to an equivalent ordinary differential equation for the Wigner quasi-probability distribution.

The second step consists in computing the time evolution of observables.

The starting point is the master equation for a single bosonic mode —written in terms of creation and annihilation operators— discussed in [chapter 2](#) and given by

$$\frac{\partial \hat{\rho}(t)}{\partial t} = \frac{1}{i\hbar} [\hat{H}, \hat{\rho}(t)] + \kappa \mathcal{D}[\hat{a}] \hat{\rho}(t) \quad (3.18)$$

where \hat{H} is the Hamiltonian of the system, describing its coherent evolution. The Lindblad superoperator $\mathcal{D}[\hat{a}] \hat{\rho}(t) = \hat{a} \hat{\rho}(t) \hat{a}^\dagger - \frac{1}{2} (\hat{a}^\dagger \hat{a} \hat{\rho}(t) + \hat{\rho}(t) \hat{a}^\dagger \hat{a})$ account for (incoherent) coupling to the external bath with jump operators \hat{a} and dissipation rate κ .

Typically, the right hand side of eq. (3.18) involves products of the density operator with the ladder operators.

The time-evolution equation for the density matrix eq. (3.18) can be transformed into an equivalent partial differential equation for the Wigner distribution [\[457\]](#), using the recipe of operator correspondences of eqs. (3.15).

3.4.1 Partial differential equation for the Wigner distribution

The mappings (3.15) allow the reformulation of the master equation eq. (3.18) in terms of a partial differential equation (PDE) for the Wigner function

$$\frac{\partial W(\boldsymbol{\alpha}, t)}{\partial t} = \hat{L}(\boldsymbol{\alpha})W(\boldsymbol{\alpha}, t), \quad (3.19)$$

where

$$\hat{L}(\boldsymbol{\alpha}) = - \sum_j \frac{\partial}{\partial \alpha_j} A_j(\boldsymbol{\alpha}) + \frac{1}{2} \sum_{jk} \frac{\partial^2}{\partial \alpha_j \partial \alpha_k^*} D_{jk}(\boldsymbol{\alpha}) + \sum_{jkl} \frac{\partial^3}{\partial \alpha_j \partial \alpha_k^* \partial \alpha_l} \dots \quad (3.20)$$

The indices j and k run over the $2N$ components of the vector of a finite set of continuous variables $\boldsymbol{\alpha} = (\alpha, \alpha^*)$.

Here $A_j(\boldsymbol{\alpha})$ is the *drift vector*²⁹ (first derivative), and $D_{jk}(\boldsymbol{\alpha})$ is the *diffusion matrix*³⁰ (second order derivative), and the equation may contain third or higher order derivatives. The formulation in eq. (3.19) is equivalent to the master equation eq. (3.18). Due to the fact that this PDE contains third or higher order derivatives, it is called a generalized Fokker Planck (Fokker Planck-like or also sometimes Wigner–Moyal) equation for the Wigner distribution [287, 318, 501]³¹.

The PDE of the form given in eq (3.19) and (3.20) is common in quantum optics [450] and are in general difficult to solve numerically.

But we do not sail in sight. Based on the concept of Itô calculus that maps FPE onto a set of coupled SDEs, our goal is to transform the generalized FPE (3.19) into a FPE. There are two conditions necessary that the generalized FPE eq. (3.20) is a FPE:

- a) positive-semidefinite diffusion matrix i.e. the diffusion matrix can be written under the form $D = BB^T$, and
- b) no derivatives of higher order than two.

3.5 From PDE to FPE : the Truncated-Wigner approximation

The PDE involves third- and higher order derivatives with respect to the phase space variable, originating both from the nonlinear term in the Hamiltonian, and loss terms. It can be justified to neglecting the third and higher order derivatives in the generalized FPE [287, 413, 502].

This approximation is called the *truncated Wigner approximation (TWA)*. If in addition the diffusion matrix is positive-semi-definite, the resulting equation becomes a *Fokker-Planck equation (FPE)* for the Wigner quasi-distribution function [126, 137, 412].

²⁹The drift term causes probability to flow deterministically.

³⁰The diffusion term causes probability to spread away from some give point.

³¹It is the quantum-mechanical version of the Liouville equation for a classical phase-space distribution.

Validity criteria for the truncated Wigner method. This powerful approximation is legitimate in the case of weak interaction and large modes occupation. Note that in some cases, such as e.g. the treatment of the Bose-Hubbard model in the framework of a closed system, the diffusion matrix is equal to zero and the SDEs reduce further to a set of nonlinear ordinary differential equations.

The validity of this truncation is not trivial and is discussed e.g. in refs. [410, 416, 431, 432, 503, 504].

Intuitively, the truncation justifies for systems with “almost classical” quantum states, where we expect that the system dynamics is essentially governed by classical equation of motions.

For this case, we expect the Wigner function to behave as a sharply peaked probability distribution centered around a macroscopic mean value. It can be showed [417] that the contribution from the third-order derivative terms is negligible provided the mean value is large^{32,33}.

3.6 The Truncated Wigner-function Fokker-Planck equation

Equivalence FPEs-SDEs. The obtained FPE governing the time evolution of the Wigner function can then be mapped to a set of *stochastic differential equations* (or Langevin equations) [448, 505] for a set complex-valued fields $\alpha_j(t)$ ³⁴.

This partial differential equation can be solved by simulating a “large” number of trajectories governed by the (Itô) stochastic differential equation (SDE).

The theory behind the connection between FPEs and SDEs is described and explained e.g. in ref. [448] and is established via Feynman–Kac formula and Itô rules [507, 508]. This mapping leads to the *truncated Wigner-function Fokker-Planck equation*

$$d\alpha_j = A_j(\boldsymbol{\alpha})dt + B_{ij}(\boldsymbol{\alpha})d\chi_j(t) \quad (3.21)$$

with $B(\boldsymbol{\alpha})$ is the factorized diffusion matrix with $B(\boldsymbol{\alpha})B(\boldsymbol{\alpha})^\dagger = D(\boldsymbol{\alpha})$. The random complex delta-correlated gaussian noise $d\chi_j$ can be decomposed as $d\chi_j = dW_1 + idW_2$, where dW_n are real-valued independent Wiener processes with

$$\overline{dW_n(t)dW_m(t')} = dt\delta_{nm}\delta(t-t') . \quad (3.22)$$

The set of equations defined in (3.21) can be efficiently simulated numerically.

Thus, instead of computing the full Wigner distribution, we obtain the expectation values by averaging over N_{traj} trajectories of the stochastic equations (3.21).

The quantum fluctuations present in this equation accounts for the decay and dephasing.

³²Actually, the third-order derivative terms give a correction to the classical trajectories (quantum scattering processes) [417].

³³Notice that even if a term is small, this doesn’t exclude the possibility that the build-up of this small term during the time evolution leads to distortion.

³⁴In fact, this comes back to solve the FPE using a stochastic Montecarlo approach [506] for the $\alpha_j(t)$ ’s.

Initial condition. Within the TWA method, the initial values of the complex valued field $\alpha_j(0)$ are non-deterministic and are obtained by stochastic sampling in the coherent state phase space according to a given positive semi-definite Wigner distribution $W(\alpha, \alpha^*, 0)$. This is pictured in Fig.3.1.

Thus, the quantum fluctuations are included in the initial condition via the stochastic sampling of a Wigner distribution [414]. This sampling is designed to correspond to the underlying (strictly positive) Wigner distribution³⁵ e.g. normalized random complex gaussian noise.

Accordingly, every unoccupied mode has vacuum fluctuations equivalent to one half of a particle, modeling correctly the uncertainty between conjugate variables [417].

It is thus important to include the modes with low occupation in the initial condition. On the other hand, it is also necessary to truncate the number of modes taken into account to avoid divergences.

The quantum corrections. In this method, the quantum corrections manifest themselves in two ways:

- Stochastic initial condition reconstructing the Wigner distribution. The initial conditions are constructed based on the Wigner transform of the initial density matrix.
- Stochastic evolution due to third order truncation. Quantum scattering processes occur during the time propagation.

Consequently, the TWA allows one to go beyond the mean-field approximation and takes into account quantum fluctuations of lowest-order.

Now that we have the time evolution of the fields, we can access the expectation values.

3.7 Expectation values within the TWA formalism

Finally, the (approximate) expectation values of symmetrically ordered operator expressions³⁶ are obtained by

- integrating Eq. (3.21) over a set α_j of independent time-evolved trajectories, and
- averaging the solution of Eq. (3.21) over the stochastic trajectories.

For a sufficiently number of trajectories and with initial values sampled according to the Wigner distribution $W(\alpha, t = 0)$, we can use the Wigner distribution as in classical probability theory to compute expectation values of (symmetrically ordered) operators as

$$\left\langle \left\{ \hat{O}(\hat{a}, \hat{a}^\dagger) \right\}_{sym} \right\rangle = \overline{O(\alpha, \alpha^*)} . \quad (3.23)$$

³⁵Note that even if this method doesn't allow for the exact inclusion of quantum fluctuations, it can do it approximately by stochastic sampling of a Wigner distribution.

³⁶Notice that other representation returns other ordering for the expectation values: e.g. the P representations returns normally ordered averages.

Here $\{\dots\}_{sym}$ indicates symmetrization, and $\overline{\dots}$ indicates stochastic averages over numerically evaluated truncated Wigner trajectories i.e.

$$\overline{O} \equiv \lim_{N_{traj} \rightarrow \infty} \frac{1}{N_{traj}} \sum_j O(\alpha^{(j)}, (\alpha^{(j)})^*) \quad (3.24)$$

where N_{traj} is the number of stochastic trajectories.

We obtain for example $\left\langle (\hat{a}^\dagger \hat{a})_{sym} \right\rangle = \overline{|\alpha|^2} - 1/2$.

3.8 Remarks

3.8.1 Accuracy

The Wigner approach seems to generate accurate results for the description of optical systems in the large photon limit, where we expect the contribution of the third-order quantum noise to be small.

3.8.2 Limitations of this numerical technique

Approximate nature. This method is intrinsically an approximation due to the truncation procedure. This can in some cases lead to demonstrably wrong results [509]. Attempts to *exactly* map the master equation onto a Wigner representation were undertaken [510]. Yet these attempts didn't result in easily and widely applicable methods.

Ultraviolet divergence. The noise modeling (in an approximate way) the quantum vacuum fluctuations leads to an ultraviolet divergence if all physically allowed modes are included.

Multi-time commutators. The TWA returns symmetrized products of operators, and do not give in general access to quantities like expectation values of time-normally ordered operator products³⁷, unequal time averages like e.g. the different time correlation functions or correlation functions for the full multimode field operator [414, 511]. With the exception of the two-time normally ordered correlation function for coherent initial states [512].

3.8.3 Single trajectory interpretation

In the case of highly populated fields, the behavior of a single trajectory obtained with the TWA corresponds approximately to a possible outcome of an individual experiment [410, 414, 436, 439, 513–517].

3.8.4 Extensions

In recent years, the TWA for bosons as described here has been transposed to study the dynamics of spin-boson systems [414, 416, 518].

³⁷These quantities can however be obtained by within the P representation formalism.

3.8.5 Exact limit

The TWA is exact in the limit of non-interacting modes, which can be used for benchmarking. The TWA is also exact in the fully classical limit, where coherences in the density matrix vanish and the dynamics is governed by classical rate equations.

3.8.6 Connection with path-integral approach

Notably, the TWA including the different concepts of Wigner function, Weyl ordering and quantum corrections, can be recovered within the Feynman's path integral formalism [410, 417].

3.9 Application to the driven dissipative harmonic oscillator

We close this chapter with a concrete application of the TWA method to a simple case of a single mode of a dissipative optical resonator driven by a coherent laser field. The Hamiltonian describing this system is

$$\hat{H} = \hbar\omega\hat{a}^\dagger\hat{a} + \hbar(F\hat{a}^\dagger + F^*a) \quad (3.25)$$

where ω is the frequency of the resonator, and F denotes the driving strength. A realistic model accounting for the dissipative nature of the quantum system is provided by the master equation

$$\frac{\partial \hat{\rho}}{\partial t} = -\frac{i}{\hbar}[\hat{H}, \hat{\rho}] + \frac{\gamma}{2}(2\hat{a}\hat{\rho}\hat{a}^\dagger - \hat{a}^\dagger\hat{a}\hat{\rho} - \hat{\rho}\hat{a}^\dagger\hat{a}). \quad (3.26)$$

By taking this equation as a starting point and by unrolling the reasoning outlined above —among which using the operator correspondences of eq. (3.15)— leads to the equation of motion for the Wigner function

$$\begin{aligned} \frac{\partial W}{\partial t} = & \left[\frac{\partial}{\partial \alpha} \left(i\omega\alpha + \frac{\gamma}{2}\alpha + iF \right) + \frac{\partial}{\partial \alpha^*} \left(-i\omega\alpha^* + \frac{\gamma}{2}\alpha^* - iF^* \right) \right] W(\alpha, \alpha^*, t) \\ & + \frac{\gamma}{2} \frac{\partial^2}{\partial \alpha \partial \alpha^*} W(\alpha, \alpha^*, t). \end{aligned} \quad (3.27)$$

This equation is a FPE with a drift term (the first derivative term in the first line) as well as a diffusion term (the second derivative term in the second line).

This FPE can be mapped onto the SDE

$$d\alpha = (-i\omega - \gamma/2)\alpha dt - iFdt + \sqrt{\gamma/2}dw(t), \quad (3.28)$$

where the dissipative process translates into a diffusive term in the SDE (the last term). The complex Gaussian noise satisfies $\langle dw(t) \rangle = 0$ and $\langle dw^+(t)dw(t) \rangle = dt$. The initial conditions $\alpha(0)$ is sampled from $W(\alpha, \alpha^*, 0)$.

Chapter 4

Dissipative phase transition and dissipative time crystals

Faster, lighter and smaller could be the leitmotiv of future quantum devices. In nanoscale systems, fluctuations around ordered states are of particular importance. This remains true even at absolute zero temperature due to the presence of quantum fluctuations. Whether the fluctuations are of classical (thermal) or quantum nature (or both), they can lead to critical behaviors and trigger the occurrence of phase transitions, with the emergence of new, exotic phases of matter.

This is also true for open quantum system. As discussed in the previous chapter, dissipation and irreversible effects are typically associated with the convergence of a quantum system towards an asymptotic stationary state, by definition invariant under time translations. However, groundbreaking recent works suggest that this is not necessarily the case, leading to the concept of non-stationarity in open quantum manybody systems.

The study of such phase transitions is of paramount importance, both from a fundamental and technological perspective.

This chapter starts in [section 4.1](#) with a review of some basic notions about classical and quantum phase transitions in systems at equilibrium. In open quantum systems, the competition between the coherent and dissipative dynamics can lead to the critical phenomenon of *dissipative phase transitions* (DPTs), which we explore in more details in [section 4.2](#). Then, in [subsection 4.3.1](#) we will introduce the notion of *time crystal*, which is the first observed “out-of-equilibrium” phase of matter. Not only can time crystals be implemented in open quantum systems, but driving and dissipation can even be key to its formation, giving rise to the so-called dissipative time crystals (DTCs). We will address some aspects of DTCs in [subsection 4.3.2](#). In particular, in [section 4.4](#), we will explore the paradigmatic example in quantum optics of the optical bistability occurring in driven-dissipative nonlinear Kerr oscillators. Finally, we will present a numerical

study of dissipative time crystals in an asymmetric nonlinear photonic dimer [section 4.5](#), reproducing the research paper [\[1\]](#) of the author.

Contents

4.1	Equilibrium phase transition	82
4.1.1	Classical phase transitions	82
4.1.2	Quantum phase transition	84
4.2	Dissipative phase transitions	89
4.2.1	Theoretical framework	90
4.2.2	Universal critical behavior and scaling invariance	92
4.2.3	Optical bistability	92
4.2.4	Numerical methods	93
4.3	Dissipative time crystals	93
4.3.1	Time crystals	93
4.3.2	Dissipative time crystals	96
4.3.3	Theoretical description of dissipative time-crystals	97
4.4	One mode critical phenomena: dynamical optical hysteresis in the Kerr model	100
4.4.1	Semiclassical analysis	100
4.4.2	Quantum analysis	101
4.5	Two mode critical phenomena: dissipative time crystal in an asymmetric nonlinear photonic dimer	101

4.1 Equilibrium phase transition

4.1.1 Classical phase transitions

Equilibrium or quasi-equilibrium classical systems are described within the well-established theoretical framework provided by classical statistical physics. Within this paradigm, the physical properties of a system in (thermal) equilibrium allow to classify states of matter into different phases.

Phase of matter. A *phase of matter* corresponds to a region in the space of thermodynamic variables (pressure, temperature, etc.) where the physical properties of a system (e.g. density, symmetries) are the same. Typical examples are the solid, liquid, gas, superconducting, superfluid, and magnetic phases of matter.

Phase transitions. As the name suggests, *phase transitions* [\[519, 520\]](#)¹ are transitions from one phase of matter to another that occur when an external system parameter (e.g. temperature, pressure, magnetic field, chemical potential, external field) varies. They are a prime example of collective phenomenon occurring in macroscopic systems.² Classical phase transitions are accompanied by a critical behavior resulting in an abrupt, possibly discontinuous change in the physical properties of the system. They follow

¹The concept of phase transition is present and attracts attention in a wide variety of physical, chemical, and biological systems and at all energy scales ranging from cosmology [\[521–526\]](#) to high energy physics, as well as in condensed matter physics.

²To be more precise, let us mention that equilibrium phase transitions can only appear in the thermodynamic limit of infinite size/many-particle systems. For finite systems, there exist no-go theorems forbidding such transitions.

from the competition between two processes : entropy maximization on the one hand and energy minimization on the other hand. Energy minimization tends to keep the system in an ordered phase of matter, while entropy maximization tends to push it away from it. In classical phase transitions, the critical behavior is driven only by thermal fluctuations; broadly speaking, ordering is destroyed by thermal fluctuations.³ Widespread examples of classical phase transitions are the liquid-gas transition (non-analyticity of the density) or the paramagnet-ferromagnet transition (non-analyticity of the magnetization). Phase transitions are usually classified into first-order and continuous phase transitions depending on the precise nature of the non-analyticity.

First-order phase transitions. *First order phase transitions*⁴ present a discontinuity in the first order derivative of the free energy with respect to some thermodynamic variables. They involve latent heat and phase coexistence.

Examples of first order thermal phase transitions include the melting of ice due to the thermal motion of the water molecules destroying the crystal lattice, or the ferromagnetic-paramagnetic transition at the Curie point due to the thermal motion of the spins.

Continuous phase transitions. In contrast, for *continuous phase transitions*, the first derivative of the free energy is continuous, with discontinuities only appearing at higher order.⁵ At the transition point, the two phases are indistinguishable; the system does not display coexistence of phases and there is no latent heat.

An example of a continuous phase transition is the ferromagnetic transition of iron at the Curie temperature (770°C), above which the material loses its magnetic properties — the magnetic moment vanishes.

Interestingly, also infinite order continuous phase transitions exist. These do not break any symmetries. A famous example is the Berezinsky-Kosterlitz-Thouless transition in the two-dimensional XY model [528–530].

Critical phenomena and scale-invariance. In the case of continuous phase transitions, the phase transition point —the point in the phase diagram that separates the two phases — is called *critical point* and the behavior near it is referred to as *critical phenomena*.

Close to the critical point both the typical length scale —the correlation length ξ — and typical time scale —the correlation time τ_c — diverge following a power law

$$\xi \propto |t|^{-\nu} \quad \text{and} \quad \tau_c \propto |t|^{-z}, \quad (4.1)$$

where ν (respectively z) is the correlation length (respectively time) critical exponent characterizing the transition. The dimensionless quantity t is a measure of the distance to the critical point (for instance for a thermal phase transition $t = |T - T_c|/T_c$, where T_c is the critical point).

³In contrast, quantum phase transitions are only driven by quantum fluctuations.

⁴The name refers to Ehrenfest’s classification of phase transitions [527].

⁵Ehrenfest further subdivided continuous transitions into second order transitions, third order transitions and so on according to which derivative of the free energy is discontinuous. Today, this subdivision is not used very much because there are few qualitative differences between the sub-classes.

The divergences in (4.1) as $t \rightarrow 0$ trigger a critical phenomena. Long-range correlations emerge, with fluctuations occurring on all length- and time-scales. The system is said to be scale-invariant.

In fact, close to the critical point, all observables in the system depend on t via power laws similar to (4.1) and the behaviour of the system is completely characterized by the set of corresponding critical exponents. This implies a notion of universality.

Spontaneous symmetry breaking. Symmetry is a transformation that doesn't change the physics of the system, i.e. it does not change the expectation values of the physical observables nor the probabilities.

Spontaneous symmetry breaking⁶ (SSB) refers to the fact that the solution of a problem⁷ does not necessarily have the symmetry of the problem.

SSB is a widespread concept in various areas of modern physics — playing a key role in atomic and condensed matter physics, high energy particle physics and even cosmology. It gives rise to a wide spectrum of phenomena observed in nature, such as superconductivity, superfluidity and Bose Einstein condensation, (anti)ferromagnets, any crystal, electroweak interaction, and Higgs mechanism.

A prime example is when the continuous spatial translation symmetry is broken to a discrete one, leading to crystallization (the formation of space crystals). The atoms spontaneously localize in a periodic arrangement across the three dimensional space, e.g. the carbon lattice of a diamond. This is the mechanism at work at the liquid to solid transition.

4.1.2 Quantum phase transition

Up to this point, we discussed some general properties of phase transition occurring at finite temperature where thermal fluctuations are responsible for destroying the ordered phase.

At absolute zero temperature thermal fluctuations are no longer present, but a different kind of phase transition, of quantum nature, can occur.

Quantum phase transitions. *Quantum phase transitions* (QPTs) [48, 531–539] are phase transitions that occur at absolute zero-temperature, between two quantum phases of matter (phases of matter at $T = 0\text{K}$) when a non-temperature parameter such as pressure or magnetic field varies. QPTs rely on the presence of quantum fluctuations, rather than thermal fluctuations as it was the case for classical phase transitions.

Motivation. QPTs have attracted a lot of interest over the past several decades, as the increase of experimental capabilities made it possible to reach the low temperature regime needed for such transitions to appear. Various QPTs have been investigated

⁶A symmetry is broken when a system switches from a symmetric state to an asymmetric one. This can either occur through an *explicit* or the *spontaneous* symmetry breaking process. In the *Explicit symmetry breaking* case, the symmetry is broken by additional objects. In the *Spontaneous symmetry breaking* case, the underlying system remains symmetric but the symmetry is hidden in the ground state.

⁷Lorentz symmetry or translation invariance are examples of symmetries of laws of nature.

and observed experimentally [540–542]. Besides, the creation of entanglement in QPTs [543, 544] is of particular relevance in the field of quantum computation.⁸

This intense research not only led to the explanation of critical behaviors at low temperature, but also to the tailoring of novel states of matter displaying desired features (e.g. superconductors or topological insulators [533, 547–549]).

However, QPTs still remain largely unexplored, and there is a lot to discover, see [550, 551] or last section in [552].

QPTs differ in fact in many ways from their finite-temperature phase transition counterparts. For example, the specific role played by the additional dimension of time corresponds to a fundamental distinction between QPTs and thermal phase transitions. Due to the non-commutativity of position and momentum in quantum mechanics, the spatial and temporal fluctuations are linked together close to the critical point.

Examples. Some paradigmatic examples of QPTs in systems at thermodynamic equilibrium are the

- Bose-Hubbard model and its superfluid-Mott insulator transition [553–559],
- one-dimensional Ising model with transverse magnetic field (shows continuous and first-order quantum transitions) [560–573],
- Dicke-model quantum phase transition [574–580].

A broad spectrum of physical systems can exhibit QPTs, among them magnets [581], superconductors and cold atomic gases [582, 583].

Ground state behaviour under QPT. A quantum system at zero temperature is always in its ground state. To understand QPTs, it is therefore useful to analyse the behavior of the ground state as one approaches the critical point. At the critical point, two qualitatively different ground states compete. A small change in the external parameter controlling the transition then selects one ground state, with the other one becoming the first excited state.

The quantum states on either side of the critical point show different types of order. In the typical scenario, one goes from a symmetric or disordered state, which reflects the symmetries of the Hamiltonian, to a broken-symmetry or ordered state, which does not possess (all of) these symmetries.

In QPTs, order is destroyed by quantum fluctuations instead of thermal fluctuations. More mathematically, for a system modeled with a Hamiltonian $H(g)$, where g is a (dimensionless) control parameter, the QPT occurs at the critical value $g = g_c$ for which the gap $\Delta(g) = E_1(g) - E_0(g)$ between the energy of the first excited state $E_1(g)$ and the energy of the ground state $E_0(g)$ closes, $\Delta(g_c) = 0$. (see fig. 4.2). To keep track of the two different ground states, it is necessary to introduce an order parameter – a quantity that distinguishes the degenerate ground states. The typical behavior in the critical region of the order parameter $O(g)$ and the gap $\Delta(g)$ is depicted in fig. 4.1. At the critical point, the ground state observables are characterized by non-analytical behavior.

⁸E.g. the adiabatic quantum algorithms can be interpreted as a sweep through a quantum phase transition [545, 546].

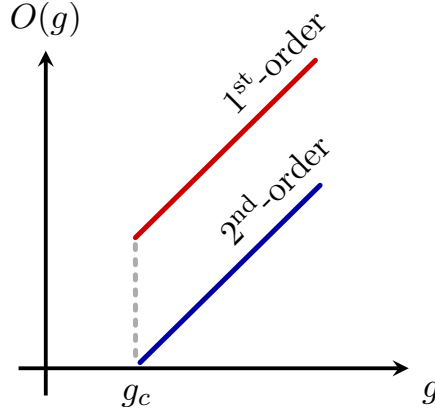


Figure 4.1: Typical behavior of the order parameter $O(g)$ versus the control parameter g in the case of a first (red) and continuous (blue) phase transition.

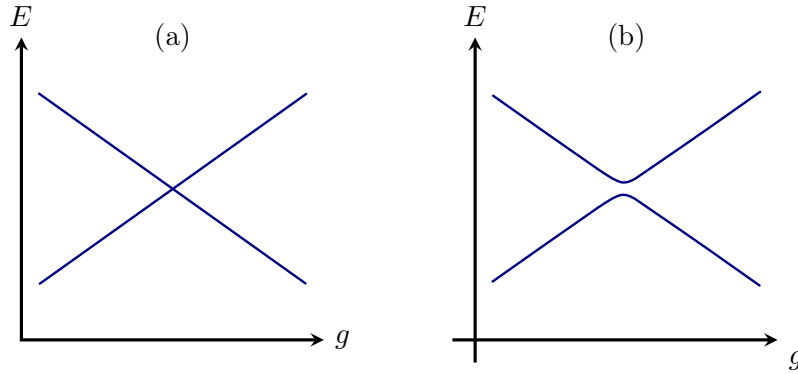


Figure 4.2: Typical behavior of the energy gap at a first (a) and continuous (b) phase transition. In (a) there is an energy level crossing between ground state and the first excited state. In (b) there is no level crossing, but the gap closes when approaching the thermodynamic limit.

Similarly to thermally driven phase transitions, QPTs can be classified into first-order and continuous phase transitions. The two classes are discriminated by how the order parameter $O(g)$ behaves at the critical point, see right panel of Fig. 4.1.

4.1.2.1 First order quantum phase transitions

First order QPTs are characterized, in the thermodynamic limit, by a jump in the order parameter $O(g)$ and a non-analytic change in the ground state properties of the Hamiltonian. In particular, this implies that at the critical point, the derivative of the energy e with respect to the control parameter g

$$\left. \frac{\partial e}{\partial g} \right|_{g=g_c}, \quad (4.2)$$

is discontinuous. First order QPTs have been predicted and observed experimentally [584–588].

There is a strong analogy between first-order quantum and first-order thermal phase transitions. There is no diverging length or time and no scale invariance when tuning the control parameter towards the critical point. In fact, the correlation length exponent is given by $\nu = 1/(d + z)$.

First order quantum phase transitions correspond to energy level crossings at which two different ground states are exactly degenerate. The system is in two different states on each side of the transition, and the system jumps from one state to the other when crossing the transition at $g = g_c$. In the vicinity of the critical point there can be a region with coexistence of the two stable phases, this is the concept of bistability.

Bistability. Bistability is a major feature of first-order phase transitions. It corresponds to the coexistence of the two stable phases with distinct properties. Bistability is at the heart of the phenomenon of hysteresis. The phase in which the system will be depends from which side the control parameter will approach the critical point. We will see more about the phenomenon of bistability in [subsection 4.2.3](#), and [section 4.4](#).

4.1.2.2 Continuous quantum phase transitions

Second order (continuous) QPTs have a continuous order parameter $O(g)$, but there is a gradual change in the ground state properties, between a phase with long range order and a disordered phase [589, 590]. A discontinuity appears in

$$\left. \frac{\partial^n e}{\partial g^n} \right|_{g=g_c}, \quad (4.3)$$

for some $n \geq 2$.

In complete analogy with the classical second order phase transitions, QPTs lead to “quantum criticality”.

Quantum criticality. Two hallmarks of second order QPTs are the scaling hypothesis and universality.

The quantum critical points are characterized by diverging length and time scales [591], leading to temporal and spatial scale invariance. This latter translates into a vanishing characteristic energy scale.

In particular at a critical point, quantum fluctuations are of vanishing energy and spread over all time and length-scales.

Also, a critical point has diverging correlation length⁹ —leading to long ranged entanglement— and relaxation time —leading to the concept of critical slowing down.

Similarly to their classical counterparts, quantum critical regions exhibit universal power-law behaviors¹⁰ with the set of critical exponents completely characterizing the critical behavior.

⁹The correlation length corresponds to the length scale over which some variables —for instance fluctuations— are related.

¹⁰E.g. power-law decay of correlation functions or power law dependence of the observables on the external parameters.

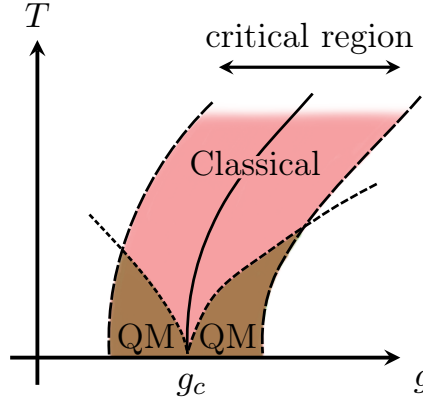


Figure 4.3: Schematic view of the vicinity of the quantum critical point $g = g_c$ in the (g, T) space. Depicted are the critical region, and the part of the critical region dominated by the classical (red) and quantum mechanical (brown) critical behaviour.

For continuous QPTs, the *quantum-classical mapping* establishes an equivalence between a quantum model in d dimensions and an effective classical system in $d + z$ dimensions [532, 536, 560].

In the specific case of multi-critical points in a finite size system, finite size scaling can be used to determine whether the system is subject to first or second order phase transitions [592].

Examples. Examples of second order QPTs are the self-organization of a Bose-Einstein condensate [53, 593], or the paramagnetic to ferromagnetic phase transition¹¹.

4.1.2.3 Extension to Finite Temperatures

While absolute zero temperature is hardly accessible in experiments, it is still possible to detect signatures of quantum phase transitions at low temperatures, as long as quantum fluctuations dominate over thermal fluctuations.

Let us take a system with characteristic energy $\hbar\omega_c$ in thermal equilibrium at temperature T . The system is subject to two types of fluctuations: thermal fluctuations with energy scale $k_B T$ and quantum fluctuations with energy scale $\hbar\omega_c$.

While the quantum transition point $g = g_c$ is present only at $T = 0$, influence of the transition can be detected in a region of “quantum criticality” around g_c , where $\hbar\omega_c > k_B T$, as depicted in fig. 4.3.

This quantum critical region is subject to competition between classical and quantum fluctuations.

4.1.2.4 Symmetry Breaking and phase transitions

Phase transitions are intimately linked with symmetry breaking, which occurs when the ordered ground state does not share the symmetry of the system’s Hamiltonian. QPTs are often associated to a spontaneous symmetry breaking pattern or a change in the topological order. However, it is worth mentioning that phase transitions do not necessarily imply a symmetry breaking.

¹¹The magnets on your fridge door are Ferromagnets.

An example is the thermal first order phase transition between liquid and gas. Both phases share the same symmetries (translation and rotation invariance).

Another example featuring such a symmetry breaking is the quantum phase transition between quantum spin-liquid states.

Finally, the Berezinskii-Kosterlitz-Thouless transition, which has already been addressed, is a continuous phase transition without symmetry breaking.

4.2 Dissipative phase transitions

While phase transitions in systems at equilibrium have been extensively studied, until recently, much less work was devoted to phase transitions in out of equilibrium systems [594, 595]. Different paradigms — both in isolated and open quantum systems — can lead to nonequilibrium dynamics:

- a) quench scenario [596–603]: A parameter of the system undergoes an abrupt change between two values corresponding to different equilibrium phases (closed system). This realm leads to the concept of dynamical quantum phase transition, which has attracted both theoretical [604–614] and experimental [70, 615–623] interests, notably for the realization of time crystals.
- b) let the system time-evolve from a specific initial condition (closed system),
- c) steady-state dynamics of a driven dissipative system (open system).

In this thesis, we will focus on this last case and study non-equilibrium phase transitions occurring in a driven dissipative system. They are called *dissipative phase transitions*.

Dissipative phase transitions. Just like their equilibrium counterparts, non-equilibrium phase transitions are transitions between two phases with distinct properties, separated by a critical point. However, while equilibrium phase transitions come in two different categories — classical or quantum phase transitions — this distinction fades away in non-equilibrium steady-state (NESS) quantum phase transitions. This directly follows from the coexistence of classical and quantum fluctuations, which leads to the occurrence of typical features of both thermal phase transitions and zero temperature quantum phase transitions. On the one hand the ordered phase is continuously connected to a thermal state, which is a feature of thermal phase transitions, and on the other hand the transition is driven by interactions, which is characteristic of quantum phase transitions.

In driven-dissipative quantum systems, the competition and interplay between coherent dynamics and dissipation can lead the system towards a NESS [126, 624, 625], with new, non-equilibrium phases and phase transitions.

The system steady state $\hat{\rho}_{SS}(g)$ depends on g a system and environment parameter. As g is varied, the steady state abruptly changes [49], leading to a dissipative phase transition (DPT) [14, 33, 49, 57, 69, 72, 73, 76, 77, 84, 92, 166, 604, 626–631]¹².

¹²Here, note that DPT is denoted Dissipative Phase Transition and not Dynamical Phase Transition, which is another kind of PT.

Motivations. DPTs occur in very various systems, such as active biological matter [632, 633], self-organized systems and quantum fluids of light [82, 634, 635]. The advent of new experimental techniques allowed their experimental observation. Moreover, the development of tools for manipulating quantum systems has allowed physicists to realize new phases of quantum matter with no equilibrium counterpart, as for example the discrete time crystals (see next section).

Theoretical investigations. The perspective of experimental implementation of DPTs is driving the interest devoted to DPTs [126, 624, 625]. Indeed, the possible observation of DPTs is highlighted in several studies and for various platforms, e.g. for photonic systems [52–56, 60, 62–64, 68, 74, 80, 81, 84, 85, 92, 166, 636, 637], lossy polariton condensates [50, 82, 83] and coupled spins models [69, 71, 72, 79, 349].

Experimental realizations. The experimental advances of the last decade, especially in the controllability, allowed the observations of DTCs in various experimental platforms. Among them, photonic systems are of particular relevance,¹³ and DTCs have been observed and studied e.g. in ultra cold atoms [51, 53, 54, 57, 70, 84, 260, 636, 637, 639, 640], trapped ions [239, 641], exciton-polariton condensates [67, 126], semiconductor microcavity [78], and arrays of coupled cavities QED [642] and circuit QED [60, 92, 166, 643–645].

Let us also mention the case of a strongly driven Jaynes–Cummings system, where the breakdown of photon blockade can lead to a first-order dissipative phase transition [60]. This was recently realised in a circuit-QED experiment [92]. Other examples include the observation of bistability in one-dimensional circuit QED lattices [166], as well as the probing of the dynamic optical hysteresis in the quantum regime [63, 78].

Technological applications. The exploration of driven-dissipative phase transitions in open quantum systems is rapidly increasing, and the development of new nonequilibrium quantum states with controllable properties are of particular interest for applications in quantum sensing and quantum information processing.

To date, the potential of DPTs for technological applications are numerous, and will for sure expand.

For example, quantum sensors based on DPTs [646] are specially robust against disorder or decoherence. Moreover, their quantum properties are highly controlled by the coupling with their environment.

Another example are quantum transducer¹⁴ [647].

4.2.1 Theoretical framework

While the (free-) energy analysis proves to be a valuable paradigm for investigating thermal or quantum phase transitions, it cannot necessarily be applied for the study of their dissipative counterparts.

¹³Photonic systems are particularly suitable to explore dissipative phase transitions described by Bose-Hubbard-like models [126, 624, 625, 638].

¹⁴Quantum transduction convert quantum signals from one form of energy to another. It is an important ingredient of quantum science and technology.

Signatures of quantum critical phenomena in dissipative phase transitions are in the dynamical properties. As we have seen in [chapter 2](#), the Lindblad master equation $\dot{\hat{\rho}} = \mathcal{L}\hat{\rho}$, where \mathcal{L} is the Lindbladian superoperator, and $\hat{\rho}$ is the density matrix, is a valuable equation for the description of open quantum systems.

DTCs are characterized by a non-analytical change of the steady state as a function of a single parameter [\[49, 75\]](#)¹⁵, due to the competition between coherent interactions, drivings, and dissipation.

This thermodynamic non-analyticity can be observed in finite-size systems[\[49, 75\]](#), and where experimentally demonstrated [\[67, 78, 166\]](#).

Dissipative phase transitions of M -th order are characterized with a singularity in a thermodynamic limit¹⁶

$$\lim_{g \rightarrow g_c} \left| \frac{\partial^M}{\partial g^M} \lim_{N \rightarrow +\infty} \text{Tr}(\hat{\rho}_{ss}(g, N) \hat{O}) \right| = +\infty \quad (4.4)$$

N is the thermodynamic parameter, counting the number of sites, modes or particles in the system.

In what follows, we will write $\mathcal{L}(g)$ and $\hat{\rho}_{ss}(g)$ to express the fact that these quantities depend on a parameter g . Thus, we have

$$\partial_t \hat{\rho}_{ss}(g) = 0 = \mathcal{L}(g) \hat{\rho}_{ss}(g). \quad (4.5)$$

The Liouvillian —and in particular its spectrum— are of key interest for the study of DPTs [\[75\]](#). If the Liouvillian spectral gap [\[49\]](#) closes in some thermodynamical limit then we expect a DPT to occur.

At the critical point $g = g_c$, a *dissipative phase transition* (DPT) is signaled by a non-analytic (discontinuous) change in the steady-state density matrix $\hat{\rho}_{ss}(g)$. For a critical point g_c , this translates mathematically to,

$$\lim_{g \rightarrow g_c} \partial_g^n \hat{\rho}_{ss}(g) \rightarrow \infty \quad (4.6)$$

for some integer n . The system is said to undergo a n -th order DPT.

It can be noticed that, in a very similar fashion to the close system case, where the energy gap $\Delta(g)$ of the system's Hamiltonian closes at the critical point, here it is the Liouvillian gap which closes [\[49, 75, 648\]](#). In other words, the eigenvalue $\lambda(g)$ with the smallest nonzero real part (in absolute value) vanishes. The mode associated to this eigenvalue then experiences an infinite lifetime and hence dominates the long-time dynamics of the system. This leads to a slowing down of the system's relaxation towards its steady state. This phenomenon is known as critical slowing down, and it has lately been investigated in driven-dissipative lattice systems as for example in ref. [\[87\]](#).

There exist strong analogies between QPTs and DPTs:

¹⁵To make connection with QPTs, note that the steady state in open quantum systems is the analogous of the ground state in closed systems.

¹⁶For lattice systems, the thermodynamic limit corresponds to the number of sites going to infinity, while for bosons, there is the additional thermodynamic limit characterized by the number of particles per site going to infinity.

	QPT	DPT
Dynamical operator	$H = H^\dagger$	$\mathcal{L} \neq \mathcal{L}^\dagger$
State	Ground state $H \psi_0\rangle = E_0 \psi_0\rangle$	Steady state $\mathcal{L}\hat{\rho}_{ss} = 0$
Transition in the thermodynamic limit	<ul style="list-style-type: none"> • Singularity of some GS observables at critical point • Closing of Hamiltonian gap 	<ul style="list-style-type: none"> • Singularity of some SS observables at critical point • Closing of Liouvillian gap

Examples of DPTs. Here are some paradigmatic examples of DPTs

- first-order transitions in the driven-dissipative nonlinear Kerr oscillators.
- the Dicke model reveals first- and second-order phase transitions, multistability and bipartite entanglement [649–653].

Note that equilibrium phase transitions in systems of one dimension (with only one optical cavity) is prohibited [654], this is not the case in nonequilibrium phase transitions in one dimension.

- The breakdown of photon blockade is the first observation of first order quantum phase transition [60, 92].

4.2.2 Universal critical behavior and scaling invariance

The same critical behaviors present in QPTs can be observed in DPTs, namely critical slowing down, divergence of the spatial fluctuations of the order parameter, as well as power-law behavior.

While DPTs occur in the thermodynamic limit, their marks can already be caught in finite-size scaling. In particular, the analysis of the spectrum of the Liouvillian allows to witness the divergence of the timescales in the system.

4.2.3 Optical bistability

A particularly interesting feature associated to DPTs are optical bistabilities [375, 402, 412, 649, 655–675].

Optical bistabilities are first order dissipative phase transitions characterized by the coexistence—in a generic nonlinear system described within the mean-field approximation—of two distinct stable NESS within a regime of parameters. The effective state of the system depends on the history of the system.

On the contrary, within a quantum treatment going beyond the mean-field analysis—e.g. the Lindblad master equation—a unique solution is predicted [318].

Experimental studies have shown optical hysteresis cycles [663–665, 669, 676, 677], in accordance with the semiclassical mean-field predictions.

The contradiction between the mean-field and quantum approach [375, 656] originates from the quantum fluctuations triggering switches between the two metastable states. The unique steady-state solution corresponds to the average.

A paradigmatic example in quantum optics is the optical bistability occurring in driven-dissipative nonlinear Kerr oscillators. This phenomenon received lot of attention and was intensively studied both theoretically [63, 678] and experimentally [78]. We will discuss the main aspects in [section 4.4](#).

4.2.4 Numerical methods

Let’s get straight to the point: there is no powerful systematic method addressing DPTs. Except for very few specific problems that can be solved exactly [679, 680], numerical techniques have to be used to characterize DPTs. Lots of them are not adequate as they can only describe one-dimensional (e.g., t-DMRG [681]) or infinite-dimensional (nonequilibrium dynamical mean-field theory [682, 683]) situations, or because they simply cannot be applied to nonequilibrium systems (e.g. path-integral Monte Carlo [684]). Moreover, while approximate methods such as mean-field theory have been abundantly used [14, 66, 71, 402, 668, 673, 685–687], they can lead to wrong results [688–690]. This led to the development of various numerical methods and framework to tackle DPTs: variational methods [688, 689], generalized Gutzwiller mean field approximation [686], Keldysh action formalism [382, 384], third quantization [376, 691], and approximate rate equations [690], and the study of exceptional points [692, 693] and Liouvillian gaps [49, 75].

4.3 Dissipative time crystals

4.3.1 Time crystals

Breaking of time translation symmetry. Perhaps one of the most fascinating symmetry breaking pattern, which gave food for thoughts for both scientists and philosophers alike — as showed by the many attempts over time to propose a viable *perpetuum mobile*¹⁷ — is the breaking of time translation symmetry.

While the breaking of spatial translation in crystals or spin rotation in magnets can easily be visualised, time translation symmetry breaking (TTSB) are much less intuitive. In spatial crystals, the continuous translational symmetry¹⁸ in space is broken, with only the discrete translation symmetry of the periodic crystal retained. This is a spontaneous symmetry breaking: while the Hamiltonian (or equations of motion) of the system is invariant under continuous translation symmetry, the ground state of the system (the crystal lattice) is not. Only a discrete translation symmetry remains, corresponding to the lattice spacing. Similarly, the spontaneous breaking of the continuous time¹⁹ translational symmetry can lead to a ground state that is periodic in time, rather than space, with only the discrete time period as a remnant symmetry (see Fig. 4.4). Phases of matter with such ground states are dubbed *time crystals*. See [694, 695] and e.g. [93] for a review.²⁰

¹⁷A *perpetuum mobile* is a machine or arrangement supposed to indefinitely keep in motion. Oh wait, yes, this violates the first law of thermodynamics (energy conservation law).

¹⁸(and rotational symmetry)

¹⁹A little digression here: the existence of “time” (the thermodynamic arrow of time) can be explained by the fact that the universe is not in equilibrium.

²⁰While this definition is rather intuitive, it is not very rigorous. Later, when considering *discrete*

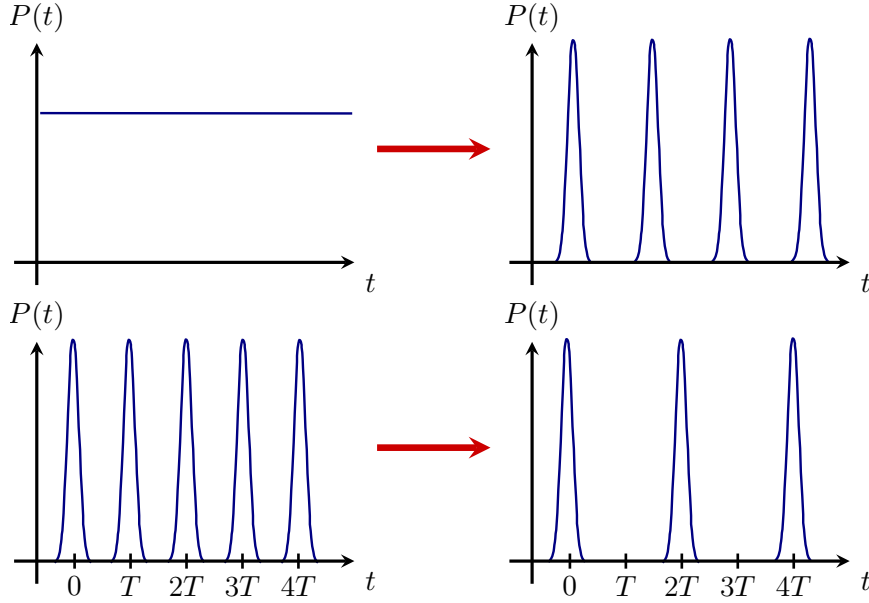


Figure 4.4: Sketch of the behavior of the probability of detecting a system—at a fixed position— versus time leading to the time crystal formation. The case of the spontaneous breaking of a continuous (top) and discrete (bottom) time-translation symmetry is depicted. In the case of the discrete spontaneous symmetry breaking, the initial discrete time-translational symmetry of the system—characterized by a periodicity T — is replaced by another discrete time-translational symmetry, but with another period, here taken to be $2T$.

An entirely new phase of matter. Because it is the ground state—which by definition is the state with lowest energy— itself that is subject to a periodic behavior, time crystals cannot come to rest by releasing energy to the environment. In other words, they cannot reach thermal equilibrium. This makes time crystals the first example of *non-equilibrium matter*²¹, an entirely new phase of matter [696, 697]. It is completely robust, in the sense that no fine-tuning of parameters is needed.

Time crystals and the laws of thermodynamics. There is a crucial difference between spatial and temporal directions. Unlike space, the passage of time is intimately linked with the first and second law of thermodynamics, which state that 1) the total energy of an isolated system is conserved and 2) that the entropy—the amount of randomness or disorder in a closed system— cannot decrease over time. Those laws make the *perpetuum mobile* impossible. So what about time crystals? By definition, their ground state exhibits a perpetual periodic motion. Even though this sounds suspiciously similar to a “perpetuum mobile”, time crystals actually do not break any laws of physics. It turns out that there is no (conventional) kinetic energy associated to this periodic motion— so that the first law is obeyed— and

rather than *continuous* time crystals (breaking respectively discrete and continuous time translation symmetry, the former being the ones that have been observed in experiments) we will provide a more robust definition, which also makes it clear that time crystals are no example of a *perpetuum mobile*.

²¹In contrast to *equilibrium matter* of condensed matter physics such as metals or insulators.

the entropy remains constant — which (marginally) complies with the second law of thermodynamics. Concretely, time crystals are asymptotic non-stationary states, in constant oscillation without addition of energy. These structures have movement even at their lowest energy state.

Discrete time crystals. The pioneering idea and subsequent tweaking gave birth to *discrete time crystals*, a concept first put forward in 2016 [698–700] and soon afterwards experimentally observed [696, 697]. Discrete time crystals²² refer to the spontaneous breaking of the discrete time translation symmetry (dTTS) that can arise in a Floquet system —closed quantum systems subject to a periodic driving.

Concretely, let us consider a Floquet system and call T the period of the driving. The system is not invariant under arbitrary time translations, but retains a *discrete* time translation symmetry (dTTS) corresponding to shifts by a discrete amount $t \rightarrow t + T$. In particular, the Hamiltonian of the system obeys $H(t + T) = H(t)$ for any time t . In a Floquet time-crystal, the dTTS is spontaneously broken: observables present a “subharmonic” response and oscillate with a period that is an integer multiple of the driving period. In other words, the response is only invariant under time translations $t \rightarrow t + nT$ with $n \in \mathbb{N}, n > 1$. As an example, in [700] it was observed that in the regime of strong disorder and interactions, the constituents of a closed spin system organize themselves into a recurring spatial configuration with a period that is doubled with respect to the driving one ($n = 2$) see Fig. 4.4.

An important ingredient for the stability of the emerging discrete time crystal is the presence of strong disorder in the system. This leads to many-body localization [701], preventing the system from absorbing the driving energy [702–704].

Another way of stabilizing the emerging discrete time crystal is through dissipation, and will be discussed in subsection 4.3.2.

The essence of the discrete time-crystalline phase is an emergent, collective, subharmonic temporal response, and can be identified by exhibiting:

- (I) Discrete time-translational symmetry breaking: after a possible transient period, the system oscillates with a period strictly greater than the driving force.
- (II) Crypto-equilibrium: the subharmonic oscillations do not produce any entropy, which allows their infinite persistence in the thermodynamic limit²³.
- (III) Rigid long-range order: rigidity on the subharmonic response. The subharmonic oscillations are synchronized over arbitrarily long distances and time.

To date, an impressive amount of theoretical and experimental works have proven the existence of discrete time crystals [696–698, 700, 705–721]. While strolling in the literature, we can notice that discrete time crystals are often also referred to as π -spin glasses [705] or Floquet time crystals [698].

²²I refrain from using the usual short DTC for Discrete Time Crystal, since this will be used for “Dissipative Time Crystal” (subsection 4.3.2).

²³This ensures that time crystals are not in contraction with the second law of thermodynamics.

4.3.2 Dissipative time crystals

We will now explore the possibility of having a time-crystal phase in open quantum systems. From a general perspective, dissipation, decoherence and fluctuations are expected to induce relaxation towards a stationary steady state and destroy the quantum properties. This is why a lot of efforts have been undertaken to isolate systems from the environment in order to experimentally realize (discrete) time crystals.

However, it turns out that this perspective is too naive. The fine tuning of the coupling parameters of the system to its environment can actually stabilize the persistent periodic motion within the system, instead of destroying it [709, 712, 716, 722, 723], giving rise to so-called *dissipative time crystals* (DTCs).

DTCs [1, 95, 352, 648, 709, 711, 716, 722, 724–748] are many-body open quantum systems exhibiting non-trivial persistent periodic oscillations arising spontaneously in some system observable after a given evolution time and for generic initial conditions, in an otherwise (discrete or continuous) time translation invariant system [722]. What is the stabilization mechanism in DTCs? While discrete time crystals in closed systems are stabilized through disorder, in DTCs, the stabilization mechanism relies on the dissipation into the environment.

It is interesting to point out that a subtype of DTCs are not driven [352]. However, in these cases the driving enters in a particular way, so that its time-dependence can be removed by using a rotating frame [1, 648, 725, 728, 730, 732, 734, 741, 744, 747]. They are therefore realizations of continuous time crystals.

The conditions required for DTCs to arise in finite systems imply the existence of strong dynamical symmetries [722].

The concept of DPT is particularly interesting from the perspective of an experimental realization of time crystals, since in a real world realization, the quantum system would inevitably be subject to some degree of external noise from an environment that cannot be completely suppressed nor controlled. DTC have been observed experimentally e.g. in [728, 729, 749].

The concept of DTC can be interpreted as a critical phenomenon in the spirit of the discussion in subsection 4.2.1 [353].

Continuous dissipative time crystals versus boundary time crystals. There is sometimes confusion in the literature about the distinction between dissipative time crystals and boundary time crystals.

For boundary time crystals, the crystalline behavior is observed at the system boundaries in the thermodynamic limit [352].

It is worth to emphasize that DTCs must be distinguished from their related boundary time crystals [352, 750]. Indeed, these latter are usually considered systems exhibiting sustained oscillations in spite of (and not due to) the dissipation processes. If these systems were taken to the closed limit, they would still oscillate and exhibit Rabi oscillations instead of evolving towards a steady-state (cf. [748]).

From Wilczek’s proposal to experimental observations and technological applications. The existence of time crystals was first argued by Nobel laureate and

physicist Frank Wilczek²⁴ in 2012. He proposed it might be possible for atoms to change over time even while at their lowest energy²⁵, in the classical [695] and quantum [694] domain. This proposal generated a fair amount of excitement and discussions [751–753]. Shortly after the proposal was made, no-go theorems ruling out the occurrence of spontaneous breaking of time translation symmetry in the ground state of equilibrium many-body systems [752, 754, 755] were derived. The essence of the argument is that these systems have time-independent observables by construction.

This crucial insight has guided the explorations towards the possibility of realizing time crystals in *non-equilibrium* quantum systems [352, 698, 700, 705, 706, 722, 727, 730, 734, 756–764], leading to the development of an active area of research [93, 94, 765–773]. Today, number of researchers have conducted experiments that show atoms behaving in ways that could qualify as a time crystal.

Time crystals are expected to be very useful platforms for precision measurements [774, 775] and quantum simulation [776]. Not later than at the end of last year, Google has implemented the first time crystal inside a quantum computer [777]²⁶.

There are several definitions of time crystals for closed [94, 755], coherently driven [94, 696, 697, 756] and incoherently driven systems [732].

4.3.3 Theoretical description of dissipative time-crystals

Let us recall that in the context of Markovian open quantum systems, the time evolution of a system with Hamiltonian H weakly coupled to its environment, is governed by the Lindblad master equation (see chapter 2)

$$\dot{\hat{\rho}}(t) = \mathcal{L}[\hat{\rho}(t)] , \quad (4.7)$$

where $\hat{\rho}$ is the density matrix and \mathcal{L} the Liouvillian superoperator.

We will assume the Liouvillian to be time-independent unless otherwise stated. The formal solution of the master equation (4.7) then takes the form

$$\hat{\rho}(t) = e^{t\mathcal{L}}[\hat{\rho}(0)] , \quad (4.8)$$

and the quantity $e^{t\mathcal{L}}$ has the interpretation of a time-translation operator which propagates the system from the initial time $t = 0$ to the time t .

Since we assume \mathcal{L} to be time independent, one has

$$[e^{t\mathcal{L}}, \mathcal{L}] = 0 , \quad (4.9)$$

time-translation is (trivially) a continuous “symmetry” of the system.

Within the paradigm of open quantum systems, the system is expected to time-evolve towards a unique time independent/stationary steady-state i.e. $\hat{\rho}(t) \rightarrow \hat{\rho}_{ss}$ [see sketch in Fig. 4.5(a)]. The steady-state $\hat{\rho}_{ss}$ respects the time-translational invariance of the generator \mathcal{L} since by definition

$$e^{t\mathcal{L}}[\hat{\rho}_{ss}] = \hat{\rho}_{ss} , \quad (4.10)$$

²⁴He was awarded the 2004 Nobel Prize, and even if it is about time translation symmetry here, it was not for the prediction of time crystals.

²⁵Remark that superconductor can technically carry an electrical current while in its lowest energy state.

²⁶See [778] for a simplified review.

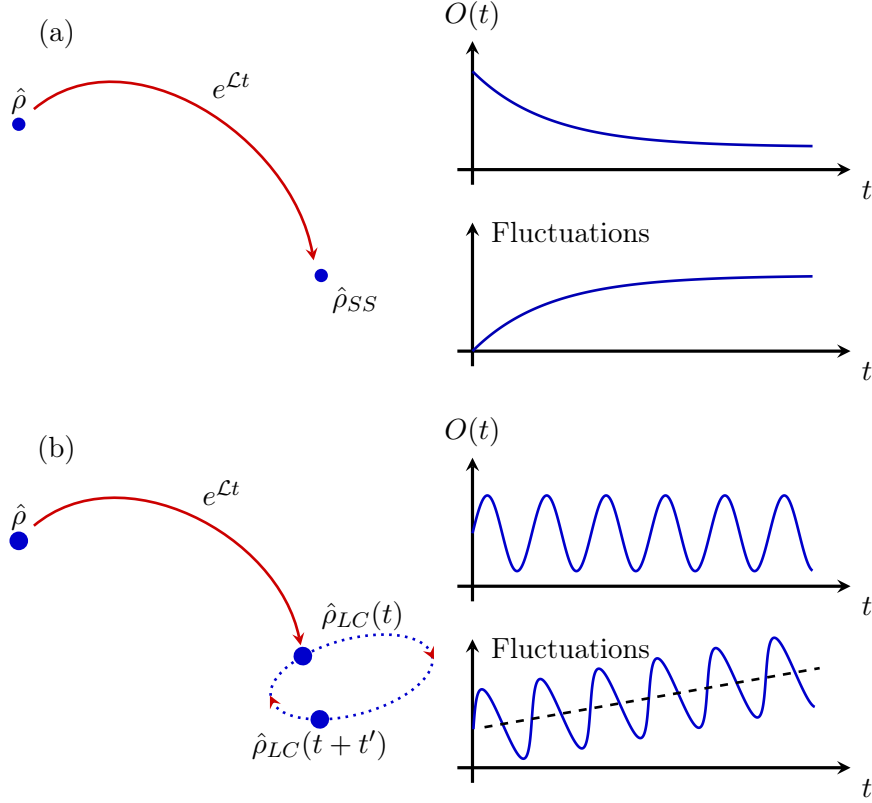


Figure 4.5: Sketch of the dynamics of a system towards a stationary phase (a) or a dissipative time-crystalline phase (b). In a system characterized by a Markovian dynamics, the Lindblad master equation described by the Liouvillian super-operator \mathcal{L} , typically time evolves towards a steady state $\hat{\rho}_{SS}$. The order parameter $O(t)$ and the fluctuations time evolve towards an asymptotic value. In the dissipative time crystal phase case, the Markovian system reaches a limit cycle, with a time-dependent state $\hat{\rho}_{LC}(t)$. In this case, typically the order parameter oscillates in time and the fluctuations increase with time.

and hence it may be regarded as a symmetric “ground state” of \mathcal{L} .

However, Markovian open quantum systems can also feature non-stationary asymptotic behaviors [722]. In this scenario, the system never reaches a steady state, but is subject to everlasting/sustained oscillations

$$\hat{\rho}(t) \rightarrow \hat{\rho}_{LC}(t), \quad (4.11)$$

dubbed as *limit cycle* [see Fig. 4.5(b)]. The system is no longer invariant under an additional time-translation since

$$e^{t'\mathcal{L}}[\hat{\rho}_{LC}(t)] = \hat{\rho}_{LC}(t' + t) \neq \hat{\rho}_{LC}(t), \quad (4.12)$$

The continuous time-translation symmetry of the generator is broken and the system forms a crystalline structure in time.

In practice, the identification of a suitable system operator \hat{O} such that the function

$$f(\tau) = \lim_{t \rightarrow \infty} \text{Tr}(\hat{O}\hat{\rho}(t + \tau)), \quad (4.13)$$

is periodic in time signals the formation of a dissipative time crystal. Importantly, the period is not limited to integer multiples of the driving period, and can take any value that can be expressed as a function of the system parameters.

4.3.3.1 Spectral Requirements for Dissipative Time Crystals

It is possible to understand both DPTs and DTCs in terms of a critical property of the spectrum of the Liouvillian superoperator [75, 352].

While DPTs emerge when one (or more) Liouvillian eigenvalues become zero in both their real and imaginary parts [49, 75], DTCs occur when the Liouvillian acquires eigenvalues with vanishing real part and nonzero imaginary part [352, 732, 779].

Moreover, a spectral analysis of the Liouvillian operator—and in particular the study of the Liouvillian gap—allows to establish an equivalence between second order DPTs and DTCs in the thermodynamic limit. In fact, DPTs and DTCs are the same phenomenon but in a different representation. This result has been established in [353].

The eigensystem of \mathcal{L} reads

$$\mathcal{L}[\hat{\rho}_k] = \lambda_k \hat{\rho}_k \quad (4.14)$$

$$\mathcal{L}^\dagger[\sigma_k] = \lambda_k \sigma_k \quad (4.15)$$

$$\text{Tr}(\sigma_k^\dagger \hat{\rho}_{k'}) = \delta_{k,k'} \quad (4.16)$$

where λ_k denotes the eigenvalues of \mathcal{L} , while the $\hat{\rho}_k$ and σ_k corresponds to respectively the right and left eigenstates associated to λ_k .

For \mathcal{L} to be a physical Liouvillian its eigenvalues λ_k must obey $\text{Re}(\lambda_k) \leq 0$.

These quantities allow to express the time evolution of any system observable.

Given an initial state $\hat{\rho}(0)$, we have

$$\langle \hat{O} \rangle(t) = \text{Tr}(\hat{O} \hat{\rho}(t)) = \sum_k O_k e^{\lambda_k t} \quad (4.17)$$

where $O_k = \text{Tr}(\sigma_k^\dagger \hat{\rho}(0)) \text{Tr}(\hat{O} \hat{\rho}_k)$.

The system exhibits non-stationarity if there are purely imaginary non-zero eigenvalues, $\lambda_k = i\omega_k$, with $\omega_k \neq 0$. Moreover, in order for this non-stationary behavior to be periodic, the further condition of nowhere-dense and commensurability²⁷ is required [734, 780, 781], that is $\omega_k/\omega_l \in \mathbb{Q}$ for all k, l .

These limit cycles emerge after a transient regime, whose duration is determined by the Liouvillian gap, as this quantity characterizes the time scale of the slowest decaying part of the system (see chapter 2).

4.3.3.2 From Finite to Infinite Dissipative Time Crystals

In closed systems, the implementation of time crystals must be performed in the thermodynamic limit in order to eliminate the oscillations arising from finite-size effects.

²⁷Two non-zero real numbers a and b are called commensurable if their ratio a/b is a rational number.

If that is not the case then a and b are incommensurable.

In the open many-body quantum systems case, however, dissipative time crystals do not necessarily need this restrictive condition [95], and refer to the general idea of non-trivial time translational symmetry breaking induced by dissipation. This is particularly an important point in the optic of the experimental implementation of DTCs, where only finite systems can be studied.

4.4 One mode critical phenomena: dynamical optical hysteresis in the Kerr model

A single Kerr oscillator subject to single-photon driving can undergo a first-order phase transition.

Interesting insight into this matter is provided e.g. in chapter 2 of [782], or chapter 4 of [783].

This realm has been studied both theoretically and experimentally.

System Hamiltonian. The Hamiltonian of a coherently driven Kerr non-linear oscillator reads:

$$\hat{H} = -\Delta \hat{a}^\dagger \hat{a} + \frac{U}{2} \hat{a}^\dagger \hat{a}^\dagger \hat{a} \hat{a} + F(\hat{a}^\dagger + \hat{a}) \quad (4.18)$$

where $\Delta = \omega_L - \omega$ with ω is the frequency of the optical mode, ω_L the laser frequency, the operator \hat{a} is the annihilation operator of the cavity mode, amplitude F the driving amplitude and U the Kerr non-linearity (self-interaction).

The regime of interest is $U \ll \kappa \ll F$ (weak nonlinearity).

4.4.1 Semiclassical analysis

The semiclassical equation of motion for the mean field of the intracavity field $\alpha = \langle \hat{a} \rangle = \text{Tr}(\hat{\rho} \hat{a})$ is given by the Gross-Pitaevskii equation

$$\partial_t \alpha = -\left(i\Delta + \frac{\gamma}{2}\right) \alpha + iU|\alpha|^2 \alpha - iF. \quad (4.19)$$

This is a cubic nonlinear equation.

For some values of the parameters, this equation admits two distinct stable steady-state solutions, thus exhibiting bistability. On the other hand, the equation of motion in the steady state satisfied by the photon number $n = |\alpha|^2$ reads

$$0 \stackrel{\uparrow}{=} U^2 n^3 - 2\Delta U n^2 + \left(\Delta^2 + \left(\frac{\gamma}{2}\right)^2\right) n - F^2 \equiv f(n) \quad (4.20)$$

Steady-state condition

If $\Delta > \sqrt{3}\gamma/2$, this equation admits three distinct solutions.

It is possible to perform a stability analysis of the different solutions by studying the derivative of the function f defined in (4.20): the solution is stable when $f'(n) > 0$, and the solution is not stable otherwise.

4.4.2 Quantum analysis

The quantum master equation reads

$$\dot{\hat{\rho}}(t) = -i\mathcal{L}\hat{\rho}(t) \quad (4.21)$$

this equation is linear and explicitly reads for a single bosonic mode

$$\partial_t \hat{\rho} = -i[\hat{H}, \hat{\rho}] + \frac{\gamma}{2} \left(2\hat{a}\hat{\rho}\hat{a}^\dagger - \hat{a}^\dagger\hat{a}\hat{\rho} - \hat{\rho}\hat{a}^\dagger\hat{a} \right) \quad (4.22)$$

This equation admits a unique steady-state.

Let me point out that the switching between the two states induced by the fluctuations present in the system can be investigated using a quantum trajectory approach, see e.g. [666, 667] and [chapter 2](#).

4.5 Two mode critical phenomena: dissipative time crystal in an asymmetric nonlinear photonic dimer

This last section reproduces the article published in *Physical Review A* [1]:

K. Seibold, R. Rota, and V. Savona, *Dissipative time crystal in an asymmetric nonlinear photonic dimer*, [Physical Review A 101, 033839 \(2020\)](#).

Resulting from a collaboration with all the authors, directed by Vincenzo Savona. My contribution to the project was to provide the theoretical development, set up the numerical implementation in Matlab and to perform the numerical simulations.

A dissipative time crystal in an asymmetric non-linear photonic dimer

Kilian Seibold,¹ Riccardo Rota,¹ and Vincenzo Savona¹

¹*Institute of Physics, Ecole Polytechnique Fédérale de Lausanne (EPFL), CH-1015, Lausanne, Switzerland**

(Dated: March 4, 2020)

We investigate the behavior of two coupled non-linear photonic cavities, in presence of inhomogeneous coherent driving and local dissipations. By solving numerically the quantum master equation, either by diagonalizing the Liouvillian superoperator or by using the approximated truncated Wigner approach, we extrapolate the properties of the system in a thermodynamic limit of large photon occupation. When the mean field Gross-Pitaevskii equation predicts a unique parametrically unstable steady-state solution, the open quantum many-body system presents highly non-classical properties and its dynamics exhibits the long lived Josephson-like oscillations typical of dissipative time crystals, as indicated by the presence of purely imaginary eigenvalues in the spectrum of the Liouvillian superoperator in the thermodynamic limit.

I. INTRODUCTION

Open many-body quantum systems [1–3] have become a major field of study over the last decade. The open nature is common to a vast class of modern experimental platforms in quantum science and technology, such as photonic systems [4], ultracold atoms [5–9], optomechanical systems [10–13] or superconducting circuits [14–16], for which driving and losses are omnipresent. Open quantum systems also display emergent physics, in particular dissipative phase transitions [17–39] and topological phases [40–45].

Several studies have highlighted the possibility for a continuous-wave driven-dissipative quantum system to reach a non-stationary state in the long time limit in which undamped oscillations arise spontaneously [46–53]. This phenomenon has been dubbed as boundary or dissipative time crystal (DTC), in analogy with the time crystals in some Hamiltonian systems [54]. Formally, DTCs are associated with the occurrence of multiple eigenvalues of the Liouvillian with vanishing real and finite imaginary part [55–57]. The experimental feasibility of DTC has been confirmed by their observation in phosphorous-doped silicon [58]. The research for further platforms showing this phenomenon is very active and important to understand the mechanisms behind the spontaneous breaking of the time-translation symmetry in open quantum many-body systems.

One of the main difficulties in the realization of DTCs in real system is related to the fragility of this phase to external perturbations which affect the symmetric structure of the model. Indeed, in most of the cases considered so far, the engineering of the DTCs relies on the exploitation of certain symmetries (either manifest [48, 52] or emergent [50]) in the Hamiltonian or in the dissipation mechanism, which can be hard to maintain in real driven-dissipative systems out of equilibrium.

In this work, we show that a DTC can arise in a simple system of two coupled photonic cavities, whose equation

of motion does not preserve any symmetry but the time-translation invariance. In a broad region of the parameter space, the dynamics of this system presents limit cycles associated to parametric instabilities [59], which can be regarded as the classical limit of a DTC. In this regime the system displays large fluctuations and entanglement, thus departing from its classical analog. As symmetries are not required for the occurrence of a DTC, this system is very robust and may be easily realized for example on a superconducting circuit architecture [60] or with coupled semiconductor micropillars [61–64]. This prototypical system is also a minimal model of dissipative Kerr solitons, that are emerging as the most suitable optical system for precision frequency generation and metrology [65], and therefore highlights the potential of these devices as sources of strongly nonclassical light. Very recently, the emergence of parametric instabilities in a photonic dimer has been observed in a classical regime of large occupation [66].

The paper is organized as follows. In Sec. II we introduce the quantum model and the theoretical tools used to calculate its properties. In Sec. III we discuss the result obtained for both the stationary-state and the dynamics of the system. In Sec. IV, we draw our conclusions.

II. THEORETICAL FRAMEWORK

We consider two coupled Kerr cavities where only one is coherently driven. The system Hamiltonian in a frame rotating with the pump frequency reads (with $\hbar = 1$)

$$\hat{\mathcal{H}} = \sum_{i=1,2} -\Delta \hat{a}_i^\dagger \hat{a}_i + \frac{U}{2} \hat{a}_i^\dagger \hat{a}_i^\dagger \hat{a}_i \hat{a}_i - J(\hat{a}_1^\dagger \hat{a}_2 + \hat{a}_1 \hat{a}_2^\dagger) + F(\hat{a}_1^\dagger + \hat{a}_1), \quad (1)$$

where \hat{a}_i is the bosonic annihilation operator of the i -th mode, Δ is the frequency detuning between the pump and the resonator, U is the on-site interaction strength, J is the hopping coupling and F is the driving amplitude. The dissipative dynamics can be described within the Born-Markov approximation, resulting in the follow-

* kilian.seibold@epfl.ch

ing Lindblad quantum master equation [67, 68] for the density matrix $\hat{\rho}$,

$$\frac{d\hat{\rho}}{dt} = \mathcal{L}\hat{\rho} = -i[\hat{\mathcal{H}}, \hat{\rho}] + \sum_{i=1,2} \kappa \mathcal{D}[\hat{a}_i] \hat{\rho}. \quad (2)$$

Here $\mathcal{D}[\hat{a}_i] \hat{\rho} = \hat{a}_i \hat{\rho} \hat{a}_i^\dagger - 1/2(\hat{a}_i^\dagger \hat{a}_i \hat{\rho} + \hat{\rho} \hat{a}_i^\dagger \hat{a}_i)$ is the dissipator in Lindblad form accounting for losses to the environment and κ the dissipation rate. \mathcal{L} is the Liouvillian superoperator and its spectrum encodes the full dynamics of the open quantum system. The expectation value of any quantum mechanical observable \hat{o} over the state characterized by the density matrix $\hat{\rho}$ is computed as $\langle \hat{o} \rangle = \text{Tr}(\hat{o} \hat{\rho})$. In the long time limit, the system evolves towards a non-equilibrium steady state $\hat{\rho}_{ss}$ satisfying the condition $d\hat{\rho}_{ss}/dt = 0$. We determine the steady-state density matrix by numerically solving the linear system $\mathcal{L}\hat{\rho}_{ss} = 0$, and imposing the condition $\text{Tr}(\hat{\rho}_{ss}) = 1$. The dynamic properties of the system are obtained by the numerical diagonalisation of the superoperator \mathcal{L} . The numerical calculations are performed in a properly truncated Hilbert space, obtained by setting a maximum value N_i^{max} ($i = 1, 2$) for the total photon occupancy per cavity. The convergence of the results versus N_i^{max} is carefully checked by varying the cutoff number of photons [69].

In order to study DTCs, that are collective phenomena arising in a thermodynamic limit with large photon number, it is necessary to define a proper scaling of the physical parameters, allowing to reach this limit in a controlled way. In this work we consider the thermodynamic limit obtained by letting the interaction strength $U \rightarrow 0$ and the driving amplitude $F \rightarrow \infty$ in Eq. (2), while keeping constant the product UF^2 . This approach has already been used to study not only DTCs [52], but also the dissipative phase transitions in photonic system of finite size [32, 33, 70–73].

In the limit of large photon occupation, the dynamics of a driven dissipative system can be generally recovered by the solution of the Gross-Pitaevskii (GP) equation [2], a mean field approach neglecting all fluctuations. The GP approximation is obtained from the master equation 2 assuming only coherent states for fields, $\hat{\rho} = |\alpha_1, \alpha_2\rangle\langle\alpha_1, \alpha_2|$. The two rescaled complex fields $\alpha_1 = \sqrt{U}\langle\hat{a}_1\rangle$ and $\alpha_2 = \sqrt{U}\langle\hat{a}_2\rangle$ evolve according to the set of coupled equations:

$$\begin{aligned} i \frac{\partial \alpha_1}{\partial t} &= (-\Delta - i\kappa/2)\alpha_1 + |\alpha_1|^2 \alpha_1 - J\alpha_2 + F\sqrt{U} \\ i \frac{\partial \alpha_2}{\partial t} &= (-\Delta - i\kappa/2)\alpha_2 + |\alpha_2|^2 \alpha_2 - J\alpha_1. \end{aligned} \quad (3)$$

The steady-state GP solutions $\alpha_{i,S}$ are obtained solving Eqs. (3) with the condition $i\partial_t \alpha_{i,S} = 0$. The stability of each solution can be assessed by evaluating the spectrum of linearized excitations around them. If all the frequencies of the linearized excitations have negative imaginary parts, then the corresponding solution is

stable and can describe the steady state of the driven-dissipative system. Otherwise, the solution is unstable. The parametric instability happens when the frequency of the excitations presents a non-zero real part.

While the Gross-Pitaevskii formalism provides a simple approximation for the dynamics of the open quantum system, it fails in the description of the mixed character of its density matrix. To overcome this limitation, we consider another approximated scheme: the truncated Wigner approximation (TWA) method [74, 75]. This numerical approach relies on the assumption that the equation of motion for the Wigner quasi-probability distribution function obtained from the master equation, Eq. (2), can be written as a Fokker-Planck equation in the limit of small non-linearities. Namely, the state of the photonic dimer can be described by two complex fields $\alpha_1(t)$ and $\alpha_2(t)$ which describe the coherence over the two modes. Their time evolution follows the stochastic differential equation

$$\begin{aligned} \frac{\partial \alpha_i}{\partial t} &= -i [-(\Delta + i\kappa/2) + U(|\alpha_i|^2 - 1)] \alpha_i \\ &\quad - iF\delta_{i,1} + iJ\alpha_{3-i} + \sqrt{\kappa/4}\chi(t), \end{aligned} \quad (4)$$

where $\chi(t)$ is a normalized random complex Gaussian noise with correlators $\langle \chi(t)\chi(t') \rangle = 0$ and $\langle \chi(t)\chi^*(t') \rangle = \delta(t-t')$ and describes the fluctuations arising in the quantum system because of photon losses. Each TWA trajectory corresponds to a different realization of the noise term $\chi(t)$. Therefore, the evolution of the density matrix can be recovered by averaging many trajectories obtained solving numerically the associated Langevin equation for the complex field, using stochastic Monte-Carlo techniques. In spite of its approximated nature, this approach is very useful for studying our system in regimes of high photon occupancy in the cavities, as it avoids the use of large cut-off in the number of photons per cavity.

III. RESULTS

A. Mean-field analysis

We start the discussion of our results by providing a mean-field analysis of our system, with the aim to determine the range of parameters where the DTC emerges. We can expect that the DTC phase appears whenever the GP approach predicts a unique parametrically unstable steady-state solution. For this reason, we calculate the number and the nature of the GP solutions as a function of the physical parameters Δ , J and $\tilde{F} = F\sqrt{U}/\kappa^{3/2}$. The results of this calculation, at the fixed value of $\Delta = 2\kappa$, are shown in the phase diagram of Fig. 1-(a). We clearly notice the emergence of a region where the GP approach predicts a unique parametrically unstable steady-state solution. In this regime, if we compute the time evolution of the mean fields $\alpha_i(t)$ by integrating

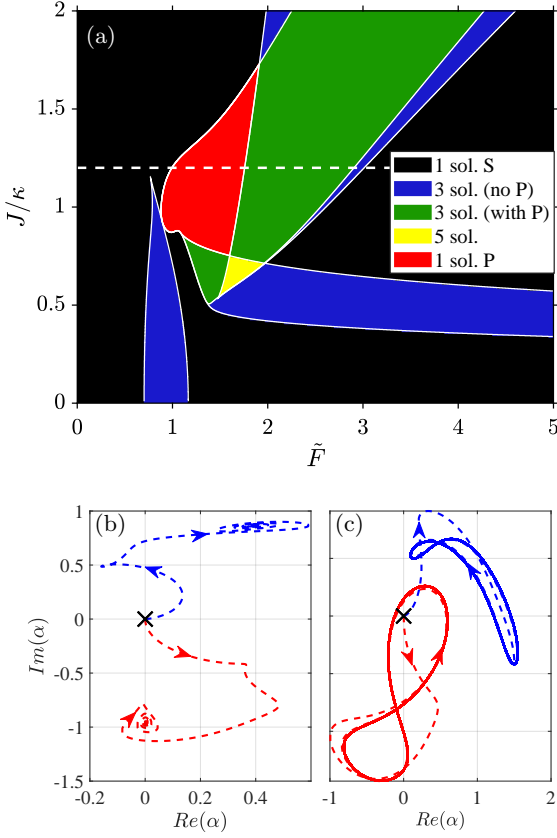


FIG. 1. Panel (a): Phase diagram for the number and the nature of the GP steady state solutions as a function of J and \tilde{F} , for the fixed value of $\Delta = 2\kappa$. In the phase diagram, we distinguish the case of a single stable solution (1 sol. S), a single parametrically unstable solution (1 sol. P), three solutions (either with or without one parametrically unstable) and five solutions. The dashed line represent the value $J = 1.2\kappa$, i.e. the value of J considered in the results of Sec. III.B and III.C. Panels (b) and (c): trajectories described by the mean fields α_1 (red curve) and α_2 (blue curve) according to the GP time evolution, for $\Delta = 2\kappa$, $J/\kappa = 1.2$ and different values of \tilde{F} : panel (b) for $\tilde{F} = 0.95$ (i.e. in the case of a single stable solution) and panel (c) for $\tilde{F} = 1.5$ (i.e. in the case of a single parametrically unstable solution). The shown trajectories are obtained by numerically integrating the GP equations (Eq. (3)) up to $t\kappa = 10^3$. The arrows indicate how the fields evolve for increasing time.

Eqs. (3), choosing the vacuum as the initial condition ($\alpha_1(0) = 0$, $\alpha_2(0) = 0$), we see the emergence of limit cycles at long times, which represent the classical limit of the dissipative time crystal in the quantum system. In Fig. 1(c), we plot the trajectories described by the two mean fields $\alpha_i(t)$ in the plane $\text{Re}(\alpha) - \text{Im}(\alpha)$: as the time increases, the fields do not evolve towards a steady state, but they display a periodic behavior. For comparison, in Fig. 1(b), we show the time evolution of a trajectory in a regime where the GP equation predicts a single steady-state solution: in this case, each of the two mean fields

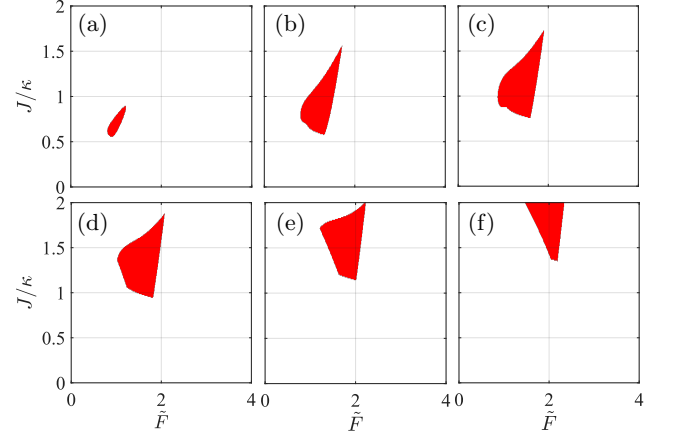


FIG. 2. Region in the parameter space where GP predicts a single parametrically unstable solution: each panel show the results as a function of the parameters J/κ and \tilde{F} , for different values of detuning: $\Delta/\kappa = 1$ (a), 1.5 (b), 2 (c), 2.5 (d), 3 (e), 3.5 (f).

α_i evolve towards a single point, which corresponds to the solution $\alpha_{i,S}$.

For sake of completeness, we have derived the phase diagram for several values of the detuning $\Delta > 0$ in Fig. 2. We notice the presence of a region with a single parametrically unstable GP solution, for all the values of Δ we have considered. Hence, it suggests that the DTC can be achieved over a finite range of values of the detuning.

In our analysis, we have considered also the case of a dimer made of two resonators with different properties. To this aim, we have solved the generalized Gross-Pitaevskii equation

$$\begin{aligned} i\frac{\partial\alpha_1}{\partial t} &= (-\Delta_1 - i\kappa_1/2)\alpha_1 + U_1|\alpha_1|^2\alpha_1 - J\alpha_2 + F \\ i\frac{\partial\alpha_2}{\partial t} &= (-\Delta_2 - i\kappa_2/2)\alpha_2 + U_2|\alpha_2|^2\alpha_2 - J\alpha_1, \end{aligned} \quad (5)$$

which assumes different values $\Delta_1 \neq \Delta_2$ for the detuning frequencies, $U_1 \neq U_2$ for the non-linearities or $\kappa_1 \neq \kappa_2$ for the loss rates of the two modes. The results of this study are presented in fig. 3. The different panels show the region in the parameter space with a unique parametrically unstable solution for the GP steady state and indicate that the DTC phase can emerge even when the dimer is formed by two resonators with different properties, highlighting the robustness of this phase in our system.

B. Steady-state properties of the quantum system

We now consider the properties of the system obtained within a fully quantum many-body approach. In Fig. 4 we show the steady-state expectation values for the photon occupation $n_1 = \langle \hat{a}_1^\dagger \hat{a}_1 \rangle$ and $n_2 = \langle \hat{a}_2^\dagger \hat{a}_2 \rangle$ in the two

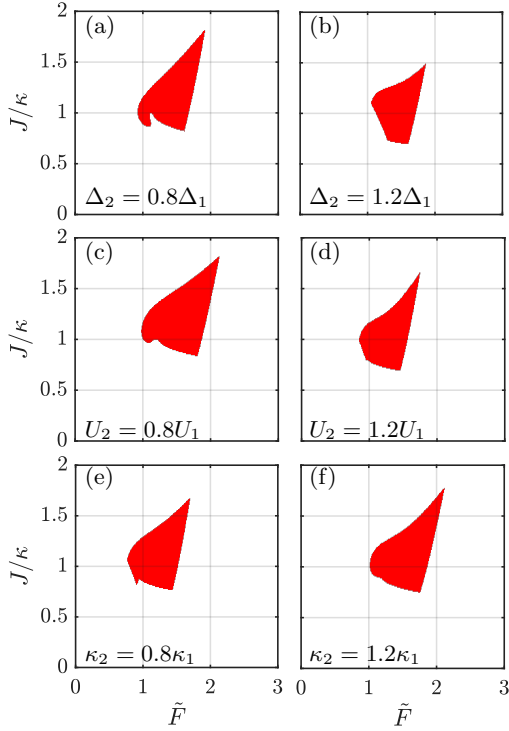


FIG. 3. Region in the parameter space where GP predicts a single parametrically unstable solution, for the case of a dimer made of resonators with different detuning frequencies [panels (a-b)], nonlinearities [panels (c-d)] or loss rates [panels (e-f)]. The coefficients for the first cavity are $\Delta_1 = 2\kappa_1$ are $U_1 = \kappa_1$, $\tilde{F} = F\sqrt{U_1}/\kappa_1^{3/2}$; the coefficients for the second cavity are specified in each panel.

cavities, as a function of the driving amplitude F , for different choices of the non-linearity U : the other Hamiltonian parameters in Eq. (1), $\Delta = 2\kappa$ and $J = 1.2\kappa$, are chosen such that the GP equation predicts the emergence of parametric instability in the system (these parameters corresponds to the dashed line plotted in the phase diagram of Fig. 1). By studying the behavior of n_1 and n_2 for decreasing U , we can extrapolate their behavior in the thermodynamic limit and compare it with the GP prediction. We see that the mean-field approach is reliable only in the limit of small and large driving, where the GP equation predicts a unique steady-state solution, but it fails for intermediate values of the rescaled driving amplitude $\tilde{F} = F\sqrt{U}/\kappa^{3/2}$. For $\tilde{F} \simeq 2$, our results show a steep increase of the photon occupancy in the two cavities as a function of \tilde{F} , which becomes steeper as the non-linearity U decreases. This behavior suggests the emergence of a discontinuity in the thermodynamic limit, and therefore the occurrence of a first-order phase transition similar to that observed in a single cavity in regimes of optical bistability [33]. Moreover, from the results in Fig. 4 we can find a broad interval of \tilde{F} values, i.e. $1 \lesssim \tilde{F} \lesssim 2$, where the expectation values computed for the quantum model do not depend strongly on U (and

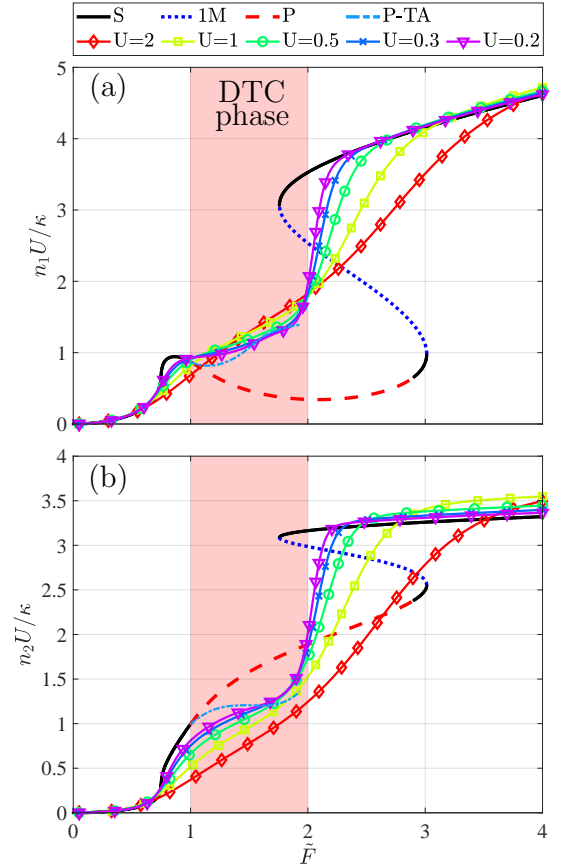


FIG. 4. Rescaled steady-state expectation value of the photon occupancy n_1 (a) and n_2 (b) in the two cavities, versus the rescaled pump amplitude \tilde{F} . The lines with markers correspond to the different values of U . The solid, dashed and dotted lines correspond to the predictions obtained from the steady-state solution of the GP equations, where the different line styles represent different nature of the solution: stable (solid black line), one mode unstable (blue dotted line) and parametrically unstable (red dashed line). The light blue dot-dashed line represents the prediction for the photon occupation calculated from the time-averaged density matrix $\hat{\rho}_{av}$ (Eq. (6)). The shaded area indicates approximately the DTC phase. The other Hamiltonian parameters are $\Delta/\kappa = 2$, $J/\kappa = 1.2$.

therefore we can safely assume that the thermodynamic limit is already reached at the lowest values of U achievable with our numerical approach) and are notably different from the GP predictions for the steady state. This interval of \tilde{F} corresponds roughly to the range where the GP approach predicts a unique parametrically unstable steady-state solution and represents the regime where the DTC is observed (henceforth, we define this range of parameters as the DTC-phase).

Due to the emergence of limit cycles in the classical regime of the DTC-phase, it is natural to ask whether a more precise prediction for the steady state of the quan-

tum system in the thermodynamic limit can be obtained from a time average of the dynamical solution of the GP equation. Knowing the solution for the field $\alpha_1(t)$ and $\alpha_2(t)$ over a limit cycle of period T , we construct the time-averaged density matrix

$$\hat{\rho}_{av} = \frac{1}{T} \int_{t_0}^{t_0+T} dt |\alpha_1(t), \alpha_2(t)\rangle \langle \alpha_1(t), \alpha_2(t)|, \quad (6)$$

where $|\alpha_1(t), \alpha_2(t)\rangle = |\alpha_1(t)\rangle \otimes |\alpha_2(t)\rangle$ is a coherent states on the two modes of the dimer. We compute the expectation values for the photon occupation on the two cavities $n_{i,av} = \text{Tr}(\hat{\rho}_{av} \hat{a}_i^\dagger \hat{a}_i)$ over this density matrix. The results for $n_{i,av}$ as a function of \tilde{F} are showed in Fig. 4 and compared with the results obtained from the steady-state solution of the master equation, Eq. (2). We notice that $n_{i,av}$ is in agreement with the quantum results in the thermodynamic limit.

However, the density matrix $\hat{\rho}_{av}$ is not able to give a complete description of the steady state $\hat{\rho}_{ss}$ of the quantum system, as evidenced by the results for the logarithmic negativity E_N and for the von-Neumann entropy, which are shown in Fig. 5. In Fig. 5-(a), we show $E_N = \log_2(\|\hat{\rho}_{ss}^{\Gamma_1}\|_1)$, where $\hat{\rho}_{ss}^{\Gamma_1}$ indicates the partial transpose with respect to the degrees of freedom of the second cavity and $\|\cdot\|_1$ the trace norm, as a function of \tilde{F} . We can see that, in the DTC-phase, $E_N > 0$ and increases for decreasing U , showing the presence of entanglement, which is absent per definition in $\hat{\rho}_{av}$ (Eq. (6)). The von-Neumann entropy $S = -\text{Tr}(\hat{\rho}_{ss} \ln(\hat{\rho}_{ss}))$, displayed in Fig. 5-(b), shows instead the mixed character of the steady state, arising because of the classical fluctuations due to the photon losses from the cavities. We see that S assumes large values for $1 \lesssim \tilde{F} \lesssim 2$ and increases for decreasing U . We notice that the classical prediction $S_{av} = -\text{Tr}(\hat{\rho}_{av} \ln(\hat{\rho}_{av}))$, also shown in Fig. 5-(b), does not agree with the quantum results in the thermodynamic limit. The analysis of E_N and S confirms the important role played by fluctuations (both quantum and classical) in the steady state of our system and therefore the inaccuracy of the GP approach in the description of the DTC-phase.

C. Quantum dynamics

In order to reveal the emergence of a DTC in the considered system, we study the dynamical properties by computing the spectrum of the eigenvalues λ_j of the Liouvillian. This is performed by numerically diagonalizing the superoperator \mathcal{L} defined in Eq. (2). In Fig. 6, we show the spectrum of the eigenvalues of \mathcal{L} with largest real part, for different values of \tilde{F} and U . Outside of the DTC-phase [see Fig. 6-(a) for $\tilde{F} = 0.8$ and Fig. 6-(f) for $\tilde{F} = 2.5$], the eigenvalue with smallest absolute value is purely real, independently of the value of U . In this regime, the dynamics of the dissipative system at long time is characterized by an exponential decaying to-

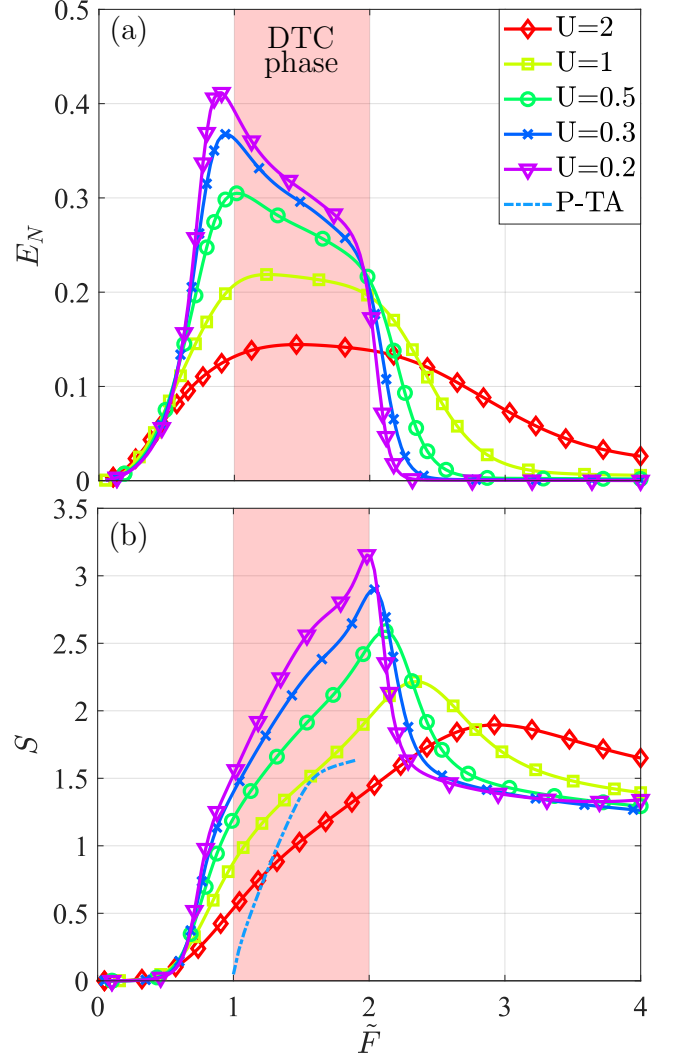


FIG. 5. Logarithmic negativity E_N (a) and Von Neumann Entropy S (b) versus the rescaled pump amplitude and for different values of the non-linearity U . The shaded area indicates approximately the DTC phase. In panel (b), the light blue line represents the prediction for the von-Neumann entropy calculated from the time-averaged density matrix $\hat{\rho}_{av}$ (Eq. (6)). The other Hamiltonian parameters are $\Delta/\kappa = 2$, $J/\kappa = 1.2$.

wards the steady state. At $\tilde{F} = 1$ [Fig. 6-(b)], the onset of long-lived oscillation at small U is revealed by the fact that the eigenvalue λ_1 with largest real part has a finite imaginary part. We also see, in this case, that the Liouvillian gap $\Lambda = |\text{Re}(\lambda_1)|$ decreases for decreasing U .

The typical Liouvillian spectrum in the DTC-phase is shown in Fig. 6-(c) ($\tilde{F} = 1.5$) and Fig. 6-(d) ($\tilde{F} = 1.8$). From these plots, we clearly notice the presence of eigenvalues which, when $U \rightarrow 0$, have a vanishing real part and finite imaginary part. This means that the time scale of the relaxation dynamics (which is determined by

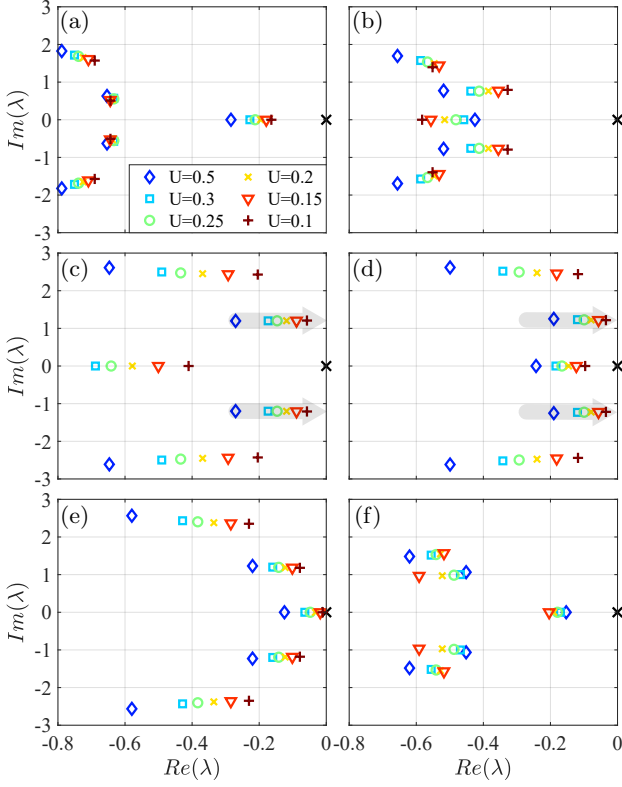


FIG. 6. Eigenvalues λ of the Liouvillian superoperator, plotted in units of κ . Each panel shows the eigenvalues with largest real part for a given pump amplitude \tilde{F} and different values of non-linearity U , corresponding to different colors and marker types. The black cross indicates the unique steady state. The different pump amplitudes corresponding to each panels are: $\tilde{F} = 0.8$ (a), $\tilde{F} = 1.0$ (b), $\tilde{F} = 1.5$ (c), $\tilde{F} = 1.8$ (d), $\tilde{F} = 2.0$ (e) and $\tilde{F} = 2.5$ (f). The other parameters are $\Delta/\kappa = 2$, $J/\kappa = 1.2$.

the inverse of the Liouvillian gap $1/\Lambda$) becomes increasingly long when approaching the thermodynamic limit. Even though the Lindblad master equation Eq. (2) predicts the existence of a time-independent steady state, the evolution of the density matrix is characterized by long lived oscillations: indeed, according to the spectral decomposition of the density matrix [70],

$$\hat{\rho}(t) = \hat{\rho}_{ss} + \sum_j c_j(0) e^{\lambda_j t} \hat{\rho}_j, \quad (7)$$

where $\hat{\rho}_j$ are the eigenmatrices of the Liouvillian superoperators associated to the eigenvalues $\lambda_j \neq 0$, and $c_j(0)$ are the components of the initial density matrix $\hat{\rho}(0)$ over the different $\hat{\rho}_j$. While all the components having λ_j with sizeable real part decay rapidly, those with $|\text{Re}(\lambda_j)| \ll |\text{Im}(\lambda_j)|$ will give rise to long lived oscillations in $\hat{\rho}(t)$.

The results in Fig. 6-(c,d) suggest also that the imaginary part of the eigenvalues with vanishing real part are

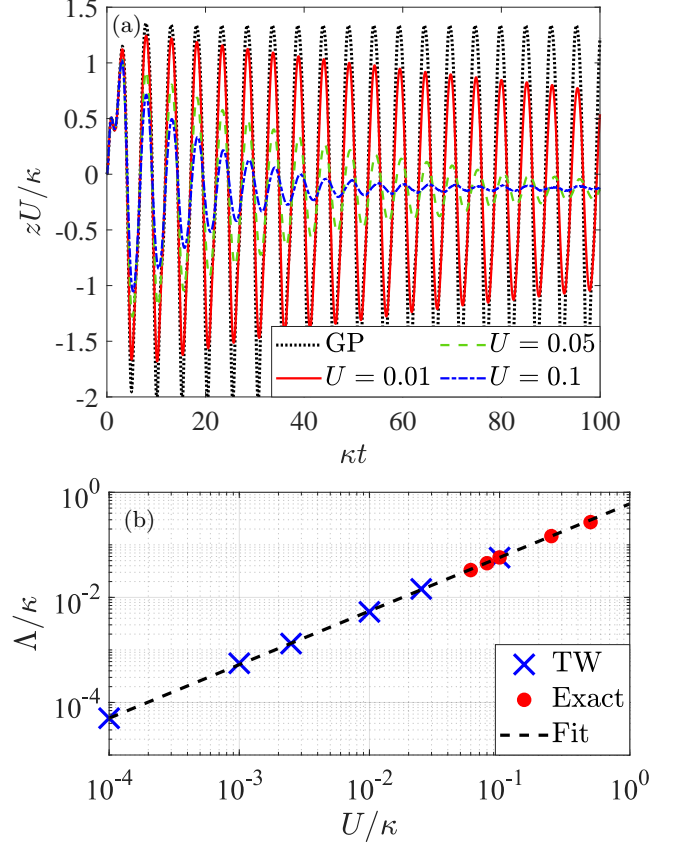


FIG. 7. (a): Time evolution of the rescaled population difference z between the two cavities for $\tilde{F} = 1.5$, $\Delta/\kappa = 2$, $J/\kappa = 1.2$ and different values of U . The results are obtained by averaging over 10^5 stochastic trajectories obtained with TWA. (b): Liouvillian gap Λ as a function of the non-linearity U for $\tilde{F} = 1.5$, $\Delta/\kappa = 2$, $J/\kappa = 1.2$. The different symbols refer to different methods to extract the value of Λ (exact diagonalization or fit of TWA results for $z(t)$). The dashed line represents a power-law fit of the data.

integer multiples of a fundamental frequency. The two features, i.e. the gapless Liouvillian spectrum and the imaginary eigenvalues of the low excitations described by bands separated by the same frequency, are the key elements of a DTC, as also pointed out in Ref. [46].

Finally, for $\tilde{F} = 2.0$ [Fig. 6-(e)], we notice that the eigenvalue with largest real part is purely real, signaling the disappearance of the long-lived oscillation of the DTC-phase. Moreover, we can notice also that this eigenvalue goes to zero in the thermodynamic limit: this behavior can be associated to the closing of the Liouvillian gap in the vicinity of a critical point, and hence supports the evidence for a first-order dissipative phase transition [70], as already indicated by the results in Fig. 4.

The occurrence of a DTC in our system is further supported by a study of the dynamics with the Truncated Wigner approximation (TWA) [74]. In Fig. 7-

(a), we show the TWA results for the time evolution of the population difference between the two cavities, $z = \langle \hat{a}_1^\dagger \hat{a}_1 - \hat{a}_2^\dagger \hat{a}_2 \rangle$, for the value of $\tilde{F} = 1.5$ inside the DTC-phase, having chosen the vacuum as the initial condition. The oscillating character of the dynamics is evident for all the values of the non-linearities considered and persists on a time scale which is large with respect to the inverse loss rate $1/\kappa$. By comparing the curves obtained for different values of U , we can see that the damping of the oscillation becomes smaller for decreasing U , but their period is almost independent. These results confirm what already observed in the analysis of the Liouvillian spectrum: when approaching the thermodynamic limit, the Liouvillian gap goes to zero, as indicated by the slowing down of the exponential decay of the oscillation; instead its imaginary part, which is related to the period of the oscillations, remains finite. The numerical estimates for the Liouvillian gap Λ and for the relevant frequencies of the oscillation can be extracted by fitting the curves $z(t)$ at long times with a sum of exponentially damped sine functions. The behavior of Λ as a function of U for $\tilde{F} = 1.5$ is shown in Fig. 7-(b). First of all, we notice that the values extracted from the fit of $z(t)$ are in good agreement with the results obtained by the exact diagonalization of the Liouvillian, confirming the validity of the TWA in this regime of small non-linearities. Furthermore, the results show a power law behavior $\Lambda \sim U^\eta$, with $\eta = 1.02 \pm 0.03$, indicating that the Liouvillian gap closes in the thermodynamical limit. Concerning the oscillatory dynamics of the system in the DTC-phase, the frequencies extracted from the fit of $z(t)$ at the largest U correspond exactly to the imaginary part of the Liouvillian eigenvalues shown in Fig. 6-(c). When U decreases, it becomes apparent that more frequency components contribute to the oscillation of $z(t)$. All the frequencies extracted from the fit are integer multiples of the same fundamental frequency: this picture strongly supports the presence of a discrete set of equally spaced Liouvillian eigenvalues, that is a sufficient condition to have a persistent non-stationarity in the dynamics of the open system [76]. A rigorous proof of this spectral structure in the thermodynamic limit is however beyond the scope of this work.

In Fig. 7, we show the quantity $z(t)$ obtained from the GP equation, when taking the vacuum as initial condition at $t = 0$. The comparison with the TWA results shows that the fluctuations do not affect the frequency of the oscillations. Fluctuations are instead only responsible for random relative phase shifts among single TWA trajectories, resulting in the damping of oscillations at long times. This last observation is verified by comparing the behavior of individual TWA trajectories. In Fig. 8, we show the evolution of the population difference between the two cavities, over five TWA trajectories, for different values of the non-linearity U and for the value of $\tilde{F} = 1.5$, inside the DTC-phase. For all the values of U , we notice that most of the single trajectories present an oscillating behavior, which persists over a longer time

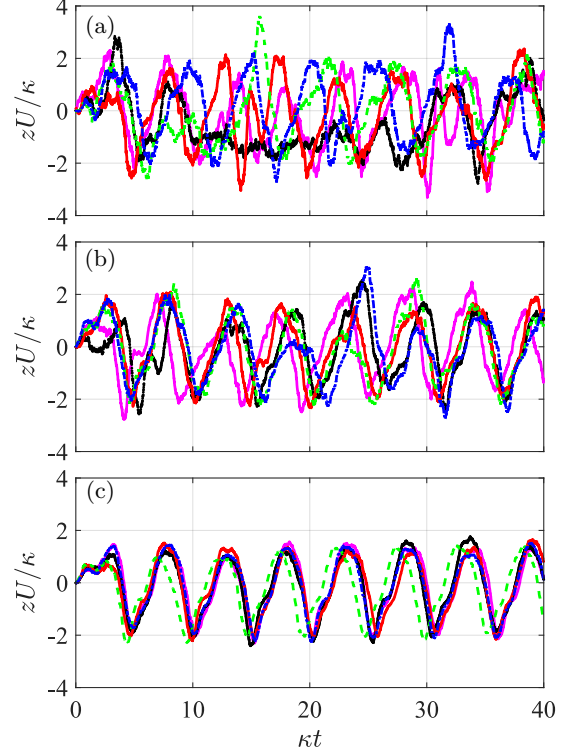


FIG. 8. Time evolution of the population difference between the two cavities obtained for 5 different TWA trajectories, starting from the vacuum at $t = 0$. The different panels show the results for different non-linearities: $U = 0.1$ (a), $U = 0.05$ (b) and $U = 0.01$ (c). The other parameters are $\tilde{F} = 1.5$, $\Delta/\kappa = 2$ and $J/\kappa = 1.2$

interval as the non-linearity decreases. From this analysis, we can deduce that the fluctuations induced by the noise term χ in Eq. (4) do not suppress the oscillating character of the trajectories, but induce a certain dephasing among them, which results in the damping towards the steady-state expectation value when the results of the single trajectories are averaged (See Fig. 7).

To have a better understanding of how the fluctuations influence the dynamics of the system in the DTC-phase, we show in Fig. 9 the distribution of the fields $\alpha_i(t)$ over a set of 12000 TWA trajectories for different times t and non-linearities U . At small time, the distribution is a Gaussian centered around the GP solution. At longer times, the effect of the noise is to spread the distribution of α_i along the limit cycles defined from the GP equation (showed in Fig. 1-(c)). Thus, even though a single TWA trajectory does not reach a steady state but presents an oscillating character similar to that of the GP parametrically unstable solution, the full distribution becomes stationary for long time, showing the emergence of a steady state. The time interval needed to reach the steady state becomes larger when U decreases.

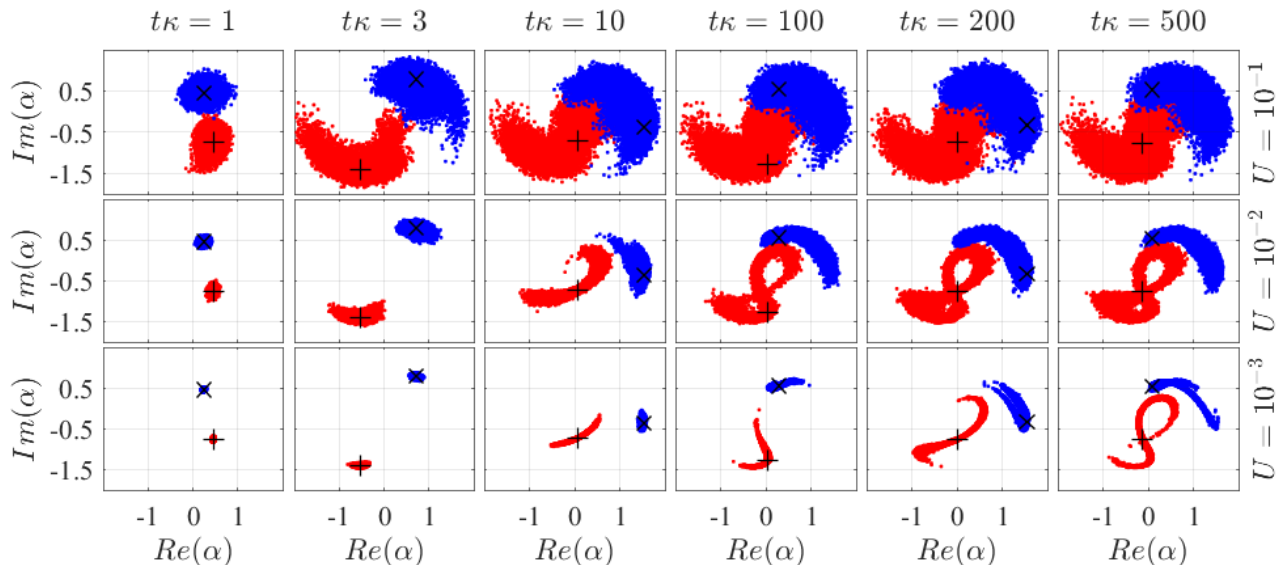


FIG. 9. Distribution of the TWA fields α_1 (in red) and α_2 (in blue) in phase space at different times t and non-linearities U . The black markers give the GP solution for the first (+) and second (x) cavity for the given time. The distributions are obtained from the realization of 1.2×10^4 TWA trajectories.

IV. CONCLUSIONS

In conclusion, we have provided strong evidences of the occurrence of a dissipative time crystal in a simple driven-dissipative system of two coupled non-linear optical resonators, under general conditions which do not rely on the presence of symmetries. The DTC phase arising over a wide range of parameters is characterized by spontaneous long lived oscillations of the system observables under continuous-wave driving, large fluctuations and non-classical correlations. The scheme we propose can be easily realized with current experimental technologies, such as superconducting circuits [60] or semiconductor micropillars [61–64], which have already been used for the investigation of other collective phenomena in open quantum system. The emergence of a DTC in

an optical dimer is directly related to the physics of Kerr solitons, for which the quantum properties of the radiation field are yet to be fully understood. The present study is an important step toward the characterization of quantum correlations and entanglement in Kerr-soliton systems, opening the way to the design of optical devices for the generation of non-classical light.

V. ACKNOWLEDGMENTS

We would like to thank Fabrizio Minganti and Wouter Verstraelen for useful discussions. We acknowledge support from the Swiss National Science Foundation through Project No. 200021_162357 and 200020_185015.

-
- [1] M. J. Hartmann, *Journal of Optics* **18**, 104005 (2016).
 - [2] I. Carusotto and C. Ciuti, *Rev. Mod. Phys.* **85**, 299 (2013).
 - [3] C. Noh and D. G. Angelakis, *Reports on Progress in Physics* **80**, 016401 (2017).
 - [4] A. Szameit and S. Nolte, *Journal of Physics B: Atomic, Molecular and Optical Physics* **43**, 163001 (2010).
 - [5] I. Bloch, J. Dalibard, and W. Zwerger, *Rev. Mod. Phys.* **80**, 885 (2008).
 - [6] F. Dimer, B. Estienne, A. S. Parkins, and H. J. Carmichael, *Phys. Rev. A* **75**, 013804 (2007).
 - [7] K. Baumann, C. Guerlin, F. Brennecke, and T. Esslinger, *Nature* **464**, 1301 (2010).
 - [8] K. Baumann, R. Mottl, F. Brennecke, and T. Esslinger, *Phys. Rev. Lett.* **107**, 140402 (2011).
 - [9] F. Brennecke, R. Mottl, K. Baumann, R. Landig, T. Donner, and T. Esslinger, *Proceedings of the National Academy of Sciences* **110**, 11763 (2013).
 - [10] M. Aspelmeyer, T. J. Kippenberg, and F. Marquardt, *Rev. Mod. Phys.* **86**, 1391 (2014).
 - [11] B. Pigeau, S. Rohr, L. Mercier de Lpinay, A. Gloppe, V. Jacques, and O. Arcizet, *Nature Communications* **6**, 8603 (2015).
 - [12] J. D. Teufel, T. Donner, D. Li, J. W. Harlow, M. S. Allman, K. Cicak, A. J. Sirois, J. D. Whittaker, K. W. Lehnert, and R. W. Simmonds, *Nature* **475**, 359 (2011).

- [13] S. Kolkowitz, A. C. Bleszynski Jayich, Q. P. Unterreithmeier, S. D. Bennett, P. Rabl, J. G. E. Harris, and M. D. Lukin, *Science* **335**, 1603 (2012).
- [14] H. J. Carmichael, *Phys. Rev. X* **5**, 031028 (2015).
- [15] J. M. Fink, A. Dombi, A. Vukics, A. Wallraff, and P. Domokos, *Phys. Rev. X* **7**, 011012 (2017).
- [16] M. Fitzpatrick, N. M. Sundaresan, A. C. Y. Li, J. Koch, and A. A. Houck, *Phys. Rev. X* **7**, 011016 (2017).
- [17] E. G. Dalla Torre, E. Demler, T. Giamarchi, and E. Altman, *Nature Physics* **6**, 806 (2010).
- [18] E. G. Dalla Torre, E. Demler, T. Giamarchi, and E. Altman, *Phys. Rev. B* **85**, 184302 (2012).
- [19] T. E. Lee, S. Gopalakrishnan, and M. D. Lukin, *Phys. Rev. Lett.* **110**, 257204 (2013).
- [20] L. M. Sieberer, S. D. Huber, E. Altman, and S. Diehl, *Phys. Rev. Lett.* **110**, 195301 (2013).
- [21] L. M. Sieberer, S. D. Huber, E. Altman, and S. Diehl, *Phys. Rev. B* **89**, 134310 (2014).
- [22] E. Altman, L. M. Sieberer, L. Chen, S. Diehl, and J. Toner, *Phys. Rev. X* **5**, 011017 (2015).
- [23] H. J. Carmichael, *Phys. Rev. X* **5**, 031028 (2015).
- [24] N. Bartolo, F. Minganti, W. Casteels, and C. Ciuti, *Phys. Rev. A* **94**, 033841 (2016).
- [25] J. J. Mendoza-Arenas, S. R. Clark, S. Felicetti, G. Romero, E. Solano, D. G. Angelakis, and D. Jaksch, *Phys. Rev. A* **93**, 023821 (2016).
- [26] W. Casteels, F. Storme, A. Le Boité, and C. Ciuti, *Phys. Rev. A* **93**, 033824 (2016).
- [27] J. Jin, A. Biella, O. Viyuela, L. Mazza, J. Keeling, R. Fazio, and D. Rossini, *Phys. Rev. X* **6**, 031011 (2016).
- [28] M. F. Maghrebi and A. V. Gorshkov, *Phys. Rev. B* **93**, 014307 (2016).
- [29] J. Marino and S. Diehl, *Phys. Rev. Lett.* **116**, 070407 (2016).
- [30] R. Rota, F. Storme, N. Bartolo, R. Fazio, and C. Ciuti, *Phys. Rev. B* **95**, 134431 (2017).
- [31] V. Savona, *Phys. Rev. A* **96**, 033826 (2017).
- [32] W. Casteels and C. Ciuti, *Phys. Rev. A* **95**, 013812 (2017).
- [33] W. Casteels, R. Fazio, and C. Ciuti, *Phys. Rev. A* **95**, 012128 (2017).
- [34] M. Foss-Feig, P. Niroula, J. T. Young, M. Hafezi, A. V. Gorshkov, R. M. Wilson, and M. F. Maghrebi, *Phys. Rev. A* **95**, 043826 (2017).
- [35] M. Biondi, G. Blatter, H. E. Türeci, and S. Schmidt, *Phys. Rev. A* **96**, 043809 (2017).
- [36] A. Biella, F. Storme, J. Lebreuilly, D. Rossini, R. Fazio, I. Carusotto, and C. Ciuti, *Phys. Rev. A* **96**, 023839 (2017).
- [37] F. Vicentini, F. Minganti, R. Rota, G. Orso, and C. Ciuti, *Phys. Rev. A* **97**, 013853 (2018).
- [38] R. Rota, F. Minganti, A. Biella, and C. Ciuti, *New Journal of Physics* **20**, 045003 (2018).
- [39] R. Rota, F. Minganti, C. Ciuti, and V. Savona, *Phys. Rev. Lett.* **122**, 110405 (2019).
- [40] L. Lu, J. D. Joannopoulos, and M. Soljai, *Nature Photonics* **8**, 821 EP (2014), review Article.
- [41] P. Roushan, C. Neill, A. Megrant, Y. Chen, R. Babbush, R. Barends, B. Campbell, Z. Chen, B. Chiaro, A. Dunsworth, A. Fowler, E. Jeffrey, J. Kelly, E. Lucero, J. Mutus, P. J. J. O'Malley, M. Neeley, C. Quintana, D. Sank, A. Vainsencher, J. Wenner, T. White, E. Kapit, H. Neven, and J. Martinis, *Nature Physics* **13**, 146 (2016).
- [42] P. St-Jean, V. Goblot, E. Galopin, A. Lemaître, T. Ozawa, L. Le Gratiet, I. Sagnes, J. Bloch, and A. Amo, *Nature Photonics* **11**, 651 (2017).
- [43] R. O. Umucalilar and I. Carusotto, *Phys. Rev. Lett.* **108**, 206809 (2012).
- [44] S. Klemmt, T. H. Harder, O. A. Egorov, K. Winkler, R. Ge, M. A. Bandres, M. Emmerling, L. Worschech, T. C. H. Liew, M. Segev, C. Schneider, and S. Höfling, *Nature* **562**, 552 (2018).
- [45] Y. L. Dong, T. Neupert, R. Chitra, and S. Schmidt, *Phys. Rev. B* **94**, 035441 (2016).
- [46] F. Iemini, A. Russomanno, J. Keeling, M. Schirò, M. Dalmonde, and R. Fazio, *Phys. Rev. Lett.* **121**, 035301 (2018).
- [47] R. R. W. Wang, B. Xing, G. G. Carlo, and D. Poletti, *Phys. Rev. E* **97**, 020202 (2018).
- [48] Z. Gong, R. Hamazaki, and M. Ueda, *Phys. Rev. Lett.* **120**, 040404 (2018).
- [49] K. Tucker, B. Zhu, R. J. Lewis-Swan, J. Marino, F. Jimenez, J. G. Restrepo, and A. M. Rey, *New Journal of Physics* **20**, 123003 (2018).
- [50] F. M. Gambetta, F. Carollo, M. Marcuzzi, J. P. Garrahan, and I. Lesanovsky, *Phys. Rev. Lett.* **122**, 015701 (2019).
- [51] J. Tindall, B. Buča, J. R. Coulthard, and D. Jaksch, *Phys. Rev. Lett.* **123**, 030603 (2019).
- [52] C. Lledó, T. K. Mavrogordatos, and M. H. Szymańska, *Phys. Rev. B* **100**, 054303 (2019).
- [53] B. Buča, J. Tindall, and D. Jaksch, *Nature Communications* **10**, 1730 (2019).
- [54] K. Sacha and J. Zakrzewski, *Reports on Progress in Physics* **81**, 016401 (2017).
- [55] V. V. Albert and L. Jiang, *Phys. Rev. A* **89**, 022118 (2014).
- [56] V. V. Albert, B. Bradlyn, M. Fraas, and L. Jiang, *Phys. Rev. X* **6**, 041031 (2016).
- [57] B. Baumgartner and H. Narnhofer, *Journal of Physics A: Mathematical and Theoretical* **41**, 395303 (2008).
- [58] J. O'Sullivan, O. Lunt, C. W. Zollitsch, M. L. W. Thewalt, J. J. L. Morton, and A. Pal, (2018), [arXiv:1807.09884](https://arxiv.org/abs/1807.09884).
- [59] D. Sarchi, I. Carusotto, M. Wouters, and V. Savona, *Phys. Rev. B* **77**, 125324 (2008).
- [60] C. Eichler, Y. Salathe, J. Mlynek, S. Schmidt, and A. Wallraff, *Phys. Rev. Lett.* **113**, 110502 (2014).
- [61] M. Abbarchi, A. Amo, V. G. Sala, D. D. Solnyshkov, H. Flayac, L. Ferrier, I. Sagnes, E. Galopin, A. Lemaître, G. Malpuech, and J. Bloch, *Nature Physics* **9**, 275 (2013).
- [62] M. Galbiati, L. Ferrier, D. D. Solnyshkov, D. Tanese, E. Wertz, A. Amo, M. Abbarchi, P. Senellart, I. Sagnes, A. Lemaître, E. Galopin, G. Malpuech, and J. Bloch, *Phys. Rev. Lett.* **108**, 126403 (2012).
- [63] K. G. Lagoudakis, B. Pietka, M. Wouters, R. André, and B. Deveaud-Plédran, *Phys. Rev. Lett.* **105**, 120403 (2010).
- [64] S. R. K. Rodriguez, A. Amo, I. Sagnes, L. Le Gratiet, E. Galopin, A. Lemaître, and J. Bloch, *Nature Communications* **7**, 11887 (2016).
- [65] T. J. Kippenberg, A. L. Gaeta, M. Lipson, and M. L. Gorodetsky, *Science* **361** (2018), [10.1126/science.aan8083](https://doi.org/10.1126/science.aan8083).
- [66] N. C. Zambon, S. R. K. Rodriguez, A. Lemaître, A. Harouri, L. L. Gratiet, I. Sagnes, P. St-Jean, S. Ravets,

- A. Amo, and J. Bloch, (2019), [arXiv:1911.02816 \[cond-mat.mes-hall\]](#).
- [67] H.-P. Breuer, *The Theory of Open Quantum Systems* (Clarendon, Oxford, 2007).
- [68] C. W. Gardiner and P. Zoller, *Quantum noise : a handbook of Markovian and non-Markovian quantum stochastic methods with applications to quantum optics*, 3rd ed., Springer series in synergetics, Vol. vol. 56 Ed.3 (Springer, Berlin, 2004).
- [69] In this work we used $N_i^{max} = 47$ for the steady-state results and $N_i^{max} = 50$ for the spectral analysis of the Liouvillian.
- [70] F. Minganti, A. Biella, N. Bartolo, and C. Ciuti, *Phys. Rev. A* **98**, 042118 (2018).
- [71] M.-J. Hwang and M. B. Plenio, *Phys. Rev. Lett.* **117**, 123602 (2016).
- [72] R. Puebla, M.-J. Hwang, J. Casanova, and M. B. Plenio, *Phys. Rev. Lett.* **118**, 073001 (2017).
- [73] M.-J. Hwang, P. Rabl, and M. B. Plenio, *Phys. Rev. A* **97**, 013825 (2018).
- [74] K. Vogel and H. Risken, *Phys. Rev. A* **39**, 4675 (1989).
- [75] B. Opanchuk and P. D. Drummond, *Journal of Mathematical Physics* **54**, 042107 (2013), <https://doi.org/10.1063/1.4801781>.
- [76] B. Buca and D. Jaksch, arXiv e-prints , arXiv:1905.12880 (2019), [arXiv:1905.12880 \[quant-ph\]](#).

Chapter 5

Dissipative Kerr solitons as dissipative time crystals

Dissipative Kerr solitons (DKSs) and their “dual” Kerr frequency combs (KFCs) have unlocked a large bandwidth of novel arena in numerous and various fields. DKSs and KFCs are characterized by strong correspondence articulated according to a frequency- or temporal-domain approach, as schematized in Fig. 5.1.

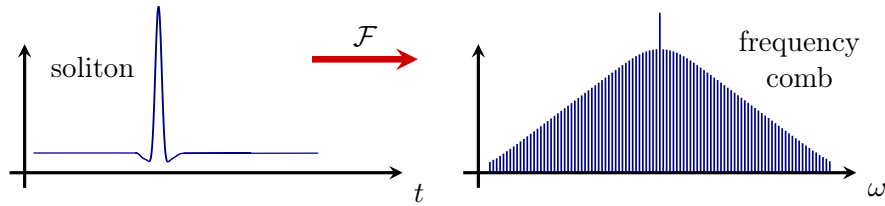


Figure 5.1: KFCs and DKSs and their relationship. Mathematically, the correspondence between KFCs and DKSs is established through the Fourier transformation.

They found application ranging from fundamental physics, metrology, precision spectroscopy to communication, biology and astronomy.

A key step on this road to applications is the downscaling of DKS sources. While in the infancy of the field of DKS, centimeter or meter-sized platforms were required to generate them, today they can be generated within compact, scalable, chip-scale platforms.

Motivated precisely by this “en marche” miniaturization, the goal of this chapter is to propose a fully quantum approach in the spirit of open quantum systems (This concept has been addressed in [chapter 2](#)).

Indeed, while DKS originate from quantum phenomena, mostly classical studies have been performed and only a handful of publications adopt a quantum approach.

This analysis leads us to make the connection between DKS and the concept of DTC addressed in the previous chapter.

We will begin this chapter by reviewing some notions related to DKSs and KFCs.

Afterwards, we will present a full study addressing the “quantum dynamics of dissipative Kerr solitons” by reproducing the research paper [3] of the author. Within this work, we provide a quantum model for DKSs within the dissipative quantum system framework, and come up with a numerical study using the truncated Wigner formalism (introduced in [chapter 3](#)). This quantum analysis allows us to interpret DKSs as dissipative time crystals.

Contents

5.1	Optical frequency combs	114
5.1.1	Introduction.	114
5.1.2	Generation of frequency combs	115
5.2	Kerr frequency combs	115
5.2.1	Kerr comb generation	116
5.3	Temporal cavity solitons	118
5.3.1	Dissipative solitons	118
5.3.2	Temporal cavity solitons	118
5.4	Dissipative Kerr soliton	119
5.4.1	A rich dynamic	119
5.4.2	Solitons and frequency combs	120
5.4.3	Theoretical description of solitons in a microresonator	120
5.4.4	Anatomy of KFCs	120
5.4.5	Lugiato–Lefever equation	121
5.5	Multi mode critical phenomena: quantum dynamics of dissipative Kerr solitons	122

5.1 Optical frequency combs

5.1.1 Introduction.

Optical frequency combs (OFCs) [784–787] are optical sources, whose spectrum is composed of discrete and equally-spaced spectral lines. More precisely, the optical frequencies ω_μ of these lines (the comb teeth) obey the comb equation

$$\omega_\mu = \mu \cdot \omega_r + \omega_0, \quad (5.1)$$

where ω_r is the repetition rate frequency, ω_0 is the carrier-envelope offset frequency [787], and μ is an integer indexing the individual comb tooth. The spectrum of an OFC spans from the infrared [788] to the visible [789] and ultraviolet [790–792].

Frequency “ruler”. The precise evenly-spaced sequence in the frequency domain turns OFCs into valuable tools for measuring unknown light frequencies and time intervals with an impressive precision¹ and speed, offering a wide range of applications. They can also be used to couple an unknown optical frequency to a radio or microwave frequency of reference [793, 794].

History. OFCs were initially developed to count the cycles of optical atomic clocks. Schematically, an atomic clock consists of an oscillator (the atom) and a counter that

¹OFCs are often called optical rulers in the literature and achieve accuracy that was previously unattainable.

counts the oscillations (the comb). In 2000 it was shown that the spectrum of OFCs can span over an octave of optical bandwidth [793, 795, 796], which is a necessary condition for many application. This opened up completely new scientific and technological perspectives and OFCs are primary elements in a wide and growing range of applications [797]². They triggered outstanding breakthroughs in frequency metrology and precision measurements [786, 793, 794], high precision spectroscopy [799, 800], communications [801, 802], microwave photonics [803], frequency synthesis [784, 804], optical ranging [805, 806], quantum sources [807, 808], metrology [809, 810] and astrocombs [811, 812].

Applications. The wide range of applications for OFCs is remarkable. OFCs have proven to be indispensable tools in various arenas and their constant downscaling³ makes them very attractive for cutting-edge technological applications. Today, state of the art OFCs have been taken out of scientific laboratories and are of chip scale, operating in any environment, commercially available, cheap and mass produced. The numerous and various fields where OFCs found applications include the gearwork in optical atomic clocks [785, 814], fundamental physics [815–818], waveform synthesis [784, 804, 819, 820] and measurement [802], X-ray and attosecond pulse generation [821], precision ranging [822], LIDAR⁴ [823], data center interconnects [824], molecular fingerprinting [825], medical diagnostics [826], gas sensing [827–829], precision time or frequency transfer over fiber and free-space [830], astronomy and cosmology [811, 812, 831, 832] including satellites [833]. The wide spectrum of scientific and technological applications is e.g. reviewed in [834].

5.1.2 Generation of frequency combs

The last two decades have witnessed the development of several principles for the generation of OFCs (see e.g. ref. [796] and in particular fig. 2 therein).

The original (and still cutting edge) method to generate OFCs are phase-stabilized mode-locked lasers [796, 835–839].

In recent years, other methods have been developed, among them electro-optic frequency combs [831, 840] and chip-scale systems based on semiconductor [841–844] and microresonators⁵ systems.

Within this thesis, we will focus on the microresonator-based frequency combs, also known as *Kerr frequency combs*.

5.2 Kerr frequency combs

Kerr frequency combs (KFCs) [845–850] are optical frequency combs arising from the interaction of a continuous wave (laser pump) with a material featuring a Kerr nonlinearity. They have first been observed in 2007 [851] and since then, they have

²The importance of OFC science has been rewarded with the Nobel Prize in Physics in 2005 [798].

³In the past two decades, the generation of OFCs turned from mode-locked lasers with cavity lengths of the order of cm to chip-scale sources based on microresonators fitting in a volume of ca. 1cm³, and working at less than 1 Watt of electrical power [813].

⁴LiDAR is the acronym for Light Detection And Ranging.

⁵Also called microring resonators, micro-cavity resonators, micro-combs or Kerr resonators. Microresonators are optical resonators whose size are typically of the micrometer order.

been demonstrated in various materials [852–861]⁶. KFCs attract lot of interest [851, 863] because they offer the vista of miniature comb systems integrated on a semiconductor chip altogether the promise to reach the full capability of their bulk counterparts [819, 864, 865].

Kerr nonlinearity. The Kerr nonlinearity/effect [866, 867] is present in media with third-order nonlinear susceptibility $\chi^{(3)}$. It provides a “self-interaction”, involving no driving fields. It can be modeled by the interaction Hamiltonian

$$H = U \hat{a}^\dagger \hat{a}^\dagger \hat{a} \hat{a} \quad (5.2)$$

where U is proportional to $\chi^{(3)}$. For instance, silica exhibits a Kerr nonlinearity.

5.2.1 Kerr comb generation

KFCs are multimode states of light generated via parametric frequency conversion [868] in high-Q⁷ microresonators. KFCs can be generated by driving —away from material resonances — a high-Q Kerr-nonlinear optical microresonator with a single-frequency continuous-wave laser pump⁸.

Depending on the regime of parameters, and in particular the strength of the driving, the Kerr nonlinearity leads to different behaviors.

In the weakly driven Kerr resonator regime, the resonator modes are populated in pairs through the spontaneous parametric processes. In this regime, the DKS can be used to generate squeezed vacuum [870–872], heralded single photons [873–875], multiphoton entangled states [807, 808, 876].

In the strongly driven Kerr resonator regime, the parametric gain can exceed the loss of the resonator and gives rise to optical parametric oscillations and the formation of bright combs.

By driving sufficiently above a power threshold determined by the Kerr nonlinearity, and under appropriate conditions for the dispersion of the microresonator optical modes, the parametric process generates a comb of evenly spaced peaks in the frequency spectrum [786, 863].

Four-wave mixing. Despite the fact that KFCs have mostly been studied classically, their emergence originates from a quantum parametric process.

Above a parametric threshold [877], the sequence of resonator modes is inter-coupled through a cascaded four-wave-mixing (FWM) process [878] —a nonlinear parametric frequency conversion— and described by the energy conservation relation

$$\hbar\omega_a + \hbar\omega_b \rightarrow \hbar\omega_c + \hbar\omega_d . \quad (5.3)$$

Here, two photons in input with frequency ω_a and ω_b coherently interact via the Kerr nonlinearity, leading to two photons in output with frequency ω_c and ω_d .

⁶A website cataloging the publications on KFCs [862].

⁷The quality factor Q of a resonator with frequency ω is given by $Q = \omega/\kappa$.

⁸KFCs can also be generated through pumped optical pulses [869]. But here we will focus on the continuous-wave laser pump case.

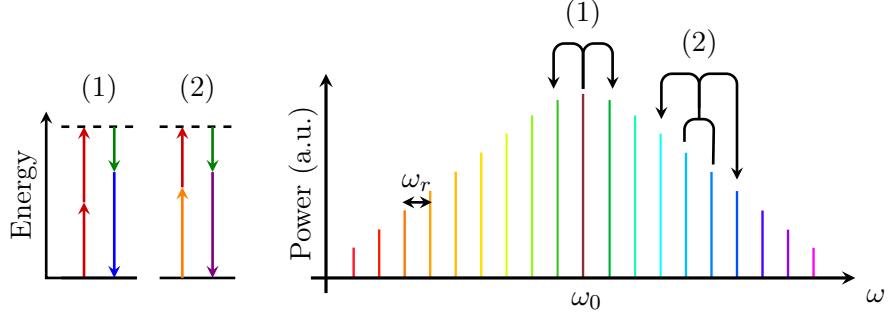


Figure 5.2: Scheme of the comb generation in a Kerr resonator through degenerate —process (1)— and non-degenerate —process (2)— FWM.

In microringresonators, the FWM process is based on the Kerr nonlinearity and can produce in the frequency domain equidistant and coherent optical lines with a spacing corresponding to the FSR of the microresonator. This mechanism is depicted in Fig. 5.2 and more details will be provided in subsection 5.4.4.

Enhanced within a high-quality (high-Q) microresonator⁹, the FWM processes initiated by only pumping one mode can excite a broad bandwidth (as many as several hundred) of equidistant cavity modes. This mechanism leads to a *coherent* optical frequency comb [851], the so-called Kerr frequency combs.

Importantly, the temporal coherence and a constant phase between the cavity modes is achieved through mode locking. Kerr resonators are modes locked through the formation of optical solitons in the cavity [879, 880]. This will be discussed in more detail in section 5.4.

More details about KFCs and the stages leading to the formation of Kerr combs can be found e.g. in Refs [881, 882].

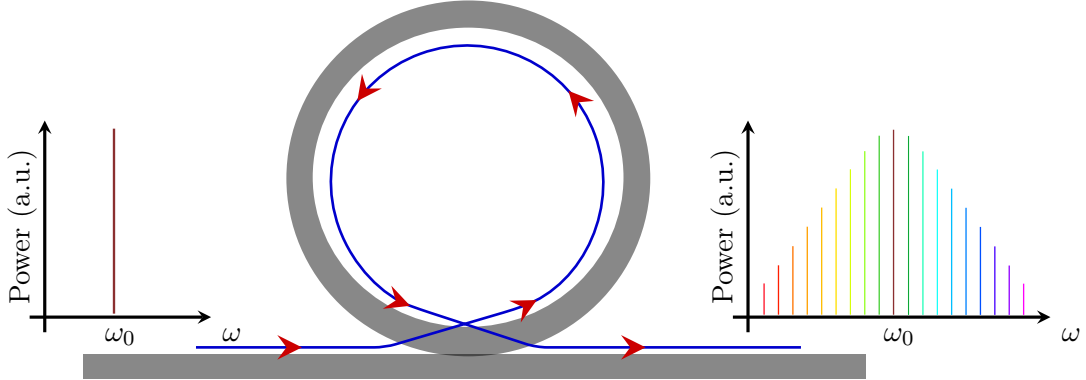


Figure 5.3: Resonator configuration.

Technological advantages and applications of Kerr combs. The interest in microresonator-based frequency combs roots from a variety of technological advantages, including low-energy requirements and robust structures that can be integrated in scalable, chip platforms [845, 863, 883–885].

⁹The recipe to enhancing light-matter interaction inside the resonator consists in increasing the quality factor and reducing the mode volume.

Applications ranging from spectroscopy and metrology [799, 886] to LIDAR¹⁰ [805, 806] and optical coherence tomography [889].

Frequency combs viewed in the frequency domain have close connection to solitons in the time domain.

5.3 Temporal cavity solitons

5.3.1 Dissipative solitons

Dissipative solitons¹¹ [890] are robust self-localized dissipative structures (LSs) that can persist *indefinitely*.

It is a concept prevalent in various nonlinear open systems driven out of equilibrium¹². These dissipative structures can be localized in space and/or in time: *temporal solitons* where the nonlinear effect balances the dispersion broadening, and *spatial solitons* [892–895] where the nonlinear effect balances the diffraction broadening.

Dissipative solitons can be found in various dissipative nonlinear systems, spanning a broad spectrum of fields of natural science [896] like .e.g. plasma physics [897, 898], hydrodynamics [899], magnetic fluids [900], tsunami waves, cloud and sand dune formation [896, 901], superconductivity [902], chemical reactions [903–905], biology [906], and optics [893, 907–912].

One common denominator of this cross-disciplinary concept is that its existence relies on a precise double balance between nonlinearity, diffusion-like processes, gain, and loss [909, 913, 914].

Robustness. The driven-dissipative nature of dissipative solitons makes these attractor states extremely stable and robust against fluctuations [896, 915].

Dissipative cavity solitons. Dissipative solitons in driven optical cavities or Dissipative cavity solitons have been investigated theoretically since the early 1990s. In experiments, they were first observed in two-dimensional spatial resonators [893] and more recently in one-dimensional Kerr cavities [909, 910].

While in a first instance the focus was on spatial dissipative cavity solitons [892, 916] the attention has now shifted towards their temporal counter-part [892, 914], which have attracted lots of interest lately [909].

5.3.2 Temporal cavity solitons

In the particular framework of nonlinear optical systems, *temporal cavity solitons* (TCSs)¹³ [909, 917] are pulses of light propagating indefinitely, which preserve their temporal and spectral shape in the course of propagation.

Their shape is maintained through an exact balance between gain and loss on one hand, and nonlinearity and dispersion on the other hand.

¹⁰Laser detection and ranging is a key technology in scientific and industrial metrology. It provides fast, long-range and high accuracy acquisition [887, 888].

¹¹The name soliton comes from the term solitary waves.

¹²To have an overview from a broader perspective, see e.g. [891].

¹³Or also sometimes called temporal dissipative solitons.

TCSs emerge in various optical systems [896] like e.g. in mode-locked lasers [835–838], coherently driven passive resonators, in particular fiber ring resonators [909] and monolithic microresonators [810, 846, 909, 914, 918, 919].¹⁴ TCSs have potential application as information carriers in all-optical memories [921]. State-of-the-art OFCs based on mode-locked lasers have been shown to exhibit relative frequency uncertainties at the level of 10^{-19} [922–925]. Recently, cavity solitons (CSs) have been demonstrated in microresonators [810, 918, 919, 926, 927].

Applications. Solitons of light propagating in optical fibers can be used for fast data transmission. Solitons can also be used in the creation of optical frequency combs in microresonators.

5.4 Dissipative Kerr soliton

Dissipative Kerr soliton (DKS)¹⁵ are temporal dissipative solitons [896, 915] emerging in Kerr nonlinear systems.

More explicitly, DKSs are stationary, localized and self-enforcing pulses of light that circulate in coherently driven nonlinear optical resonators and maintain their shape thanks to a double balance [846, 909, 918, 928].

Double balance. The shape preservation relies on an exact balance of Kerr nonlinearity and cavity dispersion (the dispersive spreading is cancelled by the self-focussing Kerr nonlinearity). The amplitude preservation is granted by the balance between parametric gain from the driving and cavity losses (the energy that is lost gets constantly replaced by new energy gained from the driving).

Dissipative Kerr solitons are the temporal representation of coherent frequency combs. DKSs were first observed in 2010 [909].

DKSs constitutes another possible state of the nonlinear cavity field.

DKSs are time-periodic solutions of an otherwise time-independent open quantum system dynamics [846, 929, 930]. This remark is important in view of the interpretation of DKSs as dissipative time crystals, as discussed in subsection 5.4.2.

Formally, solitons are solutions to the Lugiato-Lefever equation [389] and travel on top of a continuous-wave background [892, 914].

5.4.1 A rich dynamic

The DKSs can exhibit rich instability dynamics in specific regions of parameter space, including oscillations and chaotic states.

DKSs can take many forms [915], like e.g. breather solitons [931–933] and soliton crystals [848, 934].

¹⁴Lasers and passive resonator generated solitons differ by their pumping scheme, leading to profound differences between the soliton train and associated OFCs generated via these two methods [920].

¹⁵Or sometimes called Kerr cavity solitons.

Implementation. Since their discovery in microresonators, the DKSs have been observed in a variety of microresonators, ranging from bulk crystalline [918, 935] and silica microdisks [919], to photonic chip-scale devices [810, 919, 927, 936], and have been generated using both continuous-wave and pulsed excitation [869].

5.4.2 Solitons and frequency combs

The formation in the time domain of single temporal cavity solitons correspond in the frequency domain to soliton frequency combs¹⁶.

In particular, DKS provide a KFC source:

$$\text{DKS} \iff \text{phase-locked KFC}$$

Applications. DKS-based Kerr comb provide coherent optical combs, characterized by large spectral bandwidth (bandwidth exceeding one octave), low-noise comb, smooth spectral envelopes, high repetition rates from microwave to terahertz domains, low energies, and compactness (chip-scale microresonators) [918, 928, 938].

To date, these frequency comb sources have been successfully and extensively applied for counting of optical frequencies and distance measurements, dual-comb spectroscopy and telecommunications.

5.4.3 Theoretical description of solitons in a microresonator

5.4.4 Anatomy of KFCs

The (cold) resonance frequencies (eigenfrequencies) ω_μ of the μ -th mode are given through a Taylor expansion of the dispersion relation¹⁷ of the resonator around the pump frequency $\mu = 0$

$$\omega_\mu = \omega_0 + \sum_{k=1}^{+\infty} \frac{1}{k!} D_k \mu^k \quad (5.4)$$

$$= \omega_0 + D_1 \mu + D_{int}(\mu) \quad (5.5)$$

where we recall that μ is the index labelling a specific comb tooth. It represents the relative mode number with respect to the pumped mode ω_0 .

In this relation, $D_1/2\pi$ corresponds to the free spectral range (FSR) of the microresonator¹⁸ at the frequency ω_0 . In particular, we have $D_1 = 2\pi/T_R$ where T_R is the roundtrip time of the soliton in the resonator. Typically, the FSR of microresonator is of several gigahertz up to terahertz.

D_2 is the second order dispersion, and its expression reads $D_2 = -c/n_0 \cdot D_1^2 \cdot \beta_2$, with β_2 the anomalous group velocity dispersion (GVD) [878, 939], c is the speed of light and n_0 the refractive index. A positive (negative) D_2 corresponds to an anomalous

¹⁶This is the case in passive [846, 918] and active [937] media.

¹⁷Dispersion refers to the frequency dependency of the refractive index—i.e. different frequency components experience different phase velocities.

¹⁸Sometimes called reduced soliton repetition rate, in view of the comb equation eq. (5.1).

(normal) dispersion.

D_k for $\mu > 2$ are higher-order dispersion terms, given usually in units of rad/s, so that $D_k/2\pi$ are given in units of Hz.

One usually gathers D_2 and the higher-order dispersion terms $D_k, k > 2$ into the quantity D_{int} , the integrated dispersion, which describes the deviation of the resonance frequencies ω_μ from the equidistant frequency lines defined by $\omega_0 + \mu D_1$.

The intensity-dependant refractive index is responsible for a frequency shift of the modes. In order to compensate this shift and obtain an equidistant spectral grid, the FSR should increase with frequency [864]. This is the case for anomalous dispersion.

5.4.5 Lugiato–Lefever equation

The internal field in a nonlinear microresonator can be described by the paradigmatic model provided by the mean-field Lugiato-Lefever equation (LLE) [389, 928, 940–951]. This is a damped, driven, detuned nonlinear Schrödinger equation accounting for driving, dispersion, losses and Kerr nonlinearity.¹⁹

Let us start by defining the intracavity field $\mathcal{E}(\theta, t)$, where t describes time and $\theta \in [-\pi, \pi]$ is the azimuthal angle along the perimeter of the resonator. Using the parameters defined in subsection 5.4.4, the LLE governing the dynamics of this field is

$$\begin{aligned} \frac{\partial \mathcal{E}}{\partial t} = & -\kappa \mathcal{E} + i\sigma \mathcal{E} + i v_g \sum_{k=2}^K (i\Omega_{\text{FSR}})^k \frac{\beta_k}{k!} \frac{\partial^k \mathcal{E}}{\partial \theta^k} \\ & + i v_g \gamma |\mathcal{E}|^2 \mathcal{E} + \sqrt{\frac{2\kappa_{\text{ext}}}{T_{\text{FSR}}}} \sqrt{P_L}. \end{aligned}$$

In the above, $\beta_k = -\zeta_k/(-\Omega_{\text{FSR}})^k v_g$ models the dispersion, and $\sigma = \omega_L - \omega_0$ represents the detuning between the laser and the resonance frequencies. Here we assume that the normalization is such that $|\mathcal{E}|^2$ is expressed in units of watts. In the specific case of the absence of higher-order dispersion ($\beta_k = 0$ for $k > 2$) it will be convenient to change normalisation and work in terms of a new, dimensionless, total intra-cavity field $\psi \equiv (\gamma v_g / \kappa)^{1/2} \mathcal{E}$. The above equation can then be rewritten as

$$\frac{\partial \psi}{\partial \tau} = -(1 + i\alpha)\psi - i\frac{\beta}{2} \frac{\partial^2 \psi}{\partial \theta^2} + i|\psi|^2 \psi + F, \quad (5.6)$$

where $\tau = \kappa t$ is the dimensionless time, $\alpha = -\sigma/\kappa$ is the cavity detuning, $\beta = -\zeta_2/\kappa = \beta_2 v_g \Omega_{\text{FSR}}^2 / \kappa$ is the GVD (defined as normal for $\beta > 0$ and anomalous for $\beta < 0$), and $F^2 = (2\gamma v_g / T_{\text{FSR}})(\kappa_{\text{ext}} / \kappa^3) P_L$ is the dimensionless laser pump power.

Solitonic regime. The dimensionless Eq. (5.6) proves invaluable to study the nonlinear dynamics of the optical dissipation [944], and is particularly suited for a stability analysis [952]. DKSs are stable solutions of the LLE [909, 914, 953, 954]. The Lugiato–Lefever equation has been used as a valuable and handy tool for the analytical study of the nature, stability and bifurcation behaviour of solitons. It's worth

¹⁹The LLE was first introduced to describe spatial self-organization phenomena.

noting that the study of the LLE presents also interest from a purely mathematical point of view, especially regarding its dynamical properties [955–958].

The Lugiato–Lefever also provides a handy way to search for solitonic states in a microresonator. Indeed, transitions to soliton states are marked by discontinuous steps in the resonator transmission, while scanning the detuning of the driving field [918, 944, 959].

5.5 Multi mode critical phenomena: quantum dynamics of dissipative Kerr solitons

This last section reproduces the article submitted to *Physical Review A* [3]:

K. Seibold, R. Rota, F. Minganti, and V. Savona, *Quantum dynamics of dissipative kerr solitons*, *Phys. Rev. A* **105**, 053530 (2022).

Resulting from a collaboration with all the authors, directed by Vincenzo Savona, my contribution to the project was to provide the theoretical development, set up the numerical implementation in Matlab and to perform the numerical simulations. This work has benefited from the input of all the members of the LTPN group. Addressed to both, the theoretical and experimental community, the journey was marked and enriched by a subtle juggling between the different visions, concepts and jargon of these two worlds.

Quantum dynamics of Dissipative Kerr solitons

Kilian Seibold, Riccardo Rota, Fabrizio Minganti, and Vincenzo Savona

*Institute of Physics, Ecole Polytechnique Fédérale de Lausanne (EPFL), CH-1015, Lausanne, Switzerland**

(Dated: April 7, 2022)

Dissipative Kerr solitons arising from parametric gain in ring microresonators are usually described within a classical mean-field framework. Here, we develop a quantum-mechanical model of dissipative Kerr solitons in terms of the Lindblad master equation and study the model via the truncated Wigner method, which accounts for quantum effects to leading order. We show that, within this open quantum system framework, the soliton experiences a finite coherence time due to quantum fluctuations originating from losses. Reading the results in terms of the theory of open quantum systems, allows to estimate the Liouvillian spectrum of the system. It is characterized by a set of eigenvalues with finite imaginary part and vanishing real part in the limit of vanishing quantum fluctuations. This feature shows that dissipative Kerr solitons are a specific class of dissipative time crystals.

I. INTRODUCTION

Kerr frequency combs (KFCs) [1–6] are optical frequency combs generated by driving high-Q Kerr nonlinear optical microresonators with a single-frequency continuous-wave laser [7, 8]. By driving sufficiently above a power threshold determined by the Kerr nonlinearity, and under appropriate conditions for the dispersion of the microresonator optical modes, the parametric process generates a comb of evenly spaced peaks in the frequency spectrum [9, 10]. Since the first demonstration of KFCs [7], they have been observed countless times in a variety of platforms, materials, and spectral ranges, including silica microtoroid resonators [11, 12], crystalline microresonators [13], silicon nitride waveguide resonators [14–18], diamond [19], aluminum nitride [20, 21], lithium niobate [22, 23], and silicon [24].

KFCs emerge from multiple parametric resonant four-wave mixing processes. On the one hand, they result from a double balance process, where the nonlinear frequency shifts are balanced by the mode-frequency dispersion in the microresonator. On the other, the cavity losses are balanced by the gain induced by the continuous-wave driving field.

For sufficiently strong drive, the frequency spacing in the comb can be as small as the free spectral range of the microresonator. In this case, a bright pulse circulating within the resonator, called dissipative Kerr soliton (DKS) is formed [1, 10, 25–29]. DKSs are time-periodic solutions of an otherwise time-independent open quantum system dynamics [6, 30, 31]. A notable feature of DKSs is that they are dynamically stable within a classical field approach: their waveform retains its shape *indefinitely*, making DKSs a promising resource for precision measurements [6, 8], time keeping [32, 33], frequency metrology [34–37], pulse shaping [15], communication engineering [38–40], high-resolution spectroscopy [41–48], and quantum information processing [49].

The rapid development of miniaturized integrated systems for KFCs and DKSs, operating at low power where quantum effects are expected to be relevant, calls for a detailed study of the influence of quantum fluctuations on the spectral and dynamical properties of DKSs in the low-power regime. While the quantum properties of KFCs have been extensively investigated [2, 49–55], only recently the quantum mechanical properties of the DKS regime have been experimentally addressed [56]. In addition, both in the case of KFCs operated below the parametric oscillation threshold and for DKSs, quantum effects have been modeled under the assumption of linearized quantum fluctuations, resulting in Gaussian quantum fields [2, 49–57].

Here, we describe the quantum dynamics of DKSs using a Lindblad master equation, and investigate their properties via the truncated Wigner approximation [58–63] – an approximation to model driven-dissipative quantum systems in terms of stochastic *Langevin trajectories* sampled from the Wigner quasi-probability distribution. The truncated Wigner approximation reliably describes small quantum fluctuations, which are both due to the presence of nonlinearity and to the influence of the environment. These quantum fluctuations mainly introduce spatio-temporal dephasing of the DKS among different Langevin trajectories, as shown by our numerical simulations. When modeling the density operator of the system, which describes the system properties averaged over the statistical ensemble of Langevin trajectories, for any finite value of the input power the DKS does not persist indefinitely, but rather decays over time *on average*. We call the time scale, over which the soliton decays on average the *soliton coherence time*. At times longer than the soliton coherence time, the average dynamics is described by a nonequilibrium steady state that restores the time-invariant symmetry of the system. We demonstrate that the soliton coherence time varies as a power law of the strength of the nonlinearity, and the semiclassical, dynamically stable DKS emerges from the average dynamics in the limit of vanishing nonlinearity and infinite driving field amplitude.

These results allow describing the DKS as an open

* kilian.seibold@epfl.ch

quantum system. The theory of open quantum systems shows that, for any finite driving field and nonlinearity, the system must reach a translationally invariant steady state [64–66]. The decay of the DKS on average is a manifestation of the approach to this steady state. We demonstrate that the soliton coherence time corresponds to the so-called Liouvillian gap, i.e., the slowest time scale in the system.

Following the definition of Ref. [67], we can interpret the emergence of a DKS as a specific manifestation of a dissipative time crystal (DTC¹). DTCs [67, 70–89] are a peculiar phase of a driven-dissipative quantum system where the time-translational symmetry of the equation of motion is broken and non-stationary long-lived states spontaneously occur [90]. In the past years, intense research has been devoted to investigating the conditions under which dissipation can prevent a quantum many-body system from reaching a stationary state [84, 85, 90, 91]. This has led to numerous proposals of quantum systems supporting a DTC phase [67, 73, 76, 84, 92–99]. DTCs admit a natural explanation in terms of the eigenvalues of the Liouvillian superoperator, which generates the time evolution of the density matrix of an open quantum system [67, 100]. In a DTC, multiple eigenvalues of the Liouvillian exist with vanishing real and finite imaginary part [64, 101, 102], giving rise to a nonstationary dynamics with diverging relaxation time towards a steady state. The present result establishes thus a link between the long-lived DKS and the DTC phenomenon. More specifically, the Liouvillian is characterized by a set of eigenvalues whose imaginary parts are integer multiples of the frequency defining the free spectral range of the microresonator, and whose real part goes to zero in the thermodynamic limit of infinite photon number and vanishing nonlinearity.

The work is organized as follows. In Sec. II, we survey the theoretical framework used for the quantum analysis of DKSs. In Sec. III, we discuss the result obtained for the dynamics of the system: in particular, we compute the Liouvillian gap for decreasing drive power and depict a schematic representation of the spectrum of the Liouvillian. The main findings and conclusions of this work are drawn in Sec. IV.

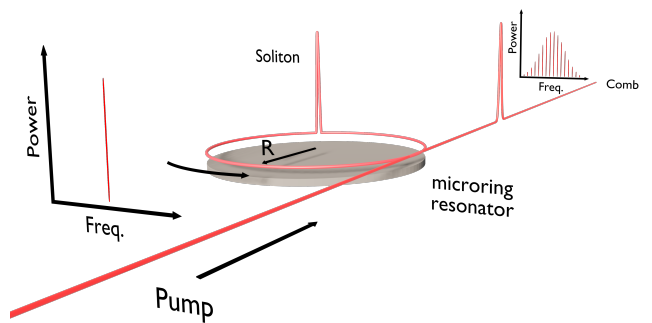


Figure 1. Schematic representation of the generation of a Kerr optical frequency comb using a high-Q Kerr optical ring microresonator. A continuous wave source drives the ring, which induces the propagation of a soliton (depicted in red) along the ring. The output signal shows the optical frequency comb. When all the resonator modes participate in the parametric process, the non-linear dynamics give rise to a DKS.

II. THEORETICAL FRAMEWORK

A. The open quantum system model and Liouvillian gap

We consider a driven high-Q continuous optical ring microresonator, whose schematic is shown in Fig. 1. The system Hamiltonian, in a frame rotating at the driving frequency, reads ($\hbar = 1$):

$$\hat{\mathcal{H}} = \sum_l \sigma_l \hat{a}_l^\dagger \hat{a}_l + \frac{\kappa}{2} F (\hat{a}_0^\dagger + \hat{a}_0) + \frac{g}{2} \sum_{m,n,p,q} \delta_{m+p,n+q} \hat{a}_n^\dagger \hat{a}_q^\dagger \hat{a}_m \hat{a}_p, \quad (1)$$

where \hat{a}_l (\hat{a}_l^\dagger) is the annihilation (creation) operator of the l -th angular momentum mode (i.e., the discrete set of whispering gallery modes), satisfying the commutation relation $[\hat{a}_j, \hat{a}_k^\dagger] = \delta_{jk}$. Only the lowest-energy mode of the microresonator ($l = 0$) is driven by an external continuous-wave laser of amplitude F . The Kerr interaction strength can be obtained from a microscopic model as $g = \hbar \omega_0^2 c n_2 / (n_0^2 A_{\text{eff}} L)$ [57, 103, 104], where c is the speed of light in vacuum, n_0 is the refractive index of the medium at the fundamental resonator frequency ω_0 , n_2 is the Kerr parameter, A_{eff} is the effective mode area, and L is the resonator length. Note that miniaturizing the resonator means decreasing the effective mode volume ($V_{\text{eff}} = A_{\text{eff}} L$) and, hence, increasing the Kerr interaction strength g . We set $\sigma_l = \sigma_0 + \omega_0 - \omega_l$, where $\sigma_0 = \omega_p - \omega_0$ is the detuning between the driving frequency ω_p and the fundamental resonator frequency ω_0 , and ω_l is the dispersion relation (which in this work is assumed parabolic, $\omega_l \propto l^2$, see also Fig. 2).

In order to account for the finite lifetime of the photons inside the microresonator, we describe the dynamics

¹ In this work, DTC stands for dissipative time crystal and not for discrete time crystal [68]. In the context of open quantum systems, time crystals have been defined in several slightly different ways. Here, we follow the definition of DTCs given in Ref. [67], where DTCs are a critical phenomenon, emerging in the thermodynamic limit, where an otherwise time-translational invariant system develops everlasting oscillations. In discrete time crystals, on the other hand, the discrete time-translation symmetry is broken in a periodically-driven system. A recent experimental demonstration of the realization of a discrete time crystal in a simple, all-optical setup constituted of one resonator [69].

of the open system in terms of its reduced density matrix $\hat{\rho}$. Assuming a weakly interacting and a memoryless environment (i.e., Born and Markov approximations), $\hat{\rho}$ solves the Lindblad quantum master equation [58, 105]:

$$\frac{d\hat{\rho}}{dt} = \mathcal{L}\hat{\rho} = -i[\hat{\mathcal{H}}, \hat{\rho}] + \kappa \sum_l \mathcal{D}[\hat{a}_l] \hat{\rho}. \quad (2)$$

Here $\mathcal{D}[\hat{a}_l]\hat{\rho} = \hat{a}_l\hat{\rho}\hat{a}_l^\dagger - 1/2(\hat{a}_l^\dagger\hat{a}_l\hat{\rho} + \hat{\rho}\hat{a}_l^\dagger\hat{a}_l)$ is the dissipator in Lindblad form accounting for the loss of photons from a mode l into the environment and κ is the dissipation rate (which we assume uniform). \mathcal{L} is the Liouvillian superoperator and its spectrum, defined by the equation $\mathcal{L}\hat{\rho}_j = \lambda_j\hat{\rho}_j$, encodes the full dynamics of an open quantum system. In most physically relevant cases, the Liouvillian superoperator \mathcal{L} has a unique zero eigenvalue, which defines the nonequilibrium steady state $d\hat{\rho}_{ss}/dt = 0$ [65, 66]. All other eigenvalues of the Liouvillian have a negative real part, determining the irreversible dissipative dynamics towards the steady state. The eigenvalue λ_j , whose real part is the smallest nonzero in modulus, defines the Liouvillian gap Λ . Λ corresponds to the inverse of the longest relaxation timescale of the system. Critical phenomena, such as dissipative phase transitions or the emergence of DTCs, are associated with a closure of the Liouvillian gap, i.e., $\Lambda \rightarrow 0$. A complete account of the spectral theory of Liouvillians can be found in, e.g., Ref. [66].

B. Classical-field approach to solitons

To numerically simulate the optical ring microresonator, we will consider a finite number of modes N_m around the $l = 0$ driven mode. Except if differently specified, we will set $N_m = 101$ (i.e., we consider only the modes $l = [-50, -49, \dots, 50]$). We verified that the results shown hereafter are only affected in one part in 10^5 on the total population, as a result of this truncation in the number of modes. Despite this simplification, the numerically exact solution of the master equation (2), in the regime of large occupation considered here, would be computationally unfeasible.

DKSs in the weakly nonlinear regime are usually modeled in terms of the classical Gross-Pitaevskii (GP) equation, whereby the classical field amplitudes of the resonator modes $\alpha_l = \langle \hat{a}_l \rangle$ obey the equation

$$\begin{aligned} \alpha_l(t + dt) = & \alpha_l(t) + i \left\{ \left(\sigma_l + i \frac{\kappa}{2} \right) \alpha_l(t) \right. \\ & + g \sum_{m,n,p} \delta_{n+l,m+p} \alpha_m(t) \bar{\alpha}_n(t) \alpha_p(t) \\ & \left. - \frac{\kappa}{2} F \delta_{l,0} \right\} dt, \end{aligned} \quad (3)$$

where $\bar{\alpha}_n$ indicates the complex conjugate of the field α_n . The GP equation leads directly to the *Lugiato-Lefever*

equation [106, 107] describing the real-space dynamics of the soliton².

Note that Eq. (3) is invariant under the scaling relation

$$\tilde{\alpha}_l = \alpha_l / \sqrt{\tilde{N}}, \quad \tilde{g} = g \tilde{N}, \quad \tilde{F} = F / \sqrt{\tilde{N}}, \quad (4)$$

where we introduced the dimensionless scaling parameter \tilde{N} . The GP solution for the rescaled field $\tilde{\alpha}_l$ only depends on the product $\tilde{F}^2 \tilde{g} = F^2 g$. In what follows, all results are obtained by setting $\tilde{F}^2 \tilde{g} = 1$, which corresponds to a case well above the threshold for soliton formation (see discussion in Sec. III A).

C. The truncated Wigner approximation

Theoretical studies of DKSs beyond the GP approximation have been mostly carried out by assuming linearized quantum fluctuations around the GP solution, i.e., Gaussian quantum fields [2, 49–57]. Quantum mechanical properties of the ring resonator can be better described with methods based on quasi-probability distributions [58, 59], such as the truncated Wigner approximation (TWA). Indeed, in cases where the quantum effects are a small (but non-negligible) correction to the classical limit of very large photon occupation, these methods account also for non-Gaussian quantum fluctuations, which become relevant when increasing g . Below, we recall the main ideas behind the TWA; for a more detailed derivation, we refer the interested reader to Refs. [58–63].

For a single mode of the electromagnetic field, the Wigner quasi-probability distribution function $W(\alpha)$ of a given quantum state expresses the quasi-probability distribution function in the phase space spanned by Q and P , with $\alpha = (Q + iP)/\sqrt{2}$. The quantities Q and P are the (real) eigenvalues of the electromagnetic field quadratures \hat{q} , and \hat{p} , with $\hat{a} = (\hat{q} + i\hat{p})/\sqrt{2}$. For N_m modes, the Wigner function $W(\vec{\alpha})$ is easily generalized in terms of N_m complex fields $\vec{\alpha} = \{\alpha_{-N_m/2}, \dots, \alpha_{N_m/2}\}$. The density matrix can be expressed in terms of the Wigner function as [109]

$$W(\vec{\alpha}) = \left(\frac{2}{\pi} \right)^{N_m} \text{Tr} \left[\prod_{l=-N_m/2}^{N_m/2} \hat{D}(\alpha_l) e^{i\pi \hat{a}_l^\dagger \hat{a}_l} \hat{D}(-\alpha_l) \hat{\rho} \right], \quad (5)$$

where $\hat{D}(\alpha_l) = \exp(\alpha_l \hat{a}_l^\dagger - \alpha_l^* \hat{a}_l)$ is the displacement operator. $W(\vec{\alpha})$ is a quasi-probability because it is real-valued, but it can take negative values. The Lindblad

² Usually, the GP (Lugiato-Lefever) equations are written as a set of coupled ordinary differential equations. Here, we represent them as a set of differential forms in order to be consistent with Eq. (6) below, which contains the stochastic term $\chi_{l,\mu}(t)$. Otherwise, its definition would require to introduce stochastic integration. We refer the interested reader to Ref. [108].

master equation for the density matrix of a quantum optical system characterized by a Kerr nonlinearity maps onto a third-order differential equation for $W(\vec{\alpha})$ in the variables $\vec{\alpha}$. The exact solution of this equation is as cumbersome as the solution of the corresponding master equation. However, when in presence of a small Kerr nonlinearity g and for sufficiently well-behaved functions, the third-order terms can be neglected, resulting in the TWA [60, 62]. The TWA correctly describes quantum fluctuations up to the lowest (i.e. second) order in \hbar with respect to the mean-field equation, holding in the limit of very large photon occupation [63].

The advantage of the TWA is that it defines a Fokker-Planck equation for the complex fields $\vec{\alpha}$. By choosing an appropriate initial distribution, the Fokker-Planck equation for $W(\vec{\alpha})$ can be cast into a set of Langevin equations for the corresponding stochastic processes on the complex fields $\alpha_{l,\mu}(t)$. Each instance of the stochastic process thus results in a Langevin trajectory, and the average solutions of the Fokker-Planck and master equations are obtained from averaging over the statistical ensemble of possible trajectories. In the case of the DKS model considered here, the Langevin equations read

$$\begin{aligned} \alpha_{l,\mu}(t+dt) = & \alpha_{l,\mu}(t) + i \left\{ \left(\sigma_l + i \frac{\kappa}{2} - g \right) \alpha_{l,\mu}(t) \right. \\ & + g \sum_{m,n,p} \delta_{n+l,m+p} \alpha_{m,\mu}(t) \bar{\alpha}_{n,\mu}(t) \alpha_{p,\mu}(t) \\ & \left. - \frac{\kappa}{2} F \delta_{l,0} \right\} dt + \sqrt{\kappa dt/2} \chi_{l,\mu}(t). \end{aligned} \quad (6)$$

Here, the index μ runs on the distinct Langevin trajectories, and the term $\chi_{l,\mu}(t)$ is a complex Gaussian stochastic variable defining each specific trajectory, and characterized by correlation functions $\langle \chi_l(t) \chi_l(t') \rangle = 0$ and $\langle \chi_l(t) \bar{\chi}_{l'}(t') \rangle = dt \delta_{l,l'} \delta(t-t')$. The noise terms $\chi_{l,\mu}(t)$ therefore account for the quantum fluctuations induced by photon losses.

Within the TWA, it is possible to obtain the expectation value of symmetrized product of operators in terms of an average over the sampled Langevin trajectories, according to the formula

$$\text{Tr} \left[\hat{\rho}(t) \left\{ (\hat{a}_j^\dagger)^n, (\hat{a}_k)^m \right\}_{\text{sym}} \right] = \langle (\bar{\alpha}_j(t))^n (\alpha_k(t))^m \rangle_{\text{stoch}}, \quad (7)$$

where we use the notation for the stochastic average $\langle \alpha_j(t) \rangle_{\text{stoch}} = \left(\sum_{\mu=1}^{N_{\text{traj}}} \alpha_{j,\mu}(t) \right) / N_{\text{traj}}$. In other words, the expectation value of any observable is obtained by sampling a sufficiently large number N_{traj} of Langevin trajectories, thus recovering the results of the Fokker-Planck equation associated to the TWA. In the following, the convergence of the results with respect to the number of considered trajectories N_{traj} used for the averaging is carefully checked.

From the solutions of the Langevin equations, the number of photons in each mode l of the microresonator is

expressed by

$$N_l(t) = \langle |\alpha_l(t)|^2 \rangle_{\text{stoch}} - \frac{1}{2}, \quad (8)$$

and the photon density at position θ is obtained as

$$N_\theta(t) = \langle |\psi_\mu(\theta, t)|^2 \rangle_{\text{stoch}} - \frac{N_m}{4\pi}, \quad (9)$$

where

$$\psi_\mu(\theta, t) = \frac{1}{\sqrt{2\pi}} \sum_l e^{i\theta l} \alpha_{l,\mu}(t). \quad (10)$$

Notice that Eqs. (8) and (9) clearly illustrate how quantum fluctuations are approximately described by the TWA. In particular, Eq. (8) shows that the classical field modeled by the Langevin equation contains quantum fluctuations corresponding to half a photon per mode. Similarly, Eq. (9) suggests that the Langevin field a discrete element of real space $\Delta\theta$, defined by the momentum cutoff introduced by truncating to m modes, contains quantum fluctuations corresponding to $N_m/4\pi$ photons.

Contrarily to the GP equation, Eq. (6) is not invariant under the rescaling introduced in Eq. (4). Indeed, applying the same rescaling to Eq. (6), one obtains

$$\begin{aligned} \tilde{\alpha}_{l,\mu}(t+dt) = & \tilde{\alpha}_{l,\mu}(t) + i \left\{ \left(\sigma_l + i \frac{\kappa}{2} - \frac{\tilde{g}}{\tilde{N}} \right) \tilde{\alpha}_{l,\mu}(t) \right. \\ & + \tilde{g} \sum_{m,n,p} \delta_{n+l,m+p} \tilde{\alpha}_{m,\mu}(t) \tilde{\alpha}_{n,\mu}(t) \tilde{\alpha}_{p,\mu}(t) \\ & \left. - \frac{\kappa}{2} \tilde{F} \delta_{l,0} \right\} dt + \sqrt{\kappa dt / (2\tilde{N})} \chi_{l,\mu}(t), \end{aligned} \quad (11)$$

which explicitly depends on \tilde{N} .

For coherent states, the scaling parameter \tilde{N} is proportional to the ratio between the field intensity and the fluctuations of the field quadratures, and therefore can be interpreted as a measure of the *classicality* of the optical system. Small values of \tilde{N} describe a regime with sizeable quantum effects, where quantum fluctuations are of the same order as the field intensity. As \tilde{N} increases, fluctuations become smaller compared to the field intensity, and quantum effects become less relevant. This interpretation of the quantity \tilde{N} holds also in the TWA, which describes quantum states beyond the coherent-state approximation. Indeed, for large values of \tilde{N} , Eq. (11) approaches the GP equation (3). Our goal is to investigate how the quantum effects influence the dynamics of a DKS by comparing the solution of Eq. (11) obtained for different values of \tilde{N} , while keeping all the other parameters unchanged. Notice that, in light of the scaling relations in Eq. (4), this procedure corresponds to solving the Lindblad master equation Eq. (2) for different values of the nonlinearity g and the pump amplitude F , in such a way that the product $F^2 g$ remains constant.

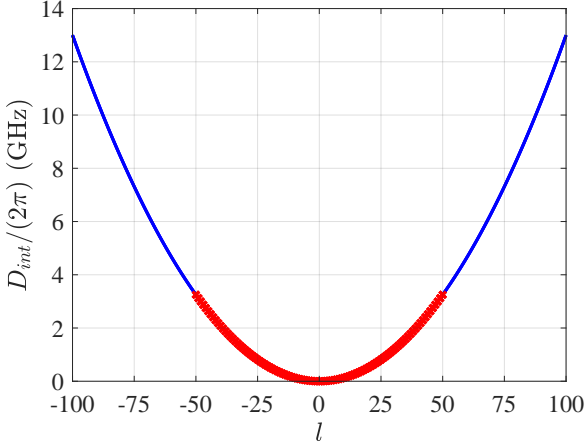


Figure 2. Integrated dispersion relation $D_{\text{int}}(l)$ versus relative mode number l . The red markers show the 101 spectral modes that are considered in the numerical simulations. The parameters are quoted in the text and correspond to typical experimental situations [18].

III. RESULTS

A. Regime of parameters

A micro-ring resonator is characterized by its radius R (and length $L = 2\pi R$), cross-section A_{eff} , quality factor Q , resonant central frequency $f_0 = \omega_0/2\pi$, refractive index n_0 , the Kerr parameter n_2 , and the group velocity dispersion β_2 . The system is driven by a laser with frequency ω_p .

From these quantities, the loss rate κ and the nonlinearity g in the Lindblad master equation (2) can be determined respectively as [57, 103, 104]

$$\kappa = \frac{\omega_0}{Q}, \quad (12)$$

$$g = \frac{\hbar\omega_0^2 cn_2}{n_0^2 A_{\text{eff}} L}, \quad (13)$$

where c is the speed of light. Close to the driving field frequency (i.e., $\omega_0 \simeq \omega_p$), the mode dispersion of the microresonator is approximated using a second-order polynomial

$$\omega_l = \omega_0 + D_1 l + \frac{1}{2} D_2 l^2, \quad (14)$$

where $D_1 = c/(n_0 R)$ is the mean free spectral range (FSR) and $D_2 = -(c/n_0) D_1^2 \beta_2$. A positive value of D_2 characterizes the anomalous dispersion regime, which is needed for the formation of DKSs [18]. The integrated dispersion relation $D_{\text{int}}(l)$ relative to the driving mode at $l = 0$ is defined by [c.f. Fig. 2]

$$D_{\text{int}}(l) \equiv \omega_l - (\omega_0 + D_1 l). \quad (15)$$

The driving parameter F is related to the power of the external driving field through the relation $P_{\text{ext}} = \hbar\omega_p \kappa F^2 / (4\eta)$, where η is the coupling efficiency (we assume critical coupling, i.e., $\eta = 1/2$).

Typical parameters for a silicon nitride (Si_3N_4) ring resonator encapsulated in silica [18, 110], with $R = 100 \mu\text{m}$, are $A_{\text{eff}} = 0.73 \times 2.5 \times 10^{-12} \text{ m}^2$ [110], $Q = 1.5 \times 10^6$ [18], $f_0 = \omega_0/2\pi = 193.5 \text{ THz}$ [111] corresponding to a wavelength $\lambda = 1.55 \mu\text{m}$ in the telecom range, $n_0 = 1.99$, $n_2 = 2.4 \times 10^{-19} \text{ m}^2/\text{W}$ [112]. Consequently, following Eqs. (12) and (13), $\kappa/2\pi = 1.3 \times 10^8 \text{ Hz}$ and $g/2\pi = 0.39 \text{ Hz} = 0.49 \times 10^{-9} \kappa$.

Necessary conditions on the driving field detuning and intensity must be fulfilled in order to observe a DKS in the solution of the GP equation. In particular, we set the driving field frequency to $\omega_p/2\pi = 193.47 \text{ THz}$, i.e., a detuning $\sigma_0/2\pi = -0.132 \text{ GHz}$ [18]. The driving field amplitude F must be larger than a minimum threshold value F_{thr} [26, 57, 107]. Expressing the minimum threshold condition in terms of the parameters of the present model results in $F_{\text{thr}}^2 g / \kappa = \tilde{F}_{\text{thr}}^2 \tilde{g} / \kappa = 1/2$. Given the values of κ and g introduced above, the minimum threshold is $\tilde{F}_{\text{thr}} = 0.9 \times 10^4$. Here, to ensure the appearance of the DKS within the GP equation [107], we set in all the analysis that follows, $F = 1.8 \times 10^4$, i.e., twice the minimum threshold, corresponding to a laser power $P_{\text{ext}} = 1.7 \times 10^{-2} \text{ W}$ (similar to that used in Ref. [18]). This value, and the value chosen for g , therefore correspond to the typical regime of current experiments, like in Refs. [18, 110], where quantum fluctuations are very small relative to the classical field. We arbitrarily set $\tilde{N} = 1$ for this choice of F and g . In what follows, we will study the results of the TWA for values of \tilde{N} ranging between $\tilde{N} = 6.3 \times 10^{-6}$ and $\tilde{N} = 1$. Values $\tilde{N} < 1$ describe cases with larger nonlinearity \tilde{g} and smaller driving field amplitude \tilde{F} , than the values of F and g quoted above, for which quantum effects are larger. Finally, we define the dimensionless time parameter $\tau = \kappa t / 2$.

B. Dynamics of the soliton

We study the time evolution of DKSs by numerically solving Eq. (11) for the rescaled fields $\tilde{\alpha}_l$ obtained using the TWA approach. Eq. (11) gives rise to a stochastic trajectory in the space of the fields $\tilde{\alpha}_l$, determined by the specific realization of the noise term $\chi_{l,\mu}(t)$. All results in what follows are obtained by averaging over several trajectories arising from different realizations of $\chi_{l,\mu}(t)$. As initial conditions, we assume each mode to be in a coherent state corresponding to the solution $\tilde{\alpha}_l^{\text{GPE}}$ of the GP equation, which in turn is obtained by numerically integrating Eq. (3) at long times. This choice has the advantage of avoiding the integration of a possibly long transient before the actual formation of a soliton within a single trajectory. In the TWA formalism, this choice of initial condition implies that the initial condition $\tilde{\alpha}_l(t=0)$ in Eq. (11) must be sampled from a Gaus-

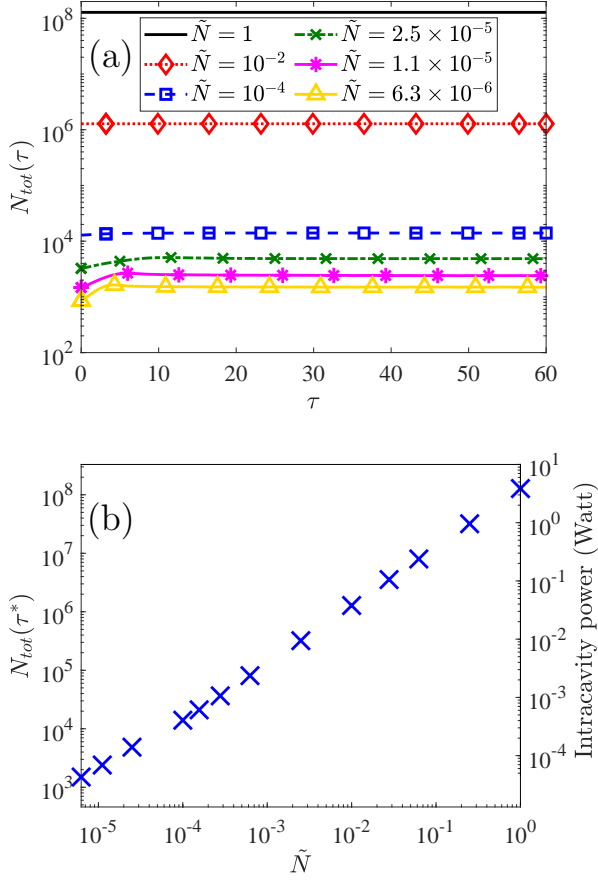


Figure 3. (a) Time evolution of the total number of photons in the ring for different values of \tilde{N} . (b) Total number of photons in the ring and intracavity power versus the scaling parameter \tilde{N} . The values are taken at $\tau^* = 60$, where the photon number reached a stationary distribution.

sian distribution of variance $1/(2\tilde{N})$ and average $\tilde{\alpha}_l^{\text{GPE}}$. More precisely, we set

$$\tilde{\alpha}_{l,\mu}(t=0) = \tilde{\alpha}_l^{\text{GPE}} + \frac{1}{\sqrt{2\tilde{N}}} \eta_{l,\mu}, \quad (16)$$

where $\eta_{l,\mu}$ is a complex random variable of zero mean, verifying $\langle \eta_{l,\mu} \eta_{l,\mu'} \rangle = 0$ and $\langle \bar{\eta}_{l,\mu} \eta_{l,\mu'} \rangle = \delta_{\mu,\mu'}$.

Fig. 3(a) displays the total number of photons in the ring N_{tot} vs time, for varying \tilde{N} . The small initial transient is due to the difference between the solution of the GP equation, which was used as initial condition, and the actual TWA solution. In what follows, when analyzing spectral features of the DKS, data will be taken in the vicinity of $\tau^* = 60$, which are not affected by the transient. In Fig. 3(b) the dependence of $N_{tot}(\tau^*)$ on \tilde{N} is shown to be linear, $N_{tot} \sim \tilde{N}$. Thus, also the intracavity power $P_I = \hbar\omega_p D_1 N_{tot}/(2\pi)$ (which is proportional to the total number of photons in the microring) depends linearly on \tilde{N} . We conclude that a small photon occupa-

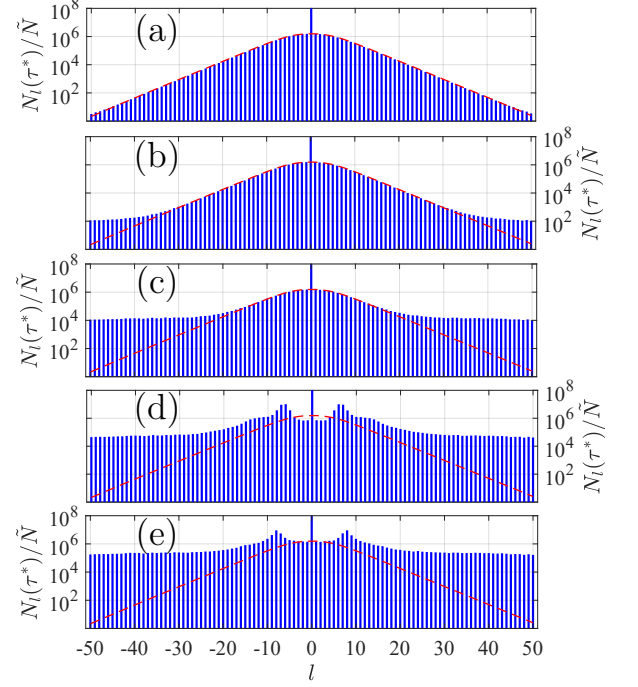


Figure 4. Snapshot of the mode occupation at τ^* for $\tilde{N} = 1$ (a), 10^{-2} (b), 10^{-4} (c), 2.5×10^{-5} (d), and 6.3×10^{-6} (e). The red dashed lines show the GPE prediction for the mode occupation. Parameter values: $\sigma_0 = -1.024\kappa$, $D_1 = 1.8587 \times 10^3 \kappa$, $D_2 = 2.02 \times 10^{-2} \kappa$, $g/2\pi = 0.49 \times 10^{-9} \kappa$ and $F = 1.8 \times 10^4$.

tion and low intracavity power is reached only for small \tilde{N} .

In Fig. 4, the photon number in the l -th mode $N_l(\tau^*)$ [c.f. Eq. (8)], is displayed for different values of \tilde{N} . For the largest value of \tilde{N} , the output field is in agreement with the prediction of the GP equation, while smaller values of \tilde{N} gradually display increasing features of quantum fluctuations.

In Fig. 5 the photon density along the ring $n(\theta, \tau) = N_\theta(\tau)/(2\pi)$, N_θ being the number of photons in the position θ [c.f. Eq. (9)]³, is displayed at increasing times τ (left-to-right) and increasing \tilde{N} (bottom-to-top). For $\tilde{N} = 1$ in Fig. 5(a-d), the soliton displays a constant profile within the considered time window. However, for smaller \tilde{N} , i.e., increasing the relevance of quantum fluctuations, the soliton profile changes in time, in particular by showing a decreasing contrast of the intensity profile along the ring. For the smallest value $\tilde{N} = 6.3 \times 10^{-6}$, Fig. 5(m-p), the photon density quickly approaches a uniform distribution over the ring. We conclude that the soliton is gradually smeared out over time by quantum fluctuations, and smaller values of \tilde{N} correspond to faster

³ Notice that this definition ensures that $N_{tot}(\tau) = \sum_l N_l(\tau) = \int d\theta n(\theta, \tau)$.

disappearance of the soliton.

Single Langevin trajectories, from which TWA results are drawn, give insight into the process leading to the disappearance of the soliton in Fig. 5, as a result of quantum fluctuations. A trajectory represents, in the limit of small nonlinearities, the possible outcome of an experiment with homodyne measurement of the output field [113]. In Fig. 6, we plot three trajectories at different values of \tilde{N} and at two different times. For $\tilde{N} = 10^{-2}$ a sharp soliton peak in the photon density persists both at short and long times. The position and height of the peak slightly vary with the sampled noise realization, but this difference is negligible with respect to the GP solution. At the intermediate value $\tilde{N} = 10^{-4}$, a similar behavior only appears at shorter times, while at longer times the trajectories differ significantly. For the smallest value $\tilde{N} = 4.4 \times 10^{-5}$ considered, we observe a faster loss of coherence between different trajectories. Since the effect increases when the nonlinearity is larger, we conclude that fluctuations, that are only responsible for a small dephasing among different trajectories at short time, accumulate as time passes, leading to a loss of spatial and temporal coherence, resulting in the smearing out of the DKS once an average is taken (see Fig. 5).

From the point of view of open quantum systems, the density matrix $\hat{\rho}(t)$, evolving under the Lindblad master equation in Eq. (2), describes the *average* time evolution of the microring resonator. Under quite general hypotheses, an open quantum system admits a unique steady state $\hat{\rho}_{ss}$, towards which the system density matrix will converge. In this sense, a system, which at $t = 0$ displays a soliton, will eventually converge to such a steady state. We can thus interpret the loss of soliton coherence in Fig. 5 as the decay towards the steady state, and call the timescale on which this process occurs the *soliton coherence time*. Thus, to quantify the soliton coherence time, we compute the Liouvillian gap Λ (i.e., the slowest decay rate). Indeed, the DKS is the longest-lived process of Eq. (2), and thus Λ is the inverse of soliton coherence time (see Sec. II A). To extract Λ , we consider the time evolution of the *contrast* of the soliton defined by

$$C(\tau) = \frac{\max_{\theta} (n(\theta, \tau))}{\int_0^{2\pi} n(\theta, \tau) d\theta / 2\pi}. \quad (17)$$

For a flat intensity profile along the ring, the value of $C(\tau)$ approaches 1. We estimate Λ by assuming an exponential behaviour vs time, $C(\tau) \simeq 1 + A \exp(-\Lambda\tau)$ and fitting the numerical results.

In Fig. 7, the Liouvillian gap is plotted as a function of \tilde{N} . For large \tilde{N} the Liouvillian gap follows a power law $\Lambda \sim \tilde{N}^a$ with $a < 0$, indicating that the gap closes in the classical limit $\tilde{N} \rightarrow \infty$. A similar power law emerges in the dependence of Λ on N_{tot} (inset of Fig. 7). Here, $\Lambda \sim N_{\text{tot}}^\eta$ with $\eta = -0.97 \pm 0.01$. This analysis indicates the range of values of the input power for which a finite soliton coherence time may be observed.

Summing up, the loss of coherence at the single trajectory level appears mainly as a change in the soliton

position with respect to the GP solution.⁴ And since this effect emerges only in Langevin trajectories (stemming from the TWA) and not in the GP equation, the loss of coherence is due to quantum (i.e., beyond semiclassical) fluctuations. Quantum fluctuations have two contributions: One comes from the noncommutative nature of the Hamiltonian terms, and the other comes from the system's interaction with the environment, which induces dissipation. The truncated Wigner approximation takes them both into account (up to order \hbar). The two additional terms accounting for these fluctuations can be obtained by comparing Eq. (6) with Eq. (3): a term proportional to g (producing a deterministic effect with respect to the GP equation), and the noise term $\chi_{l,\mu}$ (which induces random changes at a single trajectory, and thus mixness in the density matrix). It is the combined effects of these two terms which leads to the soliton finite coherence time.

C. DKS as a dissipative time crystal

The occurrence of a time-crystalline phase in a dissipative system is signaled by the emergence of several eigenvalues of the Liouvillian whose real part tends to zero in the thermodynamic limit, and whose imaginary part is a multiple of a finite frequency, as schematically shown in Fig. 8.

We extract the imaginary part of the Liouvillian eigenvalues with the largest real part, by studying the Fourier spectrum of the KFC

$$S_{\varphi}(\omega) = \left| \frac{\sqrt{2\pi}}{N_{\tau}T} \int_{t_0}^{t_0+N_{\tau}T} dt e^{i\omega t} \varphi(\theta = 0, t) \times \tilde{N} \right|^2. \quad (18)$$

where $\varphi(\theta, t) = \text{Tr} [\hat{\rho}(t) \times 1/\sqrt{2\pi} \sum_l e^{i\theta l} \hat{a}_l]$, and $T = 2\pi/D_1$ is the rotation period of the soliton along the ring. The parameters $t_0 = 20\kappa^{-1}$ and $N_{\tau} = 2 \times 10^4$ are set to ensure that the dynamics is dominated by the eigenvalues with the largest real part. Notice that, for these parameters, $S_{\varphi}(\omega)$ does not depend significantly on the position θ at which the field φ is considered.

The computed power spectra are plotted in Fig. 9. From the spectra, we extract the frequency spacing $\Omega_{\text{soliton}} = D_1 = 1.86 \times 10^3 \kappa$, which coincides with the classical prediction, indicating that quantum fluctuations affect mainly the coherence time of the soliton, while having negligible effects on the period of its motion along the ring. For the smallest value of $\tilde{N} = 6.3 \times 10^{-6}$, where $\Lambda \simeq 3 \times 10^{-2} \kappa$, the ratio $\Lambda/\Omega_{\text{soliton}}$ is of the order of 10^{-4} . These results indicate that the peculiar structure of the

⁴ While, at the single trajectory level, the processes of variation in amplitude and spatio-temporal position is dominant, for even smaller \tilde{N} and/or larger times, other phenomena like appearance of multiple peaks are observed.

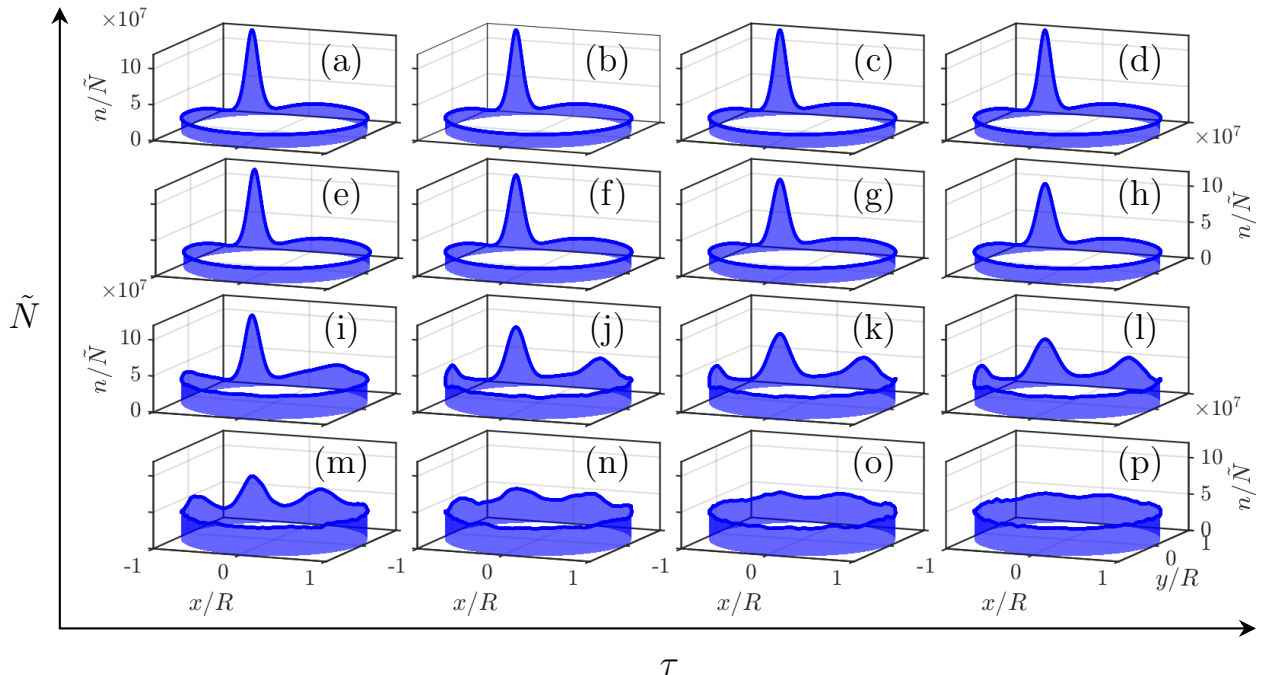


Figure 5. Snapshot of the field density in real space at $\tau = 0.5 \times 10^4 \kappa/2T \approx 8.5$ (a,e,i,m), $\tau = 1.5 \times 10^4 \kappa/2T \approx 25.4$ (b,f,j,n), $\tau = 2.5 \times 10^4 \kappa/2T \approx 42.3$ (c,g,k,o), and $\tau = 3.5 \times 10^4 \kappa/2T \approx 59.2$ (d,h,l,p), for $\tilde{N} = 10^{-2}$ (a,b,c,d), 10^{-4} (e,f,g,h), 2.5×10^{-5} (i,j,k,l), and 6.3×10^{-6} (m,n,o,p). The density is plotted as a function of the coordinates $x = R \cos(\theta)$ and $y = R \sin(\theta)$, R being the radius of the ring resonator. The soliton is depicted at times multiple of $T = 2\pi/D_1 \approx 4.2 \times 10^{-12}$ s, the rotation period of the soliton along the ring. For this choice of time, the peak of the soliton always occupies the same position in ring, allowing an easier comparison between the different plots.

frequency comb (i.e. the presence of equally spaced, narrow spectral lines) is preserved even in the regime where quantum effects produce a significant departure from the predictions of the classical GP equation.

IV. CONCLUSIONS

We have carried out a theoretical study of DKSs in microring resonators in terms of the truncated Wigner approximation, which describes quantum fluctuations to leading order in \hbar and is therefore well suited for the description of regimes of large photon occupation as in current experiments. We have shown that quantum effects are responsible of a finite coherence time of the soliton, which in the long time limit leaves place to an average solution with the field uniformly distributed along the ring. The timescale of the soliton decay towards the steady state solution depends on the relative size of quantum fluctuations, and decreases when quantum fluctuations become larger. A scaling analysis of the TWA equations indicates that a regime with large quantum effects may be achieved by decreasing the driving field intensity while correspondingly increasing the strength of the Kerr nonlinearity. The analysis provides clear indications about whether this behaviour can be observed in experiments.

We have additionally shown that the timescale asso-

ciated with the soliton disappearance is determined by the inverse Liouvillian spectral gap. More precisely, by studying the power spectrum of the DKS, we have inferred the complex eigenvalues of the Liouvillian superoperator which governs the dynamics of the DKS as an open quantum system. We have shown that the eigenvalues with the largest real part – besides the zero-eigenvalue associated to the spatially uniform steady state – are arranged to have a constant (negative) real part, defining the Liouvillian gap, and evenly spaced imaginary parts, corresponding to the Kerr frequency comb. This arrangement emerges asymptotically in the limit of large input power, and the Liouvillian gap vanishes as a power law of the total photon occupation in the microring modes. We have therefore shown that DKSs are a specific manifestation of a dissipative time crystal – a general phenomenon which can arise in open quantum systems and has been extensively studied in recent times. Establishing the link between DKSs and dissipative time crystals is an important step in the study and characterization of spontaneous time-translational symmetry breaking in quantum systems out of equilibrium.

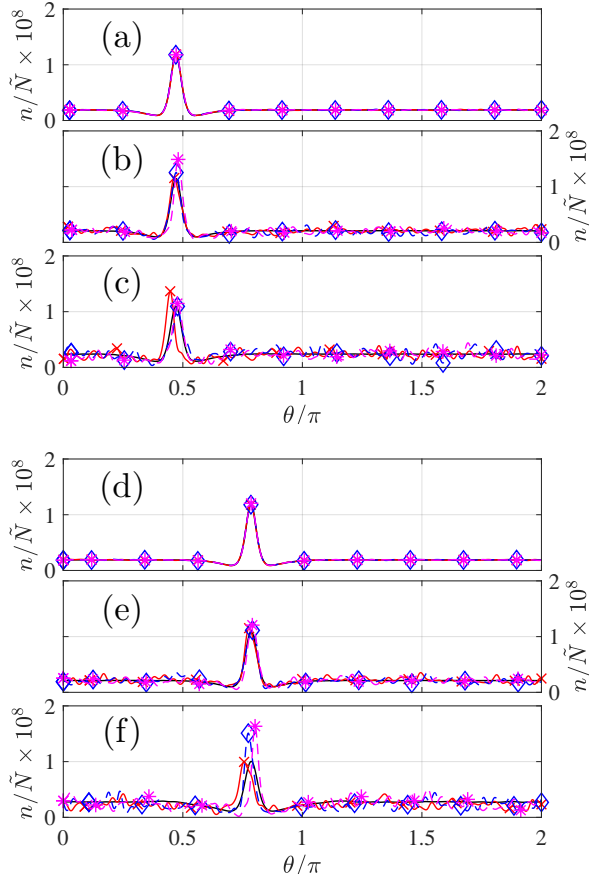


Figure 6. Occupation density in real space for $\tilde{N} = 10^{-2}$ (a,d), 10^{-4} (b,e) and 4.4×10^{-5} (c,f) at $\tau = 6$ (a,b,c) and $\tau = 15$ (d,e,f). Solid lines are averages over 10^4 trajectories, while three single trajectories are plotted as symbols (\times \star \diamond).

ACKNOWLEDGMENTS

We acknowledge enlightening discussions with Juan Pablo Vasco. This work was supported by the Swiss National Science Foundation through Project No. 200021.162357 and 200020.185015.

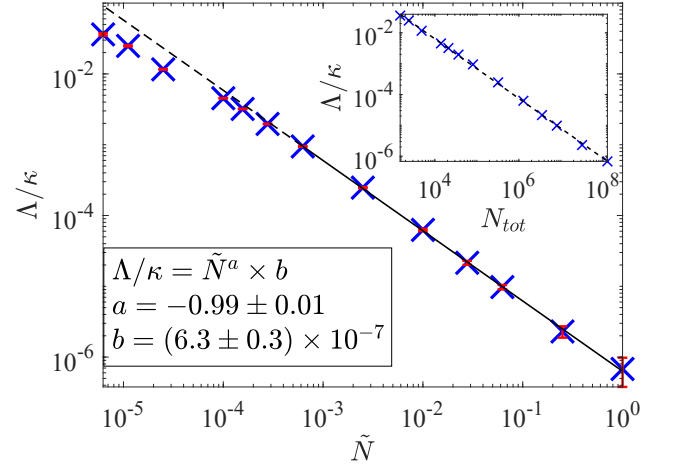


Figure 7. (a) Liouvillian gap Λ versus \tilde{N} . The error bars of the fit (in red) show the standard error (the 95% confidence interval) of each point. The power-law fit of the Liouvillian gap for $\tilde{N} \geq 6.3 \times 10^{-4}$ is shown by the continuous line. The coefficients of the fit are $\Lambda/\kappa = \tilde{N}^a \times b$ with $a = -0.99 \pm 0.01$ and $b = (6.3 \pm 0.3) \times 10^{-7}$. Inset: the Liouvillian gap versus the total number of photon inside the ring microresonator at long times (see Fig. 3). The dashed line represents a power law fit.

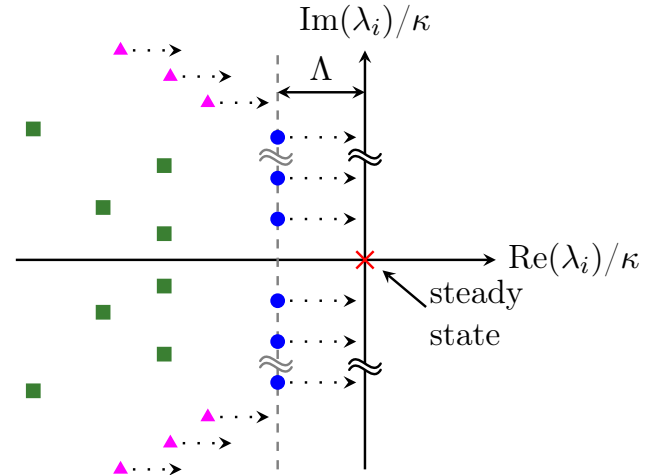


Figure 8. Schematic representation of the spectrum of the Liouvillian. The spectrum always has one zero eigenvalue, corresponding to the steady state (red cross). A set of eigenvalues with vanishing real part and equally-spaced imaginary parts emerges in the classical limit of large \tilde{N} (blue circles). The Liouvillian gap is the distance between the complex eigenvalues with the largest real part and the imaginary axis.

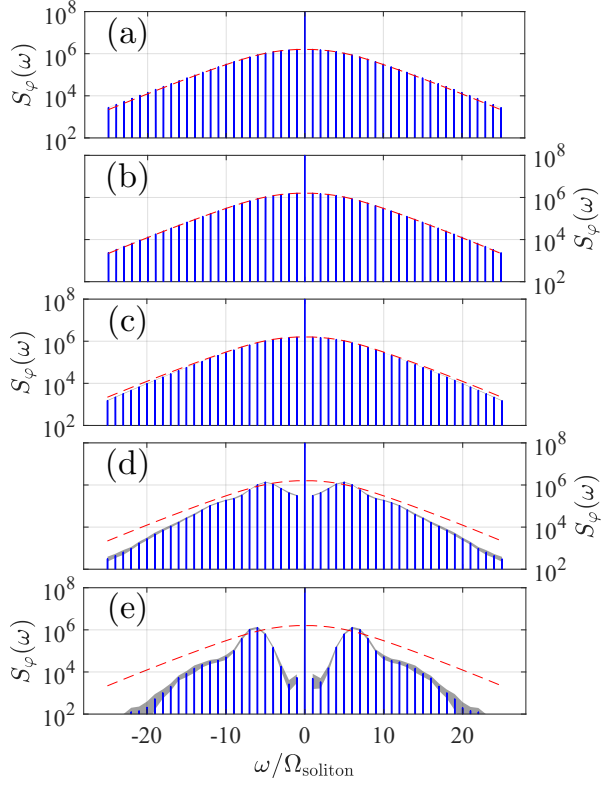


Figure 9. Fourier spectrum obtained by considering 51 modes and for $\tilde{N} = 1$ (a), $\tilde{N} = 4 \times 10^{-4}$ (b), $\tilde{N} = 10^{-4}$ (c), $\tilde{N} = 2.5 \times 10^{-5}$ (d) and $\tilde{N} = 1.1 \times 10^{-5}$ (e). The gray region shows the 95% standard deviation. The red dashed lines represent the envelope of the Fourier spectrum obtained from the GPE.

-
- [1] Y. K. Chembo, *Kerr optical frequency combs: theory, applications and perspectives*, *Nanophotonics* **5**, 214 (2016).
- [2] M. Kues, C. Reimer, J. M. Lukens, W. J. Munro, A. M. Weiner, D. J. Moss and R. Morandotti, *Quantum optical microcombs*, *Nature Photonics* **13**, 170 (2019).
- [3] M. Karpov, M. H. P. Pfeiffer, H. Guo, W. Weng, J. Liu and T. J. Kippenberg, *Dynamics of soliton crystals in optical microresonators*, *Nature Physics* **15**, 1071 (2019).
- [4] A. Kovach, D. Chen, J. He, H. Choi, A. H. Dogan, M. Ghasemkhani, H. Taheri and A. M. Armani, *Emerging material systems for integrated optical Kerr frequency combs*, *Adv. Opt. Photon.* **12**, 135 (2020).
- [5] S. A. Diddams, K. Vahala and T. Udem, *Optical frequency combs: Coherently uniting the electromagnetic spectrum*, *Science* **369** (2020), 10.1126/science.aay3676.
- [6] T. J. Kippenberg, A. L. Gaeta, M. Lipson and M. L. Gorodetsky, *Dissipative Kerr solitons in optical microresonators*, *Science* **361** (2018), 10.1126/science.aan8083.
- [7] P. Del'Haye, A. Schliesser, O. Arcizet, T. Wilken, R. Holzwarth and T. J. Kippenberg, *Optical frequency comb generation from a monolithic microresonator*, *Nature* **450**, 1214 (2007).
- [8] T. J. Kippenberg, R. Holzwarth and S. A. Diddams, *Microresonator-Based Optical Frequency Combs*, *Science* **332**, 555 (2011).
- [9] T. Udem, R. Holzwarth and T. W. Hänsch, *Optical frequency metrology*, *Nature* **416**, 233 (2002).
- [10] A. L. Gaeta, M. Lipson and T. J. Kippenberg, *Photonic-chip-based frequency combs*, *Nature Photonics* **13**, 158 (2019).
- [11] X. Yi, Q.-F. Yang, K. Y. Yang, M.-G. Suh and K. Vahala, *Soliton frequency comb at microwave rates in a high-Q silica microresonator*, *Optica* **2**, 1078 (2015).
- [12] J. Ma, L. Xiao, J. Gu, H. Li, X. Cheng, G. He, X. Jiang and M. Xiao, *Visible Kerr comb generation in a high-Q silica microdisk resonator with a large wedge angle*, *Photon. Res.* **7**, 573 (2019).
- [13] A. A. Savchenkov, A. B. Matsko, V. S. Ilchenko, I. Solomatine, D. Seidel and L. Maleki, *Tunable Optical Frequency Comb with a Crystalline Whispering Gallery Mode Resonator*, *Phys. Rev. Lett.* **101**, 093902 (2008).
- [14] J. S. Levy, A. Gondarenko, M. A. Foster, A. C. Turner-Foster, A. L. Gaeta and M. Lipson, *CMOS-compatible multiple-wavelength oscillator for on-chip optical interconnects*, *Nature Photonics* **4**, 37 (2010).
- [15] F. Ferdous, H. Miao, D. E. Leaird, K. Srinivasan, J. Wang, L. Chen, L. T. Varghese and A. M. Weiner, *Spectral line-by-line pulse shaping of on-chip microresonator frequency combs*, *Nature Photonics* **5**, 770 (2011).
- [16] Y. Okawachi, K. Saha, J. S. Levy, Y. H. Wen, M. Lipson and A. L. Gaeta, *Octave-spanning frequency comb generation in a silicon nitride chip*, *Opt. Lett.* **36**, 3398 (2011).
- [17] C. Joshi, J. K. Jang, K. Luke, X. Ji, S. A. Miller, A. Klenner, Y. Okawachi, M. Lipson and A. L. Gaeta, *Thermally controlled comb generation and soliton mode-locking in microresonators*, *Opt. Lett.* **41**, 2565 (2016).
- [18] V. Brasch, M. Geiselmann, T. Herr, G. Lihachev, M. H. P. Pfeiffer, M. L. Gorodetsky and T. J. Kippenberg, *Photonic chip-based optical frequency comb using soliton Cherenkov radiation*, *Science* **351**, 357 (2016).
- [19] B. J. M. Hausmann, I. Bulu, V. Venkataraman, P. Deotare and M. Lončar, *Diamond nonlinear photonics*, *Nature Photonics* **8**, 369 (2014).
- [20] H. Jung, C. Xiong, K. Y. Fong, X. Zhang and H. X. Tang, *Optical frequency comb generation from aluminum nitride microring resonator*, *Opt. Lett.* **38**, 2810 (2013).
- [21] H. Jung, R. Stoll, X. Guo, D. Fischer and H. X. Tang, *Green, red, and IR frequency comb line generation from single IR pump in AlN microring resonator*, *Optica* **1**, 396 (2014).
- [22] Y. He, Q.-F. Yang, J. Ling, R. Luo, H. Liang, M. Li, B. Shen, H. Wang, K. Vahala and Q. Lin, *Self-starting bi-chromatic LiNbO₃ soliton microcomb*, *Optica* **6**, 1138 (2019).
- [23] C. Wang, M. Zhang, M. Yu, R. Zhu, H. Hu and M. Loncar, *Monolithic lithium niobate photonic circuits for Kerr frequency comb generation and modulation*, *Nature Communications* **10**, 978 (2019).
- [24] A. G. Griffith, R. K. Lau, J. Cardenas, Y. Okawachi, A. Mohanty, R. Fain, Y. H. D. Lee, M. Yu, C. T. Phare, C. B. Poitras, A. L. Gaeta and M. Lipson, *Silicon-chip mid-infrared frequency comb generation*, *Nature Communications* **6**, 6299 (2015).
- [25] F. Leo, S. Coen, P. Kockaert, S.-P. Gorza, P. Emplit and M. Haelterman, *Temporal cavity solitons in one-dimensional Kerr media as bits in an all-optical buffer*, *Nature Photonics* **4**, 471 (2010).
- [26] T. Herr, V. Brasch, J. D. Jost, C. Y. Wang, N. M. Kondratiev, M. L. Gorodetsky and T. J. Kippenberg, *Temporal solitons in optical microresonators*, *Nature Photonics* **8**, 145 (2014).
- [27] A. M. Weiner, *Cavity solitons come of age*, *Nature Photonics* **11**, 533 (2017).
- [28] M. Karpov, *Dynamics and Applications of Dissipative Kerr Solitons* (2020).
- [29] V. E. Lobanov, A. E. Shitikov, R. R. Galiev, K. N. Min'kov and N. M. Kondratiev, *Generation and properties of dissipative Kerr solitons and platicons in optical microresonators with backscattering*, *Opt. Express* **28**, 36544 (2020).
- [30] P. Grelu, *Nonlinear optical cavity dynamics : from microresonators to fiber lasers* (Wiley-VCH Verlag, Weinheim, 2016).
- [31] L. Lugiato, *Nonlinear optical systems* (Cambridge University Press, Cambridge United Kingdom, 2015).
- [32] S. B. Papp, K. Beha, P. Del'Haye, F. Quinlan, H. Lee, K. J. Vahala and S. A. Diddams, *Microresonator frequency comb optical clock*, *Optica* **1**, 10 (2014).
- [33] V. Gerginov, C. E. Tanner, S. A. Diddams, A. Bartels and L. Hollberg, *High-resolution spectroscopy with a femtosecond laser frequency comb*, *Opt. Lett.* **30**, 1734 (2005).
- [34] S. B. Papp, P. Del'Haye and S. A. Diddams, *Mechanical Control of a Microrod-Resonator Optical Frequency Comb*, *Phys. Rev. X* **3**, 031003 (2013).

- [35] P. Del’Haye, O. Arcizet, A. Schliesser, R. Holzwarth and T. J. Kippenberg, *Full Stabilization of a Microresonator-Based Optical Frequency Comb*, *Phys. Rev. Lett.* **101**, 053903 (2008).
- [36] P. Del’Haye, S. B. Papp and S. A. Diddams, *Hybrid Electro-Optically Modulated Microcombs*, *Phys. Rev. Lett.* **109**, 263901 (2012).
- [37] D. T. Spencer, T. Drake, T. C. Briles, J. Stone, L. C. Sinclair, C. Fredrick, Q. Li, D. Westly, B. R. Ilic, A. Bluestone, N. Volet, T. Komljenovic, L. Chang, S. H. Lee, D. Y. Oh, M.-G. Suh, K. Y. Yang, M. H. P. Pfeiffer, T. J. Kippenberg, E. Norberg, L. Theogarajan, K. Vahala, N. R. Newbury, K. Srinivasan, J. E. Bowers, S. A. Diddams and S. B. Papp, *An optical-frequency synthesizer using integrated photonics*, *Nature* **557**, 81 (2018).
- [38] J. Pfeifle, V. Brasch, M. Lauermaun, Y. Yu, D. Wegner, T. Herr, K. Hartinger, P. Schindler, J. Li, D. Hillerkuss, R. Schmogrow, C. Weimann, R. Holzwarth, W. Freude, J. Leuthold, T. J. Kippenberg and C. Koos, *Coherent terabit communications with microresonator Kerr frequency combs*, *Nature Photonics* **8**, 375 (2014).
- [39] J. Pfeifle, A. Coillet, R. Henriët, K. Saleh, P. Schindler, C. Weimann, W. Freude, I. V. Balakireva, L. Larger, C. Koos and Y. K. Chembo, *Optimally Coherent Kerr Combs Generated with Crystalline Whispering Gallery Mode Resonators for Ultrahigh Capacity Fiber Communications*, *Phys. Rev. Lett.* **114**, 093902 (2015).
- [40] P. Marin-Palomo, J. N. Kemal, M. Karpov, A. Kordts, J. Pfeifle, M. H. P. Pfeiffer, P. Trocha, S. Wolf, V. Brasch, M. H. Anderson, R. Rosenberger, K. Vijayan, W. Freude, T. J. Kippenberg and C. Koos, *Microresonator-based solitons for massively parallel coherent optical communications*, *Nature* **546**, 274 (2017).
- [41] B. Bernhardt, A. Ozawa, P. Jacquet, M. Jacquay, Y. Kobayashi, T. Udem, R. Holzwarth, G. Guelachvili, T. W. Hänsch and N. Picqué, *Cavity-enhanced dual-comb spectroscopy*, *Nature Photonics* **4**, 55 (2010).
- [42] M. Yu, Y. Okawachi, C. Joshi, X. Ji, M. Lipson and A. L. Gaeta, *Gas-Phase Microresonator-Based Comb Spectroscopy without an External Pump Laser*, *ACS Photonics* **5**, 2780 (2018).
- [43] M. C. Stowe, F. C. Cruz, A. Marian and J. Ye, *High Resolution Atomic Coherent Control via Spectral Phase Manipulation of an Optical Frequency Comb*, *Phys. Rev. Lett.* **96**, 153001 (2006).
- [44] D. C. Heinecke, A. Bartels, T. M. Fortier, D. A. Braje, L. Hollberg and S. A. Diddams, *Optical frequency stabilization of a 10 GHz Ti:sapphire frequency comb by saturated absorption spectroscopy in ^{87}Rb* , *Phys. Rev. A* **80**, 053806 (2009).
- [45] I. Barmes, S. Witte and K. S. E. Eikema, *High-Precision Spectroscopy with Counterpropagating Femtosecond Pulses*, *Phys. Rev. Lett.* **111**, 023007 (2013).
- [46] J. Morgenweg, I. Barmes and K. S. E. Eikema, *Ramsey-comb spectroscopy with intense ultrashort laser pulses*, *Nature Physics* **10**, 30 (2014).
- [47] A. Cingöz, D. C. Yost, T. K. Allison, A. Ruehl, M. E. Fermann, I. Hartl and J. Ye, *Direct frequency comb spectroscopy in the extreme ultraviolet*, *Nature* **482**, 68 (2012).
- [48] M.-G. Suh, Q.-F. Yang, K. Y. Yang, X. Yi and K. J. Vahala, *Microresonator soliton dual-comb spectroscopy*, *Science* **354**, 600 (2016).
- [49] C. Reimer, M. Kues, P. Roztock, B. Wetzel, F. Grazioso, B. E. Little, S. T. Chu, T. Johnston, Y. Bromberg, L. Caspani, D. J. Moss and R. Morandotti, *Generation of multiphoton entangled quantum states by means of integrated frequency combs*, *Science* **351**, 1176 (2016).
- [50] M. Pyscher, Y. Miwa, R. Shahrokhshahi, R. Bloomer and O. Pfister, *Parallel Generation of Quadripartite Cluster Entanglement in the Optical Frequency Comb*, *Phys. Rev. Lett.* **107**, 030505 (2011).
- [51] J. Roslund, R. M. de Araújo, S. Jiang, C. Fabre and N. Treps, *Wavelength-multiplexed quantum networks with ultrafast frequency combs*, *Nature Photonics* **8**, 109 (2014).
- [52] M. Chen, N. C. Menicucci and O. Pfister, *Experimental Realization of Multipartite Entanglement of 60 Modes of a Quantum Optical Frequency Comb*, *Phys. Rev. Lett.* **112**, 120505 (2014).
- [53] M. Kues, C. Reimer, P. Roztock, L. R. Cortés, S. Sciara, B. Wetzel, Y. Zhang, A. Cino, S. T. Chu, B. E. Little, D. J. Moss, L. Caspani, J. Azaña and R. Morandotti, *On-chip generation of high-dimensional entangled quantum states and their coherent control*, *Nature* **546**, 622 (2017).
- [54] P. Imany, J. A. Jaramillo-Villegas, O. D. Odele, K. Han, D. E. Leaird, J. M. Lukens, P. Lougovski, M. Qi and A. M. Weiner, *50-GHz-spaced comb of high-dimensional frequency-bin entangled photons from an on-chip silicon nitride microresonator*, *Opt. Express* **26**, 1825 (2018).
- [55] Z. Yang, M. Jahanbozorgi, D. Jeong, S. Sun, O. Pfister, H. Lee and X. Yi, *A squeezed quantum microcomb on a chip*, *Nature Communications* **12**, 4781 (2021).
- [56] M. A. Guidry, D. M. Lukin, K. Y. Yang, R. Trivedi and J. Vukovi, *Quantum optics of soliton microcombs* (2021), [arXiv:2103.10517](https://arxiv.org/abs/2103.10517) [physics.optics].
- [57] Y. K. Chembo, *Quantum dynamics of Kerr optical frequency combs below and above threshold: Spontaneous four-wave mixing, entanglement, and squeezed states of light*, *Phys. Rev. A* **93**, 033820 (2016).
- [58] C. Gardiner and P. Zoller, *Quantum Noise: A Handbook of Markovian and Non-Markovian Quantum Stochastic Methods with Applications to Quantum Optics*, Springer series in synergetics (Springer, 2000).
- [59] D. Walls and G. Milburn, *Quantum Optics* (Springer Berlin Heidelberg, 2008).
- [60] K. Vogel and H. Risken, *Quasiprobability distributions in dispersive optical bistability*, *Phys. Rev. A* **39**, 4675 (1989).
- [61] B. Opanchuk and P. D. Drummond, *Functional Wigner representation of quantum dynamics of Bose-Einstein condensate*, *Journal of Mathematical Physics* **54**, 042107 (2013).
- [62] P. D. Drummond and B. Opanchuk, *Truncated Wigner dynamics and conservation laws*, *Phys. Rev. A* **96**, 043616 (2017).
- [63] A. Polkovnikov, *Phase space representation of quantum dynamics*, *Annals of Physics* **325**, 1790 (2010).
- [64] V. V. Albert and L. Jiang, *Symmetries and conserved quantities in Lindblad master equations*, *Phys. Rev. A* **89**, 022118 (2014).
- [65] D. Nigro, *On the uniqueness of the steady-state solution of the Lindblad–Gorini–Kossakowski–Sudarshan equation*, *Journal of Statistical Mechanics: Theory and Experiment* **2019**, 043202 (2019).

- [66] F. Minganti, A. Biella, N. Bartolo and C. Ciuti, *Spectral theory of Liouvillians for dissipative phase transitions*, *Phys. Rev. A* **98**, 042118 (2018).
- [67] F. Iemini, A. Russomanno, J. Keeling, M. Schirò, M. Dalmonte and R. Fazio, *Boundary Time Crystals*, *Phys. Rev. Lett.* **121**, 035301 (2018).
- [68] J. Zhang, P. W. Hess, A. Kyprianidis, P. Becker, A. Lee, J. Smith, G. Pagano, I.-D. Potirniche, A. C. Potter, A. Vishwanath, N. Y. Yao and C. Monroe, *Observation of a discrete time crystal*, *Nature* **543**, 217 (2017).
- [69] H. Taheri, A. B. Matsko, L. Maleki and K. Sacha, *All-optical dissipative discrete time crystals*, *Nature Communications* **13** (2022), 10.1038/s41467-022-28462-x.
- [70] K. Sacha and J. Zakrzewski, *Time crystals: a review*, *Reports on Progress in Physics* **81**, 016401 (2017).
- [71] K. Nakatsugawa, T. Fujii and S. Tanda, *Quantum time crystal by decoherence: Proposal with an incommensurate charge density wave ring*, *Phys. Rev. B* **96**, 094308 (2017).
- [72] R. R. W. Wang, B. Xing, G. G. Carlo and D. Poletti, *Period doubling in period-one steady states*, *Phys. Rev. E* **97**, 020202 (2018).
- [73] K. Tucker, B. Zhu, R. J. Lewis-Swan, J. Marino, F. Jimenez, J. G. Restrepo and A. M. Rey, *Shattered time: can a dissipative time crystal survive many-body correlations?*, *New Journal of Physics* **20**, 123003 (2018).
- [74] Z. Gong, R. Hamazaki and M. Ueda, *Discrete Time-Crystalline Order in Cavity and Circuit QED Systems*, *Phys. Rev. Lett.* **120**, 040404 (2018).
- [75] E. T. Owen, J. Jin, D. Rossini, R. Fazio and M. J. Hartmann, *Quantum correlations and limit cycles in the driven-dissipative Heisenberg lattice*, *New Journal of Physics* **20**, 045004 (2018).
- [76] C. Lledó, T. K. Mavrogordatos and M. H. Szymańska, *Driven Bose-Hubbard dimer under nonlocal dissipation: A bistable time crystal*, *Phys. Rev. B* **100**, 054303 (2019).
- [77] J. O'Sullivan, O. Lunt, C. W. Zollitsch, M. L. W. Thewalt, J. J. L. Morton and A. Pal, *Dissipative discrete time crystals* (2018).
- [78] F. M. Gambetta, F. Carollo, M. Marcuzzi, J. P. Garrahan and I. Lesanovsky, *Discrete Time Crystals in the Absence of Manifest Symmetries or Disorder in Open Quantum Systems*, *Phys. Rev. Lett.* **122**, 015701 (2019).
- [79] A. V. Nalitov, H. Sigurdsson, S. Morina, Y. S. Krivosenko, I. V. Iorsh, Y. G. Rubo, A. V. Kavokin and I. A. Shelykh, *Optically trapped polariton condensates as semiclassical time crystals*, *Phys. Rev. A* **99**, 033830 (2019).
- [80] H. Keßler, J. G. Cosme, M. Hemmerling, L. Mathey and A. Hemmerich, *Emergent limit cycles and time crystal dynamics in an atom-cavity system*, *Phys. Rev. A* **99**, 053605 (2019).
- [81] B. Zhu, J. Marino, N. Y. Yao, M. D. Lukin and E. A. Demler, *Dicke time crystals in driven-dissipative quantum many-body systems*, *New Journal of Physics* **21**, 073028 (2019).
- [82] N. Dogra, M. Landini, K. Kroeger, L. Hruby, T. Donner and T. Esslinger, *Dissipation-induced structural instability and chiral dynamics in a quantum gas*, *Science* **366**, 1496 (2019).
- [83] E. I. R. Chiacchio and A. Nunnenkamp, *Dissipation-Induced Instabilities of a Spinor Bose-Einstein Condensate Inside an Optical Cavity*, *Phys. Rev. Lett.* **122**, 193605 (2019).
- [84] B. Buča and D. Jaksch, *Dissipation Induced Nonstationarity in a Quantum Gas*, *Physical Review Letters* **123**, 260401 (2019).
- [85] B. Buča, J. Tindall and D. Jaksch, *Non-stationary coherent quantum many-body dynamics through dissipation*, *Nature Communications* **10**, 1730 (2019).
- [86] C. Lledó and M. H. Szymańska, *A dissipative time crystal with or without Z2 symmetry breaking*, *New Journal of Physics* **22**, 075002 (2020).
- [87] A. Lazarides, S. Roy, F. Piazza and R. Moessner, *Time crystallinity in dissipative Floquet systems*, *Phys. Rev. Research* **2**, 022002 (2020).
- [88] K. Chinzei and T. N. Ikeda, *Time Crystals Protected by Floquet Dynamical Symmetry in Hubbard Models*, *Phys. Rev. Lett.* **125**, 060601 (2020).
- [89] H. Keßler, J. G. Cosme, C. Georges, L. Mathey and A. Hemmerich, *From a continuous to a discrete time crystal in a dissipative atom-cavity system*, *New Journal of Physics* **22**, 085002 (2020).
- [90] C. Booker, B. Buča and D. Jaksch, *Non-stationarity and dissipative time crystals: spectral properties and finite-size effects*, *New Journal of Physics* **22**, 085007 (2020).
- [91] G. Engelhardt and J. Cao, *Dynamical Symmetries and Symmetry-Protected Selection Rules in Periodically Driven Quantum Systems*, *Phys. Rev. Lett.* **126**, 090601 (2021).
- [92] D. Barberena, R. J. Lewis-Swan, J. K. Thompson and A. M. Rey, *Driven-dissipative quantum dynamics in ultra-long-lived dipoles in an optical cavity*, *Phys. Rev. A* **99**, 053411 (2019).
- [93] J. G. Cosme, J. Skulte and L. Mathey, *Time crystals in a shaken atom-cavity system*, *Phys. Rev. A* **100**, 053615 (2019).
- [94] J. Tindall, B. Buča, J. R. Coulthard and D. Jaksch, *Heating-Induced Long-Range η Pairing in the Hubbard Model*, *Phys. Rev. Lett.* **123**, 030603 (2019).
- [95] K. Seibold, R. Rota and V. Savona, *Dissipative time crystal in an asymmetric nonlinear photonic dimer*, *Phys. Rev. A* **101**, 033839 (2020).
- [96] R. Hurtado-Gutiérrez, F. Carollo, C. Pérez-Espigares and P. I. Hurtado, *Building Continuous Time Crystals from Rare Events*, *Phys. Rev. Lett.* **125**, 160601 (2020).
- [97] L. F. d. Prazeres, L. d. S. Souza and F. Iemini, *Boundary time crystals in collective d-level systems*, *Phys. Rev. B* **103**, 184308 (2021).
- [98] F. Minganti, I. I. Arkhipov, A. Miranowicz and F. Nori, *Correspondence between dissipative phase transitions of light and time crystals* (2020).
- [99] H. Keßler, P. Kongkhambut, C. Georges, L. Mathey, J. G. Cosme and A. Hemmerich, *Observation of a Dissipative Time Crystal*, *Phys. Rev. Lett.* **127**, 043602 (2021).
- [100] D. A. Lidar, *Lecture Notes on the Theory of Open Quantum Systems* (2020), arXiv:1902.00967 [quant-ph].
- [101] V. V. Albert, B. Bradlyn, M. Fraas and L. Jiang, *Geometry and Response of Lindbladians*, *Phys. Rev. X* **6**, 041031 (2016).
- [102] B. Baumgartner and H. Narnhofer, *Analysis of quantum semigroups with GKS-Lindblad generators: II. General*, *Journal of Physics A: Mathematical and Theoretical* **41**, 395303 (2008).

- [103] P. E. Barclay, K. Srinivasan and O. Painter, *Nonlinear response of silicon photonic crystal microresonators excited via an integrated waveguide and fiber taper*, *Opt. Express* **13**, 801 (2005).
- [104] J. Vasco and V. Savona, *Slow-Light Frequency Combs and Dissipative Kerr Solitons in Coupled-Cavity Waveguides*, *Phys. Rev. Applied* **12**, 064065 (2019).
- [105] H.-P. Breuer, *The Theory of Open Quantum Systems* (Clarendon, Oxford, 2007).
- [106] L. A. Lugiato and R. Lefever, *Spatial Dissipative Structures in Passive Optical Systems*, *Phys. Rev. Lett.* **58**, 2209 (1987).
- [107] C. Godey, I. V. Balakireva, A. Coillet and Y. K. Chembo, *Stability analysis of the spatiotemporal Lugiato-Lefever model for Kerr optical frequency combs in the anomalous and normal dispersion regimes*, *Phys. Rev. A* **89**, 063814 (2014).
- [108] C. W. Gardiner, *Handbook of stochastic methods for physics, chemistry, and the natural sciences* (Springer-Verlag, Berlin New York, 1985).
- [109] K. E. Cahill and R. J. Glauber, *Density Operators and Quasiprobability Distributions*, *Phys. Rev.* **177**, 1882 (1969).
- [110] X. Ji, F. A. S. Barbosa, S. P. Roberts, A. Dutt, J. Cardenas, Y. Okawachi, A. Bryant, A. L. Gaeta and M. Lipson, *Ultra-low-loss on-chip resonators with sub-milliwatt parametric oscillation threshold*, *Optica* **4**, 619 (2017).
- [111] K. Liu, S. Yao and C. Yang, *Raman pure quartic solitons in Kerr microresonators*, *Opt. Lett.* **46**, 993 (2021).
- [112] K. Ikeda, R. E. Saperstein, N. Alic and Y. Fainman, *Thermal and Kerr nonlinear properties of plasma-deposited silicon nitride/silicon dioxide waveguides*, *Opt. Express* **16**, 12987 (2008).
- [113] F. Vicentini, F. Minganti, R. Rota, G. Orso and C. Ciuti, *Critical slowing down in driven-dissipative Bose-Hubbard lattices*, *Phys. Rev. A* **97**, 013853 (2018).

Chapter 6

General discussion and outlook

In this thesis we explored the physics of driven-dissipative open quantum systems, with a particular focus on the critical phenomena of dissipative Kerr solitons and dissipative time crystals. Besides the theoretical study we were careful to address the following points:

- the context and motivations in which the work is situated. Non-classical states of light are the cornerstones of the second quantum revolution, leading to a plethora of technological applications,
- the challenges involved in studying these systems numerically, with various constraints either guiding or even imposing the choice of numerical method,
- experimental feasibility in terms of experimental platforms in quantum science and technology. The emphasis is put on its implementation, in particular with respect to integration and scalability in photonic platforms.

The driving idea was to provide a quantum study of the dynamics of several quantum setups by means of the theory of open quantum systems. In particular, the quantum master equation and the spectral analysis of the Liouvillian superoperator prove to be invaluable tools for our analysis. The different results obtained in this thesis reflect the power of these theoretical methods for the study of systems subject to critical phenomena, such as dissipative phase transitions or dissipative time crystals.

On the methodology aspect, the quantum master equation was solved numerically by exact diagonalization, as well as by the approximated truncated Wigner approach — which accounts for quantum effects to lowest order.

We provide a quantum study of two different systems, characterized by a small, respectively large, number of degrees of freedom. While the properties have been obtained on systems of finite size and occupation, we extrapolated them in a “controlled” thermodynamic limit of large photon occupation.

We do also propose some experimental platforms in which these models could be implemented.

Let us summarise our findings here.

In [chapter 4](#), based on the article [1], we investigate the behavior of two coupled nonlinear photonic cavities, in the presence of inhomogeneous coherent driving and local dissipations. Importantly, we do so under very general conditions which do not rely on the presence of symmetries. We show that when the mean-field Gross-Pitaevskii equation predicts a unique parametrically unstable steady-state solution, the open quantum many-body system presents highly nonclassical properties.

This work provides strong evidence for the occurrence in this simple dissipative system of a dissipative time crystal (DTC) phase characterized by spontaneous long lived oscillations of the system observables, large fluctuations and non-classical correlations. Moreover, the study of the dynamics in terms of the theory of open quantum systems shows that this prototypical system is also a minimal model of dissipative Kerr solitons. This therefore seems to indicate that DKSs are a specific manifestation of a DTC, and the present study is an important step towards the characterization of quantum correlations and entanglement in Kerr-soliton systems. It opens the way to the design of optical devices for the generation of non-classical light.

Let us also note that this system presents interesting advantages in view of its realization with current experimental technologies. Indeed, not only does the DTC phase persist over a wide range of parameters, its occurrence does not require symmetries. This system is therefore very robust and may be easily implemented experimentally, for example on a superconducting circuit architecture or with coupled semiconductor micropillars.

In [chapter 5](#), we focus on dissipative Kerr solitons and present the findings of article [3]. This is an expansion of the former studied dimer to the continuous version of a ring resonator. We study the quantum dynamics of dissipative Kerr solitons that can form in ring microresonators from parametric gain.

While usually described within a classical mean-field framework, I develop in my thesis a quantum-mechanical model of dissipative Kerr solitons using the TWA. This allows for an estimate of the Liouvillian spectrum of the system, and hence an analysis of the phase structure. In particular, our results show that for any finite value of the input power in the microresonator, the DKS solution does not persist indefinitely but decays over time due to the presence of nonlinearity and fluctuations induced by losses.

The eigenvalues with the smallest (in absolute value) real part – besides the zeroeigenvalue associated to the spatially uniform steady state – are arranged to have a constant (negative) real part, defining the Liouvillian gap, and evenly spaced imaginary parts, corresponding to the Kerr frequency comb. Increasing the input power, the eigenvalues of the Liouvillian get closer and closer to the imaginary line (the absolute value of their real part shrinks), with the Liouvillian gap vanishing as a power law of the total photon occupation in the microring modes. Eventually, in the infinite driving strength limit, the gap closes and the DKS are expected to persist indefinitely. We demonstrate that the timescale for this steady state to be reached has a power-law behavior depending on the strength of the nonlinearity, and a true DKS emerges only

in the limit of vanishing nonlinearity and infinite driving field amplitude.

This result allows us to show that dissipative Kerr solitons are a specific manifestation of dissipative time crystals. Establishing the link between DKSs and dissipative time crystals is an important step in the study and characterization of spontaneous time-translational symmetry breaking in quantum systems out of equilibrium.

A scaling analysis of the TWA equations also indicates that a regime with large quantum effects may be achieved by decreasing the driving field intensity while correspondingly increasing the strength of the Kerr nonlinearity. The analysis provides clear indications about whether this behaviour can be observed in experiments.

We have shown that quantum effects are responsible of a finite lifetime of the soliton, which in the long time limit leaves place to a solution with the field uniformly distributed along the ring. The timescale of the soliton decay depends on the relative size of quantum fluctuations, and decreases when quantum fluctuations become larger.

Outlook

The results presented in this thesis pave the way for the possibility to use DKS as a novel approach to the generation of quantum correlated states of photons.

This opens up various avenues for further research. For instance, it could be interesting to explore in more detail the quantum properties of the soliton, like the existence of squeezing or entanglement. Moreover, while we focused on the case in which there is only one soliton in the resonator, a natural extension would be the quantum study of the scenario with two or more solitons. In that case, entanglement between the different solitons might appear.

On another side, it could be interesting to provide a detailed study of the phase transition between dissipative time crystal and the normal phase, with an in-depth investigation of how the spectrum of the Liouvillian changes between the phase characterized by one zero eigenvalue, and the phase with the eigenvalues on the imaginary axis.

We leave this study for later times and/or for future generations of enthusiastic open quantum system physicists.

Bibliography

- [1] K. Seibold, R. Rota, and V. Savona, *Dissipative time crystal in an asymmetric nonlinear photonic dimer*, [Physical Review A **101**, 033839 \(2020\)](#).
- [2] J. Vasco, D. Gerace, K. Seibold, and V. Savona, *Monolithic silicon-based nanobeam cavities for integrated nonlinear and quantum photonics*, [Physical Review Applied **13**, 034070 \(2020\)](#).
- [3] K. Seibold, R. Rota, F. Minganti, and V. Savona, *Quantum dynamics of dissipative kerr solitons*, [Phys. Rev. A **105**, 053530 \(2022\)](#).
- [4] M. D. Anderson et al., *Two-color pump-probe measurement of photonic quantum correlations mediated by a single phonon*, [Physical Review Letters **120**, 233601 \(2018\)](#).
- [5] S. T. Velez et al., *Preparation and decay of a single quantum of vibration at ambient conditions*, [Physical Review X **9**, 041007 \(2019\)](#).
- [6] M. Jammer, *The conceptual development of quantum mechanics* (Tomash Publishers American Institute of Physics, Los Angeles, Calif. Woodbury, N.Y, 1989).
- [7] A. Pais, *Einstein and the quantum theory*, [Reviews of Modern Physics **51**, 863–914 \(1979\)](#).
- [8] A. Kramida, *A critical compilation of experimental data on spectral lines and energy levels of hydrogen, deuterium, and tritium*, [Atomic Data and Nuclear Data Tables **96**, 586–644 \(2010\)](#).
- [9] C. H. Townes, *How the laser happened* (Oxford University Press, Feb. 2002).
- [10] F. Arute et al., *Quantum supremacy using a programmable superconducting processor*, [Nature **574**, 505–510 \(2019\)](#).
- [11] J. I. Cirac, R. Blatt, A. S. Parkins, and P. Zoller, *Preparation of fock states by observation of quantum jumps in an ion trap*, [Physical Review Letters **70**, 762–765 \(1993\)](#).
- [12] J. F. Poyatos, J. I. Cirac, and P. Zoller, *Quantum reservoir engineering with laser cooled trapped ions*, [Physical Review Letters **77**, 4728–4731 \(1996\)](#).
- [13] A. R. R. Carvalho, P. Milman, R. L. de Matos Filho, and L. Davidovich, *Decoherence, pointer engineering, and quantum state protection*, [Physical Review Letters **86**, 4988–4991 \(2001\)](#).
- [14] S. Diehl et al., *Quantum states and phases in driven open quantum systems with cold atoms*, [Nature Physics **4**, 878–883 \(2008\)](#).
- [15] B. Kraus et al., *Preparation of entangled states by quantum markov processes*, [Physical Review A **78**, 042307 \(2008\)](#).

- [16] G. Barontini et al., *Deterministic generation of multiparticle entanglement by quantum zeno dynamics*, [Science](#) **349**, 1317–1321 (2015).
- [17] B. Bellomo and M. Antezza, *Nonequilibrium dissipation-driven steady many-body entanglement*, [Physical Review A](#) **91**, 042124 (2015).
- [18] B. Bellomo and M. Antezza, *Steady entanglement out of thermal equilibrium*, [EPL \(Europhysics Letters\)](#) **104**, 10006 (2013).
- [19] B. Bellomo, R. L. Franco, S. Maniscalco, and G. Compagno, *Entanglement trapping in structured environments*, [Physical Review A](#) **78**, 060302 (2008).
- [20] F. Benatti and R. Floreanini, *Entangling oscillators through environment noise*, [Journal of Physics A: Mathematical and General](#) **39**, 2689–2699 (2006).
- [21] F. Benatti, R. Floreanini, and M. Piani, *Environment induced entanglement in markovian dissipative dynamics*, [Physical Review Letters](#) **91**, 070402 (2003).
- [22] D. Braun, *Creation of entanglement by interaction with a common heat bath*, [Physical Review Letters](#) **89**, 277901 (2002).
- [23] M. B. Plenio, S. F. Huelga, A. Beige, and P. L. Knight, *Cavity-loss-induced generation of entangled atoms*, [Physical Review A](#) **59**, 2468–2475 (1999).
- [24] A. Sarlette, J. M. Raimond, M. Brune, and P. Rouchon, *Stabilization of nonclassical states of the radiation field in a cavity by reservoir engineering*, [Physical Review Letters](#) **107**, 010402 (2011).
- [25] J.-W. Pan et al., *Multiphoton entanglement and interferometry*, [Reviews of Modern Physics](#) **84**, 777–838 (2012).
- [26] M. D. Reid et al., *Colloquium: the einstein-podolsky-rosen paradox: from concepts to applications*, [Reviews of Modern Physics](#) **81**, 1727–1751 (2009).
- [27] S. L. Braunstein and P. van Loock, *Quantum information with continuous variables*, [Reviews of Modern Physics](#) **77**, 513–577 (2005).
- [28] A. Gilchrist et al., *Schrödinger cats and their power for quantum information processing*, [Journal of Optics B: Quantum and Semiclassical Optics](#) **6**, S828–S833 (2004).
- [29] A. Ourjoumtsev, R. Tualle-Brouri, J. Laurat, and P. Grangier, *Generating optical schrödinger kittens for quantum information processing*, [Science](#) **312**, 83–86 (2006).
- [30] M. Mirrahimi et al., *Dynamically protected cat-qubits: a new paradigm for universal quantum computation*, [New Journal of Physics](#) **16**, 045014 (2014).
- [31] H. Goto, *Universal quantum computation with a nonlinear oscillator network*, [Physical Review A](#) **93**, 050301 (2016).
- [32] S. Puri, S. Boutin, and A. Blais, *Engineering the quantum states of light in a kerr-nonlinear resonator by two-photon driving*, [npj Quantum Information](#) **3**, 10.1038/s41534-017-0019-1 (2017).
- [33] R. Rota, F. Minganti, C. Ciuti, and V. Savona, *Quantum critical regime in a quadratically driven nonlinear photonic lattice*, [Physical Review Letters](#) **122**, 110405 (2019).

- [34] R. Rota and V. Savona, *Simulating frustrated antiferromagnets with quadratically driven QED cavities*, [Physical Review A **100**, 013838 \(2019\)](#).
- [35] M. H. Michael et al., *New class of quantum error-correcting codes for a bosonic mode*, [Physical Review X **6**, 031006 \(2016\)](#).
- [36] J. T. Barreiro et al., *An open-system quantum simulator with trapped ions*, [Nature **470**, 486–491 \(2011\)](#).
- [37] J. I. Cirac, A. S. Parkins, R. Blatt, and P. Zoller, *"dark" squeezed states of the motion of a trapped ion*, [Physical Review Letters **70**, 556–559 \(1993\)](#).
- [38] M. J. Everitt et al., *Engineering dissipative channels for realizing schrödinger cats in SQUIDS*, [Frontiers in ICT **1**, 10.3389/fict.2014.00001 \(2014\)](#).
- [39] T. Fogarty et al., *Entangling two defects via a surrounding crystal*, [Physical Review A **87**, 050304 \(2013\)](#).
- [40] G. Goldstein et al., *Environment-assisted precision measurement*, [Physical Review Letters **106**, 140502 \(2011\)](#).
- [41] H. Krauter et al., *Entanglement generated by dissipation and steady state entanglement of two macroscopic objects*, [Physical Review Letters **107**, 080503 \(2011\)](#).
- [42] C. J. Myatt et al., *Decoherence of quantum superpositions through coupling to engineered reservoirs*, [Nature **403**, 269–273 \(2000\)](#).
- [43] N. Syassen et al., *Strong dissipation inhibits losses and induces correlations in cold molecular gases*, [Science **320**, 1329–1331 \(2008\)](#).
- [44] F. Verstraete, M. M. Wolf, and J. I. Cirac, *Quantum computation and quantum-state engineering driven by dissipation*, [Nature Physics **5**, 633–636 \(2009\)](#).
- [45] K. G. H. Vollbrecht, C. A. Muschik, and J. I. Cirac, *Entanglement distillation by dissipation and continuous quantum repeaters*, [Physical Review Letters **107**, 120502 \(2011\)](#).
- [46] S. Zippilli, M. Paternostro, G. Adesso, and F. Illuminati, *Entanglement replication in driven dissipative many-body systems*, [Physical Review Letters **110**, 040503 \(2013\)](#).
- [47] E. M. L. L D Landau, *Statistical physics* (Elsevier Science & Techn., Oct. 2013), 544 pp.
- [48] L. Carr, *Understanding quantum phase transitions* (CRC Press, Boca Raton, 2011).
- [49] E. M. Kessler et al., *Dissipative phase transition in a central spin system*, [Physical Review A **86**, 012116 \(2012\)](#).
- [50] E. Altman et al., *Two-dimensional superfluidity of exciton polaritons requires strong anisotropy*, [Physical Review X **5**, 011017 \(2015\)](#).
- [51] M. P. Baden et al., *Realization of the dicke model using cavity-assisted raman transitions*, [Physical Review Letters **113**, 020408 \(2014\)](#).

- [52] N. Bartolo, F. Minganti, W. Casteels, and C. Ciuti, *Exact steady state of a kerr resonator with one- and two-photon driving and dissipation: controllable wigner-function multimodality and dissipative phase transitions*, [Physical Review A **94**, 033841 \(2016\)](#).
- [53] K. Baumann, C. Guerlin, F. Brennecke, and T. Esslinger, *Dicke quantum phase transition with a superfluid gas in an optical cavity*, [Nature **464**, 1301–1306 \(2010\)](#).
- [54] K. Baumann, R. Mottl, F. Brennecke, and T. Esslinger, *Exploring symmetry breaking at the dicke quantum phase transition*, [Physical Review Letters **107**, 140402 \(2011\)](#).
- [55] A. Biella et al., *Phase diagram of incoherently driven strongly correlated photonic lattices*, [Physical Review A **96**, 023839 \(2017\)](#).
- [56] M. Biondi, G. Blatter, H. E. Türeci, and S. Schmidt, *Nonequilibrium gas-liquid transition in the driven-dissipative photonic lattice*, [Physical Review A **96**, 043809 \(2017\)](#).
- [57] F. Brennecke et al., *Real-time observation of fluctuations at the driven-dissipative dicke phase transition*, [Proceedings of the National Academy of Sciences **110**, 11763–11767 \(2013\)](#).
- [58] P. Brookes et al., *Critical slowing down in circuit quantum electrodynamics*, [Science Advances **7**, 10.1126/sciadv.abe9492 \(2021\)](#).
- [59] L. Capriotti et al., *Dissipation-driven phase transition in two-dimensional josephson arrays*, [Physical Review Letters **94**, 157001 \(2005\)](#).
- [60] H. Carmichael, *Breakdown of photon blockade: a dissipative quantum phase transition in zero dimensions*, [Physical Review X **5**, 031028 \(2015\)](#).
- [61] H. J. Carmichael, *Analytical and numerical results for the steady state in cooperative resonance fluorescence*, [Journal of Physics B: Atomic and Molecular Physics **13**, 3551–3575 \(1980\)](#).
- [62] W. Casteels and C. Ciuti, *Quantum entanglement in the spatial-symmetry-breaking phase transition of a driven-dissipative bose-hubbard dimer*, [Physical Review A **95**, 013812 \(2017\)](#).
- [63] W. Casteels, F. Storme, A. Le Boité, and C. Ciuti, *Power laws in the dynamic hysteresis of quantum nonlinear photonic resonators*, [Phys. Rev. A **93**, 033824 \(2016\)](#).
- [64] W. Casteels, R. Fazio, and C. Ciuti, *Critical dynamical properties of a first-order dissipative phase transition*, [Physical Review A **95**, 012128 \(2017\)](#).
- [65] J. B. Curtis et al., *Critical theory for the breakdown of photon blockade*, [Physical Review Research **3**, 023062 \(2021\)](#).
- [66] S. Diehl et al., *Dynamical phase transitions and instabilities in open atomic many-body systems*, [Physical Review Letters **105**, 015702 \(2010\)](#).
- [67] T. Fink et al., *Signatures of a dissipative phase transition in photon correlation measurements*, [Nature Physics **14**, 365–369 \(2018\)](#).

- [68] M. Foss-Feig et al., *Emergent equilibrium in many-body optical bistability*, [Physical Review A **95**, 043826 \(2017\)](#).
- [69] J. Jin et al., *Cluster mean-field approach to the steady-state phase diagram of dissipative spin systems*, [Phys. Rev. X **6**, 031011 \(2016\)](#).
- [70] J. Klinder et al., *Dynamical phase transition in the open dicke model*, [Proceedings of the National Academy of Sciences **112**, 3290–3295 \(2015\)](#).
- [71] T. E. Lee, S. Gopalakrishnan, and M. D. Lukin, *Unconventional magnetism via optical pumping of interacting spin systems*, [Physical Review Letters **110**, 257204 \(2013\)](#).
- [72] M. F. Maghrebi and A. V. Gorshkov, *Nonequilibrium many-body steady states via keldysh formalism*, [Physical Review B **93**, 014307 \(2016\)](#).
- [73] J. Marino and S. Diehl, *Driven markovian quantum criticality*, [Physical Review Letters **116**, 070407 \(2016\)](#).
- [74] J. J. Mendoza-Arenas et al., *Beyond mean-field bistability in driven-dissipative lattices: bunching-antibunching transition and quantum simulation*, [Physical Review A **93**, 023821 \(2016\)](#).
- [75] F. Minganti, A. Biella, N. Bartolo, and C. Ciuti, *Spectral theory of liouvillians for dissipative phase transitions*, [Physical Review A **98**, 042118 \(2018\)](#).
- [76] A. Mitra, S. Takei, Y. B. Kim, and A. J. Millis, *Nonequilibrium quantum criticality in open electronic systems*, [Physical Review Letters **97**, 236808 \(2006\)](#).
- [77] T. Prosen and I. Pižorn, *Quantum phase transition in a far-from-equilibrium steady state of an xy spin chain*, [Physical Review Letters **101**, 105701 \(2008\)](#).
- [78] S. R. K. Rodriguez et al., *Probing a dissipative phase transition via dynamical optical hysteresis*, [Phys. Rev. Lett. **118**, 247402 \(2017\)](#).
- [79] R. Rota et al., *Critical behavior of dissipative two-dimensional spin lattices*, [Physical Review B **95**, 134431 \(2017\)](#).
- [80] R. Rota, F. Minganti, A. Biella, and C. Ciuti, *Dynamical properties of dissipative XYZ heisenberg lattices*, [New Journal of Physics **20**, 045003 \(2018\)](#).
- [81] V. Savona, *Spontaneous symmetry breaking in a quadratically driven nonlinear photonic lattice*, [Physical Review A **96**, 033826 \(2017\)](#).
- [82] L. M. Sieberer, S. D. Huber, E. Altman, and S. Diehl, *Dynamical critical phenomena in driven-dissipative systems*, [Physical Review Letters **110**, 195301 \(2013\)](#).
- [83] L. M. Sieberer, S. D. Huber, E. Altman, and S. Diehl, *Nonequilibrium functional renormalization for driven-dissipative bose-einstein condensation*, [Physical Review B **89**, 134310 \(2014\)](#).
- [84] E. G. D. Torre, E. Demler, T. Giamarchi, and E. Altman, *Quantum critical states and phase transitions in the presence of non-equilibrium noise*, [Nature Physics **6**, 806–810 \(2010\)](#).
- [85] E. G. D. Torre, E. Demler, T. Giamarchi, and E. Altman, *Dynamics and universality in noise-driven dissipative systems*, [Physical Review B **85**, 184302 \(2012\)](#).

- [86] E. G. D. Torre et al., *Keldysh approach for nonequilibrium phase transitions in quantum optics: beyond the dicke model in optical cavities*, [Physical Review A](#) **87**, 023831 (2013).
- [87] F. Vicentini et al., *Critical slowing down in driven-dissipative bose-hubbard lattices*, [Phys. Rev. A](#) **97**, 013853 (2018).
- [88] P. Werner, K. Völker, M. Troyer, and S. Chakravarty, *Phase diagram and critical exponents of a dissipative ising spin chain in a transverse magnetic field*, [Physical Review Letters](#) **94**, 047201 (2005).
- [89] J. Eisert, M. Friesdorf, and C. Gogolin, *Quantum many-body systems out of equilibrium*, [Nature Physics](#) **11**, 124–130 (2015).
- [90] H. Landa, M. Schiró, and G. Misguich, *Correlation-induced steady states and limit cycles in driven dissipative quantum systems*, [Physical Review B](#) **102**, 064301 (2020).
- [91] H. Landa, M. Schiró, and G. Misguich, *Multistability of driven-dissipative quantum spins*, [Physical Review Letters](#) **124**, 043601 (2020).
- [92] J. Fink et al., *Observation of the photon-blockade breakdown phase transition*, [Physical Review X](#) **7**, 011012 (2017).
- [93] V. Khemani, R. Moessner, and S. L. Sondhi, *A Brief History of Time Crystals*, [arXiv:1910.10745 \[cond-mat, physics:hep-th\]](#), [arXiv: 1910.10745](#) (2019).
- [94] K. Sacha and J. Zakrzewski, *Time crystals: a review*, [Reports on Progress in Physics](#) **81**, 016401 (2017).
- [95] C. Booker, B. Buča, and D. Jaksch, *Non-stationarity and dissipative time crystals: spectral properties and finite-size effects*, [New Journal of Physics](#) **22**, 085007 (2020).
- [96] C. Gerry and P. Knight, *Introductory quantum optics*, eng (Cambridge University Press, Cambridge, 2004).
- [97] M. A. Nielsen and I. L. Chuang, *Quantum computation and quantum information* (Cambridge University Press, 2009).
- [98] J.-M. R. Serge Haroche, *Exploring the quantum: atoms, cavities, and photons* (OXFORD UNIV PR, Oct. 2006), 616 pp.
- [99] J. L. Basdevant, *Mécanique quantique* (Éditions de l'École polytechnique, Palaiseau France, 2004).
- [100] A. Peres, *Quantum theory: concepts and methods* (Springer Netherlands, June 2006), 450 pp.
- [101] C. Cohen-Tannoudji, B. Diu, and F. Laloë, *III LES POSTULATS DE LA MÉCANIQUE QUANTIQUE*, fr, in [Mécanique Quantique - Tome 1](#) (EDP Sciences, Feb. 2021), pp. 215–396.
- [102] Zettili, *Quantum mechanics 2e* (John Wiley & Sons, Feb. 2009), 692 pp.
- [103] P. A. M. Dirac, *The principles of quantum mechanics* (Oxford University Press, Jan. 1981).
- [104] T. Baumgratz, M. Cramer, and M. Plenio, *Quantifying coherence*, [Physical Review Letters](#) **113**, 140401 (2014).

- [105] H. Breuer, F. Petruccione, and Petruccione, *The theory of open quantum systems* (Oxford University Press, 2002).
- [106] U. Fano, *Description of states in quantum mechanics by density matrix and operator techniques*, [Reviews of Modern Physics](#) **29**, 74–93 (1957).
- [107] J. v. Neumann, *Wahrscheinlichkeitstheoretischer aufbau der quantenmechanik*, [Nachrichten von der Gesellschaft der Wissenschaften zu Göttingen, Mathematisch-Physikalische Klasse](#) **1927**, 245–272 (1927).
- [108] T. Traxler, *Decoherence and the physics of open quantum systems, script to reinhold bertlmann's lectures*, https://homepage.univie.ac.at/reinhold.bertlmann/pdfs/decoscript_v2.pdf, [Online; accessed 28-July-2021], 2009.
- [109] L. E. Ballentine, *Quantum mechanics: a modern development* (WORLD SCIENTIFIC PUB CO INC, Mar. 1998), 672 pp.
- [110] P. A. M. Dirac, *The principles of quantum mechanics*, eng, 4th ed. 1958, repr., The international series of monographs on physics (Clarendon Press, Oxford, 1978).
- [111] P. A. M. Dirac, *The fundamental equations of quantum mechanics*, eng, Proceedings of the Royal Society of London. Series A, Containing papers of a mathematical and physical character **109**, 642–653 (1925).
- [112] J. A. Rubino-Martin, R. Rebolo, and E. Mediavilla, *The cosmic microwave background: from quantum fluctuations to the present universe* (CAMBRIDGE, Jan. 2010), 304 pp.
- [113] R. Horodecki, P. Horodecki, M. Horodecki, and K. Horodecki, *Quantum entanglement*, [Reviews of Modern Physics](#) **81**, 865–942 (2009).
- [114] C. H. Bennett et al., *Teleporting an unknown quantum state via dual classical and einstein-podolsky-rosen channels*, [Physical Review Letters](#) **70**, 1895–1899 (1993).
- [115] A. Brodutch and D. R. Terno, *Why should we care about quantum discord?*, in [Quantum science and technology](#) (Springer International Publishing, 2017), pp. 183–199.
- [116] P. Meystre, *Exploring the quantum: atoms, cavities, and photons*, [Physics Today](#) **60**, 61–62 (2007).
- [117] J. Klauder and B. Skagerstam, *Coherent states: applications in physics and mathematical physics* (World Scientific Publishing Company, 1985).
- [118] A. M. Perelomov, *Generalized coherent states and some of their applications*, [Soviet Physics Uspekhi](#) **20**, 703–720 (1977).
- [119] H. B. G. Casimir, *On the attraction between two perfectly conducting plates*, English, [Proceedings. Akadamie van Wetenschappen Amsterdam](#) **51**, 793–795 (1948).
- [120] S. Kauffman, S. Succi, A. Tiribocchi, and P. G. Tello, *Playing with casimir in the vacuum sandbox*, [The European Physical Journal C](#) **81**, 10.1140/epjc/s10052-021-09733-1 (2021).

- [121] M. S. Kim, W. Son, V. Bužek, and P. L. Knight, *Entanglement by a beam splitter: nonclassicality as a prerequisite for entanglement*, [Physical Review A](#) **65**, 032323 (2002).
- [122] J. K. Asbóth, J. Calsamiglia, and H. Ritsch, *Computable measure of nonclassicality for light*, [Physical Review Letters](#) **94**, 173602 (2005).
- [123] H. Mabuchi and A. C. Doherty, *Cavity quantum electrodynamics: coherence in context*, [Science](#) **298**, 1372–1377 (2002).
- [124] D. E. Chang, V. Vuletić, and M. D. Lukin, *Quantum nonlinear optics — photon by photon*, [Nature Photonics](#) **8**, 685–694 (2014).
- [125] D. Roy, C. Wilson, and O. Firstenberg, *Colloquium : strongly interacting photons in one-dimensional continuum*, [Reviews of Modern Physics](#) **89**, 021001 (2017).
- [126] I. Carusotto and C. Ciuti, *Quantum fluids of light*, [Rev. Mod. Phys.](#) **85**, 299–366 (2013).
- [127] V. Giovannetti, S. Lloyd, and L. Maccone, *Quantum-enhanced measurements: beating the standard quantum limit*, [Science](#) **306**, 1330–1336 (2004).
- [128] R. Demkowicz-Dobrzański and L. Maccone, *Using entanglement against noise in quantum metrology*, [Physical Review Letters](#) **113**, 250801 (2014).
- [129] D. P. DiVincenzo and D. Loss, *Quantum computers and quantum coherence*, [Journal of Magnetism and Magnetic Materials](#) **200**, 202–218 (1999).
- [130] I. Georgescu, S. Ashhab, and F. Nori, *Quantum simulation*, [Reviews of Modern Physics](#) **86**, 153–185 (2014).
- [131] A. K. Ekert, *Quantum cryptography based on bell’s theorem*, [Physical Review Letters](#) **67**, 661–663 (1991).
- [132] R. J. Glauber, *The quantum theory of optical coherence*, [Physical Review](#) **130**, 2529–2539 (1963).
- [133] H. Schlosser and P. M. Marcus, *Composite wave variational method for solution of the energy-band problem in solids*, [Physical Review](#) **131**, 2529–2546 (1963).
- [134] U. M. Titulaer and R. J. Glauber, *Correlation functions for coherent fields*, [Physical Review](#) **140**, B676–B682 (1965).
- [135] C. L. Mehta and E. C. G. Sudarshan, *Relation between quantum and semiclassical description of optical coherence*, [Physical Review](#) **138**, B274–B280 (1965).
- [136] R. Loudon, *The quantum theory of light* (OUP Oxford, Sept. 2000), 450 pp.
- [137] H. J. Carmichael, *Statistical methods in quantum optics 1* (Springer Berlin Heidelberg, 1999).
- [138] H. J. Carmichael, *Statistical methods in quantum optics 2* (Springer Berlin Heidelberg, 2008).
- [139] H. T. Dung, A. Shumovsky, and N. Bogolubov, *Antibunching and sub-poissonian photon statistics in the jaynes-cummings model*, [Optics Communications](#) **90**, 322–328 (1992).
- [140] X. T. Zou and L. Mandel, *Photon-antibunching and sub-poissonian photon statistics*, [Physical Review A](#) **41**, 475–476 (1990).

- [141] E. Schrödinger, *Der stetige übergang von der mikro- zur makromechanik*, [Die Naturwissenschaften](#) **14**, 664–666 (1926).
- [142] R. J. Glauber, *Coherent and incoherent states of the radiation field*, [Physical Review](#) **131**, 2766–2788 (1963).
- [143] R. J. Glauber, *Photon correlations*, [Phys. Rev. Lett.](#) **10**, 84–86 (1963).
- [144] E. C. G. Sudarshan, *Equivalence of semiclassical and quantum mechanical descriptions of statistical light beams*, [Physical Review Letters](#) **10**, 277–279 (1963).
- [145] A. B. C. DeWitt and C. Cohen-Tannoudji, *Quantum optics and electronics*, [Nuclear Physics](#) **72**, 696 (1965).
- [146] C. L. Mehta, *Diagonal coherent-state representation of quantum operators*, [Phys. Rev. Lett.](#) **18**, 752–754 (1967).
- [147] I. I. Rabi, *On the process of space quantization*, [Physical Review](#) **49**, 324–328 (1936).
- [148] I. I. Rabi, *Space quantization in a gyrating magnetic field*, [Physical Review](#) **51**, 652–654 (1937).
- [149] E. Jaynes and F. Cummings, *Comparison of quantum and semiclassical radiation theories with application to the beam maser*, [Proceedings of the IEEE](#) **51**, 89–109 (1963).
- [150] G. Lin and Y. K. Chembo, *(INVITED) monolithic total internal reflection resonators for applications in photonics*, [Optical Materials: X](#) **2**, 100017 (2019).
- [151] J. P. Vasco and V. Savona, *Global optimization of an encapsulated Si/SiO₂ L3 cavity with a 43 million quality factor*, [Scientific Reports](#) **11**, 10.1038/s41598-021-89410-1 (2021).
- [152] A. Wallraff et al., *Strong coupling of a single photon to a superconducting qubit using circuit quantum electrodynamics*, [Nature](#) **431**, 162–167 (2004).
- [153] A. F. Kockum and F. Nori, *Quantum bits with josephson junctions*, in [Fundamentals and frontiers of the josephson effect](#) (Springer International Publishing, 2019), pp. 703–741.
- [154] V. Bouchiat et al., *Quantum coherence with a single cooper pair*, [Physica Scripta](#) **T76**, 165 (1998).
- [155] Y. Nakamura, Y. A. Pashkin, and J. S. Tsai, *Coherent control of macroscopic quantum states in a single-cooper-pair box*, [Nature](#) **398**, 786–788 (1999).
- [156] D. Vion et al., *Manipulating the quantum state of an electrical circuit*, [Science](#) **296**, 886–889 (2002).
- [157] J. Koch et al., *Charge-insensitive qubit design derived from the cooper pair box*, [Physical Review A](#) **76**, 042319 (2007).
- [158] C. H. van der Wal et al., *Quantum superposition of macroscopic persistent-current states*, [Science](#) **290**, 773–777 (2000).
- [159] T. P. Orlando et al., *Superconducting persistent-current qubit*, [Physical Review B](#) **60**, 15398–15413 (1999).

- [160] J. E. Mooij et al., *Josephson persistent-current qubit*, [Science](#) **285**, 1036–1039 (1999).
- [161] J. M. Martinis, S. Nam, J. Aumentado, and C. Urbina, *Rabi oscillations in a large josephson-junction qubit*, [Physical Review Letters](#) **89**, 117901 (2002).
- [162] J. M. Martinis and K. Osborne, *Superconducting Qubits and the Physics of Josephson Junctions*, [arXiv:cond-mat/0402415](#), [arXiv: cond-mat/0402415](#) (2004).
- [163] A. Wallraff et al., *Quantum information processing with superconducting qubits and cavities*, in [2007 european conference on lasers and electro-optics and the international quantum electronics conference](#) (2007).
- [164] X. Gu et al., *Microwave photonics with superconducting quantum circuits*, [Physics Reports](#) **718-719**, 1–102 (2017).
- [165] G. Wendin, *Quantum information processing with superconducting circuits: a review*, [Reports on Progress in Physics](#) **80**, 106001 (2017).
- [166] M. Fitzpatrick et al., *Observation of a dissipative phase transition in a one-dimensional circuit QED lattice*, [Physical Review X](#) **7**, 011016 (2017).
- [167] R. J. Schoelkopf and S. M. Girvin, *Wiring up quantum systems*, [Nature](#) **451**, 664–669 (2008).
- [168] M. Pierre et al., *Storage and on-demand release of microwaves using superconducting resonators with tunable coupling*, [Applied Physics Letters](#) **104**, 232604 (2014).
- [169] Y. Yin et al., *Catch and release of microwave photon states*, [Physical Review Letters](#) **110**, 107001 (2013).
- [170] N. Ofek et al., *Extending the lifetime of a quantum bit with error correction in superconducting circuits*, [Nature](#) **536**, 441–445 (2016).
- [171] C. Wang et al., *A schrödinger cat living in two boxes*, [Science](#) **352**, 1087–1091 (2016).
- [172] C. Axline et al., *An architecture for integrating planar and 3d cQED devices*, [Applied Physics Letters](#) **109**, 042601 (2016).
- [173] L. Villa and G. D. Chiara, *Cavity assisted measurements of heat and work in optical lattices*, [Quantum](#) **2**, 42 (2018).
- [174] F. Brennecke et al., *Cavity QED with a bose–einstein condensate*, [Nature](#) **450**, 268–271 (2007).
- [175] M. Lewenstein et al., *Ultracold atomic gases in optical lattices: mimicking condensed matter physics and beyond*, [Advances in Physics](#) **56**, 243–379 (2007).
- [176] D. Jaksch and P. Zoller, *The cold atom hubbard toolbox*, [Annals of Physics](#) **315**, 52–79 (2005).
- [177] I. Bloch, J. Dalibard, and W. Zwerger, *Many-body physics with ultracold gases*, [Reviews of Modern Physics](#) **80**, 885–964 (2008).
- [178] C. Gross and I. Bloch, *Quantum simulations with ultracold atoms in optical lattices*, [Science](#) **357**, 995–1001 (2017).

- [179] C. Gardiner and P. Zoller, *The quantum world of ultra-cold atoms and light book II: the physics of quantum-optical devices* (IMPERIAL COLLEGE PRESS, 2014).
- [180] L. Fallani and A. Kastberg, *Cold atoms: a field enabled by light*, [EPL \(Europhysics Letters\) **110**, 53001 \(2015\)](#).
- [181] D. J. Wineland, J. C. Bergquist, W. M. Itano, and R. E. Drullinger, *Double-resonance and optical-pumping experiments on electromagnetically confined, laser-cooled ions*, [Optics Letters **5**, 245 \(1980\)](#).
- [182] D. J. Wineland, *Trapped ions, laser cooling, and better clocks*, [Science **226**, 395–400 \(1984\)](#).
- [183] A. D. Ludlow et al., *Optical atomic clocks*, [Reviews of Modern Physics **87**, 637–701 \(2015\)](#).
- [184] M. A. Cazalilla and A. M. Rey, *Ultracold fermi gases with emergent $SU(n)$ symmetry*, [Reports on Progress in Physics **77**, 124401 \(2014\)](#).
- [185] C. Balzer et al., *Electrodynamically trapped Yb^+ ions for quantum information processing*, [Physical Review A **73**, 041407 \(2006\)](#).
- [186] A. J. Daley, *Quantum computing and quantum simulation with group-II atoms*, [Quantum Information Processing **10**, 865–884 \(2011\)](#).
- [187] I. Bloch, J. Dalibard, and S. Nascimbène, *Quantum simulations with ultracold quantum gases*, [Nature Physics **8**, 267–276 \(2012\)](#).
- [188] M. Greiner et al., *Quantum phase transition from a superfluid to a mott insulator in a gas of ultracold atoms*, [Nature **415**, 39–44 \(2002\)](#).
- [189] P. W. Anderson, *Absence of diffusion in certain random lattices*, [Physical Review **109**, 1492–1505 \(1958\)](#).
- [190] J. yoon Choi et al., *Exploring the many-body localization transition in two dimensions*, [Science **352**, 1547–1552 \(2016\)](#).
- [191] L. F. Wei, Y. xi Liu, and F. Nori, *Engineering quantum pure states of a trapped cold ion beyond the lamb-dicke limit*, [Physical Review A **70**, 063801 \(2004\)](#).
- [192] F. Marquardt and S. M. Girvin, *Optomechanics*, en, [Physics **2**, 40 \(2009\)](#).
- [193] M. Aspelmeyer, T. J. Kippenberg, and F. Marquardt, *Cavity optomechanics*, [Reviews of Modern Physics **86**, 1391–1452 \(2014\)](#).
- [194] P. Meystre, *A short walk through quantum optomechanics*, [Annalen der Physik **525**, 215–233 \(2012\)](#).
- [195] I. Favero and K. Karrai, *Optomechanics of deformable optical cavities*, [Nature Photonics **3**, 201–205 \(2009\)](#).
- [196] C. Genes, A. Mari, D. Vitali, and P. Tombesi, *Chapter 2 quantum effects in optomechanical systems*, in [Advances in atomic, molecular, and optical physics](#) (Elsevier, 2009), pp. 33–86.
- [197] W. Bowen and G. Milburn, *Quantum optomechanics* (CRC Press, Boca Raton, 2016).

- [198] S. Barzanjeh et al., *Optomechanics for quantum technologies*, [Nature Physics](#) **18**, 15–24 (2021).
- [199] A. Schliesser et al., *Resolved-sideband cooling of a micromechanical oscillator*, [Nature Physics](#) **4**, 415–419 (2008).
- [200] A. Schliesser et al., *Resolved-sideband cooling and position measurement of a micromechanical oscillator close to the heisenberg uncertainty limit*, [Nature Physics](#) **5**, 509–514 (2009).
- [201] J. Chan et al., *Laser cooling of a nanomechanical oscillator into its quantum ground state*, [Nature](#) **478**, 89–92 (2011).
- [202] A. D. O’Connell et al., *Quantum ground state and single-phonon control of a mechanical resonator*, [Nature](#) **464**, 697–703 (2010).
- [203] A. Szorkovszky, A. C. Doherty, G. I. Harris, and W. P. Bowen, *Mechanical squeezing via parametric amplification and weak measurement*, [Physical Review Letters](#) **107**, 213603 (2011).
- [204] E. E. Wollman et al., *Quantum squeezing of motion in a mechanical resonator*, [Science](#) **349**, 952–955 (2015).
- [205] F. Lecocq et al., *Quantum nondemolition measurement of a nonclassical state of a massive object*, [Physical Review X](#) **5**, 041037 (2015).
- [206] J.-M. Pirkkalainen et al., *Squeezing of quantum noise of motion in a micromechanical resonator*, [Physical Review Letters](#) **115**, 243601 (2015).
- [207] A. H. Safavi-Naeini et al., *Squeezed light from a silicon micromechanical resonator*, [Nature](#) **500**, 185–189 (2013).
- [208] T. P. Purdy et al., *Strong optomechanical squeezing of light*, [Physical Review X](#) **3**, 031012 (2013).
- [209] D. W. C. Brooks et al., *Non-classical light generated by quantum-noise-driven cavity optomechanics*, [Nature](#) **488**, 476–480 (2012).
- [210] R. Riedinger et al., *Non-classical correlations between single photons and phonons from a mechanical oscillator*, [Nature](#) **530**, 313–316 (2016).
- [211] R. Riedinger et al., *Remote quantum entanglement between two micromechanical oscillators*, [Nature](#) **556**, 473–477 (2018).
- [212] S. Kiesewetter, R. Teh, P. Drummond, and M. Reid, *Pulsed entanglement of two optomechanical oscillators and furry’s hypothesis*, [Physical Review Letters](#) **119**, 023601 (2017).
- [213] L. Tian, *Optoelectromechanical transducer: reversible conversion between microwave and optical photons*, [Annalen der Physik](#) **527**, 1–14 (2014).
- [214] H. Xu, L. Jiang, A. A. Clerk, and J. G. E. Harris, *Nonreciprocal control and cooling of phonon modes in an optomechanical system*, [Nature](#) **568**, 65–69 (2019).
- [215] Z. Shen et al., *Experimental realization of optomechanically induced non-reciprocity*, [Nature Photonics](#) **10**, 657–661 (2016).
- [216] K. Fang et al., *Generalized non-reciprocity in an optomechanical circuit via synthetic magnetism and reservoir engineering*, [Nature Physics](#) **13**, 465–471 (2017).

- [217] N. R. Bernier et al., *Nonreciprocal reconfigurable microwave optomechanical circuit*, [Nature Communications](#) **8**, 10.1038/s41467-017-00447-1 (2017).
- [218] L. M. de Lépinay, C. F. Ockeloen-Korppi, D. Malz, and M. A. Sillanpää, *Nonreciprocal transport based on cavity floquet modes in optomechanics*, [Physical Review Letters](#) **125**, 023603 (2020).
- [219] S. Barzanjeh et al., *Mechanical on-chip microwave circulator*, [Nature Communications](#) **8**, 10.1038/s41467-017-01304-x (2017).
- [220] T. Corbitt and N. Mavalvala, *Review: quantum noise in gravitational-wave interferometers*, [Journal of Optics B: Quantum and Semiclassical Optics](#) **6**, S675–S683 (2004).
- [221] M. Arndt and K. Hornberger, *Testing the limits of quantum mechanical superpositions*, [Nature Physics](#) **10**, 271–277 (2014).
- [222] D. Loss and D. P. DiVincenzo, *Quantum computation with quantum dots*, [Physical Review A](#) **57**, 120–126 (1998).
- [223] B. E. Kane, *A silicon-based nuclear spin quantum computer*, [Nature](#) **393**, 133–137 (1998).
- [224] R. Vrijen et al., *Electron-spin-resonance transistors for quantum computing in silicon-germanium heterostructures*, [Physical Review A](#) **62**, 012306 (2000).
- [225] R. de Sousa, J. D. Delgado, and S. D. Sarma, *Silicon quantum computation based on magnetic dipolar coupling*, [Physical Review A](#) **70**, 052304 (2004).
- [226] L. C. L. Hollenberg, A. D. Greentree, A. G. Fowler, and C. J. Wellard, *Two-dimensional architectures for donor-based quantum computing*, [Physical Review B](#) **74**, 045311 (2006).
- [227] A. Morello et al., *Single-shot readout of an electron spin in silicon*, [Nature](#) **467**, 687–691 (2010).
- [228] A. Imamoglu et al., *Quantum information processing using quantum dot spins and cavity QED*, [Physical Review Letters](#) **83**, 4204–4207 (1999).
- [229] J. R. Petta et al., *Coherent manipulation of coupled electron spins in semiconductor quantum dots*, [Science](#) **309**, 2180–2184 (2005).
- [230] D. Englund et al., *Controlling the spontaneous emission rate of single quantum dots in a two-dimensional photonic crystal*, [Physical Review Letters](#) **95**, 013904 (2005).
- [231] R. Hanson et al., *Spins in few-electron quantum dots*, [Reviews of Modern Physics](#) **79**, 1217–1265 (2007).
- [232] A. Kavokin, J. J. Baumberg, G. Malpuech, and F. P. Laussy, *Microcavities* (Oxford University Press, 2007).
- [233] C. Weisbuch, M. Nishioka, A. Ishikawa, and Y. Arakawa, *Observation of the coupled exciton-photon mode splitting in a semiconductor quantum microcavity*, [Physical Review Letters](#) **69**, 3314–3317 (1992).
- [234] J. J. Hopfield, *Theory of the contribution of excitons to the complex dielectric constant of crystals*, [Physical Review](#) **112**, 1555–1567 (1958).

- [235] J. I. Cirac and P. Zoller, *Quantum computations with cold trapped ions*, [Physical Review Letters](#) **74**, 4091–4094 (1995).
- [236] D. Leibfried, R. Blatt, C. Monroe, and D. Wineland, *Quantum dynamics of single trapped ions*, [Reviews of Modern Physics](#) **75**, 281–324 (2003).
- [237] R. Blatt and D. Wineland, *Entangled states of trapped atomic ions*, [Nature](#) **453**, 1008–1015 (2008).
- [238] H. HAFFNER, C. ROOS, and R. BLATT, *Quantum computing with trapped ions*, [Physics Reports](#) **469**, 155–203 (2008).
- [239] R. Blatt and C. F. Roos, *Quantum simulations with trapped ions*, [Nature Physics](#) **8**, 277–284 (2012).
- [240] R. Hanson, O. Gywat, and D. D. Awschalom, *Room-temperature manipulation and decoherence of a single spin in diamond*, [Physical Review B](#) **74**, 161203 (2006).
- [241] M. V. G. Dutt et al., *Quantum register based on individual electronic and nuclear spin qubits in diamond*, [Science](#) **316**, 1312–1316 (2007).
- [242] J. A. Gyamfi, *Fundamentals of quantum mechanics in liouville space*, [European Journal of Physics](#) **41**, 063002 (2020).
- [243] J. Łuczka, *Spin in contact with thermostat: exact reduced dynamics*, [Physica A: Statistical Mechanics and its Applications](#) **167**, 919–934 (1990).
- [244] B. L. Hu, J. P. Paz, and Y. Zhang, *Quantum brownian motion in a general environment: exact master equation with nonlocal dissipation and colored noise*, [Physical Review D](#) **45**, 2843–2861 (1992).
- [245] B. M. Garraway, *Nonperturbative decay of an atomic system in a cavity*, [Physical Review A](#) **55**, 2290–2303 (1997).
- [246] J. Fischer and H.-P. Breuer, *Correlated projection operator approach to non-markovian dynamics in spin baths*, [Physical Review A](#) **76**, 052119 (2007).
- [247] A. Smirne and B. Vacchini, *Nakajima-zwanzig versus time-convolutionless master equation for the non-markovian dynamics of a two-level system*, [Physical Review A](#) **82**, 022110 (2010).
- [248] L. Diósi and L. Ferialdi, *General non-markovian structure of gaussian master and stochastic schrödinger equations*, [Physical Review Letters](#) **113**, 200403 (2014).
- [249] L. Ferialdi, *Exact closed master equation for gaussian non-markovian dynamics*, [Physical Review Letters](#) **116**, 120402 (2016).
- [250] M. O. Scully and M. S. Zubairy, *Quantum optics* (Cambridge University Press, 1997).
- [251] M. S. Kim and V. Bužek, *Photon statistics of superposition states in phase-sensitive reservoirs*, [Physical Review A](#) **47**, 610–619 (1993).
- [252] R. E. Slusher et al., *Observation of squeezed states generated by four-wave mixing in an optical cavity*, [Physical Review Letters](#) **55**, 2409–2412 (1985).
- [253] C. M. Caves, *Quantum-mechanical noise in an interferometer*, [Physical Review D](#) **23**, 1693–1708 (1981).

- [254] S. Suomela, A. Kutvonen, and T. Ala-Nissila, *Quantum jump model for a system with a finite-size environment*, [Physical Review E](#) **93**, 062106 (2016).
- [255] M. O. Scully and W. E. Lamb, *Quantum theory of an optical maser. i. general theory*, [Physical Review](#) **159**, 208–226 (1967).
- [256] B. Mollow and M. Miller, *The damped driven two-level atom*, [Annals of Physics](#) **52**, 464–478 (1969).
- [257] R. K. Wangsness and F. Bloch, *The dynamical theory of nuclear induction*, [Physical Review](#) **89**, 728–739 (1953).
- [258] R. Kubo, *A stochastic theory of line shape*, in [Advances in chemical physics](#) (John Wiley & Sons, Inc., 2007), pp. 101–127.
- [259] A. G. Redfield, *On the theory of relaxation processes*, [IBM Journal of Research and Development](#) **1**, 19–31 (1957).
- [260] M. Müller, S. Diehl, G. Pupillo, and P. Zoller, *Engineered open systems and quantum simulations with atoms and ions*, in [Advances in atomic, molecular, and optical physics](#), Vol. 61, edited by P. Berman, E. Arimondo, and C. Lin, *Advances In Atomic, Molecular, and Optical Physics* (Academic Press, 2012), pp. 1–80.
- [261] E. Kapit, M. Hafezi, and S. H. Simon, *Induced self-stabilization in fractional quantum hall states of light*, [Physical Review X](#) **4**, 031039 (2014).
- [262] R. Ma et al., *A dissipatively stabilized mott insulator of photons*, [Nature](#) **566**, 51–57 (2019).
- [263] J. P. Martínez et al., *A tunable josephson platform to explore many-body quantum optics in circuit-QED*, [npj Quantum Information](#) **5**, 10.1038/s41534-018-0104-0 (2019).
- [264] I. Carusotto et al., *Photonic materials in circuit quantum electrodynamics*, [Nature Physics](#) **16**, 268–279 (2020).
- [265] V. Giovannetti, S. Lloyd, and L. Maccone, *Advances in quantum metrology*, [Nature Photonics](#) **5**, 222–229 (2011).
- [266] G. McCauley, B. Cruikshank, S. Santra, and K. Jacobs, *Ability of markovian master equations to model quantum computers and other systems under broadband control*, [Physical Review Research](#) **2**, 013049 (2020).
- [267] Z. Leghtas et al., *Confining the state of light to a quantum manifold by engineered two-photon loss*, [Science](#) **347**, 853–857 (2015).
- [268] S. Vinjanampathy and J. Anders, *Quantum thermodynamics*, [Contemporary Physics](#) **57**, 545–579 (2016).
- [269] P. Kómár et al., *A quantum network of clocks*, [Nature Physics](#) **10**, 582–587 (2014).
- [270] P. Gehring, J. M. Thijssen, and H. S. J. van der Zant, *Single-molecule quantum-transport phenomena in break junctions*, [Nature Reviews Physics](#) **1**, 381–396 (2019).

- [271] P. Benioff, *The computer as a physical system: a microscopic quantum mechanical hamiltonian model of computers as represented by turing machines*, [Journal of Statistical Physics](#) **22**, 563–591 (1980).
- [272] R. P. Feynman, *Simulating physics with computers*, [International Journal of Theoretical Physics](#) **21**, 467–488 (1982).
- [273] I. L. Chuang, N. Gershenfeld, and M. Kubinec, *Experimental implementation of fast quantum searching*, [Physical Review Letters](#) **80**, 3408–3411 (1998).
- [274] J. A. Jones and M. Mosca, *Implementation of a quantum algorithm on a nuclear magnetic resonance quantum computer*, [The Journal of Chemical Physics](#) **109**, 1648–1653 (1998).
- [275] I. L. Chuang et al., *Experimental realization of a quantum algorithm*, [Nature](#) **393**, 143–146 (1998).
- [276] R. Hughes et al., *The los alamos trapped ion quantum computer experiment*, [Fortschritte der Physik](#) **46**, 329–361 (1998).
- [277] P. Hänggi, P. Talkner, and M. Borkovec, *Reaction-rate theory: fifty years after kramers*, [Reviews of Modern Physics](#) **62**, 251–341 (1990).
- [278] P. G. Wolynes, *Quantum theory of activated events in condensed phases*, [Physical Review Letters](#) **47**, 968–971 (1981).
- [279] G. A. Voth, D. Chandler, and W. H. Miller, *Rigorous formulation of quantum transition state theory and its dynamical corrections*, [The Journal of Chemical Physics](#) **91**, 7749–7760 (1989).
- [280] R. Ianculescu and E. Pollak, *Activated quantum diffusion in a periodic potential above the crossover temperature*, [The Journal of Chemical Physics](#) **151**, 024703 (2019).
- [281] G. S. Engel et al., *Evidence for wavelike energy transfer through quantum coherence in photosynthetic systems*, [Nature](#) **446**, 782–786 (2007).
- [282] E. Collini et al., *Coherently wired light-harvesting in photosynthetic marine algae at ambient temperature*, [Nature](#) **463**, 644–647 (2010).
- [283] R. E. Blankenship et al., *Comparing photosynthetic and photovoltaic efficiencies and recognizing the potential for improvement*, [Science](#) **332**, 805–809 (2011).
- [284] N. Lambert et al., *Quantum biology*, [Nature Physics](#) **9**, 10–18 (2012).
- [285] J. Cao et al., *Quantum biology revisited*, [Science Advances](#) **6**, 10.1126/sciadv.aaz4888 (2020).
- [286] G. Panitchayangkoon et al., *Long-lived quantum coherence in photosynthetic complexes at physiological temperature*, [Proceedings of the National Academy of Sciences](#) **107**, 12766–12770 (2010).
- [287] C. Gardiner and P. Zoller, “Quantum noise, a handbook of markovian and non-markovian quantum stochastic methods with applications to quantum optics”, in (Jan. 2004).
- [288] W. H. Zurek, *Decoherence and the transition from quantum to classical*, [Physics Today](#) **44**, 36–44 (1991).

- [289] C. Cohen-Tannoudji, B. Diu, and F. Laloe, *Quantum mechanics 1* (Wiley-VCH GmbH, Oct. 2019).
- [290] B. D. Franck Laloe, *Quantum mechanics 2* (Wiley-VCH GmbH, Oct. 2019), 688 pp.
- [291] S. Shandera, N. Agarwal, and A. Kamal, *Open quantum cosmological system*, [Physical Review D](#) **98**, 083535 (2018).
- [292] M. Tegmark and J. A. Wheeler, *100 years of quantum mysteries*, [Scientific American](#) **284**, 68–75 (2001).
- [293] J. J. Sakurai and J. Napolitano, *Modern quantum mechanics* (Cambridge University Press, 2017).
- [294] E. Merzbacher, *Quantum mechanics* (John Wiley & Sons, Dec. 1997), 676 pp.
- [295] C. Ciuti, *Open Quantum Many-Body Systems*, FR, [video file] Retrieved from <https://www.college-de-france.fr/site/jean-dalibard/seminar-2021-04-02-11h00.htm>, Apr. 2021.
- [296] S. Mukamel, *Principles of Nonlinear Optical Spectroscopy*, en, Google-Books-ID: k_7uAAAAMAAJ (Oxford University Press, 1995).
- [297] C. Neuenhahn, B. Kubala, B. Abel, and F. Marquardt, *Recent progress in open quantum systems: non-gaussian noise and decoherence in fermionic systems*, [physica status solidi \(b\)](#) **246**, 1018–1023 (2009).
- [298] M.-D. Choi, *Completely positive linear maps on complex matrices*, [Linear Algebra and its Applications](#) **10**, 285–290 (1975).
- [299] W. F. Stinespring, *Positive functions on c^* -algebras*, [Proceedings of the American Mathematical Society](#) **6**, 211–216 (1955).
- [300] M.-D. Choi, *Positive linear maps on c^* -algebras*, [Canadian Journal of Mathematics](#) **24**, 520–529 (1972).
- [301] M. Hotta, J. Matsumoto, and G. Yusa, *Quantum energy teleportation without a limit of distance*, [Physical Review A](#) **89**, 012311 (2014).
- [302] K. Kraus, A. Böhm, J. D. Dollard, and W. H. Wootters, eds., *States, effects, and operations fundamental notions of quantum theory* (Springer Berlin Heidelberg, 1983).
- [303] K. Jacobs, *Quantum measurement theory and its applications* (Cambridge University Press, 2014).
- [304] Barnett, *Quantum information omsp p* (OUP UK, May 2009), 314 pp.
- [305] M. G. A. Paris, *The modern tools of quantum mechanics*, [The European Physical Journal Special Topics](#) **203**, 61–86 (2012).
- [306] C. J. Wood, J. D. Biamonte, and D. G. Cory, *Tensor networks and graphical calculus for open quantum systems*, [Quantum Information and Computation](#) **15**, 759–811 (2015).
- [307] M. M. Wilde, *Quantum information theory* (Cambridge University Press, Feb. 2018), 776 pp.

- [308] I. Bengtsson and K. Życzkowski, *Geometry of quantum states* (Cambridge University Press, 2006).
- [309] H.-P. Breuer, E.-M. Laine, J. Piilo, and B. Vacchini, *Colloquium: non-markovian dynamics in open quantum systems*, [Reviews of Modern Physics](#) **88**, 021002 (2016).
- [310] Á. Rivas, S. F. Huelga, and M. B. Plenio, *Quantum non-markovianity: characterization, quantification and detection*, [Reports on Progress in Physics](#) **77**, 094001 (2014).
- [311] I. de Vega and D. Alonso, *Dynamics of non-markovian open quantum systems*, [Reviews of Modern Physics](#) **89**, 015001 (2017).
- [312] T. Prosen, *OpenXXZSpin chain: nonequilibrium steady state and a strict bound on ballistic transport*, [Physical Review Letters](#) **106**, 217206 (2011).
- [313] J. Metz, M. Trupke, and A. Beige, *Robust entanglement through macroscopic quantum jumps*, [Physical Review Letters](#) **97**, 040503 (2006).
- [314] D. A. Lidar, I. L. Chuang, and K. B. Whaley, *Decoherence-free subspaces for quantum computation*, [Physical Review Letters](#) **81**, 2594–2597 (1998).
- [315] T. A. Brun, *Continuous measurements, quantum trajectories, and decoherent histories*, [Physical Review A](#) **61**, 042107 (2000).
- [316] M. A. Schlosshauer, *Decoherence* (Springer Berlin Heidelberg, Nov. 2010), 436 pp.
- [317] M. B. Plenio and S. F. Huelga, *Dephasing-assisted transport: quantum networks and biomolecules*, [New Journal of Physics](#) **10**, 113019 (2008).
- [318] D. Walls and G. J. Milburn, eds., *Quantum optics* (Springer Berlin Heidelberg, 2008).
- [319] G. S. Agarwal, *Quantum statistical theories of spontaneous emission and their relation to other approaches*, in [Springer tracts in modern physics](#) (Springer Berlin Heidelberg, 1974), pp. 1–128.
- [320] D. Chruściński and S. Pascazio, *A brief history of the GKLS equation*, [Open Systems & Information Dynamics](#) **24**, 1740001 (2017).
- [321] G. Lindblad, *On the generators of quantum dynamical semigroups*, [Communications in Mathematical Physics](#) **48**, 119–130 (1976).
- [322] V. Gorini, A. Kossakowski, and E. C. G. Sudarshan, *Completely positive dynamical semigroups of n -level systems*, [Journal of Mathematical Physics](#) **17**, 821–825 (1976).
- [323] M. J. Collett and C. W. Gardiner, *Squeezing of intracavity and traveling-wave light fields produced in parametric amplification*, [Physical Review A](#) **30**, 1386–1391 (1984).
- [324] C. W. Gardiner and M. J. Collett, *Input and output in damped quantum systems: quantum stochastic differential equations and the master equation*, [Physical Review A](#) **31**, 3761–3774 (1985).
- [325] R. Alicki and K. Lendi, *Quantum dynamical semigroups and applications*, Lecture Notes in Physics (Springer Berlin Heidelberg, 2007).

- [326] B. Yurke and J. S. Denker, *Quantum network theory*, [Physical Review A](#) **29**, 1419–1437 (1984).
- [327] R. Kosloff, *Propagation methods for quantum molecular dynamics*, [Annual Review of Physical Chemistry](#) **45**, 145–178 (1994).
- [328] F. Lucas and K. Hornberger, *Optimally convergent quantum jump expansion*, [Physical Review A](#) **89**, 012112 (2014).
- [329] R. Sweke, I. Sinayskiy, D. Bernard, and F. Petruccione, *Universal simulation of markovian open quantum systems*, [Physical Review A](#) **91**, 062308 (2015).
- [330] J. F. Haase et al., *Precision limits in quantum metrology with open quantum systems*, [Quantum Measurements and Quantum Metrology](#) **5**, 13–39 (2016).
- [331] C. Maier et al., *Environment-assisted quantum transport in a 10-qubit network*, [Physical Review Letters](#) **122**, 050501 (2019).
- [332] L. Magazzú et al., *Probing the strongly driven spin-boson model in a superconducting quantum circuit*, [Nature Communications](#) **9**, 10.1038/s41467-018-03626-w (2018).
- [333] A. W. Chin, S. F. Huelga, and M. B. Plenio, *Quantum metrology in non-markovian environments*, [Physical Review Letters](#) **109**, 233601 (2012).
- [334] R. Alicki, M. Horodecki, P. Horodecki, and R. Horodecki, *Dynamical description of quantum computing: generic nonlocality of quantum noise*, [Physical Review A](#) **65**, 062101 (2002).
- [335] Y. Dong et al., *Non-markovianity-assisted high-fidelity deutsch–jozsa algorithm in diamond*, [npj Quantum Information](#) **4**, 10.1038/s41534-017-0053-z (2018).
- [336] C.-F. Li, G.-C. Guo, and J. Piilo, *Non-markovian quantum dynamics: what is it good for?*, [EPL \(Europhysics Letters\)](#) **128**, 30001 (2020).
- [337] S. Flannigan, F. Damanet, and A. J. Daley, *Many-body quantum state diffusion for non-Markovian dynamics in strongly interacting systems*, [arXiv:2108.06224 \[quant-ph\]](#), [arXiv: 2108.06224](#) (2021).
- [338] P. Bocchieri and A. Loinger, *Quantum recurrence theorem*, [Physical Review](#) **107**, 337–338 (1957).
- [339] I. C. Percival, *Almost periodicity and the quantal \hbar theorem*, [Journal of Mathematical Physics](#) **2**, 235–239 (1961).
- [340] D. A. Tieri, *Open Quantum Systems with Applications to Precision Measurements*, <http://id.loc.gov/vocabulary/iso639-2/eng>.
- [341] D. A. Lidar, *Lecture Notes on the Theory of Open Quantum Systems*, (2020).
- [342] n. Rivas and S. F. Huelga, *Open Quantum Systems: An Introduction*, en, Google-Books-ID: FGCuYsIZAA0C (Springer Science & Business Media, Oct. 2011).
- [343] V. V. Albert and L. Jiang, *Symmetries and conserved quantities in lindblad master equations*, [Phys. Rev. A](#) **89**, 022118 (2014).
- [344] D. Nigro, *On the uniqueness of the steady-state solution of the lindblad-gorini-kossakowski-sudarshan equation*, [Journal of Statistical Mechanics: Theory and Experiment](#) **2019**, 043202 (2019).

- [345] H. Spohn, *Approach to equilibrium for completely positive dynamical semigroups of n -level systems*, [Reports on Mathematical Physics](#) **10**, 189–194 (1976).
- [346] H. Spohn, *An algebraic condition for the approach to equilibrium of an open n -level system*, [Letters in Mathematical Physics](#) **2**, 33–38 (1977).
- [347] A. Jamiołkowski, *Linear transformations which preserve trace and positive semidefiniteness of operators*, [Reports on Mathematical Physics](#) **3**, 275–278 (1972).
- [348] M. Zwolak and G. Vidal, *Mixed-state dynamics in one-dimensional quantum lattice systems: a time-dependent superoperator renormalization algorithm*, [Phys. Rev. Lett.](#) **93**, 207205 (2004).
- [349] A. Kshetrimayum, H. Weimer, and R. Orús, *A simple tensor network algorithm for two-dimensional steady states*, [Nature Communications](#) **8**, 1291 (2017).
- [350] A. Gilchrist, D. R. Terno, and C. J. Wood, *Vectorization of quantum operations and its use*, 2011.
- [351] F. Minganti and D. Huybrechts, *Arnoldi-Lindblad time evolution: Faster-than-the-clock algorithm for the spectrum of (Floquet) open quantum systems*, [arXiv:2109.01648 \[quant-ph\]](#), [arXiv: 2109.01648](#) (2021).
- [352] F. Iemini et al., *Boundary time crystals*, [Physical Review Letters](#) **121**, 035301 (2018).
- [353] F. Minganti, I. I. Arkhipov, A. Miranowicz, and F. Nori, *Correspondence between dissipative phase transitions of light and time crystals*, 2020.
- [354] J. Tindall, C. S. Muñoz, B. Buča, and D. Jaksch, *Quantum synchronisation enabled by dynamical symmetries and dissipation*, [New Journal of Physics](#) **22**, 013026 (2020).
- [355] C. S. Muñoz et al., *Symmetries and conservation laws in quantum trajectories: dissipative freezing*, [Physical Review A](#) **100**, 042113 (2019).
- [356] C. Navarrete-Benlloch, *Open systems dynamics: Simulating master equations in the computer*, [arXiv:1504.05266 \[quant-ph\]](#), [arXiv: 1504.05266](#) (2015).
- [357] D. Bohm, *A suggested interpretation of the quantum theory in terms of "hidden" variables. i*, [Physical Review](#) **85**, 166–179 (1952).
- [358] L. d. Broglie, “Recherches sur la théorie des Quanta”, fr, PhD thesis (Migration - université en cours d’affectation, Nov. 1924).
- [359] N. Gisin and I. C. Percival, *The quantum-state diffusion model applied to open systems*, [Journal of Physics A: Mathematical and General](#) **25**, 5677–5691 (1992).
- [360] L. Diósi, N. Gisin, J. Halliwell, and I. C. Percival, *Decoherent histories and quantum state diffusion*, [Physical Review Letters](#) **74**, 203–207 (1995).
- [361] J. Dalibard, Y. Castin, and K. Mølmer, *Wave-function approach to dissipative processes in quantum optics*, [Phys. Rev. Lett.](#) **68**, 580–583 (1992).
- [362] K. Mølmer, Y. Castin, and J. Dalibard, *Monte carlo wave-function method in quantum optics*, [J. Opt. Soc. Am. B](#) **10**, 524–538 (1993).

- [363] P. Marte et al., *Quantum wave function simulation of the resonance fluorescence spectrum from one-dimensional optical molasses*, [Physical Review Letters](#) **71**, 1335–1338 (1993).
- [364] Y. Castin and K. Mølmer, *Monte carlo wave-function analysis of 3d optical molasses*, [Physical Review Letters](#) **74**, 3772–3775 (1995).
- [365] P. Marte, R. Dum, R. Taïeb, and P. Zoller, *Resonance fluorescence from quantized one-dimensional molasses*, [Physical Review A](#) **47**, 1378–1390 (1993).
- [366] R. Dum, P. Zoller, and H. Ritsch, *Monte carlo simulation of the atomic master equation for spontaneous emission*, [Physical Review A](#) **45**, 4879–4887 (1992).
- [367] R. Dum, A. S. Parkins, P. Zoller, and C. W. Gardiner, *Monte carlo simulation of master equations in quantum optics for vacuum, thermal, and squeezed reservoirs*, [Physical Review A](#) **46**, 4382–4396 (1992).
- [368] H. Carmichael, *An open systems approach to quantum optics*, Lecture notes in physics monographs (Springer, Berlin, 1993).
- [369] G. C. Hegerfeldt, *How to reset an atom after a photon detection: applications to photon-counting processes*, [Physical Review A](#) **47**, 449–455 (1993).
- [370] G. C. Hegerfeldt, *The quantum jump approach and quantum trajectories*, in [Irreversible quantum dynamics](#) (Springer Berlin Heidelberg, 2003), pp. 233–242.
- [371] A. J. Daley, *Quantum trajectories and open many-body quantum systems*, [Advances in Physics](#) **63**, 77–149 (2014).
- [372] H.-P. Breuer, W. Huber, and F. Petruccione, *Stochastic wave-function method versus density matrix: a numerical comparison*, [Computer Physics Communications](#) **104**, 46–58 (1997).
- [373] W. Verstraelen, *Gaussian quantum trajectories for the variational simulation of open quantum systems, with photonic applications*, en, [10.13140/RG.2.2.18971.08480](#) (2020).
- [374] H. Weimer, A. Kshetrimayum, and R. Orús, *Simulation methods for open quantum many-body systems*, [Rev. Mod. Phys.](#) **93**, 015008 (2021).
- [375] P. D. Drummond and D. F. Walls, *Quantum theory of optical bistability. i. nonlinear polarisability model*, [Journal of Physics A: Mathematical and General](#) **13**, 725–741 (1980).
- [376] T. Prosen, *Third quantization: a general method to solve master equations for quadratic open fermi systems*, [New Journal of Physics](#) **10**, 043026 (2008).
- [377] M. Nakagawa, N. Kawakami, and M. Ueda, *Exact liouvillian spectrum of a one-dimensional dissipative hubbard model*, [Physical Review Letters](#) **126**, 110404 (2021).
- [378] M. Foss-Feig et al., *Solvable family of driven-dissipative many-body systems*, [Physical Review Letters](#) **119**, 190402 (2017).
- [379] C. Guo and D. Poletti, *Analytical solutions for a boundary-driven XY chain*, [Physical Review A](#) **98**, 052126 (2018).

- [380] M. V. Medvedyeva, F. H. Essler, and T. Prosen, *Exact bethe ansatz spectrum of a tight-binding chain with dephasing noise*, [Physical Review Letters](#) **117**, 137202 (2016).
- [381] T. Prosen, *Exact nonequilibrium steady state of a strongly driven OpenXXZChain*, [Physical Review Letters](#) **107**, 137201 (2011).
- [382] L. M. Sieberer, M Buchhold, and S Diehl, *Keldysh field theory for driven open quantum systems*, [Reports on Progress in Physics](#) **79**, 096001 (2016).
- [383] T. Müller et al., *Shape effects of localized losses in quantum wires: dissipative resonances and nonequilibrium universality*, [Physical Review B](#) **104**, 155431 (2021).
- [384] A. Kamenev, *Field theory of non-equilibrium systems* (Cambridge University Press, Aug. 2014), 356 pp.
- [385] L. V. Keldysh, *Diagram technique for nonequilibrium processes*, *Zh. Eksp. Teor. Fiz.* **47**, 1515–1527 (1964).
- [386] A. C. Y. Li, F. Petruccione, and J. Koch, *Resummation for nonequilibrium perturbation theory and application to open quantum lattices*, [Phys. Rev. X](#) **6**, 021037 (2016).
- [387] A. Biella et al., *Linked cluster expansions for open quantum systems on a lattice*, [Physical Review B](#) **97**, 035103 (2018).
- [388] R. v. L. Gianluca Stefanucci, *Nonequilibrium many-body theory of quantum systems* (Cambridge University Press, July 2015), 620 pp.
- [389] L. A. Lugiato and R. Lefever, *Spatial dissipative structures in passive optical systems*, [Physical Review Letters](#) **58**, 2209–2211 (1987).
- [390] S. Finazzi et al., *Corner-space renormalization method for driven-dissipative two-dimensional correlated systems*, [Phys. Rev. Lett.](#) **115**, 080604 (2015).
- [391] K. Donatella, Z. Denis, A. Le Boité, and C. Ciuti, *Continuous-time dynamics and error scaling of noisy highly entangling quantum circuits*, [Phys. Rev. A](#) **104**, 062407 (2021).
- [392] W. Verstraelen and M. Wouters, *Gaussian quantum trajectories for the variational simulation of open quantum-optical systems*, [Applied Sciences](#) **8**, 10.3390/app8091427 (2018).
- [393] J. Cui, J. I. Cirac, and M. C. Bañuls, *Variational matrix product operators for the steady state of dissipative quantum systems*, [Physical Review Letters](#) **114**, 220601 (2015).
- [394] F. A. Y. N. Schröder and A. W. Chin, *Simulating open quantum dynamics with time-dependent variational matrix product states: towards microscopic correlation of environment dynamics and reduced system evolution*, [Physical Review B](#) **93**, 075105 (2016).
- [395] A. Nagy and V. Savona, *Variational quantum monte carlo method with a neural-network ansatz for open quantum systems*, [Phys. Rev. Lett.](#) **122**, 250501 (2019).

- [396] M. J. Hartmann and G. Carleo, *Neural-network approach to dissipative quantum many-body dynamics*, [Phys. Rev. Lett. **122**, 250502 \(2019\)](#).
- [397] F. Vicentini, A. Biella, N. Regnault, and C. Ciuti, *Variational neural-network ansatz for steady states in open quantum systems*, [Phys. Rev. Lett. **122**, 250503 \(2019\)](#).
- [398] N. Yoshioka and R. Hamazaki, *Constructing neural stationary states for open quantum many-body systems*, [Phys. Rev. B **99**, 214306 \(2019\)](#).
- [399] W. Casteels and M. Wouters, *Optically bistable driven-dissipative bose-hubbard dimer: gutzwiller approaches and entanglement*, [Physical Review A **95**, 043833 \(2017\)](#).
- [400] W. Casteels, R. M. Wilson, and M. Wouters, *Gutzwiller monte carlo approach for a critical dissipative spin model*, [Physical Review A **97**, 062107 \(2018\)](#).
- [401] H. Pichler, J. Schachenmayer, A. J. Daley, and P. Zoller, *Heating dynamics of bosonic atoms in a noisy optical lattice*, [Physical Review A **87**, 033606 \(2013\)](#).
- [402] A. Le Boité, G. Orso, and C. Ciuti, *Steady-state phases and tunneling-induced instabilities in the driven dissipative bose-hubbard model*, [Phys. Rev. Lett. **110**, 233601 \(2013\)](#).
- [403] A. Ishizaki and G. R. Fleming, *Unified treatment of quantum coherent and incoherent hopping dynamics in electronic energy transfer: reduced hierarchy equation approach*, [The Journal of Chemical Physics **130**, 234111 \(2009\)](#).
- [404] Y. Tanimura and R. Kubo, *Two-time correlation functions of a system coupled to a heat bath with a gaussian-markoffian interaction*, [Journal of the Physical Society of Japan **58**, 1199–1206 \(1989\)](#).
- [405] Y. Tanimura, *Stochastic liouville, langevin, fokker–planck, and master equation approaches to quantum dissipative systems*, [Journal of the Physical Society of Japan **75**, 082001 \(2006\)](#).
- [406] R. P. Feynman, *Space-time approach to non-relativistic quantum mechanics*, [Reviews of Modern Physics **20**, 367–387 \(1948\)](#).
- [407] N. Makri and D. E. Makarov, *Tensor propagator for iterative quantum time evolution of reduced density matrices. i. theory*, [The Journal of Chemical Physics **102**, 4600–4610 \(1995\)](#).
- [408] P Nalbach, J Eckel, and M Thorwart, *Quantum coherent biomolecular energy transfer with spatially correlated fluctuations*, [New Journal of Physics **12**, 065043 \(2010\)](#).
- [409] A. D. Somoza et al., *Dissipation-assisted matrix product factorization*, [Physical Review Letters **123**, 100502 \(2019\)](#).
- [410] A. Polkovnikov, *Phase space representation of quantum dynamics*, [Annals of Physics **325**, 1790–1852 \(2010\)](#).
- [411] E. Wigner, *On the quantum correction for thermodynamic equilibrium*, [Phys. Rev. **40**, 749–759 \(1932\)](#).
- [412] K. Vogel and H. Risken, *Quasiprobability distributions in dispersive optical bistability*, [Physical Review A **39**, 4675–4683 \(1989\)](#).

- [413] M. Werner and P. Drummond, *Robust algorithms for solving stochastic partial differential equations*, [Journal of Computational Physics](#) **132**, 312–326 (1997).
- [414] M. J. Steel et al., *Dynamical quantum noise in trapped bose-einstein condensates*, [Physical Review A](#) **58**, 4824–4835 (1998).
- [415] W. P. Schleich, *Quantum optics in phase space* (Wiley, 2001).
- [416] A. Sinatra, C. Lobo, and Y. Castin, *The truncated wigner method for bose-condensed gases: limits of validity and applications*, [Phys. Rev. A](#) **65**, 3599–3631 (2002).
- [417] A. Polkovnikov, *Quantum corrections to the dynamics of interacting bosons: beyond the truncated wigner approximation*, [Phys. Rev. A](#) **68**, 053604 (2003).
- [418] I. Carusotto and C. Ciuti, *Spontaneous microcavity-polariton coherence across the parametric threshold: quantum monte carlo studies*, [Physical Review B](#) **72**, 125335 (2005).
- [419] B. Berg et al., *Commuting heisenberg operators as the quantum response problem: time-normal averages in the truncated wigner representation*, [Physical Review A](#) **80**, 033624 (2009).
- [420] P. D. Drummond and B. Opanchuk, *Truncated wigner dynamics and conservation laws*, [Physical Review A](#) **96**, 043616 (2017).
- [421] C. Mink et al., *Variational truncated wigner approximation for weakly interacting bose fields: dynamics of coupled condensates*, [SciPost Physics](#) **12**, 10.21468/scipostphys.12.2.051 (2022).
- [422] K. Sakmann, A. I. Streltsov, O. E. Alon, and L. S. Cederbaum, *Exact quantum dynamics of a bosonic josephson junction*, [Physical Review Letters](#) **103**, 220601 (2009).
- [423] C. M. Caves and C. A. Fuchs, *Quantum information: How much information in a state vector?*, [arXiv:quant-ph/9601025](#), [arXiv: quant-ph/9601025](#) (1996).
- [424] H. B. published, *How many atoms are in the observable universe?*, en, [website] Retrieved from <https://www.livescience.com/how-many-atoms-in-universe.html>, July 2021.
- [425] E. Gross, *Classical theory of boson wave fields*, [Annals of Physics](#) **4**, 57–74 (1958).
- [426] E. P. Gross, *Quantum theory of interacting bosons*, [Annals of Physics](#) **9**, 292–324 (1960).
- [427] E. P. Gross, *Structure of a quantized vortex in boson systems*, [Il Nuovo Cimento](#) **20**, 454–477 (1961).
- [428] E. P. Gross, *Hydrodynamics of a superfluid condensate*, [Journal of Mathematical Physics](#) **4**, 195–207 (1963).
- [429] L. P. Pitaevskii, *Vortex lines in an imperfect Bose gas*, [Sov. Phys. JETP](#) **13**, 451–454 (1961).
- [430] F. Dalfovo, S. Giorgini, L. P. Pitaevskii, and S. Stringari, *Theory of bose-einstein condensation in trapped gases*, [Reviews of Modern Physics](#) **71**, 463–512 (1999).

- [431] A. A. Norrie, R. J. Ballagh, and C. W. Gardiner, *Quantum turbulence and correlations in bose-einstein condensate collisions*, [Phys. Rev. A **73**, 043617 \(2006\)](#).
- [432] P. Deuar and P. D. Drummond, *Correlations in a BEC collision: first-principles quantum dynamics with 150 000 atoms*, [Physical Review Letters **98**, 120402 \(2007\)](#).
- [433] P. D. Drummond and J. F. Corney, *Quantum dynamics of evaporatively cooled bose-einstein condensates*, [Physical Review A **60**, R2661–R2664 \(1999\)](#).
- [434] J. J. Hope and M. K. Olsen, *Quantum superchemistry: dynamical quantum effects in coupled atomic and molecular bose-einstein condensates*, [Physical Review Letters **86**, 3220–3223 \(2001\)](#).
- [435] U. V. Poulsen and K. Mølmer, *Quantum states of bose-einstein condensates formed by molecular dissociation*, [Physical Review A **63**, 023604 \(2001\)](#).
- [436] P. Blakie et al., *Dynamics and statistical mechanics of ultra-cold bose gases using c-field techniques*, [Advances in Physics **57**, 363–455 \(2008\)](#).
- [437] U. Shrestha, J. Javanainen, and J. Ruostekoski, *Quantum dynamics of instability-induced pulsations of a bose-einstein condensate in an optical lattice*, [Physical Review A **79**, 043617 \(2009\)](#).
- [438] K. Dechoum, M. D. Hahn, R. O. Vallejos, and A. Z. Khoury, *Semiclassical wigner distribution for a two-mode entangled state generated by an optical parametric oscillator*, [Physical Review A **81**, 043834 \(2010\)](#).
- [439] A. D. Martin and J. Ruostekoski, *Quantum and thermal effects of dark solitons in a one-dimensional bose gas*, [Physical Review Letters **104**, 194102 \(2010\)](#).
- [440] A. D. Martin and J. Ruostekoski, *Nonequilibrium quantum dynamics of atomic dark solitons*, [New Journal of Physics **12**, 055018 \(2010\)](#).
- [441] M. Egorov et al., *Long-lived periodic revivals of coherence in an interacting bose-einstein condensate*, [Physical Review A **84**, 021605 \(2011\)](#).
- [442] B. Opanchuk, Q. Y. He, M. D. Reid, and P. D. Drummond, *Dynamical preparation of einstein-podolsky-rosen entanglement in two-well bose-einstein condensates*, [Physical Review A **86**, 023625 \(2012\)](#).
- [443] B. Opanchuk et al., *Quantum noise in three-dimensional BEC interferometry*, [EPL \(Europhysics Letters\) **97**, 50003 \(2012\)](#).
- [444] A. Altland, V. Gurarie, T. Kriecherbauer, and A. Polkovnikov, *Nonadiabaticity and large fluctuations in a many-particle landau-zener problem*, [Physical Review A **79**, 042703 \(2009\)](#).
- [445] J. D. Sau, S. R. Leslie, D. M. Stamper-Kurn, and M. L. Cohen, *Theory of domain formation in inhomogeneous ferromagnetic dipolar condensates within the truncated wigner approximation*, [Physical Review A **80**, 023622 \(2009\)](#).
- [446] J. F. Corney et al., *Many-body quantum dynamics of polarization squeezing in optical fibers*, [Physical Review Letters **97**, 023606 \(2006\)](#).
- [447] W. Louisell, *Quantum statistical properties of radiation* (Wiley, New York, 1973).

- [448] C. W. Gardiner, *Handbook of stochastic methods for physics, chemistry, and the natural sciences* (Springer, Berlin New York, 2004).
- [449] R. F. Pawula, *Approximation of the linear boltzmann equation by the fokker-planck equation*, [Physical Review](#) **162**, 186–188 (1967).
- [450] C. Gardiner and P. Zoller, *Quantum noise* (Springer Berlin Heidelberg, Aug. 2004), 476 pp.
- [451] D. F. Styer et al., *Nine formulations of quantum mechanics*, [American Journal of Physics](#) **70**, 288–297 (2002).
- [452] P. A. M. Dirac, *The Lagrangian in quantum mechanics*, *Phys. Z. Sowjetunion* **3**, 64–72 (1933).
- [453] H. Weyl, *The theory of groups and quantum mechanics*, Dover Books on Mathematics (Dover Publications, 1950).
- [454] J. v. Neumann, *Die eindeutigkeit der schrödingerschen operatoren*, [Mathematische Annalen](#) **104**, 570–578 (1931).
- [455] H. Groenewold, *On the principles of elementary quantum mechanics*, [Physica](#) **12**, 405–460 (1946).
- [456] P. D. Drummond and C. W. Gardiner, *Generalised p-representations in quantum optics*, [Journal of Physics A: Mathematical and General](#) **13**, 2353–2368 (1980).
- [457] J. E. Moyal, *Quantum mechanics as a statistical theory*, [Mathematical Proceedings of the Cambridge Philosophical Society](#) **45**, 99–124 (1949).
- [458] F. A. Berezin, *Feynman path integrals in a phase space*, [Soviet Physics Uspekhi](#) **23**, 763–788 (1980).
- [459] F. E. S. Jr. and F. E. Schroeck, *Quantum mechanics on phase space* (Springer Netherlands, Dec. 2010), 692 pp.
- [460] T. L. Curtright, D. B. Fairlie, and C. K. Zachos, *Quantum mechanics in phase space: an overview with selected papers* (WORLD SCIENTIFIC PUB CO INC, Dec. 2005), 560 pp.
- [461] D. A. Dubin, M. A. Hennings, and T. B. Smith, *Mathematical aspects of weyl quantization and phase* (WORLD SCIENTIFIC, 2000).
- [462] T. L. Curtright, D. B. Fairlie, and C. K. Zachos, *A concise treatise on quantum mechanics in phase space* (WORLD SCIENTIFIC, 2014).
- [463] H. Weyl, *Quantenmechanik und gruppentheorie*, [Zeitschrift für Physik](#) **46**, 1–46 (1927).
- [464] H. Weyl, *The theory of groups and quantum mechanics* (Martino Fine Books, Feb. 2014), 448 pp.
- [465] B. Koczor, R. Zeier, and S. J. Glaser, *Continuous phase-space representations for finite-dimensional quantum states and their tomography*, [Physical Review A](#) **101**, 022318 (2020).
- [466] U. Leonhardt, *Measuring the quantum state of light* (Cambridge University Press, Apr. 2003), 208 pp.

- [467] M. K. Olsen, L. I. Plimak, M. J. Collett, and D. F. Walls, *Quantum-nondemolition criteria in traveling-wave second-harmonic generation*, [Physical Review A](#) **62**, 023802 (2000).
- [468] P. D. Drummond, P. Deuar, T. G. Vaughan, and J. F. Corney, *Quantum dynamics in phase space: from coherent states to the gaussian representation*, [Journal of Modern Optics](#) **54**, 2499–2512 (2007).
- [469] F. T. Arecchi, *Laser handbook* (North-Holland Pub. Co./American Elsevier Pub. Co, Amsterdam, New York, 1972).
- [470] K. Husimi, *Some formal properties of the density matrix*, Proceedings of the Physico-Mathematical Society of Japan. 3rd Series **22**, 264–314 (1940).
- [471] K. E. Cahill and R. J. Glauber, *Density operators and quasiprobability distributions*, [Phys. Rev.](#) **177**, 1882–1902 (1969).
- [472] M. A. de Gosson, *Phase space quantization and the uncertainty principle*, [Physics Letters A](#) **317**, 365–369 (2003).
- [473] D. Ferraro et al., *Wigner function approach to single electron coherence in quantum hall edge channels*, [Physical Review B](#) **88**, 205303 (2013).
- [474] R. P. Rundle et al., *Visualization of correlations in hybrid discrete—continuous variable quantum systems*, [Journal of Physics Communications](#) **4**, 025002 (2020).
- [475] S. Olivares, *Quantum optics in the phase space*, [The European Physical Journal Special Topics](#) **203**, 3–24 (2012).
- [476] W. P. Schleich, *Quantum optics in phase space* (Wiley-VCH GmbH, Dec. 2015), 696 pp.
- [477] C. H. H. Schulte et al., *Quadrature squeezed photons from a two-level system*, [Nature](#) **525**, 222–225 (2015).
- [478] R. P. Rundle and M. J. Everitt, *Overview of the phase space formulation of quantum mechanics with application to quantum technologies*, [Advanced Quantum Technologies](#) **4**, 2100016 (2021).
- [479] D. K. Ferry, *Wigner functions*, in [The wigner function in science and technology](#) (IOP Publishing, 2018).
- [480] D. K. Ferry et al., *Complex systems in phase space*, [Entropy](#) **22**, 1103 (2020).
- [481] J. Weinbub and D. K. Ferry, *Recent advances in wigner function approaches*, [Applied Physics Reviews](#) **5**, 041104 (2018).
- [482] W. H. Zurek and J. P. Paz, *Quantum chaos: a decoherent definition*, [Physica D: Nonlinear Phenomena](#) **83**, 300–308 (1995).
- [483] R. Jasiak, G. Manfredi, P.-A. Hervieux, and M. Haefele, *Quantum–classical transition in the electron dynamics of thin metal films*, [New Journal of Physics](#) **11**, 063042 (2009).
- [484] S. Habib et al., *Quantum-classical transition in nonlinear dynamical systems*, [Physical Review Letters](#) **88**, 040402 (2002).
- [485] M. te Vrugt, H. Löwen, and R. Wittkowski, *Classical dynamical density functional theory: from fundamentals to applications*, [Advances in Physics](#) **69**, 121–247 (2020).

- [486] M. Hillery, R. O'Connell, M. Scully, and E. Wigner, *Distribution functions in physics: fundamentals*, [Physics Reports](#) **106**, 121–167 (1984).
- [487] W. B. Case, *Wigner functions and weyl transforms for pedestrians*, [American Journal of Physics](#) **76**, 937–946 (2008).
- [488] R. L. Stratonovich, *On a Method of Calculating Quantum Distribution Functions*, [Soviet Physics Doklady](#) **2**, ADS Bibcode: 1957SPhD....2..416S, 416 (1957).
- [489] B. G. Englert, *On the operator bases underlying wigner's, kirkwood's and glauber's phase space functions*, [Journal of Physics A: Mathematical and General](#) **22**, 625–640 (1989).
- [490] C. Brif and A. Mann, *Phase-space formulation of quantum mechanics and quantum-state reconstruction for physical systems with lie-group symmetries*, [Physical Review A](#) **59**, 971–987 (1999).
- [491] H. Waalkens, R. Schubert, and S. Wiggins, *Wigner's dynamical transition state theory in phase space: classical and quantum*, [Nonlinearity](#) **21**, R1–R118 (2007).
- [492] F. Bopp, “Werner heisenberg und die physik unserer zeit”, in *Werner heisenberg und die physik unserer zeit* (Vieweg+Teubner Verlag, Braunschweig, 1961), p. 128.
- [493] R. Kubo, *Wigner representation of quantum operators and its applications to electrons in a magnetic field*, [Journal of the Physical Society of Japan](#) **19**, 2127–2139 (1964).
- [494] M. A. D. Gosson, *Symplectic methods in harmonic analysis and in mathematical physics* (Springer Basel, July 2011), 364 pp.
- [495] R. Hudson, *When is the wigner quasi-probability density non-negative?*, [Reports on Mathematical Physics](#) **6**, 249–252 (1974).
- [496] F. Soto and P. Claverie, *When is the wigner function of multidimensional systems nonnegative?*, [Journal of Mathematical Physics](#) **24**, 97–100 (1983).
- [497] T. Bröcker and R. F. Werner, *Mixed states with positive wigner functions*, [Journal of Mathematical Physics](#) **36**, 62–75 (1995).
- [498] A. Mandilara, E. Karpov, and N. J. Cerf, *Extending hudson's theorem to mixed quantum states*, [Physical Review A](#) **79**, 062302 (2009).
- [499] K. Nagao, “Phase space methods for quantum dynamics”, in *Fluctuations and non-equilibrium phenomena in strongly-correlated ultracold atoms* (Springer Singapore, Singapore, 2020), pp. 31–52.
- [500] O. V. Bychuk and B. J. Haughey, *Basics of probability theory*, in [Hedging market exposures](#) (John Wiley & Sons, Inc., 2015), pp. 227–245.
- [501] H. Risken, *The fokker-planck equation* (Springer Berlin Heidelberg, 1984).
- [502] P. Kinsler, *Drift, diffusion, and third order derivatives in Fokker-Planck equations: one specific case*, [arXiv:1309.3427 \[physics\]](#), [arXiv: 1309.3427](#) (2013).
- [503] P. D Drummond and A. D Hardman, *Simulation of quantum effects in raman-active waveguides*, [Europhysics Letters \(EPL\)](#) **21**, 279–284 (1993).
- [504] J. Ruostekoski and L. Isella, *Dissipative quantum dynamics of bosonic atoms in a shallow 1d optical lattice*, [Physical Review Letters](#) **95**, 110403 (2005).

- [505] H. Risken, *The fokker-planck equation: methods of solution and applications* (Springer Berlin Heidelberg, 1989).
- [506] C. Rackauckas, and Q. Nie, *Adaptive methods for stochastic differential equations via natural embeddings and rejection sampling with memory*, [Discrete & Continuous Dynamical Systems - B](#) **22**, 2731–2761 (2017).
- [507] B. Opanchuk and P. D. Drummond, *Functional wigner representation of quantum dynamics of bose-einstein condensate*, [Journal of Mathematical Physics](#) **54**, 042107 (2013).
- [508] A. I. Streltsov, O. E. Alon, and L. S. Cederbaum, *Formation and dynamics of many-boson fragmented states in one-dimensional attractive ultracold gases*, [Physical Review Letters](#) **100**, 130401 (2008).
- [509] P. Kinsler and P. D. Drummond, *Comment on "langevin equation for the squeezing of light by means of a parametric oscillator"*, [Physical Review A](#) **44**, 7848–7850 (1991).
- [510] L. I. Plimak, M. K. Olsen, M. Fleischhauer, and M. J. Collett, *Beyond the fokker-planck equation: stochastic simulation of complete wigner representation for the optical parametric oscillator*, [Europhysics Letters \(EPL\)](#) **56**, 372–378 (2001).
- [511] L. I. Plimak, M. Fleischhauer, M. K. Olsen, and M. J. Collett, *Quantum-field-theoretical techniques for stochastic representation of quantum problems*, [arXiv:cond-mat/0102483](#), [arXiv: cond-mat/0102483](#) (2001).
- [512] C. Bertulani, *Proceedings of the international workshop on collective excitations in fermi and bose systems : serra negra, são paulo, brazil, 14-17 september 1998* (World Scientific, Singapore River Edge, NJ, 1999).
- [513] A. Sinatra, C. Lobo, and Y. Castin, *Classical-field method for time dependent bose-einstein condensed gases*, [Physical Review Letters](#) **87**, 210404 (2001).
- [514] E. Witkowska, P. Deuar, M. Gajda, and K. Rzzewski, *Solitons as the early stage of quasicondensate formation during evaporative cooling*, [Physical Review Letters](#) **106**, 135301 (2011).
- [515] T. Karpiuk et al., *Spontaneous solitons in the thermal equilibrium of a quasi-1d bose gas*, [Physical Review Letters](#) **109**, 205302 (2012).
- [516] J. Javanainen and J. Ruostekoski, *Emergent classicality in continuous quantum measurements*, [New Journal of Physics](#) **15**, 013005 (2013).
- [517] M. D. Lee and J. Ruostekoski, *Classical stochastic measurement trajectories: bosonic atomic gases in an optical cavity and quantum measurement backaction*, [Physical Review A](#) **90**, 023628 (2014).
- [518] J. Schachenmayer, A. Pikovski, and A. Rey, *Many-body quantum spin dynamics with monte carlo trajectories on a discrete phase space*, [Physical Review X](#) **5**, 011022 (2015).
- [519] S. keng Ma, *Modern theory of critical phenomena* (Routledge, 2018).
- [520] N. Goldenfeld, *Lectures on phase transitions and the renormalization group* (CRC Press, 2018).

- [521] M. Morikawa, *Cosmological inflation as a quantum phase transition*, [Progress of Theoretical Physics](#) **93**, 685–709 (1995).
- [522] T. W. B. Kibble, *Topology of cosmic domains and strings*, [Journal of Physics A: Mathematical and General](#) **9**, 1387–1398 (1976).
- [523] T. Kibble, *Some implications of a cosmological phase transition*, [Physics Reports](#) **67**, 183–199 (1980).
- [524] W. H. Zurek, *Cosmological experiments in superfluid helium?*, [Nature](#) **317**, 505–508 (1985).
- [525] W. Zurek, *Cosmological experiments in condensed matter systems*, [Physics Reports](#) **276**, 177–221 (1996).
- [526] M. B. Hindmarsh and T. W. B. Kibble, *Cosmic strings*, [Reports on Progress in Physics](#) **58**, 477–562 (1995).
- [527] P. Ehrenfest, *Phasenumwandlungen im üblichen und erweiterten sinn, klassifiziert nach den entsprechenden singularitäten des thermodynamischen potenziales* (NV Noord-Hollandsche Uitgevers Maatschappij, 1933).
- [528] V. L. Berezinsky, *Destruction of long range order in one-dimensional and two-dimensional systems having a continuous symmetry group. I. Classical systems*, [Sov. Phys. JETP](#) **32**, 493–500 (1971).
- [529] J. M. Kosterlitz and D. J. Thouless, *Ordering, metastability and phase transitions in two-dimensional systems*, [Journal of Physics C: Solid State Physics](#) **6**, 1181–1203 (1973).
- [530] H.-Q. Ding and M. S. Makivić, *Kosterlitz-thouless transition in the two-dimensional quantumXYmodel*, [Physical Review B](#) **42**, 6827–6830 (1990).
- [531] S. Sachdev, *Quantum phase transitions*, 2nd ed. (Cambridge University Press, 2011).
- [532] S. L. Sondhi, S. M. Girvin, J. P. Carini, and D. Shahar, *Continuous quantum phase transitions*, [Reviews of Modern Physics](#) **69**, 315–333 (1997).
- [533] M. Vojta, *Quantum phase transitions*, [Reports on Progress in Physics](#) **66**, 2069–2110 (2003).
- [534] S. Sachdev and B. Keimer, *Quantum criticality*, [Physics Today](#) **64**, 29–35 (2011).
- [535] D. Belitz and T. Vojta, *How generic scale invariance influences quantum and classical phase transitions*, [Reviews of Modern Physics](#) **77**, 579–632 (2005).
- [536] A. Dutta et al., *Quantum phase transitions in transverse field spin models* (Cambridge University Press, 2015).
- [537] J. Dziarmaga, A. Smerzi, W. H. Zurek, and A. R. Bishop, *Dynamics of quantum phase transition in an array of josephson junctions*, [Physical Review Letters](#) **88**, 167001 (2002).
- [538] A. Polkovnikov, *Universal adiabatic dynamics in the vicinity of a quantum critical point*, [Physical Review B](#) **72**, 161201 (2005).
- [539] W. H. Zurek, U. Dorner, and P. Zoller, *Dynamics of a quantum phase transition*, [Physical Review Letters](#) **95**, 105701 (2005).

- [540] D. Chen, M. White, C. Borries, and B. DeMarco, *Quantum quench of an atomic mott insulator*, [Physical Review Letters](#) **106**, 235304 (2011).
- [541] M. Anquez et al., *Quantum kibble-zurek mechanism in a spin-1 bose-einstein condensate*, [Physical Review Letters](#) **116**, 155301 (2016).
- [542] L. W. Clark, L. Feng, and C. Chin, *Universal space-time scaling symmetry in the dynamics of bosons across a quantum phase transition*, [Science](#) **354**, 606–610 (2016).
- [543] G. Vidal, J. I. Latorre, E. Rico, and A. Kitaev, *Entanglement in quantum critical phenomena*, [Physical Review Letters](#) **90**, 227902 (2003).
- [544] U. Dorner et al., *Entangling strings of neutral atoms in 1d atomic pipeline structures*, [Physical Review Letters](#) **91**, 073601 (2003).
- [545] E. Farhi et al., *A quantum adiabatic evolution algorithm applied to random instances of an NP-complete problem*, [Science](#) **292**, 472–475 (2001).
- [546] R. Schützhold and G. Schaller, *Adiabatic quantum algorithms as quantum phase transitions: first versus second order*, [Physical Review A](#) **74**, 060304 (2006).
- [547] E. Kim and M. H. W. Chan, *Probable observation of a supersolid helium phase*, [Nature](#) **427**, 225–227 (2004).
- [548] D. Belitz and T. R. Kirkpatrick, *The anderson-mott transition*, [Reviews of Modern Physics](#) **66**, 261–380 (1994).
- [549] M. Z. Hasan and C. L. Kane, *Colloquium: topological insulators*, [Reviews of Modern Physics](#) **82**, 3045–3067 (2010).
- [550] A. Rosch, *Quantum phase transitions: introduction and some open problems*, in [Quantum theory from small to large scales](#) (Oxford University Press, 2012), pp. 411–428.
- [551] L.-Y. Qiu et al., *Observation of generalized kibble-zurek mechanism across a first-order quantum phase transition in a spinor condensate*, [Science Advances](#) **6**, 10.1126/sciadv.aba7292 (2020).
- [552] M. Heyl, *Dynamical quantum phase transitions: a review*, [Reports on Progress in Physics](#) **81**, 054001 (2018).
- [553] S. Biermann, L. de’Medici, and A. Georges, *Non-fermi-liquid behavior and double-exchange physics in orbital-selective mott systems*, [Physical Review Letters](#) **95**, 206401 (2005).
- [554] C. Maschler, I. B. Mekhov, and H. Ritsch, *Ultracold atoms in optical lattices generated by quantized light fields*, [The European Physical Journal D](#) **46**, 545–560 (2008).
- [555] J. Larson, B. Damski, G. Morigi, and M. Lewenstein, *Mott-insulator states of ultracold atoms in optical resonators*, [Physical Review Letters](#) **100**, 050401 (2008).
- [556] J. Larson, S. Fernández-Vidal, G. Morigi, and M. Lewenstein, *Quantum stability of mott-insulator states of ultracold atoms in optical resonators*, [New Journal of Physics](#) **10**, 045002 (2008).

- [557] M. J. Bhaseen, M. Hohenadler, A. O. Silver, and B. D. Simons, *Polaritons and pairing phenomena in bose-hubbard mixtures*, [Physical Review Letters](#) **102**, 135301 (2009).
- [558] A. O. Silver, M. Hohenadler, M. J. Bhaseen, and B. D. Simons, *Bose-hubbard models coupled to cavity light fields*, [Physical Review A](#) **81**, 023617 (2010).
- [559] S. F. Caballero-Benitez and I. B. Mekhov, *Quantum optical lattices for emergent many-body phases of ultracold atoms*, [Physical Review Letters](#) **115**, 243604 (2015).
- [560] M. Suzuki, *Relationship between d -dimensional quantal spin systems and $(d+1)$ -dimensional ising systems: equivalence, critical exponents and systematic approximations of the partition function and spin correlations*, [Progress of Theoretical Physics](#) **56**, 1454–1469 (1976).
- [561] P. Pfeuty, *The one-dimensional ising model with a transverse field*, [Annals of Physics](#) **57**, 79–90 (1970).
- [562] M. Campostrini, J. Nespola, A. Pelissetto, and E. Vicari, *Finite-size scaling at first-order quantum transitions*, [Physical Review Letters](#) **113**, 070402 (2014).
- [563] M. Campostrini, A. Pelissetto, and E. Vicari, *Finite-size scaling at quantum transitions*, [Physical Review B](#) **89**, 094516 (2014).
- [564] A. Pelissetto, D. Rossini, and E. Vicari, *Finite-size scaling at first-order quantum transitions when boundary conditions favor one of the two phases*, [Physical Review E](#) **98**, 032124 (2018).
- [565] M. Campostrini, A. Pelissetto, and E. Vicari, *Quantum transitions driven by one-bond defects in quantum ising rings*, [Physical Review E](#) **91**, 042123 (2015).
- [566] A. Pelissetto, D. Rossini, and E. Vicari, *Scaling properties of the dynamics at first-order quantum transitions when boundary conditions favor one of the two phases*, [Physical Review E](#) **102**, 012143 (2020).
- [567] J. Wu, L. Zhu, and Q. Si, *Crossovers and critical scaling in the one-dimensional transverse-field ising model*, [Physical Review B](#) **97**, 245127 (2018).
- [568] R. Jullien, P. Pfeuty, J. N. Fields, and S. Doniach, *Zero-temperature renormalization method for quantum systems. i. ising model in a transverse field in one dimension*, [Physical Review B](#) **18**, 3568–3578 (1978).
- [569] J. Wu, M. Kormos, and Q. Si, *Finite-temperature spin dynamics in a perturbed quantum critical ising chain with an E_8 symmetry*, [Physical Review Letters](#) **113**, 247201 (2014).
- [570] E. Barouch and B. M. McCoy, *Statistical mechanics of the XY Model. II. spin-correlation functions*, [Physical Review A](#) **3**, 786–804 (1971).
- [571] M. Suzuki, *Relationship among exactly soluble models of critical phenomena. i.*, [Progress of Theoretical Physics](#) **46**, 1337–1359 (1971).
- [572] A. Kopp and S. Chakravarty, *Criticality in correlated quantum matter*, [Nature Physics](#) **1**, 53–56 (2005).
- [573] Z. Wang et al., *Quantum criticality of an ising-like spin- $1/2$ antiferromagnetic chain in a transverse magnetic field*, [Physical Review Letters](#) **120**, 207205 (2018).

- [574] R. H. Dicke, *Coherence in spontaneous radiation processes*, [Physical Review](#) **93**, 99–110 (1954).
- [575] F. T. Hioe, *Phase transitions in some generalized dicke models of superradiance*, [Physical Review A](#) **8**, 1440–1445 (1973).
- [576] H. Carmichael, C. Gardiner, and D. Walls, *Higher order corrections to the dicke superradiant phase transition*, [Physics Letters A](#) **46**, 47–48 (1973).
- [577] G. C. Duncan, *Effect of antiresonant atom-field interactions on phase transitions in the dicke model*, [Physical Review A](#) **9**, 418–421 (1974).
- [578] Y. K. Wang and F. T. Hioe, *Phase transition in the dicke model of superradiance*, [Physical Review A](#) **7**, 831–836 (1973).
- [579] P. Nataf, T. Champel, G. Blatter, and D. M. Basko, *Rashba cavity QED: a route towards the superradiant quantum phase transition*, [Physical Review Letters](#) **123**, 207402 (2019).
- [580] P. Nataf and C. Ciuti, *No-go theorem for superradiant quantum phase transitions in cavity QED and counter-example in circuit QED*, [Nature Communications](#) **1**, 10.1038/ncomms1069 (2010).
- [581] H. v. Löhneysen, A. Rosch, M. Vojta, and P. Wölfle, *Fermi-liquid instabilities at magnetic quantum phase transitions*, [Reviews of Modern Physics](#) **79**, 1015–1075 (2007).
- [582] A. Rançon and N. Dupuis, *Quantum XY criticality in a two-dimensional bose gas near the mott transition*, [EPL \(Europhysics Letters\)](#) **104**, 16002 (2013).
- [583] M. Endres et al., *The ‘higgs’ amplitude mode at the two-dimensional superfluid/mott insulator transition*, [Nature](#) **487**, 454–458 (2012).
- [584] Z. Guguchia et al., *Multiple quantum phase transitions of different nature in the topological kagome magnet $\text{Co}_3\text{Sn}_2\text{-xIn}_x\text{S}_2$* , [npj Quantum Materials](#) **6**, 10.1038/s41535-021-00352-3 (2021).
- [585] S. I. Mukhin and N. V. Gnezdilov, *First-order dipolar phase transition in the dicke model with infinitely coordinated frustrating interaction*, [Physical Review A](#) **97**, 053809 (2018).
- [586] K. Hu and X. Wu, *First- and second-order quantum phase transitions in the one-dimensional transverse-field ising model with boundary fields*, [Physical Review B](#) **103**, 024409 (2021).
- [587] A. Trenkwalder et al., *Quantum phase transitions with parity-symmetry breaking and hysteresis*, [Nature Physics](#) **12**, 826–829 (2016).
- [588] V. Piazza et al., *First-order phase transitions in a quantum hall ferromagnet*, [Nature](#) **402**, 638–641 (1999).
- [589] J. A. Hertz, *Quantum critical phenomena*, [Physical Review B](#) **14**, 1165–1184 (1976).
- [590] M. Continentino, *Quantum scaling in many-body systems* (Cambridge University Press, 2017).
- [591] A. Kremen et al., *Imaging quantum fluctuations near criticality*, [Nature Physics](#) **14**, 1205–1210 (2018).

- [592] A Yuste, C Cartwright, G. D. Chiara, and A Sanpera, *Entanglement scaling at first order quantum phase transitions*, [New Journal of Physics](#) **20**, 043006 (2018).
- [593] D. Nagy, G. Szirmai, and P. Domokos, *Self-organization of a bose-einstein condensate in an optical cavity*, [The European Physical Journal D](#) **48**, 127–137 (2008).
- [594] D. N. Basov, R. D. Averitt, and D. Hsieh, *Towards properties on demand in quantum materials*, [Nature Materials](#) **16**, 1077–1088 (2017).
- [595] A. de la Torre et al., *Colloquium: nonthermal pathways to ultrafast control in quantum materials*, [Reviews of Modern Physics](#) **93**, 041002 (2021).
- [596] M. Uhlmann, R. Schützhold, and U. R. Fischer, *Vortex quantum creation and winding number scaling in a quenched spinor bose gas*, [Physical Review Letters](#) **99**, 120407 (2007).
- [597] A. Bermudez, D. Patanè, L. Amico, and M. A. Martin-Delgado, *Topology-induced anomalous defect production by crossing a quantum critical point*, [Physical Review Letters](#) **102**, 135702 (2009).
- [598] A. Polkovnikov, K. Sengupta, A. Silva, and M. Vengalattore, *Colloquium: nonequilibrium dynamics of closed interacting quantum systems*, [Reviews of Modern Physics](#) **83**, 863–883 (2011).
- [599] J. Dziarmaga and W. H. Zurek, *Quench in the 1d bose-hubbard model: topological defects and excitations from the kosterlitz-thouless phase transition dynamics*, [Scientific Reports](#) **4**, 10.1038/srep05950 (2014).
- [600] L. Chomaz et al., *Emergence of coherence via transverse condensation in a uniform quasi-two-dimensional bose gas*, [Nature Communications](#) **6**, 10.1038/ncomms7162 (2015).
- [601] J. Sonner, A. del Campo, and W. H. Zurek, *Universal far-from-equilibrium dynamics of a holographic superconductor*, [Nature Communications](#) **6**, 10.1038/ncomms8406 (2015).
- [602] B. Gardas, J. Dziarmaga, and W. H. Zurek, *Dynamics of the quantum phase transition in the one-dimensional bose-hubbard model: excitations and correlations induced by a quench*, [Physical Review B](#) **95**, 104306 (2017).
- [603] K. Shimizu, Y. Kuno, T. Hirano, and I. Ichinose, *Dynamics of a quantum phase transition in the bose-hubbard model: kibble-zurek mechanism and beyond*, [Physical Review A](#) **97**, 033626 (2018).
- [604] M. Heyl, A. Polkovnikov, and S. Kehrein, *Dynamical quantum phase transitions in the transverse-field ising model*, [Physical Review Letters](#) **110**, 135704 (2013).
- [605] N. Tsuji, M. Eckstein, and P. Werner, *Nonthermal antiferromagnetic order and nonequilibrium criticality in the hubbard model*, [Physical Review Letters](#) **110**, 136404 (2013).
- [606] F. Andraschko and J. Sirker, *Dynamical quantum phase transitions and the loschmidt echo: a transfer matrix approach*, [Physical Review B](#) **89**, 125120 (2014).

- [607] M. Heyl, *Dynamical quantum phase transitions in systems with broken-symmetry phases*, [Physical Review Letters](#) **113**, 205701 (2014).
- [608] M. Heyl, *Scaling and universality at dynamical quantum phase transitions*, [Physical Review Letters](#) **115**, 140602 (2015).
- [609] J. C. Budich and M. Heyl, *Dynamical topological order parameters far from equilibrium*, [Physical Review B](#) **93**, 085416 (2016).
- [610] Z. Huang and A. V. Balatsky, *Dynamical quantum phase transitions: role of topological nodes in wave function overlaps*, [Physical Review Letters](#) **117**, 086802 (2016).
- [611] A. A. Zvyagin, *Dynamical quantum phase transitions (review article)*, [Low Temperature Physics](#) **42**, 971–994 (2016).
- [612] S. Sharma, U. Divakaran, A. Polkovnikov, and A. Dutta, *Slow quenches in a quantum ising chain: dynamical phase transitions and topology*, [Physical Review B](#) **93**, 144306 (2016).
- [613] C. Karrasch and D. Schuricht, *Dynamical quantum phase transitions in the quantum potts chain*, [Physical Review B](#) **95**, 075143 (2017).
- [614] L. Zhou, Q. hai Wang, H. Wang, and J. Gong, *Dynamical quantum phase transitions in non-hermitian lattices*, [Physical Review A](#) **98**, 022129 (2018).
- [615] H. Bernien et al., *Probing many-body dynamics on a 51-atom quantum simulator*, [Nature](#) **551**, 579–584 (2017).
- [616] N. Fläschner et al., *Observation of dynamical vortices after quenches in a system with topology*, [Nature Physics](#) **14**, 265–268 (2017).
- [617] P. Jurcevic et al., *Direct observation of dynamical quantum phase transitions in an interacting many-body system*, [Physical Review Letters](#) **119**, 080501 (2017).
- [618] J. Zhang et al., *Observation of a many-body dynamical phase transition with a 53-qubit quantum simulator*, [Nature](#) **551**, 601–604 (2017).
- [619] S. Smale et al., *Observation of a transition between dynamical phases in a quantum degenerate fermi gas*, [Science Advances](#) **5**, 10.1126/sciadv.aax1568 (2019).
- [620] T. Tian et al., *Observation of dynamical phase transitions in a topological nanomechanical system*, [Physical Review B](#) **100**, 024310 (2019).
- [621] K. Wang et al., *Simulating dynamic quantum phase transitions in photonic quantum walks*, [Physical Review Letters](#) **122**, 020501 (2019).
- [622] X.-Y. Guo et al., *Observation of a dynamical quantum phase transition by a superconducting qubit simulation*, [Physical Review Applied](#) **11**, 044080 (2019).
- [623] J. A. Muniz et al., *Exploring dynamical phase transitions with cold atoms in an optical cavity*, [Nature](#) **580**, 602–607 (2020).
- [624] M. J. Hartmann, *Quantum simulation with interacting photons*, [Journal of Optics](#) **18**, 104005 (2016).
- [625] C. Noh and D. G. Angelakis, *Quantum simulations and many-body physics with light*, [Reports on Progress in Physics](#) **80**, 016401 (2016).

- [626] A. Mitra and A. J. Millis, *Coulomb gas on the keldysh contour: anderson-yuval-hamann representation of the nonequilibrium two-level system*, [Physical Review B **76**, 085342 \(2007\)](#).
- [627] A. Mitra and A. J. Millis, *Current-driven quantum criticality in itinerant electron ferromagnets*, [Physical Review B **77**, 220404 \(2008\)](#).
- [628] A. Mitra and A. J. Millis, *Current-driven defect-unbinding transition in an XY-ferromagnet*, [Physical Review B **84**, 054458 \(2011\)](#).
- [629] S. Ajisaka, F. Barra, and B. Žunkovič, *Nonequilibrium quantum phase transitions in the XY model: comparison of unitary time evolution and reduced density operator approaches*, [New Journal of Physics **16**, 033028 \(2014\)](#).
- [630] G. Dagvadorj et al., *Nonequilibrium phase transition in a two-dimensional driven open quantum system*, [Physical Review X **5**, 041028 \(2015\)](#).
- [631] C. Klöckner, C. Karrasch, and D. Kennes, *Nonequilibrium properties of berezinskii-kosterlitz-thouless phase transitions*, [Physical Review Letters **125**, 147601 \(2020\)](#).
- [632] P. Digregorio et al., *Full phase diagram of active brownian disks: from melting to motility-induced phase separation*, [Physical Review Letters **121**, 098003 \(2018\)](#).
- [633] L. F. Cugliandolo, P. Digregorio, G. Gonnella, and A. Suma, *Phase coexistence in two-dimensional passive and active dumbbell systems*, [Physical Review Letters **119**, 268002 \(2017\)](#).
- [634] A. Zamora et al., *Tuning across universalities with a driven open condensate*, [Physical Review X **7**, 041006 \(2017\)](#).
- [635] R. Hanai, A. Edelman, Y. Ohashi, and P. B. Littlewood, *Non-hermitian phase transition from a polariton bose-einstein condensate to a photon laser*, [Physical Review Letters **122**, 185301 \(2019\)](#).
- [636] J. Keeling, F. M. Marchetti, M. H. Szymańska, and P. B. Littlewood, *Collective coherence in planar semiconductor microcavities*, [Semiconductor Science and Technology **22**, R1–R26 \(2007\)](#).
- [637] F. Dimer, B. Estienne, A. S. Parkins, and H. J. Carmichael, *Proposed realization of the dicke-model quantum phase transition in an optical cavity QED system*, [Physical Review A **75**, 013804 \(2007\)](#).
- [638] A. Amo and J. Bloch, *Exciton-polaritons in lattices: a non-linear photonic simulator*, [Comptes Rendus Physique **17**, 934–945 \(2016\)](#).
- [639] H. Ritsch, P. Domokos, F. Brennecke, and T. Esslinger, *Cold atoms in cavity-generated dynamical optical potentials*, [Reviews of Modern Physics **85**, 553–601 \(2013\)](#).
- [640] J. Li et al., *Observation of parity-time symmetry breaking transitions in a dissipative floquet system of ultracold atoms*, [Nature Communications **10**, 10.1038/s41467-019-08596-1 \(2019\)](#).
- [641] T. Feldker et al., *Buffer gas cooling of a trapped ion to the quantum regime*, [Nature Physics **16**, 413–416 \(2020\)](#).
- [642] A. Tomadin and R. Fazio, *Many-body phenomena in QED-cavity arrays [invited]*, [Journal of the Optical Society of America B **27**, A130 \(2010\)](#).

- [643] A. A. Houck, H. E. Türeci, and J. Koch, *On-chip quantum simulation with superconducting circuits*, [Nature Physics](#) **8**, 292–299 (2012).
- [644] S. Schmidt and J. Koch, *Circuit QED lattices: towards quantum simulation with superconducting circuits*, [Annalen der Physik](#) **525**, 395–412 (2013).
- [645] R. Labouvie, B. Santra, S. Heun, and H. Ott, *Bistability in a driven-dissipative superfluid*, [Physical Review Letters](#) **116**, 235302 (2016).
- [646] M. Raghunandan, J. Wrachtrup, and H. Weimer, *High-density quantum sensing with dissipative first order transitions*, [Physical Review Letters](#) **120**, 150501 (2018).
- [647] T. L. Heugel, M. Biondi, O. Zilberberg, and R. Chitra, *Quantum transducer using a parametric driven-dissipative phase transition*, [Physical Review Letters](#) **123**, 173601 (2019).
- [648] C. Lledó, T. K. Mavrogordatos, and M. H. Szymańska, *Driven bose-hubbard dimer under nonlocal dissipation: a bistable time crystal*, [Physical Review B](#) **100**, 054303 (2019).
- [649] H. M. Gibbs, S. L. McCall, and T. N. C. Venkatesan, *Differential gain and bistability using a sodium-filled fabry-perot interferometer*, [Physical Review Letters](#) **36**, 1135–1138 (1976).
- [650] S. V. Lawande, R. R. Puri, and S. S. Hassan, *Non-resonant effects in the fluorescent dicke model. i. exact steady state analysis*, [Journal of Physics B: Atomic and Molecular Physics](#) **14**, 4171–4189 (1981).
- [651] R. Puri, S. Lawande, and S. Hassan, *Dispersion in the driven dicke model*, [Optics Communications](#) **35**, 179–184 (1980).
- [652] R. Bonifacio and L. A. Lugiato, *Optical bistability and cooperative effects in resonance fluorescence*, [Physical Review A](#) **18**, 1129–1144 (1978).
- [653] S. Schneider and G. J. Milburn, *Entanglement in the steady state of a collective-angular-momentum (dicke) model*, [Physical Review A](#) **65**, 042107 (2002).
- [654] M. R. Evans, *Phase transitions in one-dimensional nonequilibrium systems*, [Brazilian Journal of Physics](#) **30**, 42–57 (2000).
- [655] R. Bonifacio and L. Lugiato, *Cooperative effects and bistability for resonance fluorescence*, [Optics Communications](#) **19**, 172–176 (1976).
- [656] R. Bonifacio and L. A. Lugiato, *Photon statistics and spectrum of transmitted light in optical bistability*, [Physical Review Letters](#) **40**, 1023–1027 (1978).
- [657] R. Roy and L. Mandel, *Optical bistability and first order phase transition in a ring dye laser*, [Optics Communications](#) **34**, 133–136 (1980).
- [658] L. A. Lugiato, *II theory of optical bistability*, in [Progress in optics](#) (Elsevier, 1984), pp. 69–216.
- [659] H. Gibbs, *Optical bistability : controlling light with light* (Academic Press, Orlando, 1985).
- [660] H. Risken, C. Savage, F. Haake, and D. F. Walls, *Quantum tunneling in dispersive optical bistability*, [Physical Review A](#) **35**, 1729–1739 (1987).

- [661] K. Vogel and H. Risken, *Quantum-tunneling rates and stationary solutions in dispersive optical bistability*, [Physical Review A **38**, 2409–2422 \(1988\)](#).
- [662] H. Risken and K. Vogel, *Quantum tunneling rates in dispersive optical bistability for low cavity damping*, [Physical Review A **38**, 1349–1357 \(1988\)](#).
- [663] A. Baas, J. P. Karr, H. Eleuch, and E. Giacobino, *Optical bistability in semiconductor microcavities*, [Physical Review A **69**, 023809 \(2004\)](#).
- [664] D. Bajoni et al., *Optical bistability in a GaAs-based polariton diode*, [Physical Review Letters **101**, 266402 \(2008\)](#).
- [665] T. K. Paraíso et al., *Multistability of a coherent spin ensemble in a semiconductor microcavity*, [Nature Materials **9**, 655–660 \(2010\)](#).
- [666] J. Kerckhoff, M. A. Armen, and H. Mabuchi, *Remnants of semiclassical bistability in the few-photon regime of cavity QED*, [Optics Express **19**, 24468 \(2011\)](#).
- [667] H. Mabuchi, *Coherent-feedback control strategy to suppress spontaneous switching in ultralow power optical bistability*, [Applied Physics Letters **98**, 193109 \(2011\)](#).
- [668] T. E. Lee, H. Häffner, and M. C. Cross, *Antiferromagnetic phase transition in a nonequilibrium lattice of rydberg atoms*, [Physical Review A **84**, 031402 \(2011\)](#).
- [669] F. R. Ong et al., *Circuit QED with a nonlinear resonator: ac-stark shift and dephasing*, [Physical Review Letters **106**, 167002 \(2011\)](#).
- [670] F. Nissen et al., *Nonequilibrium dynamics of coupled qubit-cavity arrays*, [Physical Review Letters **108**, 233603 \(2012\)](#).
- [671] A. Dombi, A. Vukics, and P. Domokos, *Optical bistability in strong-coupling cavity QED with a few atoms*, [Journal of Physics B: Atomic, Molecular and Optical Physics **46**, 224010 \(2013\)](#).
- [672] C. Carr et al., *Nonequilibrium phase transition in a dilute rydberg ensemble*, [Physical Review Letters **111**, 113901 \(2013\)](#).
- [673] M. Marcuzzi et al., *Universal nonequilibrium properties of dissipative rydberg gases*, [Physical Review Letters **113**, 210401 \(2014\)](#).
- [674] J. Jin et al., *Steady-state phase diagram of a driven QED-cavity array with cross-kerr nonlinearities*, [Physical Review A **90**, 023827 \(2014\)](#).
- [675] A. L. Boité, G. Orso, and C. Ciuti, *Bose-hubbard model: relation between driven-dissipative steady states and equilibrium quantum phases*, [Physical Review A **90**, 063821 \(2014\)](#).
- [676] I. Siddiqi et al., *RF-driven josephson bifurcation amplifier for quantum measurement*, [Physical Review Letters **93**, 207002 \(2004\)](#).
- [677] H. Abbaspour et al., *Stochastic resonance in collective exciton-polariton excitations inside a GaAs microcavity*, [Physical Review Letters **113**, 057401 \(2014\)](#).
- [678] W. Casteels et al., *Truncated correlation hierarchy schemes for driven-dissipative multimode quantum systems*, [New Journal of Physics **18**, 093007 \(2016\)](#).
- [679] V. Popkov and T. Prosen, *Infinitely dimensional lax structure for the one-dimensional hubbard model*, [Physical Review Letters **114**, 127201 \(2015\)](#).

- [680] E. Ilievski and T. Prosen, *Exact steady state manifold of a boundary driven spin-1 lai–sutherland chain*, [Nuclear Physics B](#) **882**, 485–500 (2014).
- [681] H. Pichler, A. J. Daley, and P. Zoller, *Nonequilibrium dynamics of bosonic atoms in optical lattices: decoherence of many-body states due to spontaneous emission*, [Physical Review A](#) **82**, 063605 (2010).
- [682] J. K. Freericks, V. M. Turkowski, and V. Zlatić, *Nonequilibrium dynamical mean-field theory*, [Physical Review Letters](#) **97**, 266408 (2006).
- [683] H. Aoki et al., *Nonequilibrium dynamical mean-field theory and its applications*, [Reviews of Modern Physics](#) **86**, 779–837 (2014).
- [684] D. M. Ceperley, *Path integrals in the theory of condensed helium*, [Reviews of Modern Physics](#) **67**, 279–355 (1995).
- [685] T. E. Lee, H. Häffner, and M. C. Cross, *Collective quantum jumps of rydberg atoms*, [Physical Review Letters](#) **108**, 023602 (2012).
- [686] A. Tomadin, S. Diehl, and P. Zoller, *Nonequilibrium phase diagram of a driven and dissipative many-body system*, [Physical Review A](#) **83**, 013611 (2011).
- [687] M. H. Szymańska, J. Keeling, and P. B. Littlewood, *Mean-field theory and fluctuation spectrum of a pumped decaying bose-fermi system across the quantum condensation transition*, [Physical Review B](#) **75**, 195331 (2007).
- [688] H. Weimer, *Variational principle for steady states of dissipative quantum many-body systems*, [Physical Review Letters](#) **114**, 040402 (2015).
- [689] H. Weimer, *Variational analysis of driven-dissipative rydberg gases*, [Physical Review A](#) **91**, 063401 (2015).
- [690] M. Hoening, W. Abdussalam, M. Fleischhauer, and T. Pohl, *Antiferromagnetic long-range order in dissipative rydberg lattices*, [Physical Review A](#) **90**, 021603 (2014).
- [691] T. Prosen and T. H. Seligman, *Quantization over boson operator spaces*, [Journal of Physics A: Mathematical and Theoretical](#) **43**, 392004 (2010).
- [692] W. D. Heiss, *The physics of exceptional points*, [Journal of Physics A: Mathematical and Theoretical](#) **45**, 444016 (2012).
- [693] R. El-Ganainy et al., *Non-hermitian physics and PT symmetry*, [Nature Physics](#) **14**, 11–19 (2018).
- [694] F. Wilczek, *Quantum time crystals*, [Physical Review Letters](#) **109**, 160401 (2012).
- [695] A. Shapere and F. Wilczek, *Classical time crystals*, [Physical Review Letters](#) **109**, 160402 (2012).
- [696] J. Zhang et al., *Observation of a discrete time crystal*, [Nature](#) **543**, 217–220 (2017).
- [697] S. Choi et al., *Observation of discrete time-crystalline order in a disordered dipolar many-body system*, [Nature](#) **543**, 221–225 (2017).
- [698] D. V. Else, B. Bauer, and C. Nayak, *Floquet time crystals*, [Physical Review Letters](#) **117**, 090402 (2016).

- [699] W. W. Ho, S. Choi, M. D. Lukin, and D. A. Abanin, *Critical time crystals in dipolar systems*, [Physical Review Letters](#) **119**, 010602 (2017).
- [700] N. Yao, A. Potter, I.-D. Potirniche, and A. Vishwanath, *Discrete time crystals: rigidity, criticality, and realizations*, [Physical Review Letters](#) **118**, 030401 (2017).
- [701] R. Nandkishore and D. A. Huse, *Many-body localization and thermalization in quantum statistical mechanics*, [Annual Review of Condensed Matter Physics](#) **6**, 15–38 (2015).
- [702] L. D’Alessio and M. Rigol, *Long-time behavior of isolated periodically driven interacting lattice systems*, [Physical Review X](#) **4**, 041048 (2014).
- [703] A. Lazarides, A. Das, and R. Moessner, *Equilibrium states of generic quantum systems subject to periodic driving*, [Physical Review E](#) **90**, 012110 (2014).
- [704] P. Ponte, A. Chandran, Z. Papić, and D. A. Abanin, *Periodically driven ergodic and many-body localized quantum systems*, [Annals of Physics](#) **353**, 196–204 (2015).
- [705] V. Khemani, A. Lazarides, R. Moessner, and S. Sondhi, *Phase structure of driven quantum systems*, [Physical Review Letters](#) **116**, 250401 (2016).
- [706] C. W. von Keyserlingk, V. Khemani, and S. L. Sondhi, *Absolute stability and spatiotemporal long-range order in floquet systems*, [Physical Review B](#) **94**, 085112 (2016).
- [707] A. Russomanno, F. Iemini, M. Dalmonte, and R. Fazio, *Floquet time crystal in the lipkin-meshkov-glick model*, [Physical Review B](#) **95**, 214307 (2017).
- [708] B. Huang, Y.-H. Wu, and W. V. Liu, *Clean floquet time crystals: models and realizations in cold atoms*, [Physical Review Letters](#) **120**, 110603 (2018).
- [709] Z. Gong, R. Hamazaki, and M. Ueda, *Discrete time-crystalline order in cavity and circuit QED systems*, [Physical Review Letters](#) **120**, 040404 (2018).
- [710] A. Lazarides, S. Roy, F. Piazza, and R. Moessner, *Time crystallinity in dissipative floquet systems*, [Physical Review Research](#) **2**, 022002 (2020).
- [711] F. Gambetta et al., *Discrete time crystals in the absence of manifest symmetries or disorder in open quantum systems*, [Physical Review Letters](#) **122**, 015701 (2019).
- [712] N. Y. Yao, C. Nayak, L. Balents, and M. P. Zaletel, *Classical discrete time crystals*, [Nature Physics](#) **16**, 438–447 (2020).
- [713] K. Mizuta, K. Takasan, M. Nakagawa, and N. Kawakami, *Spatial-translation-induced discrete time crystals*, [Physical Review Letters](#) **121**, 093001 (2018).
- [714] A. Pizzi, J. Knolle, and A. Nunnenkamp, *Period- n discrete time crystals and quasicrystals with ultracold bosons*, [Physical Review Letters](#) **123**, 150601 (2019).
- [715] A. Pizzi, J. Knolle, and A. Nunnenkamp, *Higher-order and fractional discrete time crystals in clean long-range interacting systems*, [Nature Communications](#) **12**, 10.1038/s41467-021-22583-5 (2021).
- [716] B. Zhu et al., *Dicke time crystals in driven-dissipative quantum many-body systems*, [New Journal of Physics](#) **21**, 073028 (2019).

- [717] F. M. Surace et al., *Floquet time crystals in clock models*, [Physical Review B](#) **99**, 104303 (2019).
- [718] F. M. Gambetta et al., *Classical stochastic discrete time crystals*, [Physical Review E](#) **100**, 060105 (2019).
- [719] A. Russomanno et al., *Homogeneous floquet time crystal protected by gauge invariance*, [Physical Review Research](#) **2**, 012003 (2020).
- [720] J. Rovny, R. L. Blum, and S. E. Barrett, *Observation of discrete-time-crystal signatures in an ordered dipolar many-body system*, [Physical Review Letters](#) **120**, 180603 (2018).
- [721] S. Pal, N. Nishad, T. Mahesh, and G. Sreejith, *Temporal order in periodically driven spins in star-shaped clusters*, [Physical Review Letters](#) **120**, 180602 (2018).
- [722] B. Buča, J. Tindall, and D. Jaksch, *Non-stationary coherent quantum many-body dynamics through dissipation*, [Nature Communications](#) **10**, 1730 (2019).
- [723] R. Chitra and O. Zilberberg, *Dynamical many-body phases of the parametrically driven, dissipative dicke model*, [Physical Review A](#) **92**, 023815 (2015).
- [724] C.-K. Chan, T. E. Lee, and S. Gopalakrishnan, *Limit-cycle phase in driven-dissipative spin systems*, [Physical Review A](#) **91**, 051601 (2015).
- [725] E. I. R. Chiacchio and A. Nunnenkamp, *Dissipation-induced instabilities of a spinor bose-einstein condensate inside an optical cavity*, [Phys. Rev. Lett.](#) **122**, 193605 (2019).
- [726] D. Barberena, R. J. Lewis-Swan, J. K. Thompson, and A. M. Rey, *Driven-dissipative quantum dynamics in ultra-long-lived dipoles in an optical cavity*, [Phys. Rev. A](#) **99**, 053411 (2019).
- [727] J. G. Cosme, J. Skulte, and L. Mathey, *Time crystals in a shaken atom-cavity system*, [Physical Review A](#) **100**, 053615 (2019).
- [728] N. Dogra et al., *Dissipation-induced structural instability and chiral dynamics in a quantum gas*, [Science](#) **366**, 1496–1499 (2019).
- [729] P. Zupancic et al., *P -band induced self-organization and dynamics with repulsively driven ultracold atoms in an optical cavity*, [Physical Review Letters](#) **123**, 233601 (2019).
- [730] B. Buča and D. Jaksch, *Dissipation induced nonstationarity in a quantum gas*, [Physical Review Letters](#) **123**, 260401 (2019).
- [731] A. Riera-Campenya, M. Moreno-Cardoner, and A. Sanpera, *Time crystallinity in open quantum systems*, [Quantum](#) **4**, 270 (2020).
- [732] K. Tucker et al., *Shattered time: can a dissipative time crystal survive many-body correlations?*, [New Journal of Physics](#) **20**, 123003 (2018).
- [733] O. Scarlatella, R. Fazio, and M. Schiró, *Emergent finite frequency criticality of driven-dissipative correlated lattice bosons*, [Physical Review B](#) **99**, 064511 (2019).
- [734] H. Keßler et al., *Emergent limit cycles and time crystal dynamics in an atom-cavity system*, [Physical Review A](#) **99**, 053605 (2019).

- [735] M. Marconi et al., *Mesoscopic limit cycles in coupled nanolasers*, [Physical Review Letters](#) **124**, 213602 (2020).
- [736] C. Lledó and M. H. Szymańska, *A dissipative time crystal with or without z_2 symmetry breaking*, [New Journal of Physics](#) **22**, 075002 (2020).
- [737] G. Kónya, D. Nagy, G. Szirmai, and P. Domokos, *Nonequilibrium polariton dynamics in a bose-einstein condensate coupled to an optical cavity*, [Physical Review A](#) **98**, 063608 (2018).
- [738] M. Soriente, T. Donner, R. Chitra, and O. Zilberberg, *Dissipation-induced anomalous multicritical phenomena*, [Physical Review Letters](#) **120**, 183603 (2018).
- [739] M. Hongo, S. Kim, T. Noumi, and A. Ota, *Effective field theory of time-translational symmetry breaking in nonequilibrium open system*, [Journal of High Energy Physics](#) **2019**, 10.1007/jhep02(2019)131 (2019).
- [740] J. Fan, G. Chen, and S. Jia, *Atomic self-organization emerging from tunable quadrature coupling*, [Physical Review A](#) **101**, 063627 (2020).
- [741] H. Keßler et al., *From a continuous to a discrete time crystal in a dissipative atom-cavity system*, [New Journal of Physics](#) **22**, 085002 (2020).
- [742] K. Nakatsugawa, T. Fujii, and S. Tanda, *Quantum time crystal by decoherence: proposal with an incommensurate charge density wave ring*, [Physical Review B](#) **96**, 094308 (2017).
- [743] R. R. W. Wang, B. Xing, G. G. Carlo, and D. Poletti, *Period doubling in period-one steady states*, [Physical Review E](#) **97**, 020202 (2018).
- [744] E. T. Owen et al., *Quantum correlations and limit cycles in the driven-dissipative heisenberg lattice*, [New Journal of Physics](#) **20**, 045004 (2018).
- [745] J. O’Sullivan et al., *Dissipative discrete time crystals*, [arXiv:1807.09884 \[cond-mat, physics:quant-ph\]](#), [arXiv: 1807.09884 version: 2](#) (2019).
- [746] C. S. Muñoz et al., *Non-stationary dynamics and dissipative freezing in squeezed superradiance*, 2019.
- [747] A. V. Nalitov et al., *Optically trapped polariton condensates as semiclassical time crystals*, [Physical Review A](#) **99**, 033830 (2019).
- [748] K. Chinzei and T. N. Ikeda, *Time crystals protected by floquet dynamical symmetry in hubbard models*, [Physical Review Letters](#) **125**, 060601 (2020).
- [749] H. Keßler et al., *Observation of a dissipative time crystal*, [Physical Review Letters](#) **127**, 043602 (2021).
- [750] C. S. Muñoz et al., *Non-stationary dynamics and dissipative freezing in squeezed superradiance*, 2019.
- [751] P. Nozières, *Time crystals: can diamagnetic currents drive a charge density wave into rotation?*, [EPL \(Europhysics Letters\)](#) **103**, 57008 (2013).
- [752] P. Bruno, *Impossibility of spontaneously rotating time crystals: a no-go theorem*, [Physical Review Letters](#) **111**, 070402 (2013).
- [753] T. Li et al., *Space-time crystals of trapped ions*, [Physical Review Letters](#) **109**, 163001 (2012).

- [754] P. Bruno, *Comment on “quantum time crystals”*, [Physical Review Letters](#) **110**, 118901 (2013).
- [755] H. Watanabe and M. Oshikawa, *Absence of quantum time crystals*, [Physical Review Letters](#) **114**, 251603 (2015).
- [756] K. Sacha, *Modeling spontaneous breaking of time-translation symmetry*, [Physical Review A](#) **91**, 033617 (2015).
- [757] D. V. Else, B. Bauer, and C. Nayak, *Prethermal phases of matter protected by time-translation symmetry*, [Physical Review X](#) **7**, 011026 (2017).
- [758] F. Machado et al., *Long-range prethermal phases of nonequilibrium matter*, [Physical Review X](#) **10**, 011043 (2020).
- [759] T.-S. Zeng and D. N. Sheng, *Prethermal time crystals in a one-dimensional periodically driven floquet system*, [Physical Review B](#) **96**, 094202 (2017).
- [760] S. Basak, K. A. Dahmen, and E. W. Carlson, *Period multiplication cascade at the order-by-disorder transition in uniaxial random field XY magnets*, [Nature Communications](#) **11**, 10.1038/s41467-020-18270-6 (2020).
- [761] K. Giergiel et al., *Topological time crystals*, [New Journal of Physics](#) **21**, 052003 (2019).
- [762] A. Chew, D. F. Mross, and J. Alicea, *Time-crystalline topological superconductors*, [Physical Review Letters](#) **124**, 096802 (2020).
- [763] J. O’Sullivan et al., *Signatures of discrete time crystalline order in dissipative spin ensembles*, [New Journal of Physics](#) **22**, 085001 (2020).
- [764] P. Nurwantoro, R. W. Bomantara, and J. Gong, *Discrete time crystals in many-body quantum chaos*, [Physical Review B](#) **100**, 214311 (2019).
- [765] K. Sacha, *Time crystals* (Springer International Publishing, 2020).
- [766] D. V. Else, C. Monroe, C. Nayak, and N. Y. Yao, *Discrete time crystals*, [Annual Review of Condensed Matter Physics](#) **11**, 467–499 (2020).
- [767] H. Watanabe, M. Oshikawa, and T. Koma, *Proof of the absence of long-range temporal orders in gibbs states*, [Journal of Statistical Physics](#) **178**, 926–935 (2020).
- [768] V. K. Kozin and O. Kyriienko, *Quantum time crystals from hamiltonians with long-range interactions*, [Physical Review Letters](#) **123**, 210602 (2019).
- [769] P. Öhberg and E. M. Wright, *Quantum time crystals and interacting gauge theories in atomic bose-einstein condensates*, [Physical Review Letters](#) **123**, 250402 (2019).
- [770] V. Khemani, R. Moessner, and S. L. Sondhi, *Comment on “Quantum Time Crystals from Hamiltonians with Long-Range Interactions”*, arXiv e-prints, arXiv:2001.11037, arXiv:2001.11037 (2020).
- [771] V. K. Kozin and O. Kyriienko, *Reply to “comment on “quantum time crystals from hamiltonians with long-range interactions”*”, 2020.
- [772] A. Syrwid, A. Kosior, and K. Sacha, *Comment on “quantum time crystals and interacting gauge theories in atomic bose-einstein condensates”*, [Physical Review Letters](#) **124**, 178901 (2020).

- [773] A. Syrwid, A. Kosior, and K. Sacha, *Lack of a genuine time crystal in a chiral soliton model*, [Physical Review Research](#) **2**, 032038 (2020).
- [774] P. Richerme, *How to Create a Time Crystal*, en, [Physics](#) **10**, 5 (2017).
- [775] E. Gibney, *The quest to crystallize time*, [Nature](#) **543**, 164–166 (2017).
- [776] M. P. Estarellas et al., *Simulating complex quantum networks with time crystals*, [Science Advances](#) **6**, 10.1126/sciadv.aay8892 (2020).
- [777] X. Mi et al., *Time-crystalline eigenstate order on a quantum processor*, [Nature](#) **601**, 531–536 (2021).
- [778] *Ask a Techspert: What exactly is a time crystal?*, en-us, Nov. 2021.
- [779] N. Shammah et al., *Open quantum systems with local and collective incoherent processes: efficient numerical simulations using permutational invariance*, [Physical Review A](#) **98**, 063815 (2018).
- [780] M. R. Hush et al., *Spin correlations as a probe of quantum synchronization in trapped-ion phonon lasers*, [Physical Review A](#) **91**, 061401 (2015).
- [781] P. Rotondo et al., *Open quantum generalisation of hopfield neural networks*, [Journal of Physics A: Mathematical and Theoretical](#) **51**, 115301 (2018).
- [782] F. Storme, “Dissipative phase transitions in open quantum lattice systems”, en, PhD thesis (Université Paris Diderot (Paris 7), Sorbonne Paris Cité, Nov. 2017).
- [783] X. H. H. Zhang, *Dynamics of Open Quantum Systems: Measurement, Entanglement, and Criticality*, en, (2020).
- [784] R. Holzwarth et al., *Optical frequency synthesizer for precision spectroscopy*, [Physical Review Letters](#) **85**, 2264–2267 (2000).
- [785] D. J. Jones et al., *Carrier-envelope phase control of femtosecond mode-locked lasers and direct optical frequency synthesis*, [Science](#) **288**, 635–639 (2000).
- [786] T. Udem, R. Holzwarth, and T. W. Hänsch, *Optical frequency metrology*, [Nature](#) **416**, 233–237 (2002).
- [787] S. T. Cundiff and J. Ye, *Colloquium: femtosecond optical frequency combs*, [Reviews of Modern Physics](#) **75**, 325–342 (2003).
- [788] A. V. Muraviev, V. O. Smolski, Z. E. Loparo, and K. L. Vodopyanov, *Massively parallel sensing of trace molecules and their isotopologues with broadband sub-harmonic mid-infrared frequency combs*, [Nature Photonics](#) **12**, 209–214 (2018).
- [789] S. Miller et al., *On-chip frequency comb generation at visible wavelengths via simultaneous second- and third-order optical nonlinearities*, [Optics Express](#) **22**, 26517 (2014).
- [790] C. Gohle et al., *A frequency comb in the extreme ultraviolet*, [Nature](#) **436**, 234–237 (2005).
- [791] G. Porat et al., *Phase-matched extreme-ultraviolet frequency-comb generation*, [Nature Photonics](#) **12**, 387–391 (2018).
- [792] R. J. Jones, K. D. Moll, M. J. Thorpe, and J. Ye, *Phase-coherent frequency combs in the vacuum ultraviolet via high-harmonic generation inside a femtosecond enhancement cavity*, [Physical Review Letters](#) **94**, 193201 (2005).

- [793] S. A. Diddams et al., *Direct link between microwave and optical frequencies with a 300 THz femtosecond laser comb*, [Physical Review Letters](#) **84**, 5102–5105 (2000).
- [794] J. Reichert et al., *Phase coherent vacuum-ultraviolet to radio frequency comparison with a mode-locked laser*, [Physical Review Letters](#) **84**, 3232–3235 (2000).
- [795] J. K. Ranka, R. S. Windeler, and A. J. Stentz, *Visible continuum generation in air–silica microstructure optical fibers with anomalous dispersion at 800 nm*, [Optics Letters](#) **25**, 25 (2000).
- [796] T. Fortier and E. Baumann, *20 years of developments in optical frequency comb technology and applications*, [Communications Physics](#) **2**, 10.1038/s42005-019-0249-y (2019).
- [797] N. R. Newbury, *Searching for applications with a fine-tooth comb*, [Nature Photonics](#) **5**, 186–188 (2011).
- [798] T. W. Hänsch, *Nobel lecture: passion for precision*, [Reviews of Modern Physics](#) **78**, 1297–1309 (2006).
- [799] M.-G. Suh et al., *Microresonator soliton dual-comb spectroscopy*, [Science](#) **354**, 600–603 (2016).
- [800] M. Yu et al., *Silicon-chip-based mid-infrared dual-comb spectroscopy*, [Nature Communications](#) **9**, 10.1038/s41467-018-04350-1 (2018).
- [801] J. Pfeifle et al., *Optimally coherent kerr combs generated with crystalline whispering gallery mode resonators for ultrahigh capacity fiber communications*, [Physical Review Letters](#) **114**, 093902 (2015).
- [802] P. Marin-Palomo et al., *Microresonator-based solitons for massively parallel coherent optical communications*, [Nature](#) **546**, 274–279 (2017).
- [803] W. Liang et al., *High spectral purity kerr frequency comb radio frequency photonic oscillator*, [Nature Communications](#) **6**, 10.1038/ncomms8957 (2015).
- [804] D. T. Spencer et al., *An optical-frequency synthesizer using integrated photonics*, [Nature](#) **557**, 81–85 (2018).
- [805] P. Trocha et al., *Ultrafast optical ranging using microresonator soliton frequency combs*, [Science](#) **359**, 887–891 (2018).
- [806] M.-G. Suh and K. J. Vahala, *Soliton microcomb range measurement*, [Science](#) **359**, 884–887 (2018).
- [807] C. Reimer et al., *Generation of multiphoton entangled quantum states by means of integrated frequency combs*, [Science](#) **351**, 1176–1180 (2016).
- [808] M. Kues et al., *On-chip generation of high-dimensional entangled quantum states and their coherent control*, [Nature](#) **546**, 622–626 (2017).
- [809] P. Del’Haye et al., *Phase-coherent microwave-to-optical link with a self-referenced microcomb*, [Nature Photonics](#) **10**, 516–520 (2016).
- [810] V. Brasch et al., *Photonic chip-based optical frequency comb using soliton cherenkov radiation*, [Science](#) **351**, 357–360 (2016).
- [811] E. Obrzud et al., *A microphotonic astrocomb*, [Nature Photonics](#) **13**, 31–35 (2018).

- [812] M.-G. Suh et al., *Searching for exoplanets using a microresonator astrocomb*, [Nature Photonics](#) **13**, 25–30 (2018).
- [813] A. S. Raja et al., *Electrically pumped photonic integrated soliton microcomb*, [Nature Communications](#) **10**, 10.1038/s41467-019-08498-2 (2019).
- [814] J. L. Hall, *Nobel lecture: defining and measuring optical frequencies*, [Reviews of Modern Physics](#) **78**, 1279–1295 (2006).
- [815] P. Agostini and L. F. DiMauro, *The physics of attosecond light pulses*, [Reports on Progress in Physics](#) **67**, 813–855 (2004).
- [816] S. N. Lea, *Limits to time variation of fundamental constants from comparisons of atomic frequency standards*, [Reports on Progress in Physics](#) **70**, 1473–1523 (2007).
- [817] S. Blatt et al., *New limits on coupling of fundamental constants to gravity Using Sr87 optical lattice clocks*, [Physical Review Letters](#) **100**, 140801 (2008).
- [818] R. Pohl et al., *The size of the proton*, [Nature](#) **466**, 213–216 (2010).
- [819] F. Ferdous et al., *Spectral line-by-line pulse shaping of on-chip microresonator frequency combs*, [Nature Photonics](#) **5**, 770–776 (2011).
- [820] S. T. Cundiff, J. Ye, and J. L. Hall, *Optical frequency synthesis based on mode-locked lasers*, [Review of Scientific Instruments](#) **72**, 3749–3771 (2001).
- [821] U. Keller, *Recent developments in compact ultrafast lasers*, [Nature](#) **424**, 831–838 (2003).
- [822] K. Minoshima and H. Matsumoto, *High-accuracy measurement of 240-m distance in an optical tunnel by use of a compact femtosecond laser*, [Applied Optics](#) **39**, 5512 (2000).
- [823] N. Kuse and M. E. Fermann, *Frequency-modulated comb LIDAR*, in [Conference on lasers and electro-optics](#) (2020).
- [824] D. Kong et al., *Intra-datacenter interconnects with a serialized silicon optical frequency comb modulator*, [J. Lightwave Technol.](#) **38**, 4677–4682 (2020).
- [825] S. A. Diddams, L. Hollberg, and V. Mbele, *Molecular fingerprinting with the resolved modes of a femtosecond laser frequency comb*, [Nature](#) **445**, 627–630 (2007).
- [826] M. J. Thorpe, D. Balslev-Clausen, M. S. Kirchner, and J. Ye, *Cavity-enhanced optical frequency comb spectroscopy: application to human breath analysis*, [Optics Express](#) **16**, 2387 (2008).
- [827] M. J. Thorpe et al., *Broadband cavity ringdown spectroscopy for sensitive and rapid molecular detection*, [Science](#) **311**, 1595–1599 (2006).
- [828] B. J. Bjork et al., *Direct frequency comb measurement of $OD + CO \rightarrow DOCO$ kinetics*, [Science](#) **354**, 444–448 (2016).
- [829] P. Rickly and P. S. Stevens, *Measurements of a potential interference with laser-induced fluorescence measurements of ambient OH from the ozonolysis of biogenic alkenes*, [Atmospheric Measurement Techniques](#) **11**, 1–16 (2018).
- [830] F. R. Giorgetta et al., *Optical two-way time and frequency transfer over free space*, [Nature Photonics](#) **7**, 434–438 (2013).

- [831] A. J. Metcalf et al., *Stellar spectroscopy in the near-infrared with a laser frequency comb*, [Optica](#) **6**, 233 (2019).
- [832] B. A. C. Optical Network et al., *Frequency ratio measurements at 18-digit accuracy using an optical clock network*, [Nature](#) **591**, 564–569 (2021).
- [833] M. Lezius et al., *Space-borne frequency comb metrology*, [Optica](#) **3**, 1381 (2016).
- [834] I. Coddington, N. Newbury, and W. Swann, *Dual-comb spectroscopy*, [Optica](#) **3**, 414 (2016).
- [835] M. Hofer et al., *Mode locking with cross-phase and self-phase modulation*, [EN, Optics Letters](#) **16**, 502–504 (1991).
- [836] H. Haus, *Mode-locking of lasers*, [IEEE Journal of Selected Topics in Quantum Electronics](#) **6**, 1173–1185 (2000).
- [837] F. Wang et al., *Wideband-tuneable, nanotube mode-locked, fibre laser*, [Nature Nanotechnology](#) **3**, 738–742 (2008).
- [838] K. Kieu, W. H. Renninger, A. Chong, and F. W. Wise, *Sub-100 fs pulses at watt-level powers from a dissipative-soliton fiber laser*, [Optics Letters](#) **34**, 593 (2009).
- [839] H. Tian, Y. Song, and M. Hu, *Noise measurement and reduction in mode-locked lasers: fundamentals for low-noise optical frequency combs*, [Applied Sciences](#) **11**, 7650 (2021).
- [840] D. R. Carlson et al., *Ultrafast electro-optic light with subcycle control*, [Science](#) **361**, 1358–1363 (2018).
- [841] A. Hugi et al., *Mid-infrared frequency comb based on a quantum cascade laser*, [Nature](#) **492**, 229–233 (2012).
- [842] S. M. Link et al., *Dual-comb modelocked laser*, [Optics Express](#) **23**, 5521 (2015).
- [843] M. A. Gaafar et al., *Mode-locked semiconductor disk lasers*, [Advances in Optics and Photonics](#) **8**, 370 (2016).
- [844] L. A. Sterczewski et al., *Terahertz hyperspectral imaging with dual chip-scale combs*, [Optica](#) **6**, 766 (2019).
- [845] Y. K. Chembo, *Kerr optical frequency combs: theory, applications and perspectives*, [Nanophotonics](#) **5**, 214–230 (2016).
- [846] T. J. Kippenberg, A. L. Gaeta, M. Lipson, and M. L. Gorodetsky, *Dissipative kerr solitons in optical microresonators*, [Science](#) **361**, 10.1126/science.aan8083 (2018).
- [847] M. Kues et al., *Quantum optical microcombs*, [Nature Photonics](#) **13**, 170–179 (2019).
- [848] M. Karpov et al., *Dynamics of soliton crystals in optical microresonators*, [Nature Physics](#) **15**, 1071–1077 (2019).
- [849] A. Kovach et al., *Emerging material systems for integrated optical kerr frequency combs*, [Advances in Optics and Photonics](#) **12**, 135 (2020).
- [850] S. A. Diddams, K. Vahala, and T. Udem, *Optical frequency combs: coherently uniting the electromagnetic spectrum*, [Science](#) **369**, 10.1126/science.aay3676 (2020).

- [851] P. Del’Haye et al., *Optical frequency comb generation from a monolithic microresonator*, *Nature* **450**, 1214–1217 (2007).
- [852] I. H. Agha et al., *Four-wave-mixing parametric oscillations in dispersion-compensated high-*q*-silica microspheres*, *Physical Review A* **76**, 043837 (2007).
- [853] P. Del’Haye et al., *Full stabilization of a microresonator-based optical frequency comb*, *Physical Review Letters* **101**, 053903 (2008).
- [854] A. A. Savchenkov et al., *Tunable optical frequency comb with a crystalline whispering gallery mode resonator*, *Physical Review Letters* **101**, 093902 (2008).
- [855] D. Braje, L. Hollberg, and S. Diddams, *Brillouin-enhanced hyperparametric generation of an optical frequency comb in a monolithic highly nonlinear fiber cavity pumped by a cw laser*, *Physical Review Letters* **102**, 193902 (2009).
- [856] I. S. Grudinin, N. Yu, and L. Maleki, *Generation of optical frequency combs with a CaF_2 resonator*, *Optics Letters* **34**, 878 (2009).
- [857] L. Razzari et al., *CMOS-compatible integrated optical hyper-parametric oscillator*, *Nature Photonics* **4**, 41–45 (2009).
- [858] J. S. Levy et al., *CMOS-compatible multiple-wavelength oscillator for on-chip optical interconnects*, *Nature Photonics* **4**, 37–40 (2009).
- [859] W. Liang et al., *Generation of near-infrared frequency combs from a mgf_2 whispering gallery mode resonator*, *Optics Letters* **36**, 2290 (2011).
- [860] M. A. Foster et al., *Silicon-based monolithic optical frequency comb source*, *Optics Express* **19**, 14233 (2011).
- [861] C. Y. Wang et al., *Mid-infrared optical frequency combs at $2.5\mu\text{m}$ based on crystalline microresonators*, *Nature Communications* **4**, 10.1038/ncomms2335 (2013).
- [862] *KerrFrequencyCombs.org – Following the research on Kerr frequency combs.* <https://www.kerrfrequencycombs.org/> (visited on 03/16/2022).
- [863] A. L. Gaeta, M. Lipson, and T. J. Kippenberg, *Photonic-chip-based frequency combs*, *Nature Photonics* **13**, 158–169 (2019).
- [864] T. J. Kippenberg, R. Holzwarth, and S. A. Diddams, *Microresonator-based optical frequency combs*, *Science* **332**, 555–559 (2011).
- [865] A. Pasquazi et al., *Micro-combs: a novel generation of optical sources*, *Physics Reports* **729**, 1–81 (2018).
- [866] R. Stolen and A. Ashkin, *Optical kerr effect in glass waveguide*, *Applied Physics Letters* **22**, 294–296 (1973).
- [867] M. Sheik-Bahae, D. J. Hagan, and E. W. V. Stryland, *Dispersion and band-gap scaling of the electronic kerr effect in solids associated with two-photon absorption*, *Physical Review Letters* **65**, 96–99 (1990).
- [868] J. Tucker and D. F. Walls, *Quantum theory of parametric frequency conversion*, *Annals of Physics* **52**, 1–15 (1969).
- [869] E. Obrzud, S. Lecomte, and T. Herr, *Temporal solitons in microresonators driven by optical pulses*, *Nature Photonics* **11**, 600–607 (2017).

- [870] Y. Zhao et al., *Near-degenerate quadrature-squeezed vacuum generation on a silicon-nitride chip*, [Physical Review Letters](#) **124**, 193601 (2020).
- [871] V. D. Vaidya et al., *Broadband quadrature-squeezed vacuum and nonclassical photon number correlations from a nanophotonic device*, [Science Advances](#) **6**, 10.1126/sciadv.aba9186 (2020).
- [872] J. M. Arrazola et al., *Quantum circuits with many photons on a programmable nanophotonic chip*, [Nature](#) **591**, 54–60 (2021).
- [873] D. Grassani et al., *Micrometer-scale integrated silicon source of time-energy entangled photons*, [Optica](#) **2**, 88 (2015).
- [874] J. A. Jaramillo-Villegas et al., *Persistent energy–time entanglement covering multiple resonances of an on-chip biphoton frequency comb*, [Optica](#) **4**, 655 (2017).
- [875] T. J. Steiner et al., *Ultrabright entangled-photon-pair generation from an AlGaAs-on-insulator microring resonator*, [PRX Quantum](#) **2**, 010337 (2021).
- [876] F. Samara et al., *Entanglement swapping between independent and asynchronous integrated photon-pair sources*, [Quantum Science and Technology](#) **6**, 045024 (2021).
- [877] T. J. Kippenberg, S. M. Spillane, and K. J. Vahala, *Kerr-nonlinearity optical parametric oscillation in an ultrahigh-Q Toroid microcavity*, [Physical Review Letters](#) **93**, 083904 (2004).
- [878] T. Herr et al., *Universal formation dynamics and noise of kerr-frequency combs in microresonators*, [Nature Photonics](#) **6**, 480–487 (2012).
- [879] W. H. Renninger and P. T. Rakich, *Closed-form solutions and scaling laws for kerr frequency combs*, [Scientific Reports](#) **6**, 10.1038/srep24742 (2016).
- [880] L. F. Mollenauer and R. H. Stolen, *The soliton laser*, [Optics Letters](#) **9**, 13 (1984).
- [881] F. Li et al., *Modeling frequency comb sources*, [Nanophotonics](#) **5**, 292–315 (2016).
- [882] M. A. Guidry et al., *Quantum optics of soliton microcombs*, [Nature Photonics](#) **16**, 52–58 (2021).
- [883] Y. Okawachi et al., *Octave-spanning frequency comb generation in a silicon nitride chip*, [Optics Letters](#) **36**, 3398 (2011).
- [884] J. Wang, F. Sciarrino, A. Laing, and M. G. Thompson, *Integrated photonic quantum technologies*, [Nature Photonics](#) **14**, 273–284 (2019).
- [885] B.-H. Wu, R. N. Alexander, S. Liu, and Z. Zhang, *Quantum computing with multidimensional continuous-variable cluster states in a scalable photonic platform*, [Physical Review Research](#) **2**, 023138 (2020).
- [886] E. S. Lamb et al., *Optical-frequency measurements with a kerr microcomb and photonic-chip supercontinuum*, [Physical Review Applied](#) **9**, 024030 (2018).
- [887] T. Bosch, *Laser ranging: a critical review of usual techniques for distance measurement*, [Optical Engineering](#) **40**, 10 (2001).
- [888] G. Berkovic and E. Shafir, *Optical methods for distance and displacement measurements*, [Advances in Optics and Photonics](#) **4**, 441 (2012).

- [889] P. J. Marchand et al., *Soliton microcomb based spectral domain optical coherence tomography*, [Nature Communications](#) **12**, 10.1038/s41467-020-20404-9 (2021).
- [890] K. Nozaki and N. Bekki, *Solitons as attractors of a forced dissipative nonlinear schrödinger equation*, [Physics Letters A](#) **102**, 383–386 (1984).
- [891] H. Haken, *Synergetics*, [Physics Bulletin](#) **28**, 412–414 (1977).
- [892] W. J. Firth and C. O. Weiss, *Cavity and feedback solitons*, [Optics and Photonics News](#) **13**, 54 (2002).
- [893] S. Barland et al., *Cavity solitons as pixels in semiconductor microcavities*, [Nature](#) **419**, 699–702 (2002).
- [894] T. Ackemann, W. Firth, and G.-L. Oppo, *Chapter 6 fundamentals and applications of spatial dissipative solitons in photonic devices*, in [Advances in atomic, molecular, and optical physics](#) (Elsevier, 2009), pp. 323–421.
- [895] A. Scroggie et al., *Pattern formation in a passive kerr cavity*, [Chaos, Solitons & Fractals](#) **4**, 1323–1354 (1994).
- [896] A. Ankiewicz and N. Akhmediev, *Dissipative solitons: from optics to biology and medicine* (Springer Berlin Heidelberg, 2008).
- [897] N. J. Zabusky and M. D. Kruskal, *Interaction of "solitons" in a collisionless plasma and the recurrence of initial states*, [Physical Review Letters](#) **15**, 240–243 (1965).
- [898] H. C. Kim, R. L. Stenzel, and A. Y. Wong, *Development of "cavitons" and trapping of rf field*, [Physical Review Letters](#) **33**, 886–889 (1974).
- [899] J. Wu, R. Keolian, and I. Rudnick, *Observation of a nonpropagating hydrodynamic soliton*, [Physical Review Letters](#) **52**, 1421–1424 (1984).
- [900] R. Richter and I. V. Barashenkov, *Two-dimensional solitons on the surface of magnetic fluids*, [Physical Review Letters](#) **94**, 184503 (2005).
- [901] P. B. Umbanhowar, F. Melo, and H. L. Swinney, *Localized excitations in a vertically vibrated granular layer*, [Nature](#) **382**, 793–796 (1996).
- [902] A. Ustinov, *Solitons in josephson junctions*, [Physica D: Nonlinear Phenomena](#) **123**, 315–329 (1998).
- [903] A. M. Turing, *The chemical basis of morphogenesis*, [Philosophical Transactions of the Royal Society of London. Series B, Biological Sciences](#) **237**, 37–72 (1952).
- [904] B. Ermentrout, X. Chen, and Z. Chen, *Transition fronts and localized structures in bistable reaction—diffusion equations*, [Physica D: Nonlinear Phenomena](#) **108**, 147–167 (1997).
- [905] V. K. Vanag, A. M. Zhabotinsky, and I. R. Epstein, *Oscillatory clusters in the periodically illuminated, spatially extended belousov-zhabotinsky reaction*, [Physical Review Letters](#) **86**, 552–555 (2001).
- [906] O. Lejeune, M. Tlidi, and P. Couteron, *Localized vegetation patches: a self-organized response to resource scarcity*, [Physical Review E](#) **66**, 010901 (2002).

- [907] L. F. Mollenauer, R. H. Stolen, and J. P. Gordon, *Experimental observation of picosecond pulse narrowing and solitons in optical fibers*, [Physical Review Letters](#) **45**, 1095–1098 (1980).
- [908] K. E. Strecker, G. B. Partridge, A. G. Truscott, and R. G. Hulet, *Formation and propagation of matter-wave soliton trains*, [Nature](#) **417**, 150–153 (2002).
- [909] F. Leo et al., *Temporal cavity solitons in one-dimensional kerr media as bits in an all-optical buffer*, [Nature Photonics](#) **4**, 471–476 (2010).
- [910] V Odent, M Taki, and E Louvergneaux, *Experimental evidence of dissipative spatial solitons in an optical passive kerr cavity*, [New Journal of Physics](#) **13**, 113026 (2011).
- [911] B. Schäpers, M. Feldmann, T. Ackemann, and W. Lange, *Interaction of localized structures in an optical pattern-forming system*, [Physical Review Letters](#) **85**, 748–751 (2000).
- [912] S. Barbay et al., *Homoclinic snaking in a semiconductor-based optical system*, [Physical Review Letters](#) **101**, 253902 (2008).
- [913] M. C. Cross and P. C. Hohenberg, *Pattern formation outside of equilibrium*, [Reviews of Modern Physics](#) **65**, 851–1112 (1993).
- [914] S. Wabnitz, *Suppression of interactions in a phase-locked soliton optical memory*, [Optics Letters](#) **18**, 601 (1993).
- [915] P. Grelu and N. Akhmediev, *Dissipative solitons for mode-locked lasers*, [Nature Photonics](#) **6**, 84–92 (2012).
- [916] M. Segev and G. Stegeman, *Self-trapping of optical beams: spatial solitons*, [Physics Today](#) **51**, 42–48 (1998).
- [917] N. Akhmediev and A. Ankiewicz, eds., *Dissipative solitons* (Springer Berlin Heidelberg, 2005).
- [918] T. Herr et al., *Temporal solitons in optical microresonators*, [Nature Photonics](#) **8**, 145–152 (2013).
- [919] X. Yi et al., *Soliton frequency comb at microwave rates in a high-q silica microresonator*, [Optica](#) **2**, 1078 (2015).
- [920] N. Englebert et al., *Temporal solitons in a coherently driven active resonator*, [Nature Photonics](#) **15**, 536–541 (2021).
- [921] G. S. McDonald and W. J. Firth, *Spatial solitary-wave optical memory*, [Journal of the Optical Society of America B](#) **7**, 1328 (1990).
- [922] W. F. McGrew et al., *Atomic clock performance enabling geodesy below the centimetre level*, [Nature](#) **564**, 87–90 (2018).
- [923] S. Brewer et al., *Quantum-logic clock with a systematic uncertainty below 10^{-18}* , [Physical Review Letters](#) **123**, 033201 (2019).
- [924] C. Sanner et al., *Optical clock comparison for lorentz symmetry testing*, [Nature](#) **567**, 204–208 (2019).
- [925] L.-S. Ma et al., *Optical frequency synthesis and comparison with uncertainty at the 10^{-19} level*, [Science](#) **303**, 1843–1845 (2004).

- [926] P.-H. Wang et al., *Intracavity characterization of micro-comb generation in the single-soliton regime*, [Optics Express](#) **24**, 10890 (2016).
- [927] C. Joshi et al., *Thermally controlled comb generation and soliton modelocking in microresonators*, [Optics Letters](#) **41**, 2565 (2016).
- [928] S. Coen, H. G. Randle, T. Sylvestre, and M. Erkintalo, *Modeling of octave-spanning kerr frequency combs using a generalized mean-field lugiato-lefever model*, [Optics Letters](#) **38**, 37 (2012).
- [929] P. Grelu, *Nonlinear optical cavity dynamics : from microresonators to fiber lasers*, eng (Wiley-VCH Verlag, Weinheim, 2016).
- [930] L. Lugiato, *Nonlinear optical systems*, eng (Cambridge University Press, Cambridge United Kingdom, 2015).
- [931] H. Guo et al., *Intermode breather solitons in optical microresonators*, [Physical Review X](#) **7**, 041055 (2017).
- [932] M. Yu et al., *Breather soliton dynamics in microresonators*, [Nature Communications](#) **8**, 10.1038/ncomms14569 (2017).
- [933] A. A. Afridi et al., *Breather solitons in AlN microresonators*, [Optics Continuum](#) **1**, 42 (2022).
- [934] D. C. Cole et al., *Soliton crystals in kerr resonators*, [Nature Photonics](#) **11**, 671–676 (2017).
- [935] A. B. Matsko et al., *Mode-locked kerr frequency combs*, [Optics Letters](#) **36**, 2845 (2011).
- [936] A. G. Griffith et al., *Silicon-chip mid-infrared frequency comb generation*, [Nature Communications](#) **6**, 10.1038/ncomms7299 (2015).
- [937] H. Bao et al., *Laser cavity-soliton microcombs*, [Nature Photonics](#) **13**, 384–389 (2019).
- [938] Q. Li et al., *Stably accessing octave-spanning microresonator frequency combs in the soliton regime*, [Optica](#) **4**, 193 (2017).
- [939] A. A. Savchenkov et al., *Kerr combs with selectable central frequency*, [Nature Photonics](#) **5**, 293–296 (2011).
- [940] M. Haelterman, S. Trillo, and S. Wabnitz, *Dissipative modulation instability in a nonlinear dispersive ring cavity*, [Optics Communications](#) **91**, 401–407 (1992).
- [941] J. Geddes, J. Moloney, E. Wright, and W. Firth, *Polarisation patterns in a nonlinear cavity*, [Optics Communications](#) **111**, 623–631 (1994).
- [942] M. Haelterman, S. Trillo, and S. Wabnitz, *Polarization multistability and instability in a nonlinear dispersive ring cavity*, [Journal of the Optical Society of America B](#) **11**, 446 (1994).
- [943] Y. K. Chembo and C. R. Menyuk, *Spatiotemporal lugiato-lefever formalism for kerr-comb generation in whispering-gallery-mode resonators*, [Physical Review A](#) **87**, 053852 (2013).

- [944] C. Godey, I. V. Balakireva, A. Coillet, and Y. K. Chembo, *Stability analysis of the spatiotemporal lugiato-lefever model for kerr optical frequency combs in the anomalous and normal dispersion regimes*, [Physical Review A **89**, 063814 \(2014\)](#).
- [945] P. Parra-Rivas et al., *Dynamics of localized and patterned structures in the lugiato-lefever equation determine the stability and shape of optical frequency combs*, [Physical Review A **89**, 043813 \(2014\)](#).
- [946] Y. K. Chembo, D. Gomila, M. Tlidi, and C. R. Menyuk, *Theory and applications of the lugiato-lefever equation*, [The European Physical Journal D **71**, 10.1140/epjd/e2017-80572-0 \(2017\)](#).
- [947] E. Averlant, M. Tlidi, K. Panajotov, and L. Weicker, *Coexistence of cavity solitons with different polarization states and different power peaks in all-fiber resonators*, [Optics Letters **42**, 2750 \(2017\)](#).
- [948] L. A. Lugiato, F. Prati, M. L. Gorodetsky, and T. J. Kippenberg, *From the lugiato-lefever equation to microresonator-based soliton kerr frequency combs*, [Philosophical Transactions of the Royal Society A: Mathematical, Physical and Engineering Sciences **376**, 20180113 \(2018\)](#).
- [949] A. U. Nielsen et al., *Coexistence and interactions between nonlinear states with different polarizations in a monochromatically driven passive kerr resonator*, [Physical Review Letters **123**, 013902 \(2019\)](#).
- [950] F. Copie et al., *Interplay of polarization and time-reversal symmetry breaking in synchronously pumped ring resonators*, [Physical Review Letters **122**, 013905 \(2019\)](#).
- [951] M. Saha, S. Roy, and S. K. Varshney, *Polarization dynamics of a vector cavity soliton in a birefringent fiber resonator*, [Physical Review A **101**, 033826 \(2020\)](#).
- [952] I. V. Balakireva and Y. K. Chembo, *A taxonomy of optical dissipative structures in whispering-gallery mode resonators with kerr nonlinearity*, [Philosophical Transactions of the Royal Society A: Mathematical, Physical and Engineering Sciences **376**, 20170381 \(2018\)](#).
- [953] K. Nozaki and N. Bekki, *Low-dimensional chaos in a driven damped nonlinear schrödinger equation*, [Physica D: Nonlinear Phenomena **21**, 381–393 \(1986\)](#).
- [954] A. Ankiewicz, N. Devine, N. Akhmediev, and J. Soto-Crespo, *Dissipative solitons and antisolitons*, [Physics Letters A **370**, 454–458 \(2007\)](#).
- [955] T. Miyaji, I. Ohnishi, and Y. Tsutsumi, *Bifurcation analysis to the lugiato-lefever equation in one space dimension*, [Physica D: Nonlinear Phenomena **239**, 2066–2083 \(2010\)](#).
- [956] G. Kozyreff, *Localized turing patterns in nonlinear optical cavities*, [Physica D: Nonlinear Phenomena **241**, 939–946 \(2012\)](#).
- [957] C. Godey, *A bifurcation analysis for the lugiato-lefever equation*, [The European Physical Journal D **71**, 10.1140/epjd/e2017-80057-2 \(2017\)](#).
- [958] R. Mandel and W. Reichel, *A priori bounds and global bifurcation results for frequency combs modeled by the lugiato-lefever equation*, [SIAM Journal on Applied Mathematics **77**, 315–345 \(2017\)](#).

- [959] J. Vasco and V. Savona, *Slow-light frequency combs and dissipative kerr solitons in coupled-cavity waveguides*, [Physical Review Applied](#) **12**, 064065 (2019).